A Study of Fade Mitigation and Resource Management of Satellite Networks in Rain Conditions

Eleni Noussi

The thesis is submitted in partial fulfilment of the requirements for the award of the degree of Doctor of Philosophy of the University of Portsmouth.

June 2008

Abstract

This thesis targets higher frequency satellite systems (Ku-band and above) that suffer from severe atmospheric impairments and require advanced techniques to compensate for the effects of rain attenuation.

Keeping a classical approach, based on a worst case sizing, results in fixed over-sizing of systems leading to reduced efficiency and unreasonable costs. It is therefore necessary that these systems include adaptive Fade Mitigation Techniques (FMTs) to counteract propagation impairments in real-time and use system resources efficiently.

The combination of the management of radio resources and the deployment of Fade Mitigation Techniques appears to be an outstanding challenge for Broadband Satellite Networks. DVB-RCS and DVB-S standards have not primarily been defined considering the details of rain FMTs; they have to be adapted to support FMTs, so the study of efficient FMTs and their integration within the standards is necessary. Adaptive transmission techniques, such as Adaptive Coding and Modulation (ACM), are mostly introduced as a way of achieving efficient Bandwidth on Demand (BoD). But they can also be a good framework for deploying FMTs and can provide high availabilities for powerful connections. Employing Burst Length Control (BLC) can be a useful extension of ACM to permit its dynamic range to be increased in the case of power-limited return channels, for which high-order modulation schemes cannot be used.

A design methodology of a combined FMT is proposed and presents the complex problem of system availability depending not only on the combined FMT performance, but also on the resource allocation scheme performance. A resource allocation protocol that incorporates FMT implementation within its dynamic capacity assignment strategy is developed and tested in the presence of bursty traffic when multiple links experience simultaneous fading.

Acknowledgements

I would like to express a deep thanks to my supervisor Dr Boris Grémont for providing me with the opportunity to study for a Ph.D. in the Microwave Telecommunications Systems research group, for his continuous commitment to this project and his useful comments and suggestions. Also thanks to Dr Misha Filip, Dr David Ndzi, Professor Enric Vilar, and Dr Alan Hewitt for their good advice and helpful suggestions. My gratitude to Mr Victor Dunn, Mr Frank Margrave, and also our administrative and technical support staff, especially Mrs Linda Janes, Mr Cedric Arrow, and Mr Phillip Trew. I cannot even find the right words to express how grateful I am to Mr Chris Lovett and Mrs Margaret Lovett for their faith in me and for that invaluable, altruistic and consistent moral support they have given me all these years.

Special thanks also go to all my research group colleagues, Dragana, Kostas, Nick, Cristina, Afroditi, Manish, Kenneth, Thomas, and Matt, for their enthusiasm, stimulating discussions, their friendship, their encouragement and sense of humor that cheered me up in times of despair. I would also like to thank everyone else including both current and former members, and all my other friends here who have all helped me out in many different ways and have generally put up with me!

I would like to dedicate this thesis to my parents whose continued support, encouragement and faith in me meant the world to me and have kept me going. Finally, a special thanks to those few close family members and friends of mine back home for their moral support, patience and for standing by my parents at times I couldn't be there.

Dedicated to my parents,
Demetra & Vangelis

Αφιερωμένο στους γονείς μου,
Δήμητρα & Βαγγέλη

"Life is not about waiting for the storm to pass, it is about learning how to dance in the rain."

«Ζωή δεν είναι να περιμένεις να περάσει η μπόρα, αλλά να μαθαίνεις πώς να χορεύεις στη βροχή.»

- Unknown Author

Table of Contents

Declaration: *Whilst registered as a candidate for the above Degree, I have not been registered for any other research award. The results and conclusions embodied in this thesis are the work of the named candidate and have not been submitted for any other academic award.*

List of Figures

List of Tables

List of Acronyms and Abbreviations

ABR	Available Bit Rate
ACM	Adaptive Coding and Modulation
APSK	Amplitude and Phase-Shift Keying
ATM	Asynchronous Transfer Mode
Att	Attenuation
BBI	Broadband Interactive
BER	Bit Error Rate
BIDS	Bath Information and Data Services
BLC	Burst Length Control
BoD	Bandwidth-on-Demand
BPSK	Binary Phase Shift Keying
BW	Bandwidth
CAC	Call Admission Control
CBR	Constant Bit Rate
CCDF	Complementary Cumulative Distribution Function
CDV	Cell Delay Variation
CER	Cell Error Ratio
CF-DAMA	Combined Free/Demand Assigned Multiple Access
CLR	Cell Loss Ratio
CMR	Cell Misinsertion Rate
CNIR	Carrier-to-Noise-plus-Interference Ratio
CNR	Carrier to Noise Ratio
CRA	Continuous Rate Assignment
CS	Clear Sky
CSC	Common Signalling Channel

CTD	Cell Transfer Delay
DA	Data-Aided
DAMA	Demand Assignment
DR	Dynamic Range
DRA	Dynamic Rate Adaptation
DRR	Data Rate Reduction
DVB-RCS	Digital Video Broadcast-Return Channel by Satellite
DVB-S	Digital Video Broadcasting over Satellite
EIRP	Effective Isotropic Radiated Power
EMI	Electro-Magnetic Interference
EPG	Electronic Programme Guide
ES	Earth Station
ETSI	European Telecommunications Standards Institute
FCA	Free Capacity Assignment
FCM	Fade Countermeasure
FCT	Frame Composition Table
FDMA	Frequency Division Multiple Access
FEC	Forward Error Correction
FMT	Fade Mitigation Techniques
GEO	Geosynchronous
HAP	High Altitude Platform
IBR	In-Band Requests
INSPEC	Information Service for Physics, Electronics, and Computing
IPS	Input Power for Saturation
ITU-R	International Telecommunication Union -Radiocommunication Sector
ITU-T	International Telecommunication Union -Telecommunication Standardization Sector

LAN	Local Area Network
MAC	Medium Access Control
MF-TDMA	Multi-Frequency Time Division Multiple Access
ML	Maximum-Likelihood
MPEG-TS	Moving Picture Experts Group Transport Stream
M-PSK	M-ary Phase-Shift Keying
MTS	Microwave Telecommunication Systems
NCC	Network Control Centre
NCR	Network Clock Reference
NDA	Non-Data-Aided
nrt-VBR	Non-Real-Time Variable Bit Rate
OBR	Out-of-Band Request
PC	Power Control
PCR	Peak Cell Rate
PDF	Probability Density Function
PER	Packet Error Ratio
pkt	Packet
PL	Physical Layer
PQ	Priority Queuing
PSD	Power Spectral Density
PSK	Phase Shift Keying
QoS	Quality of Service
QPSK	Quadrature Phase-Shift Keying
RA	Resource Allocation
RBDC	Rate-Based Dynamic Capacity
RC	Reserved Capacity
RCST	Return Channel Satellite Terminal
RR	Round-Robin

RTD (or RTT)	Round Trip Delay (or Round Trip Time)
rt-VBR	Real-Time Variable Bit Rate
SCT	Superframe Composition Table
SECBR	Severely Errored Cell Block Ratio
SES	Societe Europeenne des Satellites
SF	Superframe
SNR	Signal to Noise Ratio
SNV	Signal to Noise Variance
src	Source
SYNC ACQ	Synchronisation Acquisition
TBTP	Terminal Burst Time Plan
TCP/IP	Transmission Control Protocol/Internet Protocol
TCT	Timeslot Composition Table
TDMA	Time Division Multiple Access
TRF	Traffic
TS	Timeslot
TWTA	Traveling Wave Tube Amplifier
UBR	Unspecified Bit Rate
VBDC	Volume-Based Dynamic Capacity
VSAT	Very Small Aperture Terminal
WRR	Weighted Round-Robin
w.r.t.	With Respect To

List of Symbols

$\alpha \simeq 0.35$	Roll-off factor
A	Dimensionless "area" (time-bandwidth product)
$\alpha_{on}, \alpha_{off}$	Shape/tail parameter of ON and OFF time pareto distribution
α_R	Attenuation due to rain
B	Bandwidth
$\tilde{B}_i$	Allocated carrier bandwidth for connection i
B_0	Bandwidth corresponding to ACM mode 0; $(\rho, M) = (9/10, 4)$
$B_{\max}$	MF-TDMA subspace bandwidth
BO_o	Satellite output back-off
BO_i	Satellite input back-off
C	Channel capacity
C/N_o	Carrier-to-noise power spectral density ratio
$C/(N_o + I_o)$	Carrier-to-noise-plus-interference ratio
C_{tot}	Overall payload capacity
γ_R	Specific attenuation in [dB/km]
$\Delta T_{SLOT} = T_{\min}$	Timeslot (minimum burst) duration
D_a	Antenna diameter
D	End-to-end delay
D_{queue}	Queueing delay prior to transmission
ϵ	Path elevation angle
E_s/N_o	Energy-per-symbol-to-noise power spectral density ratio
E_b/N_o	Energy-per-bit-to-noise power spectral density ratio
$(E_s/N_o)_{ach}$	Acheived energy-per-symbol-to-noise spectral density ratio
$(E_s/N_o)_{req}$	Required energy-per-symbol-to-noise spectral density ratio

η	Antenna efficiency
f_c	Carrier frequency
G	Antenna gain in dB
G_C	Coding gain
G_H	BLC gain
H	Burst Length Control expansion factor
H_P	Hurst parameter of Pareto distribution
IPS	Input power for saturation
k	Location parameter (smallest possible value) of Pareto distribution
k_{on}, k_{off}	Location parameter of ON and OFF time distribution
λ	Wavelength in m
L	"Load" or level of demand placed on the channel expressed as a fraction of the total channel capacity
L_F	Feeder loss in dB
L_{Fd}	Downlink free-space loss in dB
L_{FS}	Free space loss in dB
L_{Fu}	Uplink free-space loss in dB
$L_R(R, \epsilon)$	Effective radio path length through the rain in km
μ	Median (mean value)
M	M-arity
M_o	Clear-sky link power margin
N_b	Number of bits in one ATM cell
N_c	Number of frequency carriers
N_{FMT}	Number of FMT slot intervals
N_{pkt}	Total number of packets in queue
N_{src}	Number of transmitting sources
N_{TS}	Number of traffic (payload) slots per carrier

$\pi \simeq 3.14159$	Ratio of a circle's circumference to its diameter
P_T	Transmitted power in dBW
ρ	Code rate
R	Precipitation rate in mm/h
R_b	User information bit rate
R_{bc}	Coded bit rate
R_{bg}	Bit rate "granularity"
R_{pkt}	Transmission cell rate
R_s	Symbol rate
RTD	Satellite round trip propagation delay
σ	Standard deviation
T	System noise temperature in K
$\tilde{T}_i$	Allocated Burst duration for connection i within the frame period T_F
T_F	Frame duration
T_{pkt}	Packet transmission/reception duration
T_s	Symbol duration
θ	Phase of the transmitted carrier in deg

CHAPTER 1

INTRODUCTION

1.1 The DVB-RCS System

Digital Video Broadcast-Return Channel by Satellite (DVB-RCS) is an open standard used in two-way broadband communication via geosynchronous satellites. Typically, remote terminals or networks receive transmissions on a "forward" channel and deliver requests and responses on a smaller "return" channel [1.1] and [1.2].

Broadband Interactive service (BBI), designed for Societe Europeenne des Satellites (SES), the company operating the ASTRA Satellite network ([1.3] and [1.4]) is an example of a satellite system following the DVB-RCS standard [1.1], [1.2], and [1.5]. Another satellite operator, Eutelsat, the owner of three LinkStar DVB-compatible hubs, has partnered more closely with the Comsat Laboratories division of ViaSat in order to implement a true DVB-RCS standard network enabling interoperability of terminals for enterprise services across Europe [1.6], [1.7], and [1.8].

Worldwide companies and industries are developing broadband interactive satellite systems; it has been several years since their commercial availability was announced [1.9]. It is expected that the network access demand will increase and therefore strategies to achieve high utilisation of the limited available radio resources are of great importance to accommodate the increase in demand at the lowest possible cost [1.10] and [1.14].

A result of the need to accommodate high-rate transmission is to push into increasingly higher frequency bands, namely Ka band (27-40 GHz) and V band (40-75 GHz). This trend is explained by the relatively large segments of frequency spectrum required for supporting the high data rates planned in newer systems [1.10]. Most VSAT and Digital Broadcast Satellite TV systems in operation today use portions of the Ku band [1.11].

A major drawback to the use of higher frequencies is increasingly significant rain attenuation, as this increases rapidly with increasing microwave frequency, [1.11]-[1.13]. It

can cause serious signal quality degradations of earth-space communication links and can therefore have a major impact not only on individual links, but on the whole network, which will be affected on a global basis.

1.2 Literature Survey

The purpose of the literature survey was to identify more precisely the focal point of the work within the context of Broadband Satellite links. The survey was carried out using the INSPEC on-line database through the Bath Information and Data Services (BIDS), with a personal Athens account, in combination with extensive use of the facilities of the University of Portsmouth Library and especially its inter-library loan services for obtaining relevant and extremely interesting scientific articles. Regular participation in technical conferences offered invaluable networking and exchange of up-to-date information with researchers from similar fields of other institutions from all over the world.

The following subjects were identified to be of particular interest to this project:

- *Medium Access Control* (MAC) [1.15], [1.16], [1.17]-[1.22], and [1.23]-[1.34];
- *Multi-Frequency Time Division Multiple Access* (MF-TDMA) [1.18], [1.19], [1.21], [1.22], [1.26], [1.27], and [1.33]-[1.38];
- *DVB-Return Channel by Satellite* and Bandwidth-on-Demand (BoD) [1.1], [1.5], [1.35], [1.26], and [1.38];
- Fade Mitigation Techniques in Demand Assignment TDMA [1.39]-[1.45]

A plethora of references were identified, collected and analysed. All references which are of particular importance to this work will be acknowledged in the text where appropriate and listed at the end of the respective chapter.

1.3 Objective and Scope of the Thesis

This thesis targets high frequency satellite systems that suffer from severe atmospheric impairments and hence require advanced techniques to compensate for the effects of rain attenuation.

The main objective of this work is to perform a detailed study of advanced multimedia satellite networks affected by rain-induced microwave impairments. The key point of research interest is to describe, analyse and quantify on a whole-network-level the impact of the introduction of a Fade Mitigation Technique (FMT) on the interdependent system operations.

As a first step, the choice of a realistic satellite communications scenario is necessary, with the purpose of investigating how an appropriate Fade Mitigation Technique can be implemented, preferably avoiding major modifications of the existing standards.

The combination of the management of radio resources and the deployment of fade mitigation techniques appear to be an outstanding challenge for ATM Broadband Satellite Networks. The compensation of rain fading on such systems may require the enhancement of current standards, which have not been primarily built considering the details of FMTs, so they may have to be adapted to support them, at physical and/or at MAC layer level.

Some FMTs, such as Power Control (PC), are already adopted by current systems, and others, such as Adaptive Coding and Modulation (ACM), are being introduced in the new generation of standards (DVB-S2) or are still a subject for enhancement of current standards (DVB-RCS). In fact, adaptive transmission techniques appear to be mostly introduced as a way of achieving efficient Bandwidth on Demand (BoD) [1.20]. However ACM is also a good framework for deploying FMTs and there is an attractive possibility of extending the dynamic range and link availability of power-limited return channels through Burst Length Control [1.45]. Hence a design methodology of a combined FMT with ACM and BLC is proposed.

The investigation of the impact of such a combined FMT on the resource management of the network is therefore the main objective of this work. This thesis will focus on the design of a resource allocation protocol based on the dynamic handling of the bandwidth when multiple links experience simultaneous fading.

The main objectives of the work presented in this thesis can be summarised as follows:

- To extend the FMT dynamic range of ACM with BLC, in order to improve the link availability of power-limited return channels.
- To investigate any dependance of system availability on the combined FMT dynamic range, as well as on the resource allocation scheme performance.
- To design a resource allocation protocol that incorporates FMT within a dynamic capacity assignment strategy.
- To develop a computer simulation of the proposed resource allocation scheme including an appropriate traffic model to best represent the behaviour of modern Internet traffic.
- To analyse the short-term performance of the proposed scheme and perform comparison with that of pure ACM through implementation of appropriate test scenarios.

- To ultimately develop a novel adaptive bandwidth-partitioning technique that incoroporates BLC and is compatible with the DVB-RCS standard, taking into account the real-time channel conditions as well as traffic needs of the MF-TDMA network users.

1.4 Overview/Contents of the Thesis

The content of chapter 2 is a review of broadband satellite networks and the Fade Mitigation Techniques (FMTs) relevant to them. In particular, the chapter focuses on important issues of multimedia networks regarding Quality of Service (QoS), MF-TDMA resource management, and CAC/MAC design issues. An extensive description of the suitable FMTs for the enhancement of current standards and their implications on the resource allocation process is also included. The objective is to outline the main interest and focus of this thesis.

Chapter 3 proposes a methodology on how to design a Fade Mitigation Technique (FMT) suitable for application to Ka-band Multi-Frequency-TDMA/DVB-RCS networks. The chapter starts with the description of the satellite system to be simulated. A combined FMT employing Adaptive Coding/Modulation (ACM) and Burst Length Control (BLC) will be studied. Detailed return link calculations assist in clear-sky as well as attenuated uplink and downlink performance analysis. The next step is to proceed to the consideration of a single link, in order to investigate the attenuation protection that can be offered as a function of spare resource in the form of extra timeslots, with the intention to meet the user-specified Quality of Service requirements considering a large number of links simultaneously affected by rain; both the advantages and costs of the FMT employment are demonstrated. A qualitative design approach with regards to the BLC operation, introduces the complex problem of the dependence of system availability not only on the combined FMT dynamic range, but also on the Resource Allocation (RA) scheme performance.

Chapter 4 starts with a description of the traffic generation model developed for the purposes of the network simulation. It proceeds to a review of capacity organisation and segmentation details that provide the basis for the BoD operation. The chapter then addresses the problem of FMT resource management, i.e. the problem of allocating slots to the traffic sources within the MF-TDMA channel under rain conditions, and presents the proposed resource allocation protocol incorporating FMT implementation within its dynamic capacity assignment strategy.

Chapter 5 looks at the performance of the proposed algorithm. The Bandwidth on Demand (BoD) algorithm is tested in the presence of bursty traffic and rain attenuation. In addition to improving the desired availability, the goal is to maximise channel utilisation and minimise transmission delay while maintaining the fairness among the links. The impact of the FMT enhancement on system performance, channel capacity utilisation, user throughput, buffer occupancy and transmission delay is investigated, with the aim to explore the suitability and limitations of Burst Length Control. The proposed combined FMT technique (ACM-BLC) is also compared to simulation results for the pure ACM scheme in order to evaluate the improvement and other possible consequences brought by BLC.

Finally chapter 6 is a discussion of the results obtained in the previous chapters and introduces the areas for further research work.

1.5 References

[1.1] ETSI EN 301 790 V1.3.1: "Digital Video Broadcasting (DVB); Interaction Channel for Satellite Distribution Systems" (also known as the DVB-RCS specification), Final Draft, 2002-11, retrieved June 11, 2008, from the ETSI website: http://www.etsi.org

[1.2] ETSI EN 301 790 V1.4.1: "Digital Video Broadcasting (DVB); Interaction Channel for Satellite Distribution Systems", 2005-09, retrieved June 11, 2008, from the ETSI website: http://www.etsi.org

[1.3] Fairhurst G., (2001), "Broadband Multimedia Satellite Systems", retrieved June 11, 2008, from the University of Aberdeen website: http://www.erg.abdn.ac.uk/public_html/research/future-net/digital-video/bband-sat.html

[1.4] Krause J., "The ASTRA BBI System: An overview", retrieved July 3, 2003, from http://www.luxinnovation.lu/presentations/020708_presa_krause.pdf

[1.5] ETSI TR 101 790 (V1.2.1): "Digital Video Broadcasting (DVB); Interaction Channel for Satellite Distribution Systems; Guidelines for the use of EN 301 790", 2000-01, retrieved June 11, 2008, from the ETSI website: http://www.etsi.org

[1.6] *"Eutelsat Plans Expansion of Broadband Multimedia Services"*, SKYBroadband, Issue #46, June 17, 2003, retrieved June 11, 2008, from http://www.skybroadband.info/arc/20030210/industry.html

[1.7] *"Eutelsat Will Expand Broadband Multimedia Services with Satellite Terminals from ViaSat"*, ViaSat, Press Releases, 05-02-2003, retrieved June 11, 2008, from http://www.viasat.com/news/eutelsat-will-expand-broadband-multimedia-services-satellite-terminals-viasat

[1.8] *"Eutelsat Inaugurates New Italian Teleport for Broadband Services"*, Talk Satellite, March 21, 2003, retrieved June 11, 2008, from http://www.eutelsat.org/news/press-releases-2003.html

[1.9] "Astra Broadband Interactive System Now Commercially Available", retrieved June 11, 2008, from http://www.satnews.com/stories2/4nov2001-3.html

[1.10] Hatdjitheodosiou M. H., Ephremides A., Friedman D.: "Broadband Access via Satellite", Computer Networks, vol. 31, no. 4, pp. 353-378, 1999.

[1.11] Nelson R. A., "V-band: Expansion of the Spectrum Frontier", Via Satellite, February 1998, pp. 66+.

[1.12] Touw S. I. E., "Analyses of Amplitude Scintillations for the Evaluation of the Performance of Open-Loop ULPC Systems", MSc Thesis, Eindhoven University of Technology, Eindhoven, The Netherlands, 1994.

[1.13] Ippolito L. J., "Radio propagation for space communications systems", IEEE Proceedings, vol. 69, no. 6, pp. 697-727, U.S.A., June 1981.

[1.14] Hadjitheodosiou M. H., Coakley F. P., "Networking with VSATs: From Low Bit Rate Systems to ATM Service Provision", AIAA 16th International Communications Satellite Systems Conference, 1996, pp. 854-864.

[1.15] Pech P. Bousquet M., Castanet L., Radzik J., Fabre B., "Methodology to Optimise Techniques of Resource Management for Ka-band GEO Satellite Networks from the Introduction of Propagation Information", COST280, doc. PM2015[R1], October 2001.

[1.16] Örs T., Sun Z., Evans B. G., "Analysis of an Adaptive Random/Reservation MAC Protocol for ATM over Satellite", IEEE, VTC '98, p. 1523-1527, 1998.

[1.17] A. Iera, A. Molinaro, S. Marano, "Traffic Management Techniques to face the Effects of Intrinsic Delays in Geostationary Satellite Networks", IEEE Transactions on Wireless Communications, vol. 1, no. 1, pp. 145-155, January 2002.

[1.18] C. H. Chang, H. K. Wu, Y. Tseng, "Quality of Service Support for Broadband Satellite Multimedia Service", IEEE Wireless Communications and Networking Conference, vol. 1, p. 187-91, U.S.A., 1999.

[1.19] M. Mobasseri, V. C. M. Leung, "Bandwidth Assignment for VBR Traffic in Broadband Satellite Networks", Canadian Conference on Electrical and Computer Engineering, Conference Proceedings, "Navigating to a New Era", vol. 2, p. 654-8 , U.S.A., 2000.

[1.20] A. Hung, M. J. Montpetit, G. Kesidis, "ATM via Satellite: a Framework and Implementation", Wireless Networks, vol. 4, no. 2, pp. 141-53, Netherlands, 1998.

[1.21] H. Peyravi, "Medium Access Control Protocols for Space and Satellite Communications: A Survey and Assessment", IEEE Communications Magazine, vol. 37, no. 3, pp. 62-71, 1999.

[1.22] K. H. Li, C. Chen, "An adaptive MAC protocol for satellite ATM", IEEE Proceedings, 15th International Conference on Information Networking, p. 119-126, 2001.

[1.23] P. D. Mitchell, D. Grace, T. C. Tozer, "Performance of the combined free/demand assignment multiple access protocol with combined request startegies via satellite", IEEE Personal, Indoor and Mobile Radio Communications Conference (PIMRC), vol. 2, pp. F-90-94, 2001.

[1.24] P. D. Mitchell, D. Grace, T. C. Tozer, "Comparative performance of the CFDAMA protocol with various terminal request strategies", IEEE Global Telecommunications Conference (GLOBECOM), vol. 4, pp. 2720-2724, 2001.

[1.25] P. D. Mitchell, T. C. Tozer, D. Grace, "Effective Medium Access Control for Satellite Broadband Data Traffic", IEE Seminar on Personal Broadband Satellite, vol. (Ref. No. 02/ 059), pp. 3/1-7, London, U.K., 2002.

[1.26] J. Neale, R. Green, J. Landovskis, "Impact of CF-DAMA on TCP via Satellite Performance", IEEE Global Telecommunications Conference, vol. 4, p. 2687-91, U.S.A., 2001.

[1.27] Y. Li, Z. Jiang, V. C. M. Leung, "Performance Evaluations of PRR-CFDAMA for TCP Traffic over Geosynchronous Satellite Links", IEEE Wireless Communications and Networking Conference Record, vol. 2, p. 844-8, U.S.A., 2002.

[1.28] T. Le-Ngoc, I. M. Jahangir, "Performance Analysis of CFDAMA-PB Protocol for Packet Satellite Communications", IEEE Transactions on Communications, vol. 46, no. 9, pp. 1206-1214, September 1998.

[1.29] T. Le-Ngoc, S. V. Krishnamurthy, "Performance of Combined Free/Demand Assignment Multiple Access Schemes in Satellite Communications", International Journal of Satellite Communications, vol. 14, no. 1, pp. 11-21, January-February 1996.

[1.30] T. Le-Ngoc, S. V. Krishnamurthy, "Performance of Combined Free/Demand Assignment Multi-Access (CFDAMA) Protocol with Pre-Assigned Request Slots in Integrated Voice/Data Satellite Communications", IEEE International Conference on Communications Proceedings, "Communications Gateway to Globalization", vol. 3, p. 1572-6, U.S.A., 1995.

[1.31] I. M. Jahangir, T. Le-Ngoc, "Performance Analysis of Combined Free/Demand Assignment Multiple Access (CFDAMA) Protocol for Packet Satellite Communications", IEEE International Conference on Communications, "Serving Humanity Through Communications", vol. 2, pp. 869-73, U.S.A., 1994.

[1.32] T. Le-Ngoc, I. M. Jahangir, Combined Free/Demand Assignment Multiple Access (CFDAMA) Protocols for Packet Satellite Communications", 2nd International Conference on Universal Personal Communications, "Personal Communications: Gateway to the 21st Century", vol. 2, pp. 824-8, U.S.A., 1993.

[1.33] E. A. Wibowo, A. Iuoras, P. Takats, J. Lambadaris, M. Devetsikiotis, "Guaranteeing QoS in Packet-Switched Satellites by Medium Access Control", 2nd Canadian Conf. Broadband Res., pp. 31-42, 22-24 June 1998.

[1.34] A. Iuoras, P. Takats, C. Black, R. DiGirolamo, E. Wobowo, J. Lambadaris, M. Devetsikiotis, "Quality of Service-Oriented Protocols for Resource Management in Packet-Switched Satellites", International Journal of Satellite Communications, vol. 17, no. 3, pp. 129-141, May-June 1999.

[1.35] K. D. Lee, Y. H. Cho, H. J. Lee, H. Jeong, "Optimal Scheduling for Timeslot Assignment in MF-TDMA Broadband Satellite Communications", IEEE-56th Vehicular Technology Conference Proceedings, vol. 3, p. 1560-1564, Piscataway, NJ, USA, 2002.

[1.36] J. M. Park, U. R. Savagaonkar, E. K. P. Chong, H. J. Siegel, S. D. Jones, "Efficient Resource Allocation for QoS Channels in MF-TDMA Satellite Systems", 21st Century Military Communications Proceedings, "Architectures and Technologies for Information Superiority", vol. 2, p. 645-9, U.S.A., 2000.

[1.37] A. Iera, A. Molinaro, S. Marano, M. Petrone, "QoS for Multimedia Applications in Satellite Systems", Satellite Systems, IEEE Multimedia, p. 46-53, October-December 1999.

[1.38] J. Neale, R. Green, J. Landovskis, "Interactive Channel for Multimedia Satellite Networks", IEEE Communications Magazine, vol. 41, pp. 192-198, March 2001.

[1.39] N. Celandroni, F. Potorti, "Fade Countermeasure using Signal Degradation Estimation for Demand-Assignment Satellite Systems", Journal of Communications and Networks, vol. 2, no. 3, September 2000 (ISSN 1229-2370), copyright Korean Institute of Communication Sciences.

[1.40] N. Celandroni, E. Ferro, N. James, F. Potorti, "FODA/IBEA-TDMA: A Flexible Fade Countermeasure System for Integrated Services in User Oriented Networks", International Journal of Satellite Communications, vol. 10, copyright 1992 by John Wiley & Sons, Ltd.

[1.41] N. Celandroni, F. Potorti, S. T. Rizzo, "An inexpensive Fade Countermeasure Technique for DA-TDMA Satellites Systems", Proceedings of the IEEE Global Telecommunications Conference GLOBECOM'96, vol. 2, pp. 1001-1005, London, U.K., November 18-22, 1996.

[1.42] N. Celandroni, E. Ferro, F. Potorti, "Experimental Results of a Demand-Assignment Thin Route TDMA System", International Journal of Satellite Communications, vol. 14, no. 2, copyright 1996 by John Wiley & Sons, Ltd.

[1.43] Celandroni N., Ferro E., Potorti F., Maral G., "Delay Analysis for InterLAN Traffic using two suitable TDMA Satellite Access Schemes", International Journal of Satellite Communications, vol. 15, no. 4, copyright 1997 by John Wiley & Sons, Ltd.

[1.44] Celandroni N., Ferro E., Potorti F., "Comparison between Distributed and Centralised Demand Assignment TDMA Satellite Access Schemes", International Journal of Satellite Communications, vol. 14, no. 2, copyright 1996 byJohn Wiley & Sons, Ltd.

[1.45] Carassa F., "Adaptive Methods to Counteract Rain Attenuation Effects in the 20/30 GHz Band", Space Communication and Broadcasting 2, North Holland, 1984, pp. 253-269.

CHAPTER 2

FADE MITIGATION TECHNIQUES FOR DVB-RCS LINKS

2.1 Introduction

The explosion of internet and the convergence of data, voice and video services is redefining the way we communicate. Broadband networks are being deployed at an accelerating rate to cope with the exponentially growing demand for bandwidth. Network operators employ hybrid fibre/satellite architectures to take advantage of both technologies and extend services to distant user communities that may be accessing the satellite networks through fixed and portable terminals. However, there are technical issues that need to be addressed for satellites to be able to provide seamless communications. Resource management is a major problem because of the latency and the limited capacity resource available in satellite communications [2.1].

Another major drawback associated with higher frequency microwave systems (mainly Ku/Ka-bands and above) is the large signal attenuation, caused by precipitation, that can be in the order of several tens of dBs. In particular, rain attenuation dominates the power margin needed for high reliability systems operating at 20/30 GHz. In lower frequency bands, such as the X-band and below, the normal design procedure has been to incorporate a significant fixed power margin into the system. Clearly this approach is not very acceptable in the higher frequency bands since for most of the time the attenuation is less than the built-in margin. A more efficient technique to achieve the desired availability would be to reduce the rain margin to some nominally low level and employ a Fade Countermeasure (FCM) [2.11]. Please note that this work especially targets power-limited systems incorporating small (return-channel) terminals.

This chapter provides an overview of ATM Broadband Satellite Networks and some of their remaining, outstanding challenges: resource management with fade mitigation. After identifying the various QoS classes with their characteristics and requirements, Section 2.2 proceeds to important issues and mechanisms of MF-TDMA resource management. By introducing Call Admission Control (CAC) and Bandwidth-on-Demand (BoD), the chapter

identifies the need for effective MAC algorithms coupled with successful CAC strategies. Section 2.3 addresses the compensation of fading on such systems and it reviews suitable solutions for the enhancement of current standards whilst discussing their implications on the resource allocation process. Section 2.4 then presents the possibility of an enhanced FMT to improve availability of power-limited systems. In section 2.5 the chapter ends with a brief summary outlining the main interest and focus of this thesis.

2.2 Broadband Satellite Networking

ATM (Asynchronous Transfer Mode) via Satellite has long been proposed for broadband satellite systems that can support existing and emerging multimedia services with world wide connectivity. Seeking technical solutions to a seamless integration of ATM and satellite protocols whilst delivering controlled Quality of Service (QoS) is a core target. However, the integration presents some major difficulties [2.30]:

- ATM has no error control on individual links performed for 48 bytes cell payload at physical and ATM layer, detection for misinserted cells and means to deal with cell delay variations are placed at higher layer. This enables ATM to keep up with high-speed transmission links. But, for a satellite system which suffers from fading and long propagation delay, this simplicity could bring high packet loss and serious QoS degradation.
- Problems arise due to radio transmission characteristics. New functions, such as multiple access, error control, resource management and congestion control, must be designed and incorporated seaminglessly into the ATM protocol.
- The gap in performance between ATM and ATM-satellite has to be closed. ATM takes advantage of statistical multiplexing to achieve high bandwidth utilisation and offers a wide range of quality levels from guaranteed, best effort, to non-guaranteed QoS [2.31]. This is difficult for an ATM-satellite protocol due to limited bandwidth and channel fading. Signalling and protocols of ATM-satellite must therefore be specially designed to compensate and possibly overcome these difficulties in order to maintain QoS within acceptable bounds.

These issues impose difficulties on the design of ATM-satellite signalling and protocol especially at air interface. For example, MAC protocols need to be developed in order to expand statistical multiplexing from fixed network to air interfaces. This would allow as many users as possible to access simultaneously the satellite channels whilst maintaining fairness, low delay and channel efficiency.

MAC protocols enable a terminal to gain access to the transmission medium in a shared channel system. MAC protocols must be in place for earth terminal to satellite uplink since it is a many-to-one channel. The MAC technique can have a dominant effect on the ability of the satellite network to deliver a QoS contract.

The Network Control Centre (NCC) performs the critical operations of both Call Admission Control (CAC) and Bandwidth on Demand (BoD) [2.34]. In an ATM network each connection is associated with a set of required QoS parameters. During the call establishment phase, one important network operation is the evaluation of the impact of the new connection on the already accepted connections. CAC decides if a new call should be accepted or not (a new call can be blocked if there are not enough resources) [2.33]. CAC is therefore a process that receives a connection request giving the traffic descriptor and QoS requirements of the connection and returns a response granting or denying the request. The objective of the CAC is to ensure that the network meets its QoS guarantees made to connections that are admitted to the network.

BoD is a set of MAC protocols and algorithms that allow a connection to request variable amounts of communication resources while the connection is already in progress. BoD is well suited to an environment where many bursty connections share a common medium access link. BoD can be invoked many times during the progress of some types of connections, while CAC is invoked only once at the connection set-up for every connection. These two critical network operations are described in more details in the following two sub-sections.

2.2.1 QoS in Multimedia Satellite Networks

Contemporary communication systems have to support multimedia services. The term multimedia is referred to as ([2.1]): "the representation, storage, retrieval and distribution of machine-processable information expressed in multiple media, such as text, voice, video, graphics, image, audio and video". The two main features of multimedia traffic, from the network point of view, are that it imposes strict real time performance requirements and generates large numbers of bit streams, often with high bit rates.

Types of multimedia service are:

- TV - well suited to satellite.
- Video on Demand - Ability to download minutes or hours of TV programmes.
- Electronic Programme Guide, EPG - now widely used by many digital TV users.

- E-commerce services (shopping, gaming, etc.).
- Internet proxied services (selected web, email).
- Internet access - offered by some current systems ([2.2]).
- Games - good take-up by some specific users ([2.3] and [2.4]).

Most modern broadband systems permit some level of interactivity. This is true of most current content (TV, Radio, etc.) but especially true of the new digital services, where users often wish to sort, manipulate or participate based on the received content. Although it is possible to conceive a one way internet service, one-way routed internet, most services require some form of return channel to allow two way packet flow [2.5].

A. Quality of Service Parameters

Six QoS parameters are identified by the ATM Forum ([2.6]). Three of these may be negotiated between the end-systems and the network. One or more values of the QoS parameters may be offered on a per connection basis, corresponding to the number of related performance objectives supported by the network. Support of different performance objectives can be done by routing the connection to meet different objectives, or by implementation-specific mechanisms within individual network elements.

The following QoS parameters are negotiated:

- Maximum Cell Transfer Delay (maxCTD): duration between a cell leaving the source and reaching the destination (end-to-end).
- Peak-to-peak Cell Delay Variation (peak-to-peak CDV): the variation in cell transfer delay (difference between the maximum and minimum cell transfer delay experienced during the connection).
- Cell Loss Ratio (CLR): The percentage of cells that are lost in the network, in relation to the total cells sent in a transmission (lost cells/total cells), due to error or congestion and are not received by the destination (e.g. cell loss at the ATM layer due to errors occurring in the cell header, or dropped cells when a queue is full).

The following QoS parameters are not negotiated:

- Cell Error Ratio (CER): The ratio of cells with payload errors in a transmission in relation to the total number of cells sent in a transmission (error cells/total number of cells)
- Severely Errored Cell Block Ratio (SECBR): severely errored blocks/total number of cell blocks (sequence of transmitted cells). A number of errors on a cell block creates a severely errored block.

- Cell Misinsertion Rate (CMR): The ratio of cells received at an endpoint that were not originally transmitted by the source end in relation to the total number of cells properly transmitted.

Further information on ATM layer QoS may be found in ITU-T Recommendation I.356 ([2.7]).

B. ATM Quality of Service Classes

The architecture for services provided at the ATM layer consists of the following five distinct service categories specified by the ATM Forum ([2.6]) so as to accommodate all the different applications:

- CBR Constant Bit Rate
- rt-VBR Real-Time Variable Bit Rate
- nrt-VBR Non-Real-Time Variable Bit Rate
- UBR Unspecified Bit Rate
- ABR Available Bit Rate

ITU-T Recommendation I.356 ([2.7]) in fact defines four Classes of Service:

- Class 1 (Stringent Class) is a delay sensitive class and it is intended to support Constant Bit Rate and real-time Variable Bit Rate services. Examples include telephony and videoconferencing.
- Class 2 (Tolerant Class) is a delay tolerant class and supports Available Bit Rate and non real-time Variable Bit Rate. Examples include video and data.
- Class 3 (Bi-Level Class) supports Variable Bit Rate and Available Bit Rate services. An example is high-speed data services.
- The last class, Class 4 (Unspecified Class), supports Unspecified Bit Rate services such as file transfers and email [2.1].

The following table identifies the associations of the above QoS Classes with service categories:

	Class 1 (Stringent Class)	Class 2 (Tolerant Class)	Class 3 (Bi-Level Class)	Class 4 (Unspecified Class)
CBR	✖			
rt-VBR	✖		✖	
nrt-VBR		✖	✖	
ABR		✖	✖	
UBR				✖

Table 2.1 Association of QoS classes with service categories

The following sections identify some example applications which are appropriate targets for each of the defined service categories [2.6]. ITU-T Recommendation I.211 ([2.8]) gives more examples and further details on some types of applications.

(i) Constant Bit Rate (CBR)

The CBR service category is used by connections that request a static amount of bandwidth that is continuously available during the connection lifetime. Example applications for CBR are:

- Interactive Video/Audio (e.g., videoconferencing/telephone)
- Video/Audio Distribution (e.g., television/radio)
- Video/Audio Retrieval (e.g., video on demand/audio library)
- Any data/text/image transfer application which contains smooth enough traffic or for which the end-system's response time requirements justify occupying a fully reserved CBR channel.

(ii) Real-Time Variable Bit Rate (rt-VBR)

The real-time VBR service category is intended for real-time applications, i.e. those requiring tightly constrained delay and delay variation, as would be appropriate for voice and video applications. Example applications for real-time VBR are:

- A real-time application (including those listed above for CBR) for which the end-system can benefit from statistical multiplexing by sending at a variable rate, and can tolerate or recover from a small but non-zero cell loss ratio.
- A real-time application (including those listed above for CBR) for which variable rate transmission allows more efficient use of network resources.

(iii) Non-Real-Time Variable Bit Rate (nrt-VBR)

The non-real-time VBR service category is intended for non-real-time applications which have bursty traffic characteristics. No delay bounds are associated with this service category. Example applications for non-real-time VBR are:

- Response time critical transaction processing (e.g. airline reservations, banking transactions, process monitoring)
- Frame Relay interworking

(iv) Unspecified Bit Rate (UBR)

The UBR service category is intended for non-real-time applications, i.e. those not requiring tightly constrained delay and delay variation. Examples of such applications are traditional computer communications applications, such as file transfer and email. UBR service does not specify traffic related service guarantees. Example applications for UBR are:

- Interactive Text/Data/Image Transfer (e.g. banking transaction, credit card verification)
- Text/Data/Image Messaging (email, telex, fax)
- Text/Data/Image Distribution (news feed, weather satellite pictures)
- Text/Data/Image Retrieval (file transfer, library browsing)
- Aggregate LAN (LAN interconnection or emulation)
- Remote Terminal (telecommuting, telnet)

(v) Available Bit Rate (ABR)

ABR is an ATM layer service category for which the limiting ATM layer transfer characteristics provided by the network may change subsequent to connection establishment. The ABR service does not require bounding the delay or the delay variation experienced by a given connection. It is not intended to support real-time applications. On the establishment of an ABR connection, the end-system shall specify to the network both a maximum required bandwidth and a minimum usable bandwidth. Example types of applications for ABR are:

- Any UBR application listed above that can take advantage of the ABR flow-control protocol in order to achieve a low cell loss ratio.
- Critical data transfer (e.g. defence information).
- Super computer applications.

- Data communications applications requiring better delay behaviour, such as remote procedure call, distributed file service (e.g. Network File System), or computer process swap/paging.

2.2.2 Management of MF-TDMA Resources

For the return link in DVB-RCS systems, achieving high capacity with limited radio resources is an important focus of investigation. The European Telecommunications Standards Institute's (ETSI) DVB-RCS standard [1.1] and [1.2] describes a return link using a Multi-Frequency Time Division Multiple Access (MF-TDMA) scheme.

Conventional TDMA uses only one frequency; all earth stations transmit on a single frequency, whatever the destination of the bursts, and therefore the satellite link speed is limited. MF-TDMA was proposed to solve this inefficiency. It reduces satellite antenna sizes and transmission power, and increases satellite network bandwidth [2.1]. Each station may transmit on any one frequency at a given time. If the ATM cell payload capacity on each frequency is B Mb/s and the number of frequencies is N_c, the overall payload capacity, C_{tot}, is

$$C_{tot} = N_c \times B \text{ Mb/s} \tag{2.1}$$

Figure 2.1 shows the MF-TDMA frame format [2.42], [2.38], [2.45], and [2.46]. Each frame, of 26.5 msec duration, consists typically of a number of Common Signalling Channel (CSC) slots, for initial log-on requests (using Slotted-Aloha, [2.9] and [2.10]) and Acquisition slots (for coarse synchronisation acquisition), a number of Synchronisation slots and a number of Data slots. The slot duration is considered to be fixed, as Figure 2.1 indicates. Each slot contains one ATM cell of N_b=424 bits. For a frame duration T_F=26.5 ms, and assuming N_{TS}=128 traffic slots per carrier, it is possible to generate bit rates that are multiples of 16 kbits/sec from 0 upto 2048 kbits/sec.

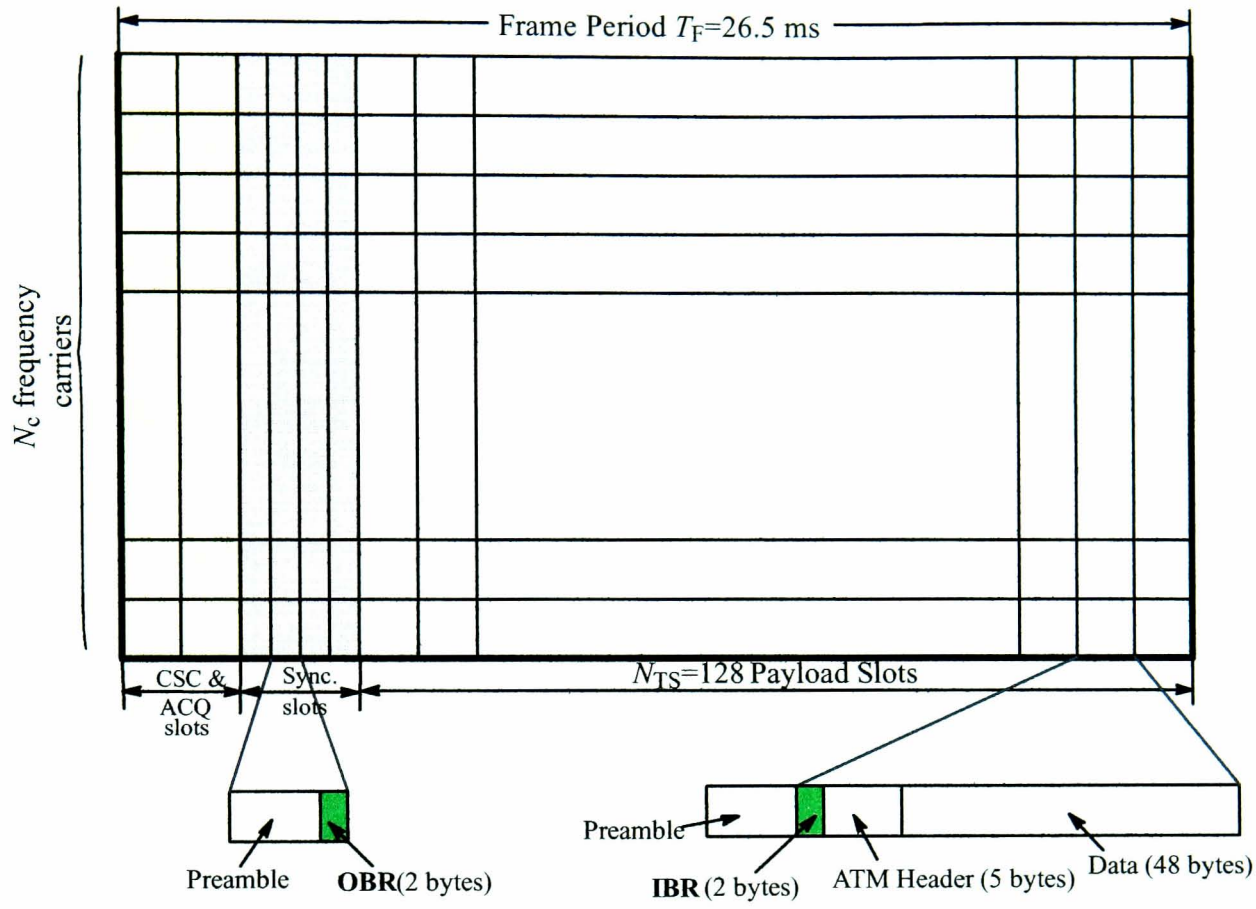

Figure 2.1 The MF-TDMA frame format

Each carrier supports a number of SYNC slots, composed of SYNC probes for synchronisation maintenance and Out-of-Band Request (OBR) minislots, used for initial capacity request (mini-slot method for requesting capacity, contention-based or periodic assignment to logged-on terminals of bursts smaller than traffic timeslots).

Data is transmitted in payload slots in ATM-like cell format, which includes an additional 2-byte header to support In-Band Requests (IBR) for uplink capacity (prefix method for requesting capacity, based on the optional prefix attached to ATM traffic bursts). Each payload slot can be used by any type of connection, be it real-time or non-real-time. A terminal is not allowed to transmit data on more than one carrier at a time, in order to minimise power output requirement and reduce hardware complexity in terminals.

The terminals access a pattern of time/frequency slots within the MF-TDMA frames. Having established knowledge of the MF-TDMA structure, the Return Channel Satellite Terminal (RCST) accesses the network (using a slotted-Aloha burst). Thereafter, traffic capacity is allocated dynamically, allowing the terminal to operate in a contentionless mode. A terminal can only transmit once it has forward channel reception. Moreover, the RCST must have been synchronised, logged in, and allocated capacity (Figure 2.2).

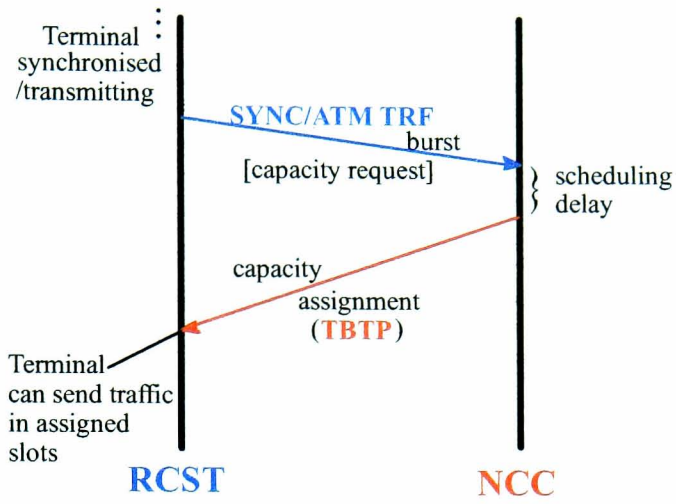

Figure 2.2 Capacity request signalling

The Network Control Centre (NCC) will allocate to each active terminal, through the Terminal Burst Time Plan (TBTP), a series of bursts, each defined by a frequency, a bandwidth, a start time and a duration. The basic principle of the MF-TDMA scheme is illustrated in Figure 2.3, where the darker slots show a possible pattern of slots allocated to one particular RCST.

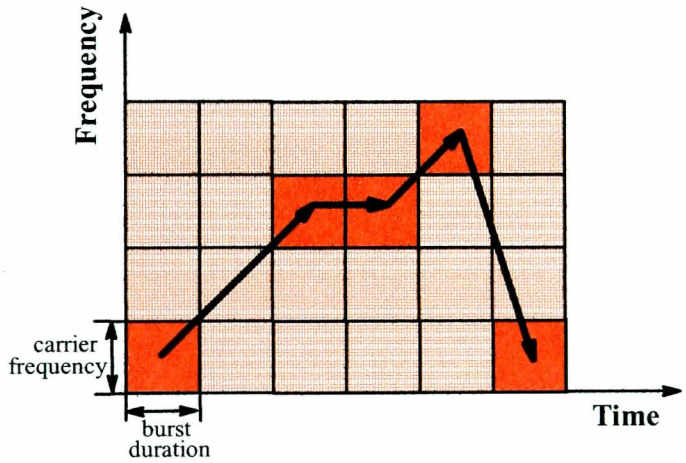

Figure 2.3 The basic principle of MF-TDMA

The MF-TDMA scheme allows the modification of transmission parameters (for example carrier frequency) on a timeslot by timeslot basis. In addition, other transmission parameters, such as coding rate and bit rate may be varied as well. The advantage is a more flexible adaptation to widely varying transmission parameters, typical of multimedia. This is at the expense of slightly more complex terminals.

A. Request Handling Mechanisms

There are four request handling mechanisms (request strategies) allowing four types of capacity assignment: Reserved Capacity (RC), Rate-Based Dynamic Capacity (RBDC),

Volume-Based Dynamic Capacity (VBDC) and Free Capacity Assignment (FCA). The prioritisation of these different categories is as per the order below, with RC having highest priority and FCA lowest priority. It should be noted that in the current discussion the terms connection and terminal are used interchangeably for simplifying reasons, however they are not identical, as a terminal may establish more than one connection. In such case it will request capacity for all of its connections [1.1], [1.2], [2.45], [2.46], and [2.47].

(i) Reserved Capacity (RC) or Continuous Rate Assignment (CRA)

This strategy is aimed toward real-time connections (such as CBR and real-time-VBR), which cannot tolerate or have strict constraints on delay and delay variation. This is especially suitable for applications with smooth traffic characteristics. Queuing is not permitted for these services, therefore for granting RC requests the network controller must allocate the required downlink capacity.

In RC assignment, a terminal states its need for uplink (and downlink) capacity at connection setup time, in terms of a fixed number of payload slots per frame. If the connection is admitted, the terminal will have its requested number of timeslots per frame assigned to it for the duration of the connection. Consequently, the Connection Admission controller (CAC) must ensure that the total reserved capacity does not exceed the total system capacity.

(ii) Rate Based Dynamic Capacity (RBDC)

In RBDC assignment strategy, a terminal may request a variable number of time slots in each frame. The request can be explicit, in the form of the number of time slots per frame. The request can also be implicit, in the sense that what is requested can remain effective for a number of frames.

The terminal will need to update its request periodically. The scheduler guarantees that an RBDC request will be granted up to the maximum value negotiated at connection set-up. This is equivalent to reserving a portion of network capacity, although the terminal may not require all of its reserved capacity in each MF-TDMA frame.

In contrast to RC strategy, RBDC strategy permits statistical multiplexing among terminals, resulting in a more efficient use of network resources. The network controller must still ensure that the total RC or maximum RBDC of all terminals does not exceed the total available capacity.

(iii) Volume Based Dynamic Capacity (VBDC)

In VBDC assignment, a terminal signals its request as a total number of payload slots required to empty its queue. The network, however, does not provide a guarantee on capacity

availability. The scheduler will only try its best to satisfy the request of this type. The request remains effective as long as not all of the requested time slots are granted or as long as the request has not timed out. This strategy is directed toward jitter-tolerant connections and it is especially suited for bursty traffic. It allows for a great deal of statistical multiplexing and thus VBDC may contribute to a very efficient use of network resources.

(iv) Free Capacity Assignment (FCA)

Finally, in FCA strategy the scheduler attempts to maximise capacity utilisation by distributing unrequested uplink capacity to all registered terminals. This strategy has the lowest priority level, i.e. the scheduler will satisfy all RC, RBDC, and VBDC requests before it performs free capacity assignment. Unlike the previous request strategies, ground terminals have no control in obtaining capacity.

FCA assigns capacity to RCSTs from capacity which would otherwise be unused. Such capacity assignment is automatic, it does not involve any signalling from the RCST to the NCC and is intended as bonus capacity which can be used to reduce delays on any traffic which can tolerate delay jitter.

Even though the four scheduling strategies aim at traffic with different characteristics, users do have flexibility in combining these strategies to match their QoS requirements. Table 2.2 below shows a possible mapping of ATM service categories into the request/assignment strategies [2.45] and [2.46].

Traffic Class	Scheduler Handling Mechanisms
CBR	RC
rt-VBR	RC
nrt-VBR	RC or RC + DC
ABR	RC + DC (+FCA)
UBR	VBDC + FCA

Table 2.2 Association of QoS classes with service categories

2.2.3 Call Admission Control

As defined by ATM forum [2.60] Call Admission Control (CAC) is the set of actions taken by the network for establishing virtual connections by determining whether a

connection can be accepted or not. A new connection will be accepted if the network has enough resources to provide the QoS requirements of that connection request without affecting the QoS of the connections already established in the network [2.61] and [2.62].

Pricing policy is an important issue in any CAC strategy. It should be based on both resource allocation as well as actual resource usage in order to maintain consistency between the two and satisfy both users and network providers.

A successful CAC strategy should achieve a good balance between the users' desire for QoS guarantees and the network provider's desire for maximum revenue. Furthermore, a CAC algorithm should be relatively easy to implement, be suitable to a wide range of traffic types, and be able to deal with time-varying traffic.

As part of a comprehensive traffic management solution, CAC needs the following two aspects:

- A traffic description method accepted by both user and network (i.e. the use of appropriate traffic descriptors such as the Peak Cell Rate (PCR)).
- An efficient underlying resource management scheme that should allocate resources to each connection to guarantee its QoS, yet allow dynamic resource sharing [2.61].

CAC will base its decision on the new connection's QoS requirements and the current condition of the network. To see whether sufficient resources are available it needs information regarding the current allocations (TBTP table), see Figure 2.4.

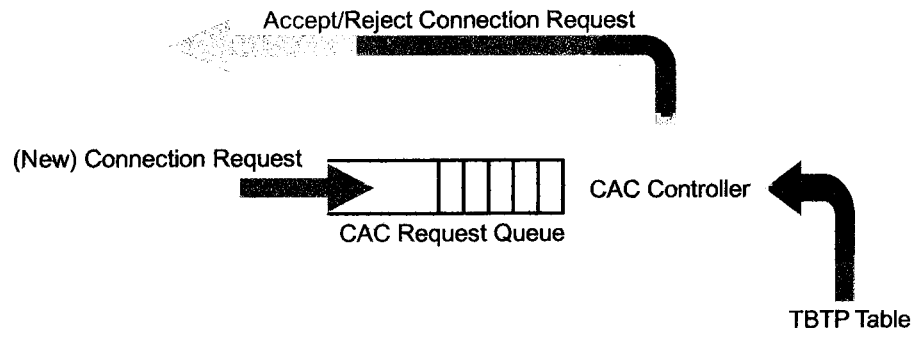

Figure 2.4 CAC Controller Model

Several CAC algorithms for ATM networks have been proposed in literature. The most widely used approaches are based either on the definition of an equivalent bandwidth for each connection or on the actual measurement of the bandwidth used by active connections.

The first approach relies on the estimation of the equivalent capacity. These CAC schemes are compared in [2.66] and [2.67]. However, due to the complexity and inaccuracy in the computation of the equivalent capacity, this approach is rarely adopted [2.68].

Other schemes, based on dynamic bandwidth allocation, exploit reactive congestion control schemes; they are effective when the roundtrip delay is not excessively long [2.67]. Therefore they cannot be effectively adopted in satellite environments.

Other interesting CAC schemes are based on the concept of fast bandwidth or buffer reservation. Some of them allow for the incremental allocation of bandwidth, but they are not suited for satellite environments due to the heavy signalling exchange they require. An interesting type of CAC is the fast buffer reservation technique [2.69]. This has the interesting property of maintaining burst integrity as a main objective, which is particularly interesting for loss-sensitive traffic. It avoids the complexity of CAC schemes based on the equivalent bandwidth computation and takes the acceptance decision considering only the source burstiness and peak bit rate [2.68].

Some methods ([2.70] and [2.71]) combine the CAC with the BoD process in order to offer QoS guarantees to services while maintaining a good level of system efficiency.

The study in [2.72] presents some encouraging results from implementing a CAC policy for DVB-RCS systems, applied to the different traffic classes and performed both at the satellite terminal and the NCC.

2.2.4 Bandwidth on Demand

MF-TDMA is an extension of TDMA considered to be the main candidate for future ATM satellite networks. The reason is that it allows the possibility of on-demand allocation of bandwidth [2.38] and therefore it takes advantage of the flexibility and statistical multiplexing capabilities of ATM.

Most new generation Ka-band satellite systems are intended to provide low-cost telecommunication services to hundreds or thousands of users. BoD can be employed in order to maximise the system capacity and support the maximum amount of users possible. On the billing side, BoD enables users to pay only for the bandwidth they utilise [2.63].

In ATM, cells containing different forms of data are time multiplexed over the same bandwidth. Each timeslot may contain cells from voice, video or data traffic types. For example, a multiplexed multimedia application may have five out of eight cells for video, two for sound and one for data [2.64] and [2.65]. This process involves dynamically assigning timeslots only to connections that need them.

In response to the set of all BoD requests, the BoD controller computes the number of timeslots for each connection. It then generates the Terminal Burst Time Plan (TBTP) table to be transmitted back to the user terminals. In creating this table, the BoD controller may also conceptually use requests provided by the CAC sublayer. This is depicted in Figure 2.5.

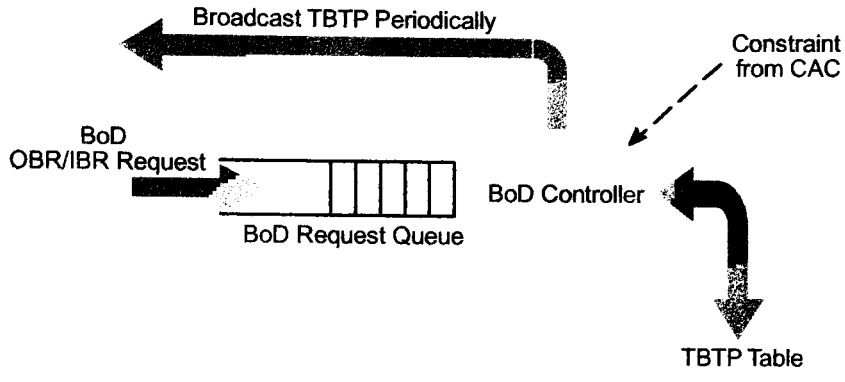

Figure 2.5 BoD Controller Model

A MAC protocol should meet two constraints: QoS provision and fairness. QoS provision means that the MAC protocol, with the aid of a well-designed admission control algorithm, will deliver the QoS contract agreed at the call setup time. Fairness refers to the fact that the protocol has to ensure a fair allocation of the shared link bandwidth even in the case of congestion. The design goal is to achieve efficiency, i.e. the protocol will maximise network resource usage [2.32].

Several researchers have studied the problem of QoS provision for multimedia traffic over ATM networks [2.35]. They propose a number of methods for assigning the bandwidth resource in the satellite network to connections of different classes. Several approaches to the problem of resource management have been proposed in order to achieve enhanced resource utilisation and better QoS provision; some proposed assignment schemes can achieve QoS delivery for the higher-class connections ([2.36], [2.37], [2.38], [2.39], and [2.40]). Others suggest scheduling strategies that can achieve a drastic reduction of the end-to-end delay experienced by lower-class connections as these receive low priority in the assignment process of the scarce satellite bandwidth resource [2.41].

Other studies have developed novel MAC protocols for MF-TDMA satellite channels [2.42] and [2.43]; Mobasseri and Leung [2.44] evaluate MAC Protocols providing Quality of Service in an ATM-based broadband satellite network. In particular, the performance of MAC schemes, Fixed Assignment, DAMA, CF-DAMA and combined Fixed/CF-DAMA, is simulated; Hung et al. [2.38] propose a simple MAC layer in which ATM service classes are mapped onto MF-TDMA uplink access methods. They show how different QoS's can be provided by using a combination of different access schemes and they address the problem of scheduling. Iuoras et al. [2.45] and [2.46] focus on bandwidth allocation and congestion avoidance in a broadband satellite with on-board switching. The CF-DAMA protocol, as the MF-TDMA primary access scheme, is combined with a congestion avoidance scheme to

achieve flexible handling of all traffic/service classes, as defined by the ATM Forum [2.48]. Their approach can guarantee a specified QoS (delay, delay variation, cell loss ratio).

Lee et al. [2.36] develop a dynamic resource allocation algorithm for MF-TDMA DVB-RCS. The algorithm gives an optimal assignment plan within a very short period of time so that the system throughput can be maximised; Neale et al. [2.49] present results of simulating Internet page transfer times using CF-DAMA. In [2.50] Pech et al. provide a methodology to optimise resource management techniques in Ka-band GEO satellite networks by use of channel propagation information incorporating FMT behaviour into ATM network considerations.

Of all the studies mentioned, none, apart from the last one, takes into account fading conditions. Even though the dynamic resource allocation in MF-TDMA systems is of great interest to this thesis, most of the above studies do not consider, to the knowledge of the author, the implementation of satellite Fade Mitigation Techniques, although they are necessary. Pech et al. [2.50] have been the only ones to introduce FMTs in resource management protocols and work on the modelling of rain affected DVB-RCS communications. Their work however only focuses on a single-link analysis. It seems therefore very desirable to extend the analysis to the management of MF-TDMA networks consisting of *multiple* links affected simultaneously by rain attenuation. The focus would be placed on the implications of rain compensation at network level on resource sharing and management. A relevant work along these lines is that of Celandroni et al. in [2.51]. They presented a complete fade countermeasure with demand assignment of capacity, but their study was only applied on TDMA.

Association of up-link power control with bit and coding rate variation gives the system the ability to cope with fade conditions [2.52], [2.53], [2.54], [2.55], and [2.56]. These studies are of great significance and an adaptation of such modelling to the case of DVB-RCS/MF-TDMA systems is of major interest to the work on this thesis.

2.2.5 CAC/MAC Design Issues

At this point some important issues involved in the design of the CAC and MAC algorithms become apparent.

Once a connection is admitted by CAC, the commitment is made to provide adequate resources. A connection request is granted only when sufficient resources such as bandwidth and buffer space are available along the path of a connection. The decision is made based on the service category, the QoS desired and the state of the network, i.e. the number and

conditions of existing connections. The total number of connections supported by the network will depend on the individual bit rates supported.

Important issues are those of queue management and traffic regulation. In the case when a traffic request is not granted, the traffic of that source can be queued. However, the queue depth has to be controlled/managed. Buffers are valuable system resources and give an extra level of freedom to the system. But they are finite and must be properly managed so as to ensure QoS. The Round-Robin (RR), the Weighted Round-Robin (WRR), and Priority Queuing (PQ) are some standard, well-known allocation mechanisms [2.58]. When queues are full, traffic congestion can cause packet discard, so further mechanisms to prevent or ease queue congestion can be employed.

Traffic shaping mechanisms can eliminate for the most part traffic jitter caused by queuing. They alter the traffic characteristics of a stream of cells on a connection to achieve better network efficiency whilst meeting the QoS objectives. The use of bandwidth can be maximised by specifying, for example peak and average traffic rates. Examples of traffic shaping are peak cell rate reduction, burst length limiting, reduction of CDV by suitably spacing cells in time, and queue service schemes.

Shaping the traffic can be seen as 'smoothing' out traffic using queues to hold up packets just delaying them until there is a trough. The most famous algorithm for traffic shaping is the leaky bucket algorithm [2.57], [2.58], and [2.59].

The possibility to vary the bandwidth and duration of successive slots allocated to an RCST is an important terminal flexibility that will add complexity to the problem of "packing" all connections in the MF-TDMA space and could therefore have an impact on the achieved channel capacity utilisation.

2.3 Fade Mitigation Techniques in DVB-RCS Systems

Satellite systems need to take into account of many parameters for adapting the offered service and in order to remain competitive with terrestrial networks. Existing classical satellite technology is being replaced by new, improved technology, in order to cope with higher system capacity and Quality of Service requirements for broadband multimedia communications.

Such solutions have to be mainly based on recognised network protocols and standards in order to reduce terminal and service cost. For two-way satcom services the use of the DVB Return Channel via Satellite (DVB-RCS) protocol [1.1] and [1.2] is a commonly accepted choice.

Improved solutions include use of higher frequency bands, such as the Ka-band (27-40 GHz) or the V-band (40-75 GHz) [1.10], and multi-beam coverage in order to increase the throughput and system capacity. A major drawback is that rain attenuation increases rapidly with carrier frequency [2.12]-[2.14] and can cause significant signal quality degradation on individual earth-space communication links. This situation will have a major impact on the link availability and thus the achievable throughput of a network. Hence the implementation of Fade Countermeasures becomes necessary and is of great importance to system designers.

Keeping a classical approach based on a worst case sizing will result in a fixed over-dimensioning of the system, reducing efficiency and resulting in unreasonable costs. It is therefore necessary that satellite systems include Fade Mitigation Techniques (FMTs) to counteract propagation impairments and use system resources efficiently. The principle of these techniques is to adapt the physical layer to the link propagation attenuation.

The current DVB-RCS and DVB-S standards have not primarily been defined considering the details of rain FMTs; they may therefore have to be adapted to support FMTs, either at physical and/or at MAC layer level [2.15]. Hence the integration of efficient FMTs within the DVB standards has been studied more precisely in the remaining of this thesis.

Some FMTs, such as Power Control (PC), are already adopted by current systems, and others, such as ACM, are being introduced in the new generation of standards (DVB-S2) or are still a subject for enhancement of current standards (DVB-RCS) [2.16]. In fact, adaptive transmission techniques appear to be the preferred solutions. They are mostly introduced as a way of achieving efficient BoD. But ACM is also a good framework for deploying FMTs. The reasons will become obvious in the following sections.

2.3.1 Availability of Satellite Links Attenuated by Rain

The satellite channel conveys information by means of modulated radio frequency carriers, which are relayed by the satellite transponder and then received by the destination station. Noise contaminates the received carriers. Therefore, the retrieved baseband signals are also contaminated: analogue signals are noisy, and recovered data may contain erroneous bits.

As a consequence, it is not feasible to provide error-free transmission at the physical level. The only hope is to limit the Bit Error Rate (BER) to an acceptable level constrained by cost considerations. It is the job of the upper layers, and especially the data link layer, to ensure error-free transmission by means of automatic repeat request protocols. The task is made easier when the physical layer already provides "clean" information, with a low enough BER; as the BER decreases, the performance improves.

Radio frequency link power budget analysis provides the means to calculate the quality of the information contents delivered to the data link control layer ([2.17]). The quality of digital information is measured by the BER, which is the ratio of the number of bits received in error to the total number of received bits. The BER depends on the type of modulation and coding performed, and on the carrier to noise power spectral density ratio, C/N_0, at the input of the receiver. C/N_0 can be considered as a quality measure of the radio frequency link. The objective of calculating the link budget is to find the most cost effective solution, for example by choosing the smallest physical size of earth station to achieve the desired performance at minimum costs.

Satellite link availability is the percentage of a year for which the link performs as per the required BER. The availability depends on the clear-sky link power budget as well as the dynamic range of the FMT employed. The clear-sky link margin plus the dynamic range of the FMT equals the overall amount of attenuation that can be tolerated over the satellite link. Whenever conditions exceed this range, the signal is assumed "lost" and the link becomes "unavailable". Typical satellite links are designed for a BER performance of 10^{-8} at an availability of 99.9%.

However the cost of an FMT must also be taken into account. Possible effects on the source bit rate, the link delay, the overall number of connections supported by the network or the packing of the connections and the capacity utilisation should be considered. It becomes apparent that, even though an FMT in general improves availability, competition for common scarce resources means that the actual availability is also dictated by the performance of the CAC and MAC schemes. So the final performance of an adaptive MF-TDMA system with FMT must be studied carefully, as shown in this thesis.

2.3.2 Adaptive Transmission Techniques as FMTs

Adaptive transmission techniques consist in modifying the signals transmitted by the nodes of a satellite network (earth stations, satellite) whenever the link quality is degraded. The different types of signal processing are available to more than one earth station on demand. Therefore, adaptive transmission techniques are considered to be resource-shared FMTs [2.18].

A. Adaptive Coding and Modulation (ACM)

Adaptive Coding and Modulation tries to maintain the bit-error ratio (BER) or packet error ratio (PER) below an agreed level while permitting a reduction of the required energy

per information bit when fading conditions get worse. This is achieved through a variable coding rate and/or by reducing the spectral efficiency when the carrier-to-noise power ratio at the input of the demodulator decreases below set thresholds due to propagation effects. Higher code rates and larger constellations can be used under less faded conditions.

Parallel concatenated convolutional coding with interleaving (turbo coding) [2.19] has attracted the interest of the satellite communications industry, leading to the standardisation of such codes for second-generation DVB-RCS terminals [1.1], [1.2], [2.15], and [2.20]. This choice extends the dynamic range of the FMT resulting in an increased throughput during unfaded conditions. Lower coding rates and/or reduced constellations are selected when the carrier-to-noise power spectral density ratio decreases due to propagation effects.

For M-PSK with code rate ρ, the user information bit rate R_b in [bps] is proportional to $B\rho \log_2 M$, where B is the bandwidth in [Hz] and ρ is the code rate. If the M-arity M can be increased from 2 to 4, 8 or 16, then the throughput R_b can be increased by a factor of 1, 2, 3, or 4 respectively. Similarly, the information bit rate can be adjusted by varying the code rate ρ. But higher-level constellations and reduced coding require higher energy-per-bit-to-noise power spectral density ratios (at the input of the receiver), so this is only feasible whenever atmospheric conditions are good enough [2.21], typically close to clear-sky conditions (provided the link power budget is large enough). Therefore, ACM is particularly useful for increasing the (clear-sky*) throughput of a connection. ACM may provide a dynamic range between 0 and 17 dB depending on the link budget [2.22]. So ACM should be able to achieve high availabilities for connections with a sufficient link power budget.

There are however situations when the negotiated information bit rate should not be changed (i.e. situations when the user data rate is constant and when the services cannot tolerate reduction of the information rate, for example voice transmission). In general, in a Bandwidth on Demand (BoD) scenario, the instantaneous information bit rate requested by the source should always be granted, provided it lies within the bounds agreed by CAC at connection set-up. Therefore ACM as an FMT results in larger bandwidth for FDMA or longer burst durations in a TDMA frame. ACM therefore translates into a reduction of the total satellite throughput when multiple links experience fading simultaneously [2.23], competing for limited transponder resources. Hence for Multi-Frequency TDMA (MF-TDMA), ACM offers a trade-off between time/bandwidth and power.

* nb: tropospheric scintillation was not considered as it was out of the scope of this thesis

(i) ACM Operation at constant Information Data Rate (ACM1)

Depending on the attenuation level, the appropriate ACM mode (i.e. the level of modulation and coding) can be chosen from the range of available ACM schemes (see Table 2.3). This is achieved using the look-up graph shown in Figure 2.6. It should be noted that the enhanced DVB-RCS standard incorporating ACM is thereon referred to as DVB-RCS2. It is assumed here that the system has a large enough link power budget to support 16APSK code rate 9/10 in clear-sky conditions. When the CNR degrades, a more robust ACM scheme is selected to keep the PER below 10^{-7}, with the bit rate kept constant at $R_b^i = \hat{R}_b^i = 2.048$ Mbps.

The dynamic range of the ACM FMT is therefore of the order of 17 dB. It is important to note that a change in ACM mode must also be accompanied by a change in bandwidth whose relative values are given in Table 2.3.

mode m	Modulation	ρ	bandwidth	Rain protection [dB]
0	16APSK	9/10	B_0	1.3
1		5/6	1.08 B_0	2.7
2		3/4	1.2 B_0	4.2
3		2/3	1.35 B_0	5.7
4	8PSK	4/5	1.5 B_0	6.2
5		3/4	1.6 B_0	7
6		2/3	1.8 B_0	8.5
7	QPSK	6/7	2.1 B_0	9.6
8		4/5	2.25 B_0	10.5
9		3/4	2.4 B_0	11.3
10		2/3	2.7 B_0	12.4
11		3/5	3 B_0	13.2
12		1/2	3.6 B_0	14.4
13		2/5	4.5 B_0	15.9
14		1/3	5.4 B_0	17
15	BPSK	1/2	7.2 B_0	17.6

Table 2.3 DVB-RCS2 carrier bandwidth variation depending on selected ACM mode assuming transmission over the full frame duration T_F

Note that in the original DVB-RCS [1.1] system, the BoD is restricted to QPSK (modes 7 to 14, see Table 2.3). For power limited systems, the original DVB-RCS system [1.1] could be used. In this case, the required link power budget would be reduced by 9 dB but the FMT dynamic range would fall to 8 dB (Figure 2.6).

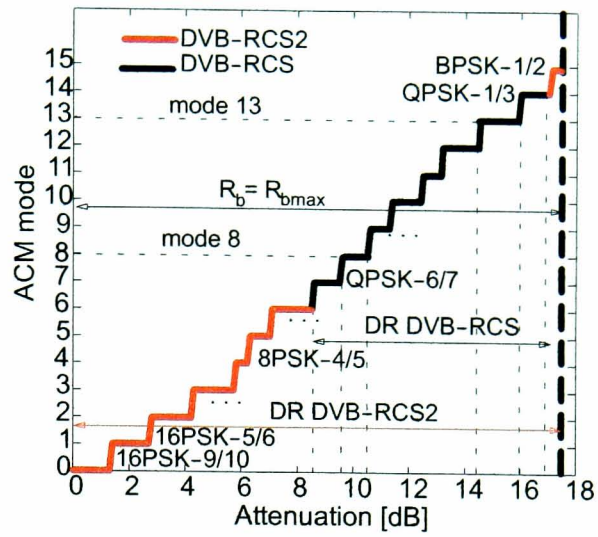

Figure 2.6 DVB-RCS2 ACM mode selection vs. SNR (E_s/N_o) degradation w.r.t. clear-sky

The maximum bit rate $\hat{R}_b^i$ available to a connection i assuming transmission over the full frame duration (T_F) is given by:

$$\hat{R}_b^i = \frac{B_i \cdot \rho(Att_i) \cdot \log_2 M(Att_i)}{(1 + \alpha)}, \quad \text{[bps]} \tag{2.2}$$

where $\alpha \simeq 0.35$ is the roll-off factor and B_i is the allocated bandwidth for connection i. Note that in Table 2.3 B_0 is the bandwidth that corresponds to mode 0 with $(\rho, M) = (9/10, 4)$.

When only using a portion of the frame lasting T_i seconds ($T_i \leq T_F$), the average bit rate $\bar{R}_b^i$ over the duration of a frame, T_F, becomes:

$$\bar{R}_b^i = \frac{B_i(Att_i)\,\rho(Att_i)\,\log_2 M(Att_i)}{T_F(1 + a)} \times T_i = k(Att_i) \times T_i, \tag{2.3}$$

$$\text{where } k(Att_i) = \frac{B_i \rho \log_2 M}{T_F(1 + a)}, \tag{2.4}$$

Equation (2.3) emphasises that the bandwidth, the code rate and the M-arity are chosen based on the attenuation (see Figure 2.6).

From the above discussion it is concluded that if the burst duration is kept constant, then the carrier bandwidth must be adjusted in order to counterbalance the change in ACM mode due to varying channel conditions.

In the context of an MF-TDMA system, such a change in ACM mode implies "switching" the transmission to a different carrier of appropriate width. This requires an appropriate segmentation of the total system bandwidth into channels with width matching the FMT needs of all connections. Thus there is a need for an adaptive resource allocation algorithm.

In DVB-RCS systems several carriers of different bandwidth are possible and depending on channel and traffic needs users can be moved from one carrier to another. This may not be optimal if the bandwidth segmentation of the MF-TDMA space is fixed and the different available carriers are not efficiently used. To avoid this, the bandwidth should be adaptively segmented, over a fixed short allocation interval, according to channel conditions and traffic needs. This is allowed by the DVB-RCS standard but, to the knowledge of the candidate, this has not been studied in great details.

Let us describe what the controller managing the BoD requests should be capable of doing in such a scenario. The BoD controller receives all the user traffic requests, $\vec{R}_b^i$, and then selects the appropriate ACM mode for each user and corresponding bandwidth B_i (Table 2.3). The controller then calculates the allocated burst duration T_i for each connection i for the following frame interval. By grouping connections using the same ACM mode (and bandwidth), it should then appropriately segment the total system bandwidth into the required number of carriers and perform an efficient resource assignment.

(ii) ACM Operation at constant Bandwidth (ACM2)

Looking at Equation (2.2) it is apparent that when the bandwidth is kept constant, the bit rate of the connection has to be reduced in rainy conditions. This FMT changes the useful data rate by choosing modulation and coding rate, but it operates at constant symbol rate. Table 2.4 shows the relative rate variation corresponding to each ACM mode, for a constant bandwidth.

mode m	Modulation	ρ	$\hat{R}_b^i$	Rain protection [dB]
0	16APSK	9/10	R_0	1.3
1		5/6	0.93 R_0	2.7
2		3/4	0.83 R_0	4.2
3		2/3	0.74 R_0	5.7
4	8PSK	4/5	0.67 R_0	6.2
5		3/4	0.62 R_0	7
6		2/3	0.56 R_0	8.5
7	QPSK	6/7	0.48 R_0	9.6
8		4/5	0.44 R_0	10.5
9		3/4	0.42 R_0	11.3
10		2/3	0.37 R_0	12.4
11		3/5	0.33 R_0	13.2
12		1/2	0.28 R_0	14.4
13		2/5	0.22 R_0	15.9
14		1/3	0.18 R_0	17
15	BPSK	1/2	0.14 R_0	17.6

Table 2.4 DVB-RCS2 supported rate variation depending on selected ACM mode

The table demonstrates the fact that, for a specified bandwidth, choosing modulation schemes with higher spectral efficiency can result in higher system capacity. ACM offers the possibility of achieving high peak rates, if required, whenever weather conditions and the link power budget allow it. For example, with a modulator operating at its maximum supported symbol rate of 4.096 MBaud [2.29], a user can achieve a maximum bit rate $\hat{R}_b^i = 14.75\,\text{Mbps}$ ($\rho = 9/10$, $M = 16$), if allowed to transmit exclusively over a 5.5 MHz carrier bandwidth. Such increase in throughput can be used to boost the overall throughput or possibly to reduce the transmission queues.

Assuming this technique has no adaptive TDMA burst allocation effect on the resource allocation process, i.e. the packing of all the connection bursts within the MF-TDMA space. This FMT comes only at the price of reducing the source bit rate when requiring change to a more robust ACM scheme and therefore, one would argue that this constraint goes against the BoD philosophy. That is sources should be offered the throughput they require when they require it.

There is however, an alternative option: transmission over a longer burst duration T'_i. It is thus possible to switch to a more robust scheme whilst keeping the same bit rate. This is only possible for sources that transmit at an average rate below the peak burst rate of the MF-TDMA system. However the limitation in this case is that the higher the average source

bit rate $\overline{R}_b^i$ the smaller the range of possible ACM modes. This greatly limits the FMT dynamic range that can be achieved.

B. Data Rate Reduction (DRR)

This technique involves the reduction of the transmission rate (symbol and information bit rate) whenever the system monitoring the next channel state predicts a possible deep fading. During clear-sky conditions, the symbol rate would be very high and it would then be gradually reduced as channel conditions get worse. For example, a reduction by 2 of the modulator symbol rate would increase the energy-per-symbol to noise-spectral-density ratio (E_s/N_o) by 3 dB, therefore offering an extra 3 dB protection against fades [2.21]. A DRR system has been designed in the framework of the OLYMPUS project [2.24] and studied in a simulation of a Ka-band VSAT videoconferencing system [2.25]. In both cases, the information data rate (2.048 Mbps) during clear-sky conditions is decreased by a factor of 2, 4, or 8 depending on the channel quality. The gains on the required E_b/N_o are thus 3, 6, and 9 dB respectively [2.18]. Figure 2.7 shows the attenuation protection offered when DRR, also known as Dynamic Rate Adaptation (DRA) [2.15] and [2.20] is used as an FMT. The principle is to adapt the modulator's symbol rate to propagation conditions keeping the same modulation constellation and the same level of error correction.

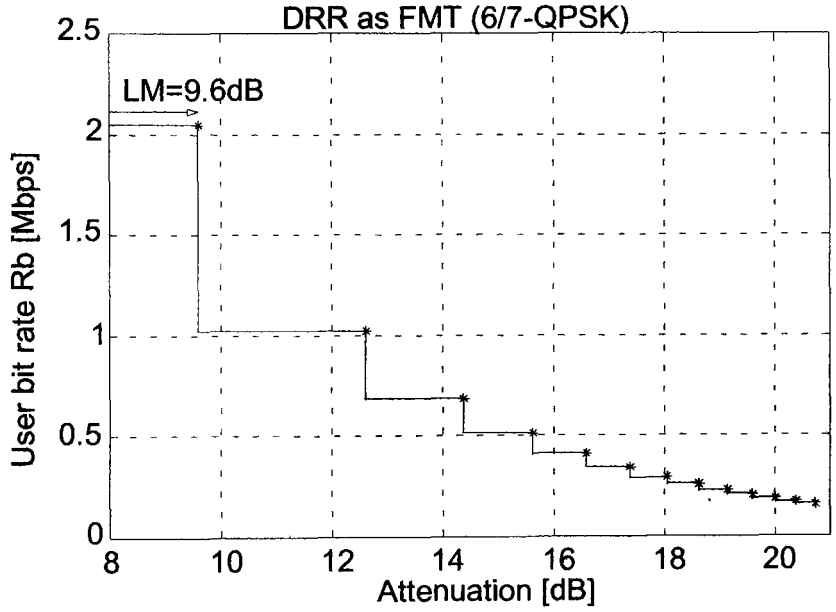

Figure 2.7 Data Rate Reduction as a function of attenuation

With DRR, the information data rate ($\overline{R}_{b_{\max}}^i$) is reduced when the link experiences fading. This translates in a decrease by an equal amount of the required C/N_o ratio when the required E_b/N_o ratio is kept constant (no change in the coding gains and constant BER). This also requires a reduction of the occupied carrier bandwidth [2.23].

This technique exhibits the advantage of equally distributing the satellite resources (bandwidth, burst length) among every user. No additional or extra resource is required for a connection affected by rain, so it imposes no reducing of the shared resource for the rest of the users. The applicability of this technique clearly depends on whether services can tolerate a significant reduction in their information rate. This is the case for example for video or data transmissions where the upper network layers are left unaffected. DRR is not suitable for voice transmissions since it requires fixed bit rate.

C. Burst Length Control (BLC)

In BLC, a variable portion of MF-TDMA burst plan is allocated to carry additional FMT timeslots whose role is to compensate for the attenuation suffered by a set of links undergoing rain. In particular, when a traffic burst is subject to fading, the burst will be allocated extra transmission time during which the original traffic burst can be expanded into. This time expansion results in an increase in average power (or energy/bit) of the signal that is used to counteract the effect of the fade [2.26].

If the duration of S_i traffic slots (emanating from source i) is spread by a factor H_i, then the number of *extra* FMT slot intervals required by the i^{th} return connection is:

$$N_{FMT}^{i} = S_i \times (H_i - 1) \tag{2.5}$$

Using time spreading, the total power margin M_i is increased to:

$$M_i = M_o^i + 10\log_{10} H_i \ \ [\text{dB}] \tag{2.6}$$

where M_o^i denotes the clear-sky power margin whereas the second term is the extra power gain brought in by BLC. Thus a spread by a factor of $H_i = 2$ produces a fade protection of 3 dB. Burst Length Control (BLC) was first described in [2.27]. The details on how BLC is implemented are given in Appendix A.

BLC operates at constant bandwidth and it can be seen as increasing the duration of the transmitted bits by increasing the symbol duration. The difference from DRR is that DRR can only be introduced at the cost of a reduced bit rate $\overline{R}_{b_{\max}}^{i}$ and equivalently a reduced bandwidth.

Deciding the value of the required spreading factor depends on the combined impact of up- and down-link attenuation on the overall CNR of the link. This will also depend on the clear-sky CNR and the desired/agreed maximum allowed BER of the link, i.e. in general:

$$H_i = f(A_i, BER_{\max}) \tag{2.7}$$

iwhere $A_i \equiv CNR_o - CNR_i$ denotes the total drop in CNR at the hub/NCC station for link i with respect to clear-sky conditions and $H_i \geq 1$. The total number of FMT slots in terms of A_i is $N^i_{FMT} = S_i \times \lfloor f(A_i, BER_{\max}) - 1 \rfloor$*.

In a previous study of a typical Ka-band return channel [2.28], QPSK with rate 7/8 convolutional coding was chosen as the system baseline (clear-sky) modulation/coding scheme providing maximum user throughput at a BER better than 10^{-8}. This system leaves a positive clear-sky link margin of $M^i_o = 2.73$ dB with a clear-sky CNR^i_o of 75.25 dB.Hz.

Combining equations (2.6) and (2.7), the power fade margin can be expressed as a function of the drop in CNR. This has been evaluated in [2.28] and is shown in Figure 2.8 with S_i set to unity. This figure shows the number of required FMT slots per traffic slot for a typical return channel. It shows that every time the burst duration is doubled in time, the FMT offers an extra 3 dB attenuation protection.

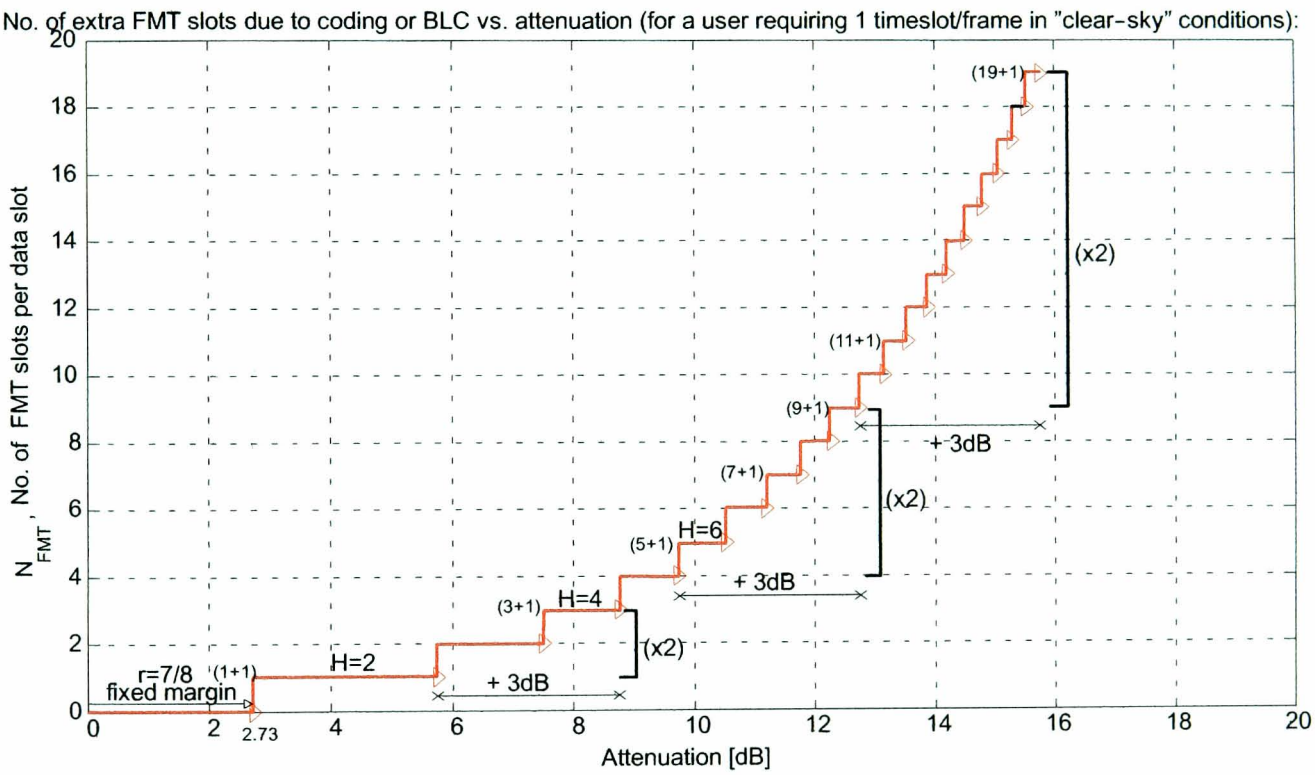

Figure 2.8 No. of extra FMT slots due to BLC vs. attenuation protection

* nb: $\lfloor 4.6 \rfloor = 4$

An important point is that Burst Length Control provides compensation for rain attenuation at the expense of total network capacity. Maintaining the BER target to achieve long-term availability will then only be limited by the dynamic range of the FMT, i.e. the maximum number of extra slots; if more slots are required, the system will not perform satisfactorily (hence the link will enter an outage state).

The above graph clearly emphasises the effect of BLC on the resource allocation process. Any fade compensation comes at the cost of extra timeslots which reduces the total capacity available to the whole MF-TDMA network. A case where multiple links experience fading simultaneously, will translate in very reduced global user throughput, as the links will compete for limited resources.

D. Summary of FMTs

The following table summarises the above FMTs and their characteristics.

FMT	BW	FMT mechanism	Max user Bit Rate R_{bmax}	BoD	MF-TDMA packing (burst characteristic)	Note
ACM1 [2.18]	variable (increased with rain) to compensate for ACM mode change	ACM gain	fixed	through burst duration up to R_{max} (depending on allocated burst duration up to T_F)	variable BW variable duration	$T_i \leq T_F$
ACM2 [2.20]	fixed	useful data rate control via modulation & coding but constant symbol rate	variable (reduced with rain) to compensate for ACM mode change	through burst duration up to R_{max} (depending on allocated burst duration up to T_F)	fixed BW variable duration	$T_i \leq T_F$
DRR [2.15] and [2.20]	variable (reduced with rain)	symbol rate reduction, fixed burst duration	variable (reduced)	same as above	variable BW fixed duration	$T_i \leq T_F$
BLC [2.27]	fixed	symbol rate reduction, burst time expansion upto frame duration T_F	fixed	same as above	fixed BW variable duration	$T_i < T_F$ *
ACM1-DRR	variable (increased to widest carrier of most robust mode, then reduced due to DRR)	ACM1/DRR gain (DR extension)	fixed until ACM DR is exhausted, variable (reduced) with DRR	same as above	variable BW variable duration	$T_i \leq T_F$
ACM2-DRR	variable (reduced due to DRR when ACM DR is exhausted)	ACM2/DRR gain (DR extension)	variable (reduced) due to ACM2/DRR	same as above	variable BW variable duration	$T_i \leq T_F$
ACM1-BLC	variable due to ACM1	ACM+BLC gain (DR extension)	fixed	same as above	variable BW variable duration	$T_i < T_F$ *
ACM2-BLC	fixed	ACM+BLC gain (DR extension)	variable (reduced) due to ACM2	same as above	fixed BW variable duration	$T_i < T_F$ *

Table 2.5 Adaptive transmission FMTs and their characteristics

* nb: BLC can only be applied when the source bit rate is below the peak bit rate $\hat{R}_b^i$, in order to allow for the necessary expansion from T_i to T_F

ACM1 seems to be the preferable scheme when keeping the user peak bit rate constant. The FMT however comes at the cost of bandwidth (change to a more robust ACM mode results in switching the transmission to a wider carrier).

ACM2 is suitable to cases where bandwidth is constrained and user bit rate can be reduced during fades. So, the symbol rate can be kept constant but bit rate reduction is required to accommodate the change in ACM mode.

In either of the above two cases, an extension of the dynamic range of ACM would be particularly useful in the case of power-limited systems for which high-order modulation schemes (e.g. 32PSK) cannot be used.

DRR can only be introduced at the price of a reduced user bit rate. The occupied carrier bandwidth can be reduced keeping the same modulation and coding scheme and adjusting the carrier symbol (and information data) rate. Simultaneous combination of ACM-DRR to keep a constant bit rate is not possible due to the opposite effects this would have in terms of FMT gain ($\hat{R}_b^i \propto \{B_i, \rho(Att_i), \log_2 M(Att_i)\}$, see equation (2.2)).

For services that cannot tolerate reductions of the information bit rate, Burst Length Control (BLC) seems to be a more attractive method. Instead of changing the user bit rate, the additional redundancy necessary to provide extra compensation against fading is introduced by a pure time extension used to transmit a time-expanded version of the original symbol stream. This has an impact on the number of connections that can be supported at any time by the network but live connections are "transparent" to fade conditions.

A possible scenario utilising a combination of all the above methods is the following: during fading conditions the ACM mode can be changed either by switching transmission to a wider carrier or, when bandwidth is constrained, the transmission bit rate can be reduced; if data rate reduction is acceptable, there is also another option: instead of changing the ACM mode, the carrier symbol rate can be reduced accordingly (i.e. DRR), keeping the same modulation and coding format. If however data rate reduction is not acceptable due to the nature of the connection, BLC allows a further option: change of ACM mode keeping data rate constant, and when the dynamic range of ACM is exhausted, then BLC can further extend the fading protection at the cost of network capacity.

Let us recall that the possibility to vary both burst duration and bandwidth, is an option supported by the standard. It can offer flexibility to the resource allocation process but at the same time add complexity to it, in terms of MF-TDMA "packing". This is important as the packing efficiency has a direct impact on the achieved channel utilisation.

On the other hand, a significant reduction in the source maximum user bit rate could have a detrimental effect on the agreed QoS of a connection, so a renegotiation would be required to ensure the source can tolerate it. Of course, renegotiation should only be a last resort situation, and for cases when reduction of the maximum bit rate is unacceptable, DRR cannot be applied and the option of variable bandwidth (ACM1) becomes necessary.

In such cases, a desirable extension of the FMT dynamic range is only possible through BLC and can prove to be useful. The following section is discussing this attractive possibility.

2.4 FMT for Power-Limited DVB-RCS Links

ACM should be able to provide high availabilities for powerful connections. Permitting the dynamic range of the FMT to be increased, thereby increasing the availability of MF-TDMA connections is particularly desirable for power-limited return links from very small terminals (for example home users).

2.4.1 BLC-enhanced ACM

The possibility of further extending the dynamic range of the ACM would be useful especially in the case of power-limited systems for which higher-order modulation schemes cannot be used. A BLC-extended ACM scheme can achieve this. In this case, the change in ACM mode is accompanied with a change of the burst duration to $H_i \times T_i \leq T_F$, while the bandwidth B_i is kept constant, where H_i is the BLC factor. The increased duration is used to transmit a time-expanded version of the original symbol stream. The impact of ACM-BLC scheme on the mode selection look-up graph is shown on the top-right of Figure 2.9.

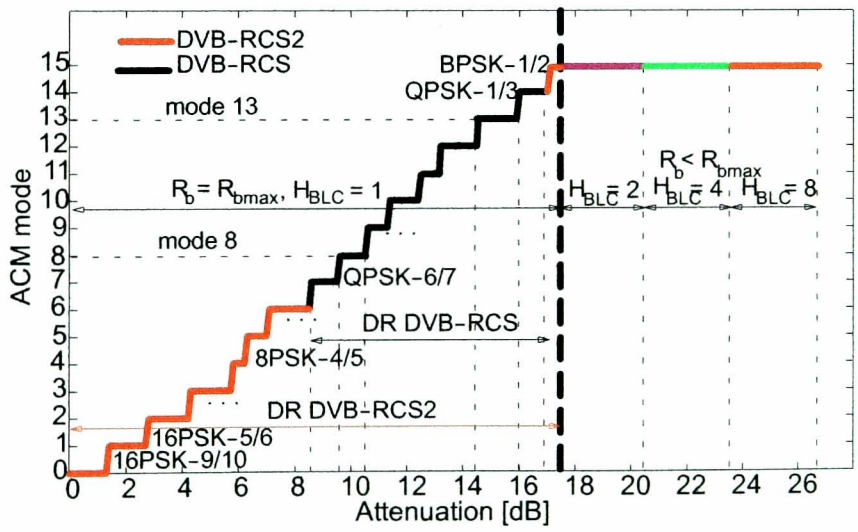

Figure 2.9 DVB-RCS2 ACM mode selection vs. SNR (E_s/N_o) degradation w.r.t. clear-sky (PER=10^{-7}) and FMT dynamic range extension due to Burst Length Control

When the ACM system's dynamic range is exhausted, BLC expansion by a factor H_i of 2, 4, 8 provides 3, 6 and 9 dB respectively of extra protection.

Figure 2.10 shows the attenuation the system would be able to cope with, by applying BLC, as a function of $\overline{R}_b^i$. It should be repeated that BLC can only be applied when the bit rate of the source is below the peak bit rate $\hat{R}_b^i$, in order to allow for the necessary expansion from T_i to $H_i \times T_i \leq T_F$. This is generally possible for bursty traffic sources that rarely transmit at peak bit rate. Clearly, the lower the $\overline{R}_b^i$ the greater the extension to the FMT's dynamic range that BLC can offer.

When BLC is used in addition to ACM, Equation (2.3) becomes:

$$\overline{R}_b^i = k'(Att_i) \times T_i, \tag{2.8}$$

where $k'(Att_i) = k(Att_i)/H_i(Att_i)$.

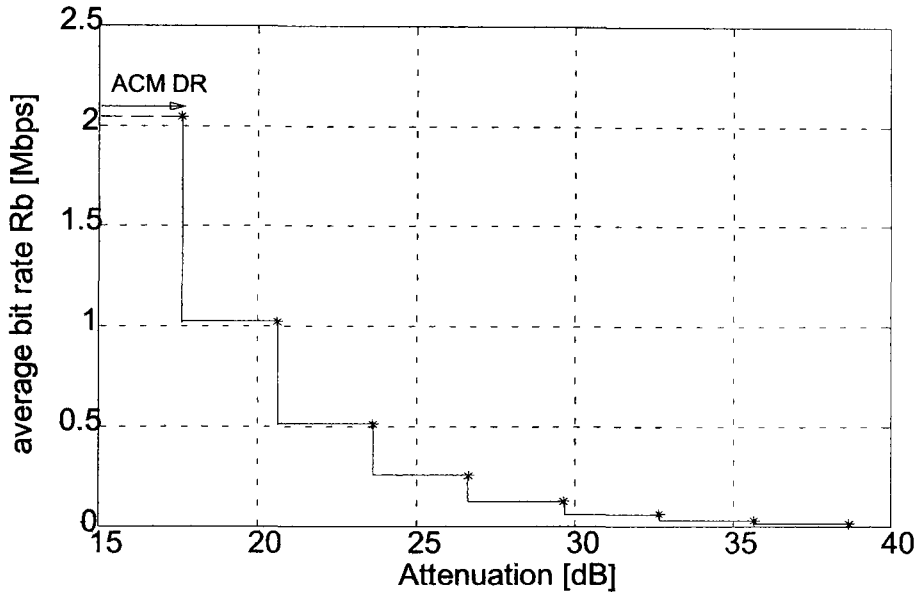

Figure 2.10 $\overline{R}_b^i$ as a function of attenuation (FMT dynamic range extension, offered by BLC)

Therefore the ACM-BLC system, with its greater dynamic range, will be able to achieve greater link availabilities. This is again at the cost of increased utilisation of MF-TDMA resources. Therefore the packing of all live connections within the MF-TDMA space, when multiple links simultaneously suffer from rain, will pose a real challenge for the resource allocation algorithm. This needs further investigations and will be presented later in this thesis.

2.5 Conclusions

The management of radio resources and the deployment of fade mitigation techniques are intrinsically linked. Study of this link appears to be an outstanding problem that will be investigated in this thesis.

The DVB-RCS protocol and physical layer allow for ACM and DRR fade mitigation techniques. However, as indicated in this chapter, the extension of ACM with BLC appears to be very attractive in order to extend the FMT dynamic range and link availability of power-limited return channels. It is proposed to study this further in this thesis.

A critical issue is that FMT, MAC and CAC operations are potentially interdependent. It is thus required to study carefully the trade-offs between link availability, user throughput, channel capacity utilisation, transmission delay and channel loading. This is addressed in the remaining pages.

2.6 References

[2.1] Awadalla H. O., "Resource Management for Multimedia Traffic over ATM Broadband Satellite Networks", PhD Thesis, Dept. of Electronic Engineering, Queen Mary and Westfield College, University of London, March 2000.

[2.2] VSAT Systems, "Broadband Satellite Internet: The Technology", retrieved June 11, 2008, from the VSAT Systems website: http://www.vsat-systems.com/broadband-satellite-internet/index.html.

[2.3] Weidenbener L. S., "Gambling via Satellite Proposed", The Courrier-Journal, 29 May 2005, retrieved July 2005, from http://www.courier-journal.com/apps/pbcs.dll/article?AID=/20050529/NEWS02/505290384.

[2.4] "Is it possible to play Quake, Half-Life, Counter-Strike games via satellite?" PlanetSky Satellite Frequently Asked Questions Area, copyright 2005-2006, retrieved December 2006, from http://www.planetsky.com/satellite_faq.php#10

[2.5] Fairhurst G., "Broadband Multimedia Satellite Systems", Jan. 2001, retrieved January 2003, from http://www.erg.abdn.ac.uk/public_html/research/future-net/digital-video/bband-sat.html.

[2.6] ATM Forum, Traffic Management Specification Version 4, af-tm-0056, April 1996, retrieved January 2003, from ftp://ftp.atmforum.com/pub/approved-specs/

[2.7] ITU-T Recommendation I.356 (2000): "B-ISDN ATM Layer Cell Transfer Performance".

[2.8] ITU-T Recommendation I.211 (1993): "B-ISDN Service Aspects".

[2.9] Kleinrock L., Lam S. S., "Packet switching in a slotted satellite channel", AFIPS Conference Proceedings, vol. 42, p. 703-710, 1973.

[2.10] Abramson N., "Packet switching with satellites", AFIPS Conference Proceedings, vol. 42, p. 695-702, 1973.

[2.11] Nelhams R. M., Barton S. K., "Adaptive TDMA for Fade Countermeasures", IEE Colloquium on Fade Countermeasures and Channel Restoration on Earth-Space Links, p. 2/1-2/6, London , UK, 2 Mar. 1990.

[2.12] Ippolito L. J.: "Radio propagation for space communications systems", IEEE Proceedings, Vol. 69, No. 6, pp. 697-727, U.S.A., June 1981.

[2.13] Nelson R. A.: "V-band: Expansion of the Spectrum Frontier", Via Satellite, February 1998, pp. 66+.

[2.14] Touw S. I. E.: "Analyses of Amplitude Scintillations for the Evaluation of the Performance of Open-Loop ULPC Systems", MSc Thesis, Eindhoven University of Technology, Eindhoven, The Netherlands, 1994.

[2.15] Moreau C.: "Protocols and Signalling for Adaptive Fade Mitigation Techniques (FMT) in DVB-RCS Multi-beam Systems" (Executive Summary), EADS Astrium and Space Engineering, 17-06-05, retrieved December 2005, from the ESA Telecommunications website: http://telecom.esa.int/telecom/www/object/index.cfm?fobjectid=11068.

[2.16] Alamanac A. B., Leconte K., Monaco M. C., Buret I.: "FMT Control Loop for the Return Link of DVB-RCS Systems", 23rd AIAA International Communications Satellite Systems Conference (ICSSC-2005), Electronic Proceedings (I000231.pdf), Aurelia Convention Centre, Rome, Italy, 25-28 September 2005.

[2.17] Haykin S., "Communication Systems", 4th edition, John Wiley & Sons, 2001, USA, ISBN 0-471-17869-1.

[2.18] Panagopoulos A. D., Arapoglou P. D. M., Cottis P. G.: "Satellite Communications at Ku, Ka and V Bands: Propagation Impairments and Mitigation Techniques", IEEE Communications Surveys & Tutorials, vol. 6, no. 3, pp. 2-14, 2004.

[2.19] Proakis J. G.: Digital Communications, McGraw Hill, 4th Ed., 2001, Chapter 8.

[2.20] "Protocols and Signalling for Fade Mitigation Techniques (FMT) in DVB-RCS Multi-beam Systems", ESA Workshop on 'Fade Mitigation Techniques for DVB-S2/DVB-RCS systems', Noordwijk, The Netherlands, 13-14 December 2004.

[2.21] Grémont B., "Fade Countermeasure Modelling for Ka-band Satellite Links", PhD Thesis, Coventry University, November 1997.

[2.22] Noussi E., Grémont B., Hewitt A.: "DVB-RCS2 Satellite Network with Dual Fade Mitigation Technique", 23rd AIAA International Communications Satellite Systems Conference (ICSSC-2005), Electronic Proceedings (I000282.pdf), Aurelia Convention Centre, Rome, Italy, 25-28 September 2005.

[2.23] Alamanac, A. B., Bousquet M.: "Millimetre-Wave Radio Systems: Guidelines on Propagation Modelling and Impairment Mitigation Techniques Research Needs", MC#3 Meeting and 1st COST280 International Workshop, Malvern, U.K., 1-3 July 2002.

[2.24] Filip M., Vilar E.: "Adaptive Modulation as a Fade Countermeasure, An OLYMPUS Experiment", International Journal of Satellite Communications, vol. 8, pp. 31-41, 1990.

[2.25] Kerschat K. et al.: "A Variable Spread-Spectrum Fade Countermeasure System for the DICE Video Conference System", Proceedings of the OLYMPUS Utilisation Conference, Seville, Spain, April 1993.

[2.26] Emerson D. J., Nelhams R. M., Clark B. L., "Adaptive TDMA for Fade Countermeasures", Olympus Utilisation Conference, ESA SP-292, Vienna, 12-14 April 1989.

[2.27] Carassa F., "Adaptive Methods to Counteract Rain Attenuation Effects in the 20/30 GHz Band", Space Communication and Broadcasting 2, North Holland, 1984, pp. 253-269.

[2.28] Noussi E., Grémont B., Filip M., "Adaptive MF-TDMA: Burst Length Control as a Rain Fade Countermeasure", Communication Systems, Networks and Digital Signal Processing (CSNDSP), 4th Int. Symposium Proceedings, University of Newcastle upon Tyne, 20-22 July 2004, p. 43-46.

[2.29] Spacebridge Semiconductor, "SB7088 Broadband Wireless Return Channel Modulator", Advance Product Information, retrieved December 2005, from http://www.spacebridge.com/products/sb7088.htm

[2.30] Fan B., Tafazolli R., Evans B. G., "A Fully Integrated Air Interface Signalling and Protocol for ATM via Satellite", 4th Ka Band Utilisation Conference Proceedings, p. 515-520, Venice, Italy, Nov. 2-4, 1998.

2.31] Bhasin K. B., Glover D. R., Ivancic W. D., vonDeak T. C., "Enhancing End-to-End Performance of Information Services over Ka-Band Global Satellite Networks", 3rd Ka Band Utilisation Conference Proceedings, p. 489-496, Sorento, Italy, Sept. 15-18, 1997.

2.32] Li K.-H., Chen C., "An adaptive MAC protocol for satellite ATM", IEEE Proceedings, 15th International Conference on Information Networking, p. 119-126, 2001.

2.33] Mertzanis I., Sfikas G., Tafazolli R., Evans B. G., "Satellite-ATM Networking and Call Performance Evaluation for Multimedia Broadband Services", 4th Ka Band Utilisation Conference Proceedings, p. 489-496, Venice, Italy, Nov. 2-4, 1998.

2.34] Dr. McCaughan D., Johanson G., Dr. Wing Lo, Dr. Abu-Amara H., "Satellite Webtone - Network Architectures for the Millennium", 4th Ka Band Utilisation Conference Proceedings, p. 497-505, Venice, Italy, Nov. 2-4, 1998.

2.35] Örs T., Sun Z., Evans B. G., "An Adaptive Random-Reservation MAC Protocol to Guarantee QoS for ATM over Satellite", Proceedings of the IFIP TC6/WG6.2 4th International Conference on Broadband Communications: The Future of Telecommunications, Stuttgart, Germany, pp. 107-118, 1-3 April 1998.

2.36] Lee K. D., Cho Y. H., Lee H. J., Jeong H., "Optimal Scheduling for Timeslot Assignment in MF-TDMA Broadband Satellite Communications", IEEE-56th Vehicular Technology Conference Proceedings, vol. 3, p. 1560-1564, Piscataway, NJ, USA, 2002.

2.37] Chang C. H, Wu H. K., Tseng Y., "Quality of Service Support for Broadband Satellite Multimedia Service", IEEE Wireless Communications and Networking Conference, vol. 1, p. 187-91, U.S.A., 1999.

2.38] Hung A., Montpetit M. J., Kesidis G., "ATM via Satellite: a Framework and Implementation", Wireless Networks, vol. 4, no. 2, pp. 141-53, Netherlands, 1998.

2.39] Mitchell P. D., Tozer T. C., Grace D., "Effective Medium Access Control for Satellite Broadband Data Traffic", IEE Seminar on Personal Broadband Satellite, vol. (Ref. No. 02/ 059), pp. 3/1-7, London, U.K., 2002.

2.40] Le-Ngoc T., Krishnamurthy S. V., "Performance of Combined Free/Demand Assignment Multiple Access Schemes in Satellite Communications", International Journal of Satellite Communications, vol. 14, no. 1, pp. 11-21, January-February 1996.

2.41] Awadalla H. O., "Resource Management for Multimedia Traffic over ATM Broadband Satellite Networks", PhD Thesis, Dept. of Electronic Engineering, Queen Mary and Westfield College, University of London, March 2000.

2.42] Li K. H., Chen C., "An adaptive MAC protocol for satellite ATM", IEEE Proceedings, 15th International Conference on Information Networking, p. 119-126, 2001.

2.43] Li Y., Jiang Z., Leung V. C. M., "Performance Evaluations of PRR-CFDAMA for TCP Traffic over Geosynchronous Satellite Links", IEEE Wireless Communications and Networking Conference Record, vol. 2, p. 844-8, U.S.A., 2002.

2.44] Mobasseri, M. Leung V. C. M., "Bandwidth Assignment for VBR Traffic in Broadband Satellite Networks", Canadian Conference on Electrical and Computer Engineering, Conference Proceedings, "Navigating to a New Era", vol. 2, p. 654-8 , U.S.A., 2000.

[2.45] Wibowo E. A., Iuoras A., Takats P., Lambadaris J., Devetsikiotis M., "Guaranteeing QoS in Packet-Switched Satellites by Medium Access Control", Proceedings of the CCBR'98 Conference, p. 31-43, Ottawa, Canada, Jun. 21-24, 1998.

[2.46] Iuoras A., Takats P., Black C., DiGirolamo R., Wibowo E., Lambadaris J., Devetsikiotis M., "Quality of Service-Oriented Protocols for Resource Management in Packet-Switched Satellites", International Journal of Satellite Communications, vol. 17, no. 3, pp. 129-141, May-June 1999.

[2.47] Keelty M., Landovskis J., Le Masson Y., "Satellite Interface Modems for Interactive Multimedia Terminals", 4th Ka Band Utilisation Conference Proceedings, p. 559-564, Venice, Italy, Nov. 2-4, 1998.

[2.48] ATM Forum, Traffic Management Specification Version 4, af-tm-0056, April 1996, retrieved January 2003, from ftp://ftp.atmforum.com/pub/approved-specs/

[2.49] Neale J., Green R., Landovskis J., "Impact of CF-DAMA on TCP via Satellite Performance", IEEE Global Telecommunications Conference, vol. 4, p. 2687-91, U.S.A., 2001.

[2.50] Pech P., Bousquet M., Castanet L., Radzik J., Fabre B., "Methodology to Optimise Techniques of Resource Management for Ka-band GEO Satellite Networks from the Introduction of Propagation Information", COST280, doc. PM2015[R1], October 2001.

[2.51] Celandroni N., Potorti F., "Fade Countermeasure using Signal Degradation Estimation for Demand-Assignment Satellite Systems", Journal of Communications and Networks, vol. 2, no. 3, September 2000 (ISSN 1229-2370), copyright Korean Institute of Communication Sciences.

[2.52] Celandroni N., Ferro E., James N., Potorti F., "FODA/IBEA-TDMA: A Flexible Fade Countermeasure System for Integrated Services in User Oriented Networks", International Journal of Satellite Communications, vol. 10, copyright 1992 by John Wiley & Sons, Ltd.

[2.53] Celandroni N., Potorti F., Rizzo S. T., "An inexpensive Fade Countermeasure Technique for DA-TDMA Satellites Systems", Proceedings of the IEEE Global Telecommunications Conference GLOBECOM'96, vol. 2, pp. 1001-1005, London, U.K., November 18-22, 1996.

[2.54] Celandroni N., Ferro E., Potorti F., "Experimental Results of a Demand-Assignment Thin Route TDMA System", International Journal of Satellite Communications, vol. 14, no. 2, copyright 1996 by John Wiley & Sons, Ltd.

[2.55] Celandroni N., Ferro E., Potorti F., Maral G., "Delay Analysis for InterLAN Traffic using two suitable TDMA Satellite Access Schemes", International Journal of Satellite Communications, vol. 15, no. 4, copyright 1997 by John Wiley & Sons, Ltd.

[2.56] Celandroni N., Ferro E., Potorti F., "Comparison between Distributed and Centralised Demand Assignment TDMA Satellite Access Schemes", International Journal of Satellite Communications, vol. 14, no. 2, copyright 1996 by John Wiley & Sons, Ltd.

[2.57] Chao H. J., Guo X., "Quality of Service Control in High-Speed Networks", John Wiley & Sons, Inc., New York, 2002, ISBN 0-471-00397-2.

[2.58] Haden R., "Quality of Service", retrieved January 2004, from http://www.rhyshaden.com/qos.htm

[2.59] "ATM Traffic Management", retrieved January 2004, from http://homepages.uel.ac.uk/u0216401/webpage/ATM%20traffic%20mgt.htm

[2.60] The ATM Forum Technical Committee, Traffic Management Specification Version 4.0, AF-TM 0056.000, April 1996.

[2.61] Liu K., Petr D. W., Braun C., "A Measurement-based CAC Strategy for ATM Networks", IEEE International Conference on Communications, Towards the Knowledge Millenium, vol. 3, p. 1714-1718, June 1997.

[2.62] Matyagina G., Shenoy N., Asenstorfer J., "Call Admission Control for a CDMA/TDMA based ATM Satellite Access Network", Proceedings of the IEEE International Conference on Telecommunications '99, Korea.

[2.63] Psomas G., "Satellite Communications: An overview", retrieved February 23, 2003, from http://www.iis.ee.ic.ac.uk/~frank/surp98/report/hdr1/.

[2.64] Le Pocher H., Leung V. C. M., Gillies D., "Evaluation of Statistical Multiplexing Performance for Real-Time ATM Traffic Employing a Frame-Based Management Strategy", IEEE Proceedings of Global Telecommunications Conference (GLOBECOM), 1997, retrieved January 2003, from http://www.ece.ubc.ca/~vleung/conference_papers/globecom97_2.pdf

[2.65] Swanson P., "Asynchronous Transfer Mode - ATM", retrieved February 23, 2003, from http://www.cyberus.ca/~swanson/ index.html.

[2.66] Perros H. G., Elsayed K. M., "Call Admission Control Schemes: A Review", IEEE Commun. Mag., vol. 34, November 1996.

[2.67] Rege K. M., Equivalent Bandwidth and related Admission Criteria for ATM systems - A Performance Study", Int. Journal Commun. Systems, vol. 7, pp. 181-197, 1994.

[2.68] Iera A., Molinaro A., Marano S., "Call Admission Control and Resource Management Issues for Real-Time VBR Traffic in ATM-Satellite Networks", IEEE Journal on Selected Areas in Communications, vol. 18, no. 11, November 2000.

[2.69] Turner J. S., "Managing Bandwidth in ATM Networks with Bursty Traffic", IEEE Network, September 1992.

[2.70] Rosenberg C., "End-to-End Resource Management for ATM On-Board Processor Geostationary Satellite Systems", 4th Ka Band Utilization Conference Proceedings, p. 481-488, Venice, Italy, November 1998.

[2.71] Acar G., Rosenberg C., "Performance study of end-to-end resource management in ATM geostationary satellite networks", Military Communications Conference (MILCOM), 2001, Communications for Network-Centric Operations: Creating the Information Force, IEEE, vol. 2, p. 764-769.

[2.72] Iera A., Molinaro A., Pulitano S., "Connection Admission Control Issues in DVB-RCS Systems", Proceedings of the 6th European Workshop on Mobile/Personal Satcoms & 2nd International Conference on Advanced Satellite Mobile Systems (ASMS) Conference, Noordwijk, The Netherlands, 21-22 September 2004.

CHAPTER 3

DVB-RCS NETWORK WITH RAIN FADE MITIGATION

3.1 The DVB-RCS Communication Scenario

Figure 3.1 illustrates a typical configuration of a broadband satellite system capable of providing multimedia services. The return link channel is shared by earth stations using the MF-TDMA scheme.

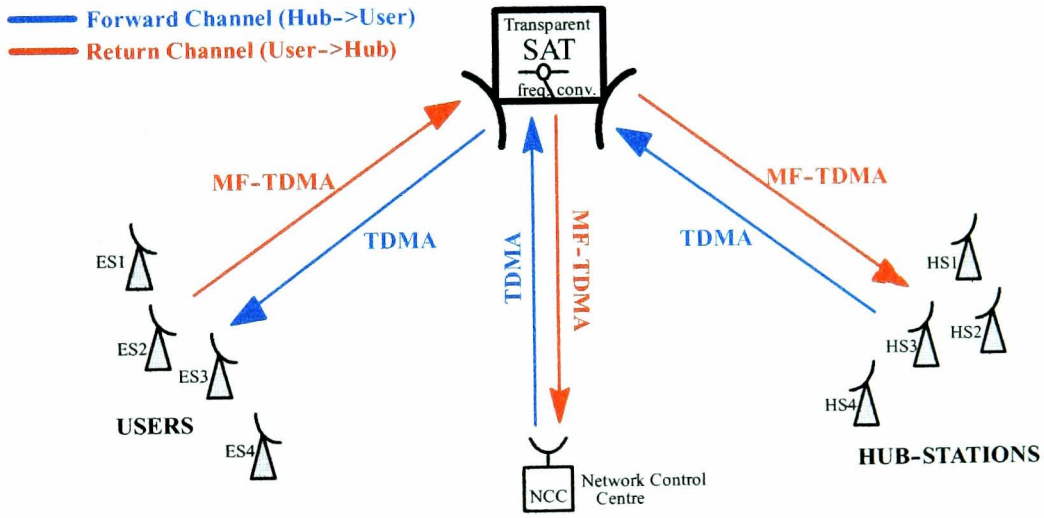

Figure 3.1 Typical configuration of a broadband satellite system

On the forward link, the access mechanism is assumed to be TDMA. The forward link transmission to the various user stations is organised in bursts. The burst is assumed to be consisting of a fixed number of timeslots, with each timeslot long enough to transmit one fixed-size packet. The combination of MF-TDMA on return links and TDMA on the forward channel allows for allocation through Bandwidth on Demand (BoD).

The system provides packet transmission from a hub to VSATs (Very Small Aperture Terminals) or RCSTs (Return Channel Satellite Terminals), through a bent-pipe satellite. The Ka-band frequencies allocated by the ITU for fixed satellite services at Ka-band have been

assumed (29.66 GHz uplink and 19.7 GHz downlink). The Network Control Centre (NCC) manages, in real-time, the communications of the whole MF-TDMA satellite network.

On the outbound link (hub to RCST) TDMA is used with a burst rate compatible with MPEG-2 (6 Mbps). Variable length packets from higher layer applications (video, audio, data) are encapsulated in an MPEG transport stream packet (188 bytes). Individual terminals identify user data from the destination address header in the broadcast stream.

The inbound link uses satellite ATM packets (48 bytes + 5 bytes header) to communicate with the hub. ATM provides a guaranteed QoS and short packet sizes (16 kbps). The RCSTs can be allocated non-overlapping slots in time and frequency (i.e. frequency "hop") across the whole MF-TDMA space to form a TDMA frame with a burst transmission rate of 2.048 Mbps. It is apparent that, for such a scenario of adaptive resource sharing in an environment where individual links may suffer occasional deep fades, MF-TDMA is especially suited and can offer flexible allocation of the return path capacity matching the bit rates of the user applications [3.1] and [3.2]. It is also well suited for deploying adaptive fade mitigation techniques when individual links suffer from occasional deep fades.

An RCST, once powered on, starts receiving general network information from the DVB-RCS NCC. The NCC provides monitoring and control functions and generates the control and timing messages required for operation of the satellite network. All messages from the NCC are sent using MPEG-2 TS (Moving Picture Experts Group Transport Stream) using private data sections. These are transmitted over the forward link. Actually, the DVB-RCS specification calls for two forward links - one for interaction control, and another for data transmission. Both links can be supported using the same DVB-S transport multiplex [3.3].

The term forward link refers to the link from the hub station which is received by the user terminal. DVB-RCS allows this communication to use the same transmission path as that used for data (that is the DVB-S receive path), or the alternate interaction path. Conversely the return link is the link from the user terminal to the hub station using the DVB interaction channel. The control messages received over the forward link also provide the Network Clock Reference (NCR). The NCR contains a 27 MHz clock reference and reception of the NCR is used by user terminals to adjust the transmit frequency of each user terminal to ensure a common reference for the MF-TDMA transmissions.

All transmissions by a user terminal are controlled by the NCC. Before a terminal can send data, it must first join the network by communicating (logon) with the NCC describing its configuration. The logon message is sent using a frequency channel also specified in the control messages (channel shared through slotted ALOHA).

After receiving a logon message from a valid terminal, the NCC returns a series of tables including the TBTP (Terminal Burst Time Plan) for each user terminal. The TBTP notifies each terminal at what specific time intervals and what specific assigned carrier frequencies it can communicate over, at an assigned transmit power. The block of information may be encoded in one of several ways (using convolutional coding, Reed-Solomon/convolutional coding or Turbo-coding). The block is prefixed by a preamble (and optional control data) and is followed by a postamble (to flush the convolutional encoder). The complete burst is typically sent using QPSK modulation. Before each terminal can use its allocated capacity it must first achieve physical layer synchronisation (of time, power, and frequency), a process completed with the assistance of special synchronisation messages sent by the terminal over the satellite channel. A terminal normally logs off the network when it has completed its communication [3.4].

3.2 ACM System and the Integration of BLC

The overall architecture for DVB-RCS with FMT is depicted in Figure 3.2. Provided the user station has been allowed a connection by the Connection Admission Controller (CAC), the RCST sends its traffic request (TRF Req), typically expressed as a bit rate or multiples of payload size (53 bytes for ATM or 188 bytes for MPEG packets, according to the encapsulation mode defined at logon) to the BoD controller. If granted, this will translate into the allocation of an "area", A_i, in the MF-TDMA subspace of a frame, as shown in Figure 3.2.

The dimensionless area A_i can be expressed as a time-bandwidth product:

$$A_i = B_i \times T_i \tag{1}$$

where B_i is the allocated carrier bandwidth (Hz) and T_i is the period over which the connection i will be allowed to transmit during the next frame period T_F.

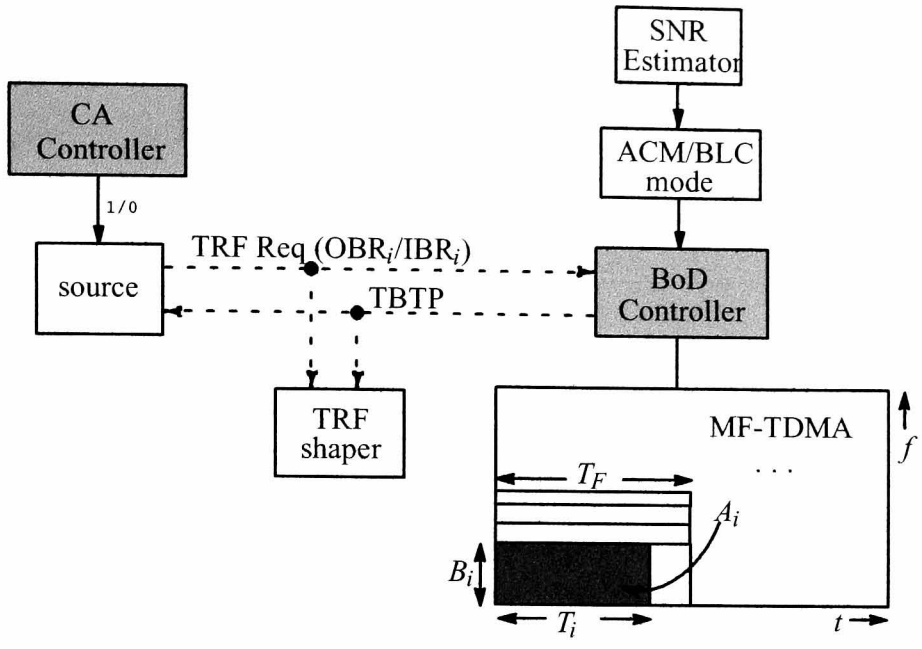

Figure 3.2 Architecture of ACM DVB-RCS

In addition, the NCC, where normally the BoD controller resides, measures the received SNR (E_S/N_0) on the return channels from the received bursts of each active RCST (Return Channel Satellite Terminal). This operation can be achieved using an appropriate SNR estimator as discussed in the following section.

3.2.1 SNR Estimation for Fade Detection

The link SNR (E_S/N_0) on the return link is estimated at the NCC and reported to the RCST. In order to reduce the amount of channel signalling, this reporting should only occur when SNR variations exceed a certain threshold. The way the actual fades can be determined or estimated is an important operation. There are in general two basic approaches:

- Open loop measurements of the fading conditions, for example using beacon detectors monitoring the amplitude of an unmodulated carrier or radiometric measurements of the sky noise temperature.
- Closed loop measurements applied to the information signal.

Open loop methods are particularly applicable to scenarios where the FMT only applies to either the up or the down-link, whereas closed loop methods are suited to FMTs trying to maintain the end-to-end QoS on the uplink/Satellite/downlink chain.

SNR estimators that rely on actual knowledge of the transmitted data are designated as Data-Aided (DA). In this case the estimator knows a priori the transmitted symbol stream (TxDA or pilot symbol estimator). Examples of this type are the Maximum-Likelihood

(ML-TxDA) and the squared Signal-to-Noise Variance (SNV Tx-DA) data-aided estimators. The alternative is an estimator that uses an estimate of the transmitted data sequence from receiver decisions (RxDA), also known as in-service, data directed or blind SNR estimators [3.5].

In this thesis, for the considerations of the dynamic Physical Layer (PL) adaptation on the return link some important assumptions have been made. For this purpose, let us first briefly consider the way that the SNR estimation can be performed on the forward link in the first place.

A. Forward-Link Dynamic PL Adaptation

Each user terminal can continuously monitor the received DVB-S2 compliant forward link and estimate the received SNR by exploiting the DVB-S2 embedded pilot symbols only (DA estimation). It can then report the estimates (together with the required transmission mode) to the gateway/NCC periodically. For this reporting SYNC bursts (that are periodically transmitted to maintain network synchronisation) can also be used. The reporting period might be 1 sec or even longer. In case the user terminal detects that a SNR estimate variation exceeds set thresholds, it can transmit a request for a FMT mode change immediately utilising a signalling channel that is operated in contention mode access.

Therefore, the user terminal estimates the channel quality on forward link continuously but only reports the estimate when a certain threshold is exceeded (and a mode change is required). The NCC can then decide its physical layer setting on the forward link based upon the reports from the associated user terminals [3.6].

B. Return-Link Dynamic PL Adaptation

For updating the actual SNR estimate of an individual return link, the NCC can utilise each forward link estimate reporting burst, a request for capacity, as well as each traffic burst. Based on the channel estimation, the NCC can then set for each user terminal an adequate transmission mode which may change from frame to frame. These mode change requests can be transferred to each associated user terminal through the TBTP via the forward link.

Similar to the forward link, the above estimation can be done using a DA estimator or alternatively a NDA or "in-service" SNR estimator can be used. In either case, the estimation will be derived from the baseband, sampled, data-bearing received signal. Let us now examine the two options and their implications more carefully.

(i) Data-Aided (DA) SNR Estimators

In this case, the estimation data must be known to the receiver. These schemes are widely considered to perform well [3.5] and [3.7], but at the price of introducing system overhead due to the known pilot symbols required for the estimation. This overhead can be a penalty to the achievable channel throughput. The only case where such estimators will not impinge upon the throughput of the channel is when the system already uses known sequences, for example, for synchronisation training. In DVB-RCS, the SYNC bursts that are periodically transmitted by the user terminals can be used for this purpose. One would then have to make sure that the transmission periodicity of these bursts is sufficient, i.e. frequent enough for the estimation process and if not any increase in this transmission frequency for the purpose of channel quality estimation would lead to the same issue of increased overheads in an environment known for its scarce channel resources.

(ii) Non Data-Aided (NDA) SNR Estimators

These techniques that derive the SNR estimates solely from the unknown, information-bearing portion of the received signal are of particular interest since they do not affect the channel throughput. However they result in a bias in the estimation of the mean SNR which increases as the M-arity of the modulator is larger. Non-linear correction for the estimator bias has been recommended in [3.5] and was proven to effectively remove the bias. This however comes at the price of an increase in the estimation error.

The main constraint of this scheme is related to the bursty nature of the return channel traffic as this can limit the frequency and possibly the accuracy of the estimation process affecting the achievable performance of the FMT. It is logical that, in order to improve further the estimation, estimates from multiple bursts for the same connection can be averaged together to reduce the estimation error. The main concern is that the amount of traffic (average number of symbols per unit time) from a RSCT can be sporadic and small which would have an impact on the accuracy of the burst SNR estimator. Simulations in [3.5] of the ML-RxDA estimator applied to MPSK described in [3.7], with the addition of a correction for the bias of the estimator at low SNRs, have shown the suitability of the technique even for very low traffic (only one ATM cell transmitted every second as a worst-case analysis). As discussed earlier, the advantage of this estimator was that, unlike data-aided schemes, it acted passively on the received symbol packets without requiring the insertion of any pilot symbols. Figure 3.3 shows that for a typical Ka band event of 15 dB, the estimated SNR remains within 1 dB of the true SNR.

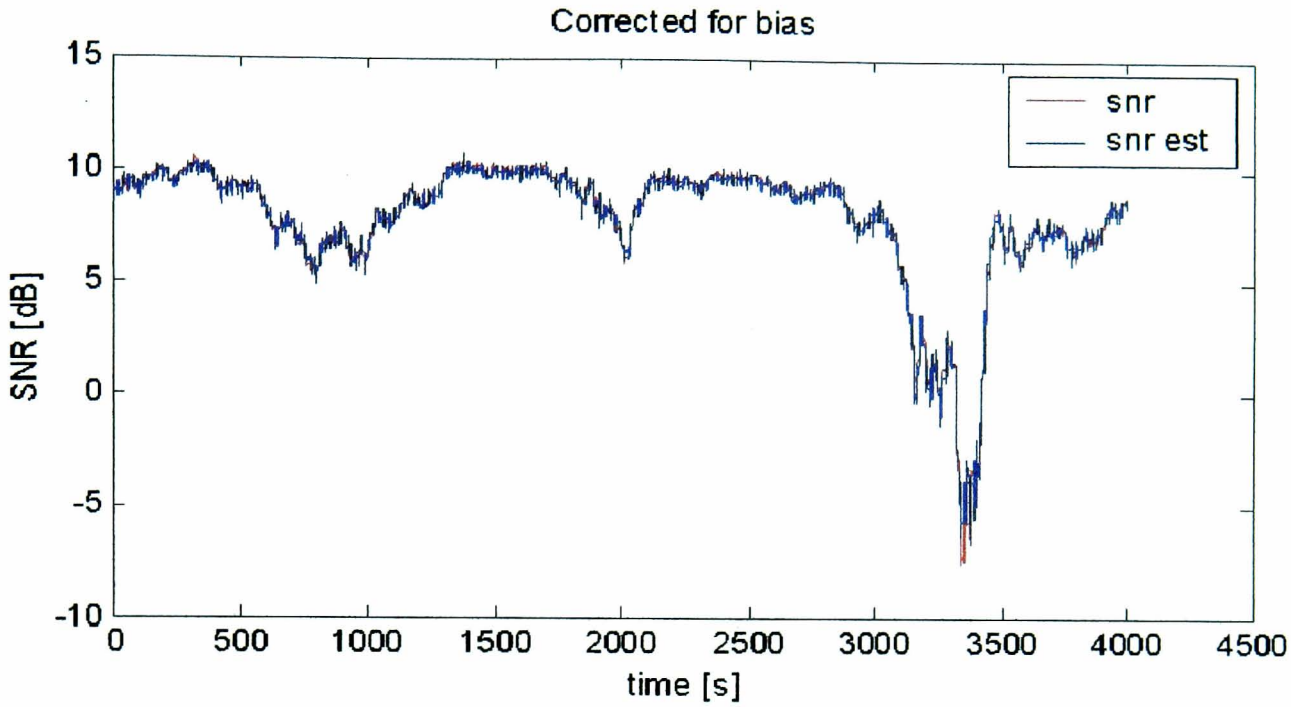

Figure 3.3 Estimated and true SNR (E_s/N_o) [3.8]

It should be noted that a common constraint for both DA and NDA schemes is the propagation delay ($\simeq$ 500 ms) in addition to the processing delay involved.

In other words, it becomes apparent that both schemes have got advantages and disadvantages and both lead to similar types of issues. Whichever the choice, any implications need to be taken into account during system design. There is no doubt that SNR estimation is an important operation and it is very crucial for the deployment and effective operation of the FMT itself. Besides, the detection range of the estimation algorithm determines whether the dynamic range offered by the FMT itself can indeed be fully utilised. However, fade detection is not the main interest of this work; it will therefore not be explored in depth and an ideal estimation will be assumed for the purposes of this thesis.

3.2.2 ACM-BLC

Based on the measured SNRs (including fading conditions) and having received the traffic requests from the user stations, the NCC can then allocate a carrier of appropriate bandwidth and duration to each connection for transmission of its bursts in the next frame period. This assignment and mode setting is achieved through the TBTP broadcasted to all stations as often as required.

In practice, the BoD controller can consider the requested MF-TDMA burst duration T_i needed by a connection assuming a BoD traffic request of $\overline{R}_b^i$ from the source and taking into

account the selected ACM mode (see Figure 3.2). It is up to the BoD controller to determine the actual allocated bandwidth, $\tilde{B}_i$, and allocated burst duration $\tilde{T}_i \leq T_i$ for the connection, taking into account all user connections and the limited amount of MF-TDMA space.

To explain the FMT scenario, let us assume that the connection is currently in ACM mode 8 ($E_s/N_o \approx$ 10 dB below clear-sky, for ACM modes please refer to Table 2.3). Due to rain let us assume that the SNR degrades further to 14.5 dB below clear-sky. Using the look-up table 2.3, the system would switch to mode 13. This switching from mode 8 to mode 13 corresponds to halving the FEC code rate from 4/5 to 2/5 with QPSK. If the source bit rate remains unchanged (i.e. it cannot be reduced and ACM2 is used), this change of mode increases the required MF-TDMA area from A_i to $A'_i = 2A_i$. The mode change expands the bandwidth by a factor of 2 (see case (a) in Figure 3.4). The duration T_i of the burst is always chosen so that it matches the required $\overline{R}_b^i$ (according to Equation (2.3)).

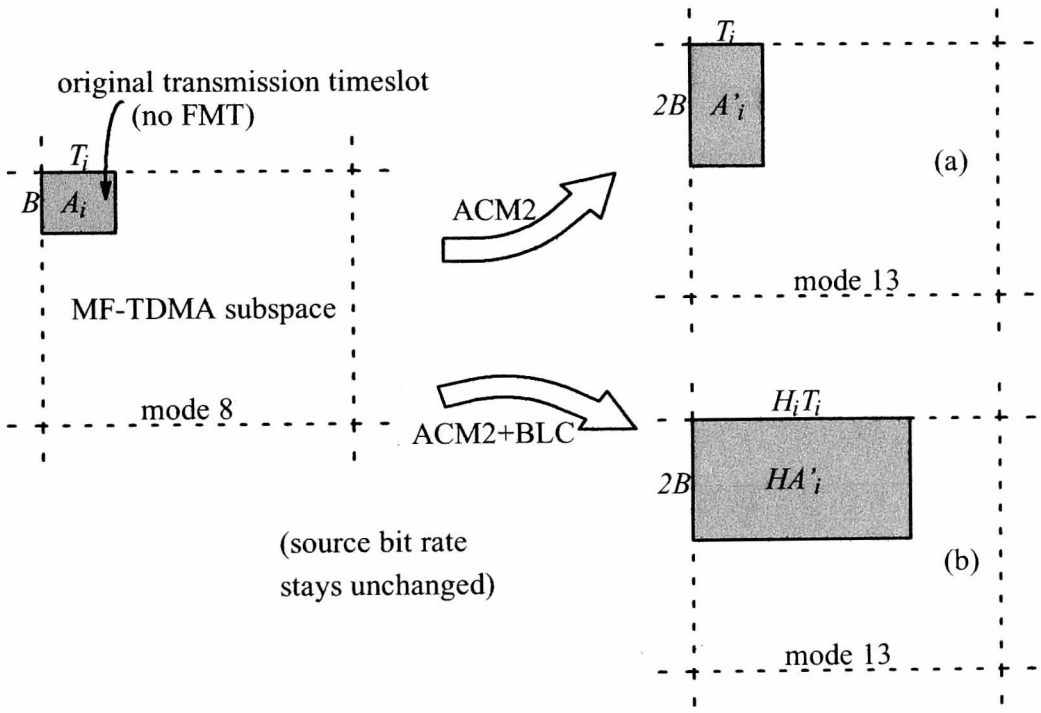

Figure 3.4 Simple example of area expansions due to FMT

It should be noted that, from the user's perspective, the BoD capability of DVB-RCS2 offers a wide range of transmission rates *if* resources are available. ACM1 provides the possibility of achieving high peak rates, if required, whenever weather conditions and the link power budget allows it. For example, with a modulator operating at its maximum supported symbol rate of 4.096 MBaud [3.9], a user can achieve a maximum bit rate $\hat{R}_b^i = 14.75$ Mbps ($\rho = 9/10,\ M = 16$), if it is allowed to transmit exclusively over a 5.5 MHz carrier bandwidth. Such increase in throughput can be used to boost the overall

throughput or possibly reduce transmission queues. But this throughput increase can only occur during no-rain conditions and does not constitute an FMT per se.

The impact of BLC on the utilisation of the MF-TDMA space is shown in Figure 3.4(b). BLC with expansion factor $H_i = 3$ is applied in addition to a change in ACM mode. This example shows that BLC would bring an extra 4.77 dB fade protection, making the system capable of coping with up to 20.5 dB of attenuation. However, due to its impact on capacity utilisation, it is clear that a more sensible approach is to apply BLC only when the most robust ACM scheme ($\rho = 1/2$, $M = 2$) cannot provide the required rain margin. In this case, BLC-ACM is solely used to increase the dynamic range of the FMT, thereby improving the availability of the return links.

3.3 Return Link Power Budget Analysis

Radio frequency link budget analysis aims at calculating the quality of the information delivered at the physical layer. The quality of digital information is measured by the BER, which is the ratio of the number of bits received in error to the total number of received bits. The BER depends on the type of modulation and coding used, and on the carrier to noise power spectral density ratio, C/N_0, at the input of the receiver. C/N_0 can be considered as a quality measure of the radio frequency link. The objective is to fully use the satellite transponder resource and the smallest physical size of earth station whilst achieving adequate BER performance at reasonable costs.

The Effective Isotropic Radiated Power (EIRP) is expressed as:

$$EIRP = P_T + G_T \quad [\text{dBW}] \tag{3.1}$$

where P_T is the power fed to the transmitting antenna, and G_T is the antenna transmit gain in the pertinent direction.

The earth station transmitter Tx with output power P_{Tx} feeds power P_T to the antenna through a feeder with feeder loss L_{FTx}. The antenna displays a transmit gain G_{Tmax} at boresight, and a reduced transmit gain G_T in the direction of the satellite as a result of the transmit depointing off-axis angle θ_T. The transmitter output power P_{Tx} is smaller than or equal to the transmitter output rated power P_{Txmax}, depending on the transmitter output back-off. In order to calculate the actual gain G_T, one needs to know more about the antenna gain pattern. When a parabolic antenna is considered, the gain is given by:

$$G = 20\log D_a - 20\log\lambda + 10\log\eta + 9.943 \quad [\text{dB}] \tag{3.2}$$

where D_a [m] is the antenna diameter, λ [m] is the wavelength and η is the antenna efficiency (a typical value is 0.6-0.7) [3.13].

The free-space loss depends on the frequency f [GHz] and the distance R [km] between the earth station and the satellite:

$$L_{FS} = 92.44 + 20\log f + 20\log R \quad [\text{dB}] \tag{3.3}$$

The figure of merit of the receiving equipment incorporates the composite gain from the antenna to the receiver input and the system noise temperature. As a factor in the expressions for C/N_0 given later (Equations (3.5) and (3.6)), it indicates the capability of the receiving equipment to build up a high value of C/N_0. It is given by:

$$\frac{G}{T} = G_R - 10\log T \quad [\text{dB/K}] \tag{3.4}$$

where G_R is the antenna receive gain at boresight and T is the receiving system noise temperature.

Starting with the sender site available earth station, EIRP_{ES}, along the transmission path to the receiver site, one can find out the achieved C/N_0.

3.3.1 Uplink Performance Analysis

The uplink carrier-to-noise spectral density ratio is given by:

$$(C/N_o)_u\,[dBHz] = EIRP_{ES}\,[dBW] - L_{Fu}\,[dB] + \left(\frac{G}{T}\right)_S [dB/K] + 228.6\,[dBJK^{-1}] \tag{3.5}$$

where L_{Fu} is the uplink free-space loss, G is the satellite antenna receiver gain and T is the uplink system noise temperature. The uplink budget is shown in Table 3.1.

Return Link Analysis		
Bit rate	2048	kbits/s
Modulation scheme	16APSK	
Coding	variable rate "new turbo" [3.14]	
Multiple access scheme	MF-TDMA	
Uplink		
Central Tx frequency, f	30	GHz
Transmitted power, P_{Tx}	1	W
Antenna diameter, D_a	0.75	m
Antenna efficiency, η_a	80	%
Earth station $EIRP_{ES}$	43.5	dBW
Free-space path loss, L_{FS}	213.76	dB
Reception Satellite		
Satellite figure of merit, G/T	18	dB/K
Inter-system interferences		
Adjacent satellite + covered terrestrial systems	23	dB
Uplink $C/(N_o+I_o)$	75.267	dBHz

Table 3.1 Return Link Analysis: Uplink Budget (RCST to Satellite)

3.3.2 Downlink Performance Analysis

The downlink carrier-to-noise spectral density ratio is given by:

$$(C/N_o)_d[dBHz] = EIRP_S[dBW] - L_{Fd}[dB] - BO_o[dB] + \left(\frac{G}{T_d}\right)_{ES}[dB/K] + 228.6[dBJK^{-1}] \tag{3.6}$$

where $EIRP_{SAT}$ is the satellite EIRP, L_{Fd} is the downlink free space loss, G is the earth station antenna receiver gain, T_d is the downlink system noise temperature ([3.16] and [3.17]) and BO_o is the satellite output back-off, which depends on the input back-off, BO_i, given by:

$$BO_o = IPS[dBW] - EIRP_{ES}[dBW] + L_{Fu}[dB] - G_S \quad [\text{dB}] \tag{3.7}$$

where IPS is the input power for saturation. For non-saturated operation, the output back-off for one carrier, BO_o, for the Olympus TWTA was approximately linearised as [3.18]:

$$BO_o \simeq 0.94 \times BO_i - 3.99 \quad [\text{dB}] \tag{3.8}$$

where BO_i is the input back-off (for one carrier), provided it is greater than 11 dB [3.19] and equals the difference between the input power for saturation of the TWTA and the total collected signal power at its input.

Return Link Analysis		
Downlink		
Central Tx frequency, f	17.7	GHz
Satellite TWTA output power	1.07	W
Antenna transmit gain	45.9	dBi
Satellite $EIRP_{SAT}$	28.22	dBW
Free-space path loss, L_{FS}	210.12	dB
Atmospheric loss, L_A	1.05	dB
Satellite output losses, L_A	3	dB
Hub		
Antenna diameter, D_a	4.5	m
Antenna efficiency, η_a	70	%
User earth station figure of merit, G/T	30.2	dB/K
Inter-system interferences		
Adjacent satellite systems	28	dBHz
Downlink $C/(N_o+I_o)$	75.54	dBHz

Table 3.2 Return Link Analysis: Downlink Budget (Satellite to Hub)

3.3.3 Overall Clear-Sky Link Performance

The overall link carrier power to noise power spectral density ratio at the earth station receiver input $(C/N_o)_t$ measures the overall link performance and conditions the quality of the baseband signal delivered to the user terminal in terms of its BER. The $(C/N_o)_t$ can be calculated from:

$$(C/N_o)_t = 10 \times \log_{10}[10^{-0.1(C/N_o)_u} + 10^{-0.1(C/N_o)_d}]^{-1} \quad \text{[dB.Hz]} \qquad (3.9)$$

Note that intermodulation, interference noise or fading have been neglected for simplicity.

All a power link budget is trying to find out is how much resource of the transponder is needed and what the transmitting ability $EIRP$ and receiving ability G/T of the earth station should be. Starting with the available satellite resource, the available transmission ability $EIRP_{ES}$ or receiving ability $(G/T)_{ES}$ can be found, which can determine the achieved $(C/N_o)_{ach}$ or $(E_s/N_o)_{ach}$.

Return Link Analysis				
Overall Link				
Available C/N_o	72.4			dBHz
E_s/N_o achieved	14.84			dB
16APSK	9/10	5/6	3/4	2/3
Required E_s/N_o (PÊR=10^{-9})	16.4	15	13.5	12
Link Margin $_{(clear\text{-}sky)}$	-1.56	-0.16	1.34	2.8

Table 3.3 Overall Clear-Sky Return Link Analysis

The subtraction from the achieved signal to noise ratio ($(E_s/N_o)_{ach}$) of that required by the modem ($(E_s/N_o)_{req}$) should give a small positive link margin. This positive margin allows to cope with all those unforeseen small fading/noise components that are still allowable without undermining the reliability of the link. Considering Table 3.3, 16APSK with code rate of 2/3 is chosen in this thesis as the system's baseline modulation/coding scheme, leaving a positive link margin of 2.8 dB.

This has consequences on the availability of the system that can be obtained from the ITU-R model [3.21], as it will be seen in section 3.5.1.

3.4 Achieved Link Availability with and without FMTs

The finding of the above section gives us useful information on the dynamic range (DR) of the FMT employed and the availability of the system. From Table 2.3 it can be seen that mode 3 ($\rho = 2/3$, $M = 16$) was chosen as a baseline, hence the full dynamic range offered by the FMT (ACM) in theory cannot be used. In chapter 2 it was seen that it is possible for ACM to offer a 17.6 dB dynamic range. The baseline mode offers a M_o of 2.8 dB, allowing for an initial possible compensation of 2.8 dB of attenuation (instead of the potential 5.7 dB protection offered by this mode, as obtained from theory, see Table 2.3, chapter 2). Furthermore, the supported ACM modes will be able to compensate for up to a maximum further attenuation of 11.9 dB. So overall, the system will be able to compensate for a maximum attenuation of 14.7 dB, which will be referred to as the *dynamic range* of ACM, DR_{ACM}.

3.4.1 Fixed Link Margin System

This section will briefly examine a couple of link design scenarios in order to demonstrate the advantages offered by ACM.

Figure 3.5 illustrates what would happen when only a small fixed margin is permanently incorporated for rain protection. This scenario, thanks to the permanent use of the least robust codulation mode supported, offers a good system throughput, however the clear-sky link margin M_o available with mode 3 will only be able to compensate for a 2.8 dB attenuation. Any deeper attenuation $A(p)$ will degrade the system's performance; in particular the link availability will be poor since the link is down whenever rain exceeds 2.8 dB (a large percentage of the time). As it will be seen in section 3.5.1, the ITU-R model [3.21] predicts a certain percentage $(p\%)$ of the time of an average year during which attenuation $A(p)$ is exceeded.

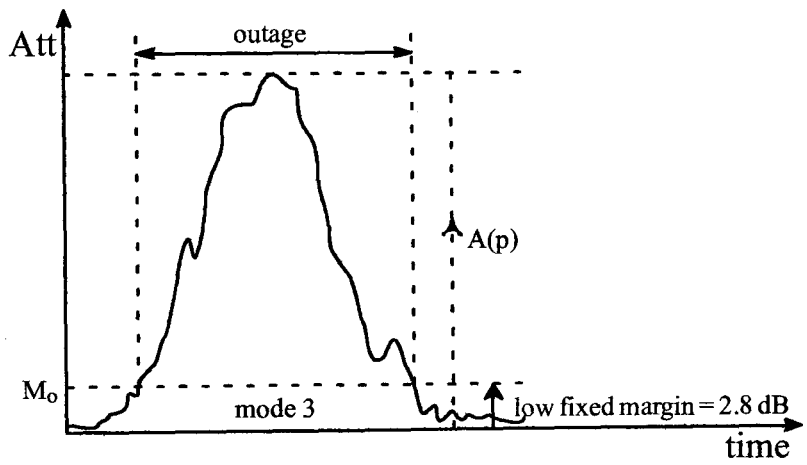

Figure 3.5 Low fixed margin standard design approach

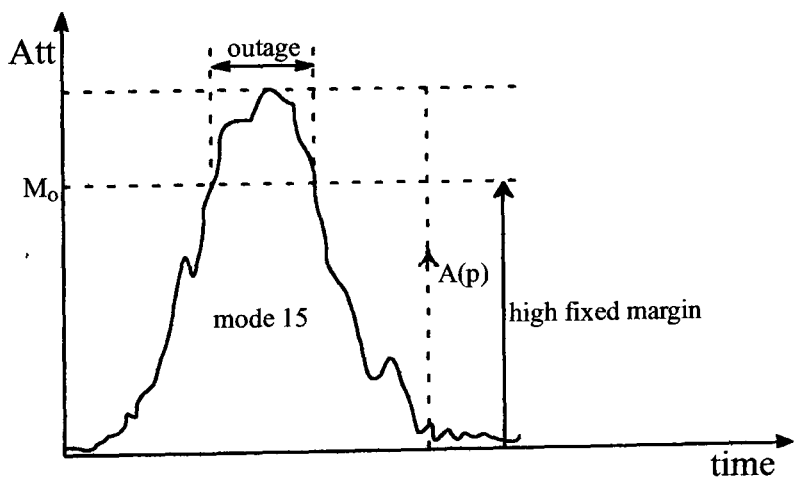

Figure 3.6 High fixed margin standard design approach

Figure 3.6 demonstrates the alternative option of permanently providing a large fixed margin using the most robust codulation scheme. This brings a great improvement to the link availability, as deeper attenuation levels can be compensated (up to 14.7 dB). However this will come at the price of poor system throughput due to the fact that all links will be using the most robust FMT mode, which has a much lower throughput, regardless of the rain conditions.

3.4.2 Switching of ACM Modes

In section 3.3.3 it was shown that ACM would be able to provide a practical dynamic range of 14.7 dB (including a clear-sky link margin of 2.8 dB). Figure 3.7 shows the operation of ACM as a fade countermeasure.

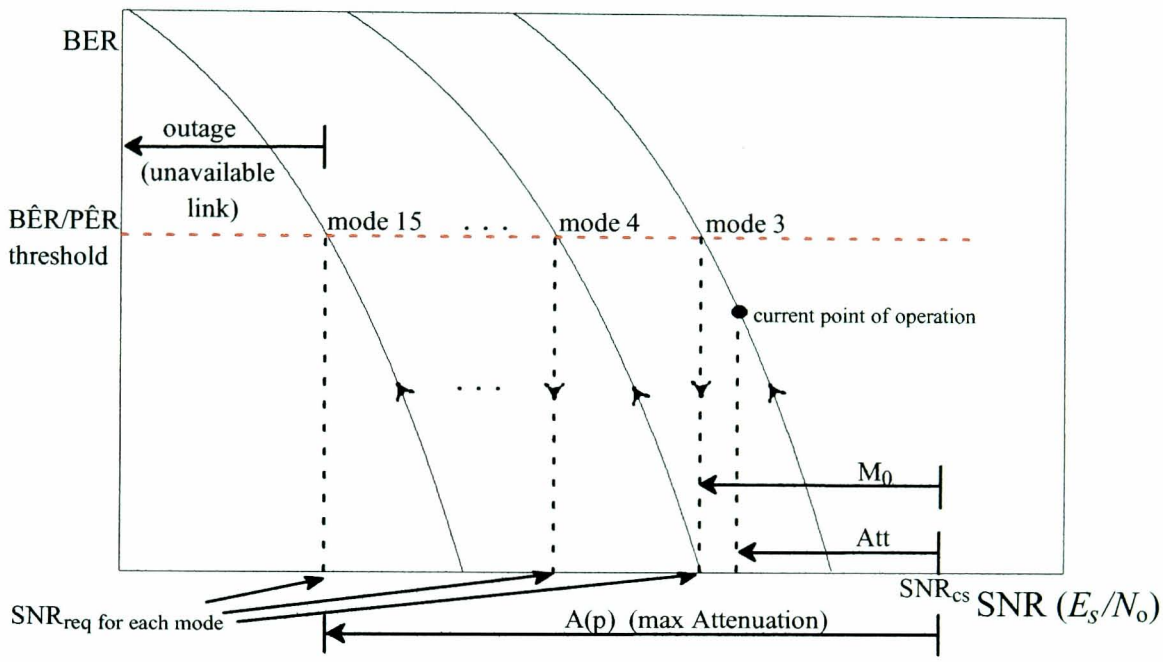

Figure 3.7 ACM mode switching during fading (theoretical performance)

When attenuation degrades beyond the system's original achieved SNR $(E_s/N_o)_{req}$ in clear-sky conditions, the system automatically switches to a more robust ACM mode so as to keep the BER/PER below a set threshold defining the required QoS of the link. The mode switching can continue if necessary up to the most robust mode (mode 15). This is when the available dynamic range is exhausted and a maximum attenuation of 14.7 dB can be compensated for. Any further attenuation cannot be compensated, resulting in a link outage (see Figure 3.8). The link is thus considered unavailable (since minimum QoS is not achieved).

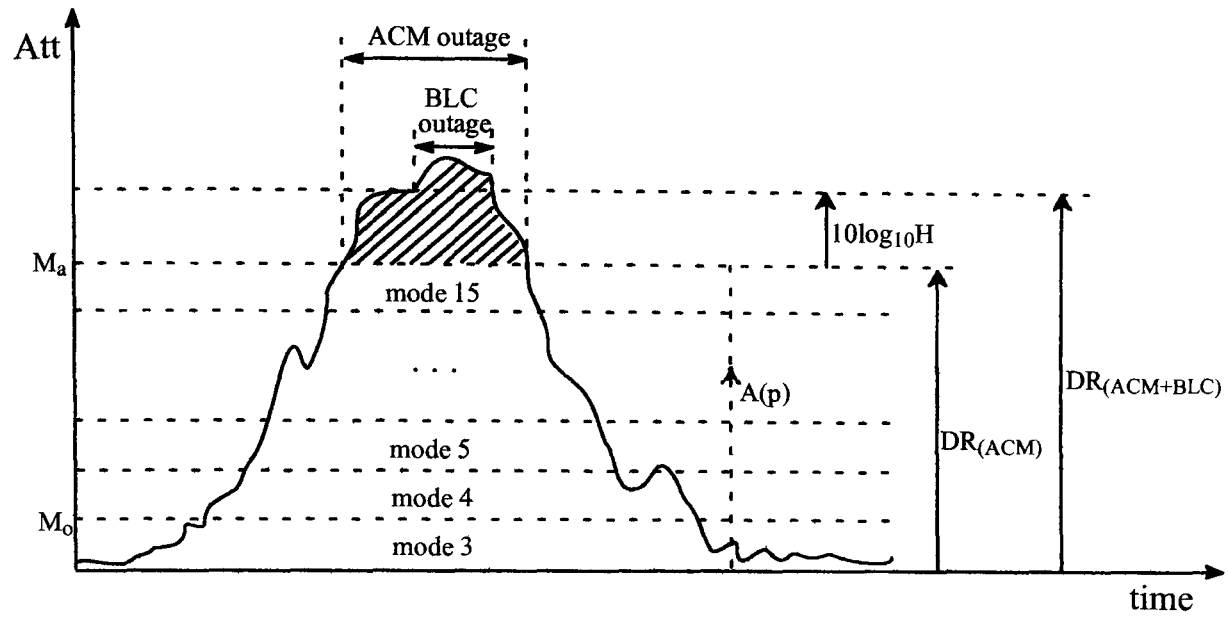

Figure 3.8 ACM mode switching in the event of a fade and possible DR extension by BLC

The advantage of the dynamic selection of the mode is apparent: dynamic selection inherits the good availability of a large fixed margin system and it also inherits the good throughput of a low fixed margin case; in fact, through the range of modes available, dynamic mode selection assists in enhancing (i.e. improving) the throughput whenever it is possible.

Looking at Figure 3.7, attenuation will be compensated as long as the attenuation $A(p)$ satisfies:

$$A(p) \leq SNR_{cs} - SNR_{req,\, mode15} \tag{3.10}$$

If (3.10) is valid, then the dynamic range of ACM, $DR_{(ACM)}$, will be capable of compensating for $A(p)$ (in dBs), otherwise $A(p)$ exceeds the dynamic range and no more compensation with ACM is possible.

3.4.3 Availability of BLC Link

This section describes a qualitative single link design approach when BLC is used as FMT and discusses its expected advantages and implications. Note at this stage that a pure BLC operation is assumed (inclusion of ACM is treated in the next chapter and the main simulation is presented later, in chapters 4 and 5).

In the event of rain in some portion of the footprint, the drop in QoS on rain attenuated links will require the deployment of the FMT to counteract for rain attenuation. Figure 3.9(a) shows the variations of the carrier-to-noise ratio for a simulated 30/20 GHz return link.

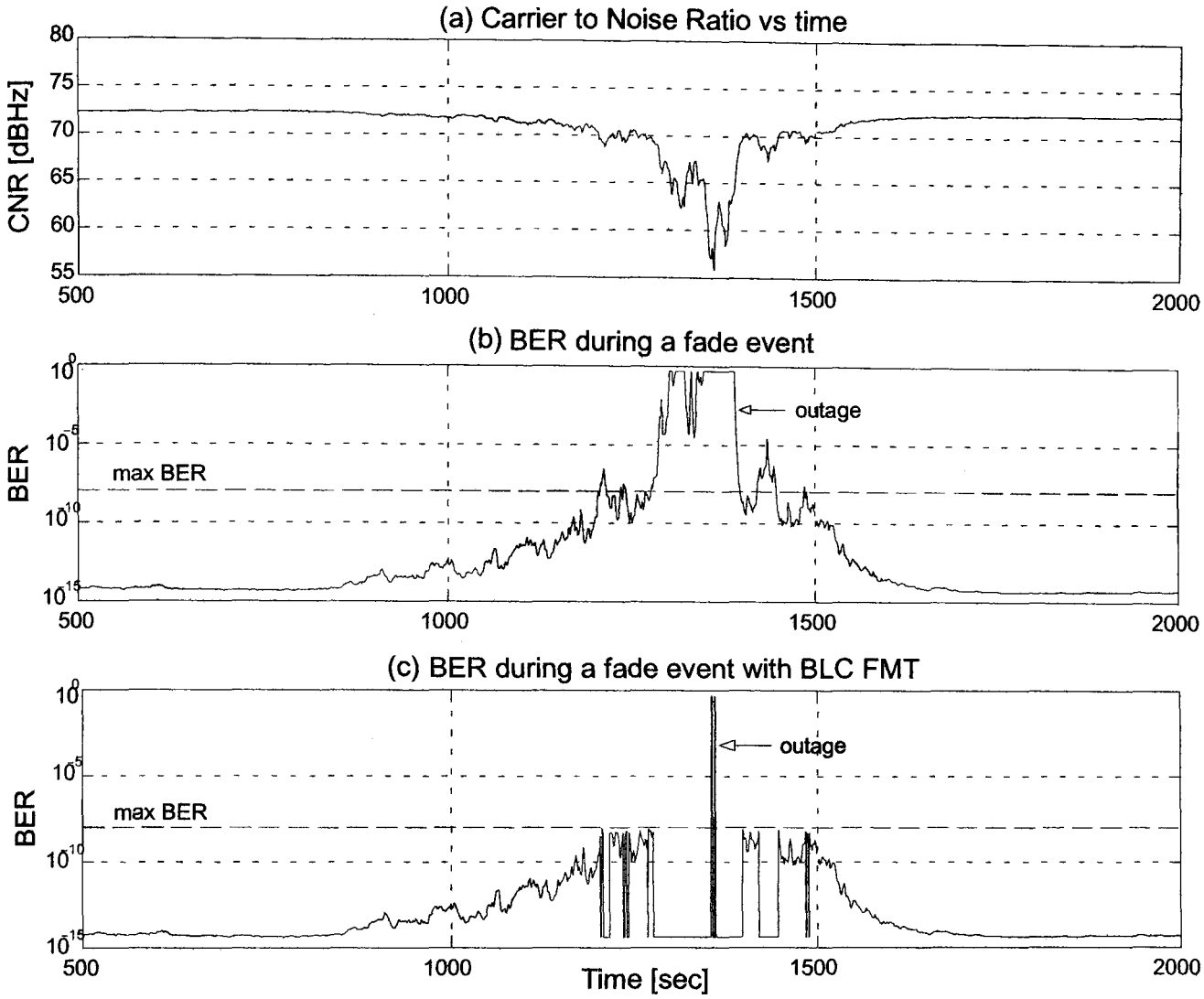

Figure 3.9 CNR degradation due to rain with/without BLC

Figure 3.9(b) shows the time-varying BER of the link without BLC, with channel variations shown in Figure 3.9(a). Figure 3.9(c) shows the BER when BLC is used. The link can maintain the BER below the maximum BER threshold of 10^{-8} for most of the time. However when the total drop in CNR nears its peak, the BER grows to a large value (0.5). This situation corresponds to a link outage that ultimately contributes towards the long-term unavailability of the link.

BLC is introduced through additional TDMA slots. Figure 3.10 shows the corresponding number of FMT BLC slots per normal traffic slot for the link undergoing rain attenuation. This is the same as the number of FMT slot intervals, N_{FMT}, introduced in section 2.3.2 C. of chapter 2 (see equation (2.5)).

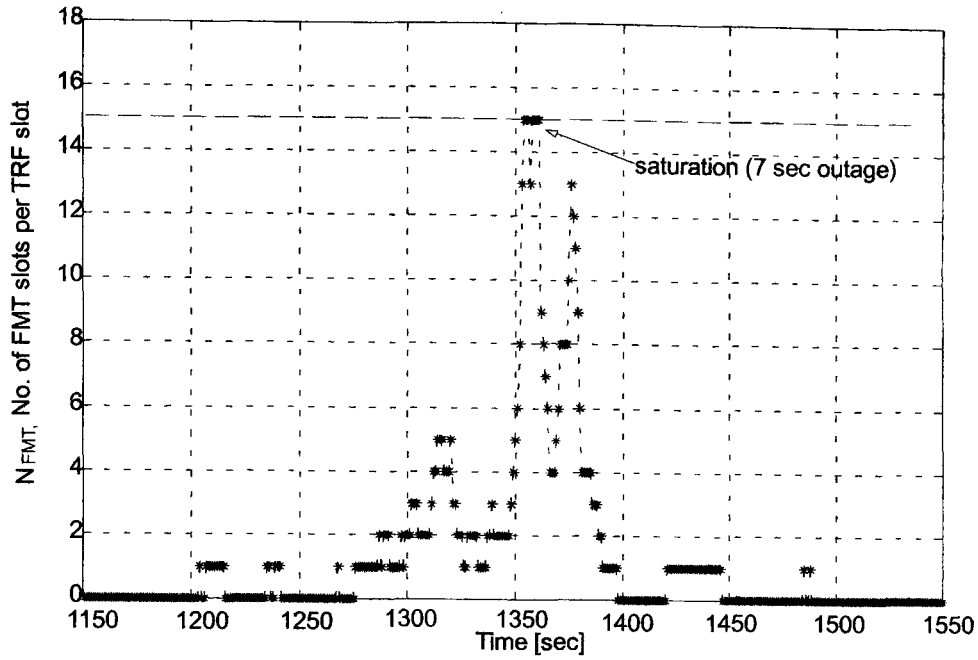

Figure 3.10 No. of FMT slots for one user during rain (pure BLC)

It can be seen that at time $t \approx 1355$ seconds, the FMT saturates to its maximum value of 15 BLC slots per traffic slot. The FMT is not able to offer any more protection and hence the link enters an outage state.

One can easily realise the advantages of such an adaptive system over a fixed one that would constantly allocate a fixed number of slots (15 extra slots for a 15 dB attenuation threshold). In the case of the adaptive BLC system, the number of BLC slots varies in time depending on the actual rain fade, as shown in Figure 3.10. On the long term, this results in a more economical use of FMT slots since rain is rare. This in turn results in a more efficient use of capacity and allows for more links affected by rain to be serviced in a set TDMA network. Maintaining the BER target to achieve long-term availability is thus primarily set by the dynamic range of the FMT, i.e. for BLC the maximum number of extra slots (15 slots in this example); for deeper rain fades more slots would be required, the system cannot provide them and so a link outage occurs.

It is also important to note that this adaptiveness should be controlled, in order to avoid unnecessary "switchings" in short periods of time (Figure 3.10) due to fast changes in attenuation levels. This will reduce the number of FMT requests and will tend to minimise FMT signalling in the network.

3.4.4 BLC-enhanced ACM Operation

If BLC is employed in addition to ACM (see section 3.4.2), a further compensation of rain becomes possible. Figure 3.8 gives the new combined FMT dynamic range:

$$DR = DR_{ACM} + 10\log_{10} H \tag{3.11}$$

where H is the BLC expansion factor.

In this case, the outage can be further reduced as BLC compensates for additional attenuation. Equation (3.11) clearly shows the improvement brought by BLC which will therefore bring an improvement of the link availability.

However, the availability of the system will not simply depend on the dynamic range. The DR extension only provides a potential theoretical improvement of availability. Whether this availability can practically be achieved for the system will also depend on the network user traffic conditions and the parameters described in section 3.5.2. The availability will also be function of the efficiency of the resource allocation algorithm that allocates bursts to sources.

For methods using a shared resource, the outage probability [3.44] on a certain link is given by the sum of the probabilities of two mutually exclusive events:

$$P_o = P(Att > M_a) + P(Att \leq M_a,\ E \text{ unavailable}) \tag{3.12}$$

where the first term $P(Att > M_a)$ is the probability that the attenuation exceeds the maximum compensable fade. The second term $P(Att \leq M_a,\ E$ unavailable) corresponds to the probability of rain being compensable by the FMT, however the shared resource E is not available (presumably E is used by other links).

To evaluate (3.12), in particular its last term, it is necessary to know the joint attenuation distribution among all the stations of the system. Interesting investigations on the joint attenuation distributions have been carried out in the framework of propagation research programmes [3.44], [3.45], and [3.46]. However the method seems difficult to extend to realistic fading scenarios and the multidimensional integration of joint density functions becomes difficult as the number of links increases.

An accurate prediction of the availability, $1-P_o$, of the link thus requires the estimation of $P(Att \leq M_a,\ E$ unavailable). A proposed approach in this thesis is to use instead a simulation approach, taking into account of stochastic traffic sources, the practical resource allocation algorithm and the fading conditions.

3.5 Rain Attenuation on Satellite Links

3.5.1 Distribution of Rain Attenuation

Raindrops cause attenuation of radio waves by both absorption and scattering. Absorption involves dissipation of some of the energy of an electromagnetic wave as heat

(thermal dissipation). Scattering involves diversion of some of the energy of the wave into directions other than the desired one.

Attenuation due to rain on a satellite link can be determined using:

$$a_R = \gamma_R L_R(R, \epsilon) \quad [\text{dB}] \tag{3.13}$$

where γ_R [dB/km] is the specific attenuation and $L_R(R, \epsilon)$ [km] is the effective radio path length through the rain [3.22] and depends on the precipitation rate, R [mm/h], and the path elevation angle ϵ. For practical applications, γ_R is calculated according to the empirical power law relation of a form aR^b [3.23] and [3.24], where the parameters a and b are frequency, elevation and polarisation dependent [3.25]. For a given frequency, a and b can be determined by [3.26]:

$$a = \frac{a_H + a_V + (a_H - a_V)\cos^2\epsilon\cos 2\tau}{2} \tag{3.14}$$

$$b = \frac{a_H b_H + a_V b_V + (a_H b_H + a_V b_V)\cos^2\epsilon\cos 2\tau}{2a} \tag{3.15}$$

where the parameters a_H, a_V, b_H, and b_V can be found in tabular form for various frequencies in [3.26], and τ is the polarisation tilt angle relative to the horizontal. The effective path length $L_R(R, \epsilon)$ can be obtained from the ITU-R model in [3.24] and the rain rate distribution can be obtained from the ITU-R prediction model [3.21]. Point rainfall intensity statistics are usually given as values of R [mm/h] that are exceeded particular percentages of the time of an average year. Therefore, for the particular frequency, polarisation and elevation, it is possible to calculate γ_R and L_R and thus obtain N data pairs:

$$(a_{R_i}, p_i), \quad i = 1,\ldots,N \tag{3.16}$$

where a_{R_i} is the total attenuation x that will be exceeded for $(100{\cdot}p)\%$ of the time of an average year, i.e.:

$$p_i = Prob\{a_R \geq x\}, \quad i = 1,\ldots,N \tag{3.17}$$

Since rain attenuation confines to the log-normal distribution law satisfactorily, it is necessary to determine its median and standard deviation. Figure 3.11 shows an estimation of the CCDF (Complementary Cumulative Distribution Function) of rain attenuation expected at one location and its lognormal fit.

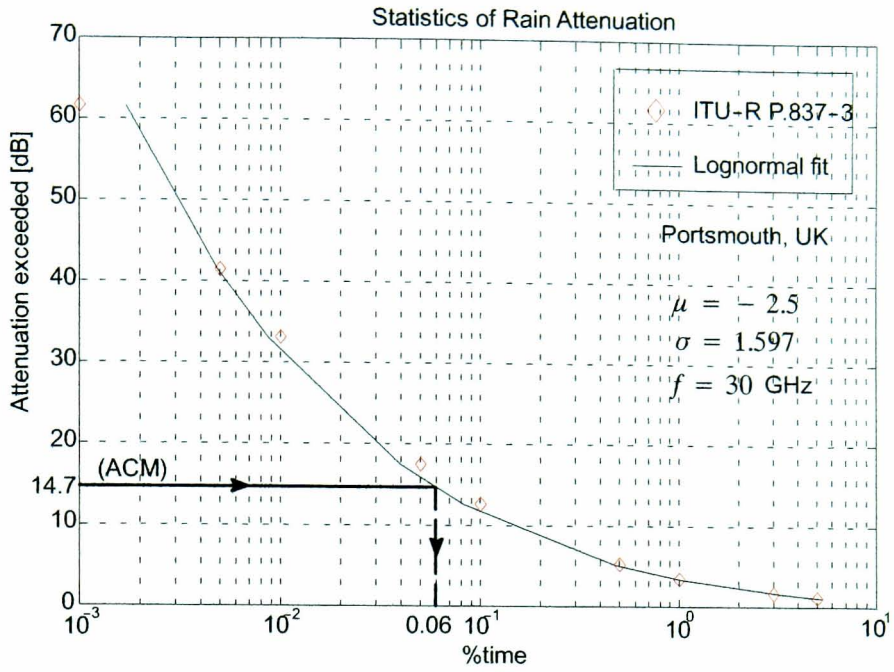

Figure 3.11 CCDF of Rain Attenuation expected at one location and its lognormal fit ([3.21])

It is easy to show that this CDF can be approximated by a log-normal distribution whose PDF is given by:

$$p(u) = \frac{1}{u\sigma\sqrt{2\pi}}\exp\left(-\frac{(\ln u - \mu)^2}{2\sigma^2}\right), \quad u > 0$$

$$p(u) = 0, \quad \text{otherwise,} \tag{3.18}$$

where μ and σ are the median and standard deviation of the distribution. These parameters can be graphically determined by plotting the obtained data on a log-normal probability paper and fitting a straight line to the plot. [3.25] illustrates the use of this conventional procedure. The CCDF of equation (3.18) is given by:

$$P_u = \int_x^{\infty} \frac{1}{u\sigma\sqrt{2\pi}}\exp\left(-\frac{(\ln u - \mu)^2}{2\sigma^2}\right)du, \quad u > 0$$

$$P_u = 0, \quad \text{otherwise.} \tag{3.19}$$

Figure 3.11 shows that the log-normal fit is appropriate for unavailability percentages sufficient for system design. In the case of Portsmouth at 30 GHz, the two lognormal parameters are $\{\mu = -2.5,\ \sigma = 1.597\}$. These values will be used throughout this thesis for the purpose of producing typical rain fade events.

Considering the 14.7 dB attenuation (the maximum attenuation compensation offered by the system incorporating ACM as discussed in the previous section), one can obtain the resulting offered availability of the system. Using Figure 3.11, the availability can be expected to be 99.94%. This is just a top estimate of the link availability. In practice, the

achievable availability will be smaller than this bound. This will be discussed further in the following chapters.

3.5.2 Impact of Rain on Satellite Networks

Figure 3.12 shows an example of rain cells over areas with active and non-active users inside the coverage area of a satellite. It should be clear that the FMT resource requirement (e.g. burst expansion into extra FMT slots) of a system will depend on:

- users' density and location (the greater the concentration of users the greater the required FMT resource needs when it rains)
- space and time characteristics of rain (for rain over large areas more FMT resource is required)
- depth of rain attenuation (the deeper the rain attenuation the more FMT resources are needed)
- actual traffic characteristics of the user stations (increased traffic will require more FMT resources in rainy conditions)
- agreed QoS parameters (higher QoS requires more network resources).

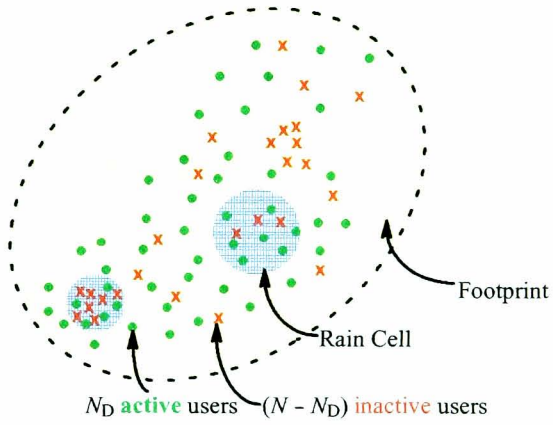

Figure 3.12 Active and non-active users in the satellite footprint in the presence of rain

Furthermore, depending on the hour of the day or the month, the rain conditions may be quite severe resulting in a much more extensive need for network resources through the FMT. This would in particular be worse if severe fades occurred at times when user traffic is high. So diurnal/seasonal variability of rain effects may also prove important for detailed studies.

Preliminary work in [3.11] investigated the effect of different probabilities of rain over different user density areas on channel capacity utilisation and total user throughput efficiency. Two cases, a correlated and a decorrelated scenario, were studied. Rain events

were generated using a random rain synthesiser [3.12]. As expected, the correlated scenario produces a large increase in required bandwidth, causing significant traffic queuing delays as the rain increases. The number of users served within only two MF-TDMA channels without any queuing delay is larger for the uncorrelated scenario, since not all sources happened to transmit at their peak rates simultaneously. This is of great significance and clearly demonstrates the potential advantages of statistical geographical multiplexing, even in the case when 50% of the links are rain affected (uncorrelated). In the uncorrelated rain scenario, outage predominantly occurs when the dynamic range of the FMT is exceeded [3.12]. In the correlated rain scenario, not all requests can be granted for high numbers of active users; even when the number of active users is small, the high variability in required bandwidth resulted in an inefficient use of capacity. In such cases, if the agreed QoS allows it, some connections could be blocked until resources become available, or more likely, the requests may be queued as long as the sources can tolerate.

3.5.3 Rainfield Modelling

There is a lot of ongoing research on the modelling and prediction of propagation channel characteristics. Modelling rainfields in space and time has been worked on over the last four decades. A number of studies have developed rain cell models from radar measurements but these are statistical in nature and do not enable the construction of typical two dimensional rainrate fields [3.27]. Other models have disadvantages in that they only deal with the spatial variation of the rainrate within a rain cell [3.28] or do not take into account the full range of rain rates that are significant for frequencies up to and beyond 20 GHz [3.29]. These models assume regular shapes to the rain cells, such as ellipses or Gaussian functions, of position centred on the area of maximum rain rate. Other studies [3.30] and [3.31] suggest that fractal methods may be of use in characterising the shapes of rain cells and clouds. Further studies have sought to find a clearer understanding of the shape, and spatial distribution of rain cells occurring in specific areas and climatic regions, leading towards more accurate models for the synthesis of rain fields, incorporating techniques of fractal geometry as well as meteorological radar data [3.32].

A study in [3.33] gives a summary of modelling approaches until 1994. A publication of particular interest is Bell's approach [3.34] where he showed, amongst other useful points, that rainfall values estimated by satellites obeyed a log-normal marginal distribution. [3.35] and [3.36] showed that radar-measured rainfield intensities are described well by a log-normal distribution and confirmed, following a suggestion in [3.37] that the spatial correlation structure of a rainfield could be described satisfactorily by a power spectrum

fitted by a power law. Work in [3.38] drew attention of the need for modellers to give proper attention to the asymmetry of the scaling behaviour of rainfields in space and time, addressed the problem of advection and derived a model using Fourier transforms. More recent studies focused on the development of models able to downscale rainfall satisfactorily in space and time [3.39] and [3.40].

To assist in studying the impact of correlated rain attenuation on the satellite footprint, a recent development at the MTS Research Group is the development of a 2D channel simulator of rainfields accompanied with its comprehensive theoretical stochastic model [3.10]. A typical snapshot of the synthesised rainfield is shown in Figure 3.13.

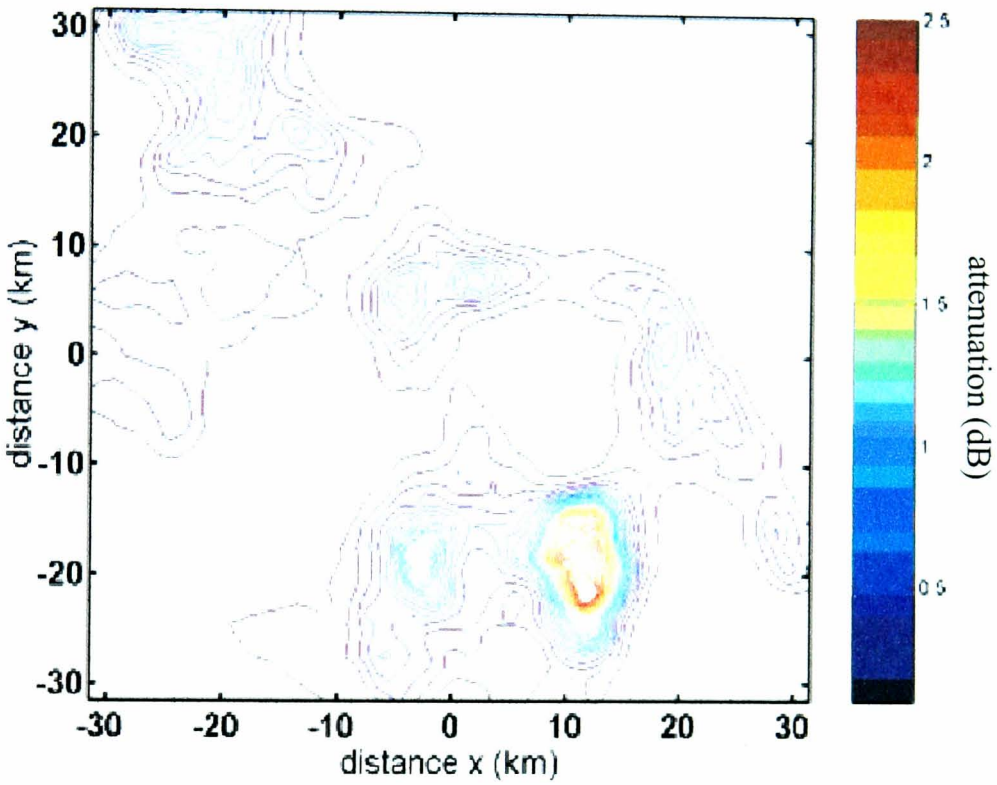

Figure 3.13 Example of synthesised rainfield

In this particular case, there is a raincell in the lower right quadrant with a small peak attenuation of about 2.5 dB. Obviously, in the case of a communication scenario, the BoD algorithm should try and avoid multiplexing together requests emanating from rainy regions because this would require a large amount of network resources (for both traffic and FMT purposes). Over a small geographical area, a uniform density of users can be assumed, so that normal and FMT traffic can be evaluated assuming realistic correlated/decorrelated rain conditions.

The main purpose of the above rainfield model is to try and replicate synthetically rain conditions (rainfall rate in mm/h) as measured on the ground. This type of simulation model

has already been applied to the performance analysis of the carrier-to-noise-plus-interference ratio (CNIR) for microcellular HAP networks [3.42].

An attractive application would also certainly be the management of high frequency broadband communication resources in the presence of spatially correlated dynamic rain fading. Once dynamic rainfall maps can be generated, it is relatively straightforward to transform them into maps of rain attenuation; incorporating these into standard link power budget equations. It is then possible to infer global network performance such as channel utilisation, interference analysis, Quality of Service provisioning in broadband communication networks and the real-time allocation of communication resources based on the user traffic demand *and* the rain fading conditions.

Despite the extreme attractiveness of the above possibility, such rainfield models, to the knowledge of the author, are not yet applicable to the real-time resource management communication scenario under study. Difficulties of their application include the minimum time resolution achieved ([3.20] and [3.40]), which is of the order of 5-6 minutes - the time between radar scans. The inappropriateness of such a time resolution can be realised by considering the fast variations of network traffic (especially with a frame duration of the order of some msec) and the relatively short time intervals that need to be incorporated in a network simulation study.

Rainfield synthesis will be, without a doubt, an invaluable tool to the designers of communications systems impacted by rain. However, based on the above review and on the nature of this thesis focusing on the trade-off analysis of the various important *network* aspects and the investigation of the intrinsic links between resource management and FMT deployment, it is believed that accurate rainfield synthesis is not yet ready for short-term analysis of networks.

Similarly, the incorporation of real data was not considered a wise approach in the case of the short-term analysis this work is focusing on. A major limitation is the availability of simultaneous attenuation time-series (which are not available to the research group in Portsmouth). Processing actual data can also be extremely time consuming and, although data driven propagation models could be used to solve the problem of representing both the spatial and temporal properties of fading [3.43], a time-series random rain synthesiser can be considered sufficient for the design of FMTs and the evaluation of the RA algorithm adaptiveness as targeted by this thesis.

3.5.4 Time-Series Random Rain Synthesiser

A simple simulator function requiring the statistical lognormal parameters $\{\mu, \sigma\}$ previously discussed was developed. A series of normally distributed random numbers, after normalisation and appropriate filtering, go through a non-linear (gaussian to log-normal) transformation, incorporating $\{\mu, \sigma\}$. An example of the time-series generated appeared in Figure 3.9(a).

Typical rain events of various amplitudes and durations (10-20 minutes on average) were produced and saved so that they could be loaded during simulation; events were chosen in order to comply with the following criteria:

- to represent typical rain conditions: light precipitation events, which are produced generally by a stratiform rain structures that occur in winter or spring, and heavy rain events that can be produced during a storm or more generally by convective rain cells, often encountered at the end of spring, in summer or autumn,
- to be able to test the system behaviour with events that require adequate compensation by the FMT,
- to introduce "worst-case" scenarios that will possibly "stretch" the abilities of the system to cope concurrently with both high FMT and traffic demands.

It is believed that the developed random rain simulator is suitable to the requirements of this work, where long-term fading is not the main interest, as it is capable of providing with appropriate test-case scenarios ("best", "worst" or typical cases).

3.6 BoD for Multiple Links with ACM-BLC FMT

For an uplink burst rate of 2048 kbps, the average bit rate $\overline{R}_{bc}^{i}$ for a connection i within a typical MF-TDMA frame of T_F=26.5 ms duration [3.2] is

$$\overline{R}_{bc}^{i}\,[kbps] = \frac{N^i \times N_b}{T_F\,[ms]} \tag{3.20}$$

where N^i is the number of allocated slots per frame for connection i, N_b=424 bits is the number of bits per slot.

Putting in the right numerical values, the number of required slots for a particular average coded bit rate is thus given by:

$$N^i = \frac{\overline{R}_{bc}^{i}[kbps]}{16} \text{ slots/frame} \tag{3.21}$$

Note that the value of 16 kbps is the rate granularity used as the basis for the bandwidth on demand process (i.e. the minimum rate that can be achieved over the period of a frame by the allocation of just one timeslot per frame).

Now, in the event of a fade, expanding the bits by a factor H would lead to a new number of required slots, N'_i':

$$N'_i = \frac{\overline{R}^i_{bc}[kbps]}{16} \times H = N^i \times H \quad \text{slots/frame} \tag{3.22}$$

From the user point of view the user bit rate, $\overline{R}^i_b(t)$, can be variable. H is a function of the attenuation level in time $Att(t)$ (as discussed in chapter 2, see Figure 2.8), the BER threshold, $\hat{BER}$, the clear-sky SNR_{cs}, and the ACM mode (ρ, M) of the system, so the number of allocated slots, $N'_i(t)$, is better written as:

$$N'_i(t) = \left\lceil \frac{\overline{R}^i_b(t)[kbps] \times H(Att(t) \mid \hat{BER}, SNR_{cs}, \rho, M)}{\rho \cdot 16} \right\rceil \tag{3.23}$$

where $\lceil x \rceil$ is the ceiling function. This rounding up ensures enough MF-TDMA resources are allocated to connection i.

The total number of required slots, N_{TOT}, of the MF-TDMA network is simply the sum of slots requested by all users and of course this should never exceed the total number of slots, N_F, existing in a MF-TDMA frame:

$$N_{TOT} = \sum N'_i \leq N_F \quad \text{for each frame} \tag{3.24}$$

where $N_F = 512$ slots per frame, according to the simplified scenario of DVB-RCS, described in [3.2].

As expected, equation (3.23) expresses the number of required FMT slots as a function of rain attenuation, QoS parameters, as well as actual traffic characteristics of the user stations. This simple mathematical model is one of the keys to the simulation and analysis of multiple links. It should also be noted that (3.23) takes the process of mode selection into account (code rate and modulation scheme).

3.7 Conclusions

Starting with the presentation of the communication scenario under study, this chapter focused on a qualitative description of important issues regarding the overall architecture of a DVB-RCS system with FMT.

Considerations of the dynamic physical layer adaptation on the return link were discussed and the essential operation of effective SNR estimation and its impact was reviewed, with the intention to clarify the main focus of this thesis.

An outline of the proposed combined FMT scenario and its effects on resource utilisation was then presented and, after a detailed clear-sky link budget analysis, an extensive discussion of its consequences on the system availability followed. In particular a combination of ACM and BLC will be studied.

The ongoing work on rain modelling and the suitability of the various methods were examined, with the study ending up to the employment of an adequate tool to assist with this work in the following chapters.

The chapter ends with a qualitative design approach with regards to the BLC operation and introduces the complex problem of the dependence of system availability not only on the combined FMT dynamic range, but also on the resource allocation scheme performance.

The need for application of this simplified analysis to a practical scenario and evaluation of the network performance through simulation means becomes necessary. This simulation study will be presented in the following chapters, where consideration of the MAC layer will give to the thesis a more practical and realistic perspective.

3.8 References

[3.1] Watson P. A., Page A., Martellucci A., "Test Case 3: V-Band VSAT Asymmetrical Data Communication System", COST 255 Final Report, Radiowave Propagation Modelling for SatCom Services at Ku-Band and above, Volume 2, pp. 6.3-3-6.3-11, Bech, Luxembourg, 1999.

[3.2] Noussi E., Grémont B. C., Filip M., "Basis for Fade Mitigation Technique Implementation over the DVB Return Channel by Satellite", Internal Research Report 03/11, University of Portsmouth, Department of Electronic & Computer Engineering, June 2003.

[3.3] ETSI EN 301 790 V1.4.1: "Digital Video Broadcasting (DVB); Interaction Channel for Satellite Distribution Systems", 2005-09, retrieved June 11, 2008, from the ETSI website: http://www.etsi.org

[3.4] Fairhurst G., "Broadband Multimedia Satellite Systems", Jan. 2001, retrieved January 2003, from http://www.erg.abdn.ac.uk/public_html/research/future-net/digital-video/bband-sat.html

[3.5] Grémont B., Castanet L., Bousquet M., Alamanac A. B., Radzik J., "Closed-Loop SNR Estimation for DVB Type Satellite Communications", Cost Action 280, PM8-020, Rome, Italy, November 2004.

[3.6] Schweikert R., Wörz A. J., Lücke O., Werner M., "Protocols and Signalling for Adaptive Fade Mitigation Techniques (FMT) in DVB-RCS Multi-Beam Systems": Executive Summary, ESA Study Contract Report, Issue 01, 12 October 2005.

[3.7] Pauluzzi D. R., Bealieu N. C.: "A comparison of SNR Estimation Techniques for the AWGN Channel", IEEE Trans. on Communications, vol. 48, no. 10, pp. 1681-1691, October 2000.

[3.8] Noussi E., Grémont B., Filip M.: "Integration of Fade Mitigation within Centrally Managed MF-TDMA/DVB-RCS Networks", Special Issue on "Satellite Network Protocols and Performances", International Journal of Space Communications (full manuscript accepted by the editorial board), to be published in 2008, available on demand from the authors.

[3.9] Spacebridge Semiconductor, "SB7088 Broadband Wireless Return Channel Modulator", Advance Product Information, retrieved December 2005, from http://www.spacebridge.com/products/sb7088.htm

[3.10] Grémont B., Filip M., "Spatio-Temporal Rain Attenuation Model for Application to Fade Mitigation Techniques", IEEE Transactions on Antennas and Propagation, vol. 52, no. 5, pp. 1245-1256, May 2004.

[3.11] Noussi E., Grémont B., Filip M., "A Demand Assignment Algorithm for FMT Resource Management in DVB-RCS Networks", PREP 2005 Proceedings, p. 32-33, 30 March-1 April 2005, University of Lancaster, UK.

[3.12] Noussi E., Grémont B., Filip M., "Adaptive MF-TDMA: Burst Length Control as a Rain Fade Countermeasure", 4th Int. Symposium on Communication Systems, Networks and Digital Signal Processing (CSNDSP 2004) Proceedings, p. 43-46, University of Newcastle upon Tyne, 20-22 July 2004.

[3.13] Filip M., "Adaptive modulation as a Fade Countermeasure", PhD Thesis, University of Portsmouth, 1992.

[3.14] "Protocols and Signalling for Fade Mitigation Techniques (FMT) in DVB-RCS Multi-beam Systems", ESA Workshop on 'Fade Mitigation Techniques for DVB-S2/DVB-RCS systems', Noordwijk, The Netherlands, 13-14 December 2004.

[3.15] "Protocols and Signalling for Fade Mitigation Techniques (FMT) in DVB-RCS Multi-beam Systems", ESA Workshop on 'Fade Mitigation Techniques for DVB-S2/DVB-RCS systems', Noordwijk, The Netherlands, 13-14 December 2004.

[3.16] Maral G., Bousquet M., "Satellite Communications Systems - Systems, Techniques & Technology", 3rd edition, John Wiley & Sons, England, 1998.

[3.17] Zong P., Filip M., "Satellite Link Budgets for COST 255 Test Case", Internal Report 98/9, University of Portsmouth, December 1998.

[3.18] Grémont B.: "Fade Countermeasure Modelling for Ka-band Satellite Links", PhD Thesis, Coventry University, November 1997.

[3.19] Ippolito L. J.: "Radio propagation for space communications systems", IEEE Proceedings, Vol. 69, No. 6, pp. 697-727, U.S.A., June 1981.

[3.20] Grémont B., "Simulation of Rainfield Attenuation for Satellite Communication Networks", COST Action 280, Propagation Impairment Mitigation for Millimetre Wave Radio Systems, 1st International Workshop, PM3014, July 2002.

[3.21] ITU, Rec. ITU-R P.837-3 1, Recommendation ITU-R P.837-3, "Characteristics of Precipitation for Propagation Modelling", 2001.

[3.22] Bhargava V. K., Haccoun D., Matyas R., Nuspl P. P, "Digital Communications by Satellite: Modulation, Multiple Access and Coding", Wiley, New York, 1981.

[3.23] Olsen R. L., Rogers D. V., Hodge D. B., "The αR^b Relation in the calculation of Rain Attenuation", IEEE Trans. Antenn. Propagat., vol. AP-26, no. 2, pp. 318-329, Feb. 1978.

[3.24] ITU-R P.618-7, Radiowave Propagation, "Propagation Data and Prediction Methods Required for the Design of Earth-Space Telecommunication Systems", 2001.

[3.25] Filip M., Vilar E., "Optimum Utilization of the Channel Capacity of a Satellite Link in the Presence of Amplitude Scintillations and Rain Attenuation", IEEE Transactions on Communications, vol. 38, no. 11, pp. 1958-1965, Nov. 1990.

[3.26] ITU-R P.838-1, Radiowave Propagation, "Specific Attenuation Model for Rain for Use in Prediction Methods", 1999.

[3.27] Crane R. K., "Electromagnetic Wave Propagation through Rain", Wiley Ser. Remote Sens., John Wiley, New York, 1996.

[3.28] Manning R. M., "A rain attenuation model for satellite link attenuation predictions incorporating the spatial inhomogeneity of rainrate", International Journal. of Satellite Communications, vol. 2, 187-197, 1984.

[3.29] Capsoni C., Fedi F., Magistroni C., Paraboni A., Pawlina A., "Data and theory for a new model of the horizontal structure of rain cells for propagation applications", Radio Science, 22(3), 395-404, 1987b.

[3.30] Lovejoy S., "Area-Perimeter Relation for Rain and Cloud Areas", Science, vol. 216, 185-187, April 1982.

[3.31] Rys F.S., Waldvogel A., "Fractal Shape of Hail Clouds", Physical Review Letters, vol. 56, no. 7, 784-787, February 1986.

[3.32] Callaghan S. A., "Fractal Analysis and Synthesis of Rain Fields for Radio Communication Systems", PhD Thesis, University of Portsmouth, March 2004.

[3.33] Foufoula-Georgiou E., Krajewski W., "Recent Advances in Rainfall Modelling, Estimation and Forecasting", Rev. Geophys., July Supplement, 1125-1137, 1995.

[3.34] Bell T. L., "A Space-Time Stochastic Model of Rainfall for Satellite Remote Sensing Studies", Journal of Geophysical Research, vol. 92, pp. 9631-9643, 1987.

[3.35] Crane R. K., "Space-Time Structure of Rain Rate Fields", J. Geophys. Res., vol. 95, pp. 2011-2020, 1990.

[3.36] Pegram G. G. S., Clothier A. N., "The String of Beads Rainfall Model and its Application in Simulation and Forecasting", Proceedings 9th SA National Hydrology Symposium, University of the Western Cape, South Africa, 1999.

[3.37] Menabde M., Harris D., Seed A. W., Austin G., "Self-Similar Random Fields and Rainfall Simulation", J. Geophys. Research, vol. 102, pp. 13509-13515, 1997.

[3.38] Marsan D., Schertzer D., Lovejoy S., "Casual Space-Time Multifractal Processes: Predictability and Forecasting Rain Fields", J. Geophys. Research, vol. 101, pp. 26333-26346, 1996.

[3.39] Seed A. W., Srikanthan R., Menabde M., "A Space and Time Model for Design Storm Rainfall", J. Geophys. Research, p. 9693-9714, 2001.

[3.40] Pegram G. G. S., Clothier A. N., "Downscaling Rainfields in Space and Time, using the String of Beads Model in Time Series Mode", Hydrology and Earth System Sciences, vol. 5, no. 2, pp. 175-186, 2001.

[3.41] Grémont B., "Simulation/Modelling of Rainfields for Terrestrial and Satellite Network Applications", Microwave Telecommunication Systems (MTS) Research Group, University of Portsmouth, retrieved June 11, 2008, from the University of Portsmouth website: http://www.port.ac.uk/research/telecoms/researchareas/satellitecommunications/simulationofrainfields/

[3.42] Spillard C., Tozer T., Gremont B., Grace D., "The Performance of High-Altitude Platform Networks in Rainy Conditions", 22nd AIAA International Communications Satellite Systems Conference, Monterey, USA, 9-12 May 2004, AIAA-2004-3220.

[3.43] Grémont B., Watson R. J., Watson P. A., Hodges D. D., "Modelling and Detection of Rain Attenuation for MF-TDMA Satellite Networks Utilizing Fade Mitigation Techniques", Int. Workshop of Cost Actions 272 and 280, Satellite Communications - From Fade Mitigation to Service Provision", p. 277-284, ESTEC, Noordwijk, The Netherlands, 26-28 May 2003.

[3.44] Carassa F., "Methods to Improve Satellite Systems Performances in the Presence of Rain", Alta Frequenza, vol. LVI, no. 1-2, pp. 173-184, Jan-Apr 1987.

[3.45] Carassa F., "Adaptive Methods to Counteract Rain Attenuation Effects in the 20/30 GHz Band", Space Communication and Broadcasting, vol. 2, pp. 253-269, 1984.

[3.46] Baptista J. P. V. P., "Simultaneous Rain Attenuation Observations in the Three SIRIO Italian Stations: Statistical Results after Five Years' Activity", Electronic Letters, 10th May 1984, vol. 20, no. 10, p. 427-429.

CHAPTER 4

RESOURCE ALLOCATION ALGORITHM FOR DVB-RCS WITH FADE MITIGATION

The application of suitable FMTs for the enhancement of current standards has been hinted at as desirable in chapter 2. A technique that could extend the dynamic range and potentially improve the link availability of power-limited return channels appears to be particularly attractive. A description of important issues regarding the overall DVB-RCS architecture with FMT has been provided in chapter 3 and a qualitative design approach with regards to the BLC operation introduced the complex problem of the dependence of system availability on the RA scheme performance.

Starting with a description of the traffic generation model, developed for the purposes of the network simulation, this chapter provides a review of capacity organisation and segmentation details that provide the basis for the BoD operation. Then, the problem of resource management under rain conditions is addressed, by presenting the proposed resource allocation protocol that incorporates FMT implementation within a dynamic capacity assignment strategy.

4.1 Traffic Source Modelling

4.1.1 Background

As already discussed so far, satellite bandwidth is a limited and expensive commodity, which must be used as efficiently as possible to support a large number of users and provide good returns for the service provider. The achievable bandwidth utilisation efficiency and the resulting Quality of Service (QoS) that users obtain are governed by the underlying multiple access scheme. Satellite systems have traditionally been used to provide telephony and TV/video broadcast services, invariably provided by fixed bandwidth allocation for the

duration of the connection. The rapid growth of the Internet has resulted in the development of a wide range of services including telephony and audio/video streaming. In sparsely populated regions of the world, satellites are often the only economic means of providing people with Internet access and so the next generation satellite systems will be required to support an increasing proportion of Internet traffic [4.1]. Internet traffic is highly bursty; demand from users accessing web browsing, file transfer and electronic mail applications is difficult to predict, very bursty and often highly asymmetric - forward channel data rates are often far in excess of return channel requirements [4.2].

The complexity of traffic in a multimedia network is a natural consequence of integrating, over a single communication channel, a diverse range of traffic source such as video, voice and data that significantly differ in their traffic patterns as well as their performance requirements. Specifically, bursty traffic patterns generated by data sources and variable bit rate (VBR) real-time applications such as compressed video and audio tend to exhibit certain degrees of correlation between arrivals, and show long-range dependence in time (self-similar traffic) [4.3]

Due to the increasing dominance of Internet traffic, the focus of this thesis is on the transport of Internet traffic and traffic sources were modelled accordingly. It is well known that Internet traffic exhibits self-similarity [4.3]-[4.9]. A great deal of previous evaluations of satellite communication protocols have been based on simple ON/OFF or Poisson traffic sources, which do not accurately reflect the behaviour of Internet traffic [4.10]. Therefore in this thesis self-similar processes with long-range dependence are employed for the traffic sources to better represent real Internet traffic.

4.1.2 Self-Similarity in Network Traffic

A. What is Self-Similarity?

A self-similar phenomenon displays structural similarities across a wide range of timescales. Traffic that is bursty on many or all timescales can be statistically described using the notion of self-similarity. Self-similar is the property associated with "fractals", which are objects whose appearances are unchanged regardless of the scale at which they are viewed [4.5]. In the case of stochastic objects such as time series, self-similarity is used in the distributed sense: when viewed at varying timescales, the object's relational structure remains unchanged. As a result, such a time series exhibits bursts at a wide range of timescales [4.3].

B. What Causes Self-Similarity?

Since self-similarity is believed to have a significant impact on network performance, understanding what causes self-similarity in traffic is important.

Research has revealed that the traffic generated by World Wide Web transfers shows self-similar characteristics. Some researchers have looked at network traffic at the packet level, identified the flows between individual source/destination pairs, and showed that transmission and idle times for those flows were heavy-tailed [4.7]. Others' work has been based on data collected at the application level rather than network level. Observations allowed them to build on the conclusions presented in [4.7] by showing that the heavy-tailed nature of transmission and idle times is not primarily a result of network protocols or user preference, but rather stems from more basic properties of information storage and processing: both transmission and user "think" times are themselves strongly heavy-tailed [4.5]. Transmission times may be heavy-tailed, primarily due to the distribution of available file sizes in the Web. Silent times may also be heavy-tailed, primarily due to the influence of user think time. Comparing the distributions of ON and OFF times, they found that the ON time distribution was heavier-tailed than the OFF time distribution. The distribution of file sizes in the Web might be the primary determiner of Web traffic self-similarity. In fact, it has been shown that the transfer of files whose sizes are drawn from a heavy-tailed distribution is sufficient to generate self-similarity in network traffic. The ON and OFF periods do not need to have the same distribution. These results suggest that the self-similarity of Web traffic is not a machine-induced artefact; in particular, changes in protocol processing and document display are not likely to remove the self-similarity of Web traffic [4.3].

C. Self-Similar Model

Self-similar traffic is bursty over a wide range of timescales and can be modelled by the superposition ON/OFF sources with heavy-tailed distribution of ON and OFF times. During each ON period, a train of packets is generated with invariant inter-arrival time, dependant on the overall activity level of the source, with each terminal contributing an equal amount of traffic to the channel. The traffic source is completely inactive during each OFF period (i.e. no packets are generated). A heavy-tailed distribution is one with a significant probability of obtaining large values. The simplest heavy-tailed distribution is the Pareto distribution, with the packet generation depicted in Figure 4.1. It is specified by [4.7]:

$$P(t) = \alpha k^{a} t^{-a-1} \qquad (a, k > 0,\ x \geq k) \tag{4.1}$$

where k represents the smallest possible value of the random variable (location parameter). The parameter α is the shape parameter and defines the tail of the distribution; as α decreases,

an arbitrarily large portion of the probability mass may be present in the tail of the distribution. The Pareto probability density function is plotted in Figure 4.2 for three different values of α. Variance is infinite when $1 \leq \alpha \leq 2$ [4.7]. The mean value of the distribution, $E(x)$ is given by:

$$E(x) = \frac{k\alpha}{\alpha - 1} \tag{4.2}$$

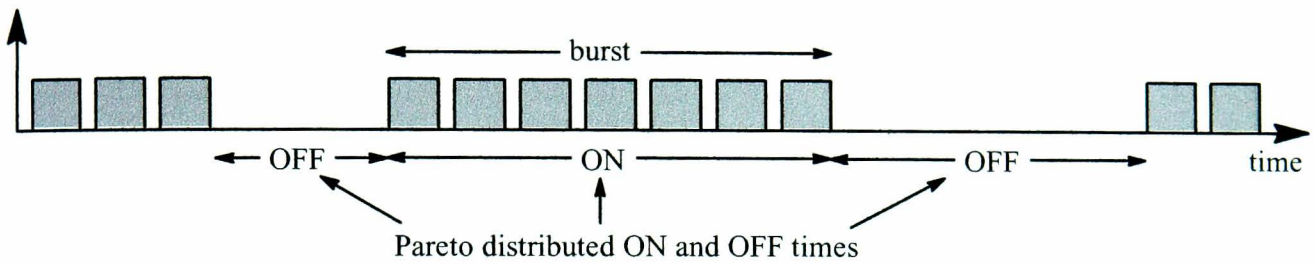

Figure 4.1 A Pareto distributed ON/OFF packet generation process

Pareto distributions have a number of properties that are qualitatively different from distributions commonly encountered such as the exponential, normal, or Poisson distributions. In practical terms, a random variable that follows a Pareto distribution can give rise to extremely large values with non-negligible probability [4.4] and [4.11].

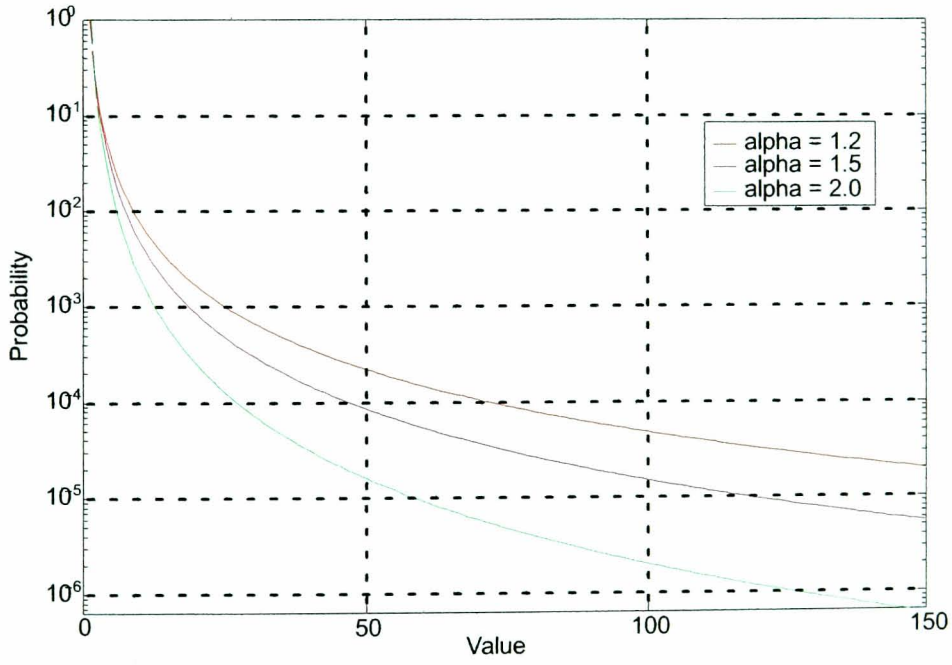

Figure 4.2 Pareto probability density function (pdf)

The way to set the parameters involved and generate values fitting a Pareto probability density function through simulation is shown later, in section 5.1.3 of the next chapter.

4.2 Resource Management at Network Level

4.2.1 Segmentation of the Return Link Capacity

In a Satellite Interactive Network, the timeslots of the return link are organised and numbered so that the network is able to allocate them to individual active RCSTs [4.12].

A. Superframes

A superframe is a portion of time and frequency of the return link. The superframe duration is actually the elementary period of time for the assignment of resources to terminals. Within a Satellite Interactive Network, a superframe identifier, "SF_ID", identifies the return link resources accessed by a given set of RCSTs.

Figure 4.3 shows how the global return link capacity may be segmented amongst sets of RCSTs; the network will then manage several SF_IDs (i.e. separate sets of carrier frequencies). In this figure a typical example of two SF_IDs (i.e. two separate sets of carrier frequencies) corresponding to two RCST groups is shown. For simplicity reasons it is assumed that these frequency sets are fixed, i.e. that superframes have fixed bandwidth (otherwise a change in a superframe's bandwidth would affect the whole arrangement and all RCSTs groups would then have to be notified and have their superframe bandwidth adjusted appropriately).

For each superframe of a given SF_ID, allocation of timeslots is communicated to the RCSTs via the TBTP table. An RCST is thereafter allowed to transmit data bursts in timeslots which were allocated to it.

As shown in Figure 4.3, the consecutive superframes (in green colour) of a given SF_ID are contiguous in time. Each occurrence of a superframe in time is labelled with a number called "SF_counter". Consider for example "SF_counter 1" and "SF_counter 2" (i.e. the first two superframes) of "SF_ID 2". They are of the same composition and duration, unless a notification that a change should be applied is provided; this is what happens at the boundary between the second and third superframe (between SF_counter 2 and SF_counter 3 of SF_ID 2), so that the third superframe is of different composition as well as duration. The superframe duration actually changes from T_1 to T_2 for SF_counter 3. This notification involves the Terminal Burst Time Plan (TBTP) and the Superframe, Frame and Timeslot Composition Tables (SCT, FCT, TCT), which will be described in detail later on.

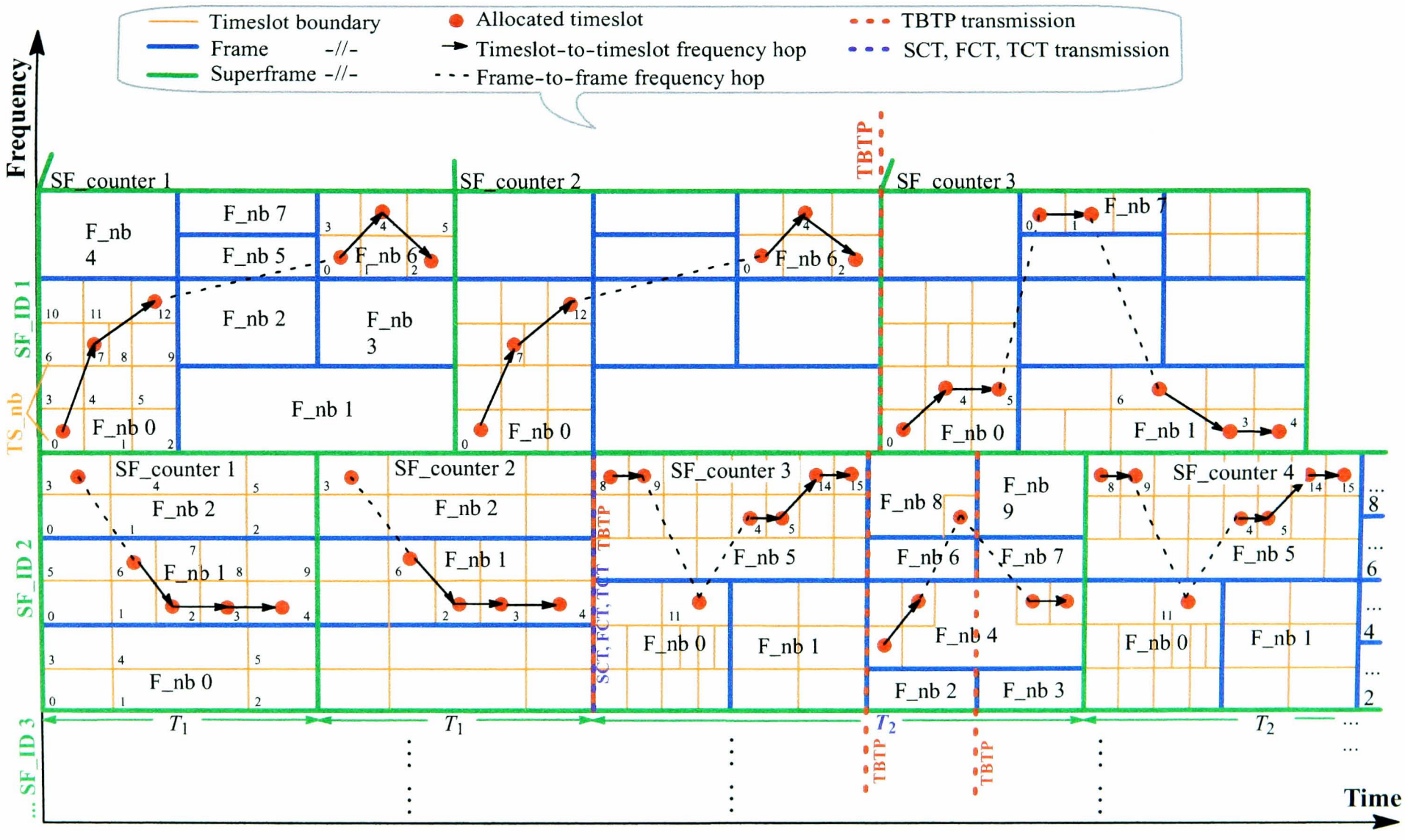

Figure 4.3 An example of global return link capacity segmentation and timeslot allocation

B. Frames

A superframe is composed of frames (Figure 4.3, in blue colour), themselves composed of timeslots (orange). The frame is at an intermediate level between the superframe and the timeslots. It is introduced for reasons of signalling efficiency (on the forward link signalling). The frame duration is not used as the basis of any timeslot allocation process.

In a superframe, frames are numbered from 0 (lowest frequency, first in time) to N (highest frequency, last in time), ordered in time then in frequency (F_nb represents the frame number) and can take the values:

$$0 \leq N \leq 31 \tag{4.3}$$

This numbering scheme used for frames [4.12] is shown in Figure 4.4. It enables the network to allocate timeslots to individual RCSTs.

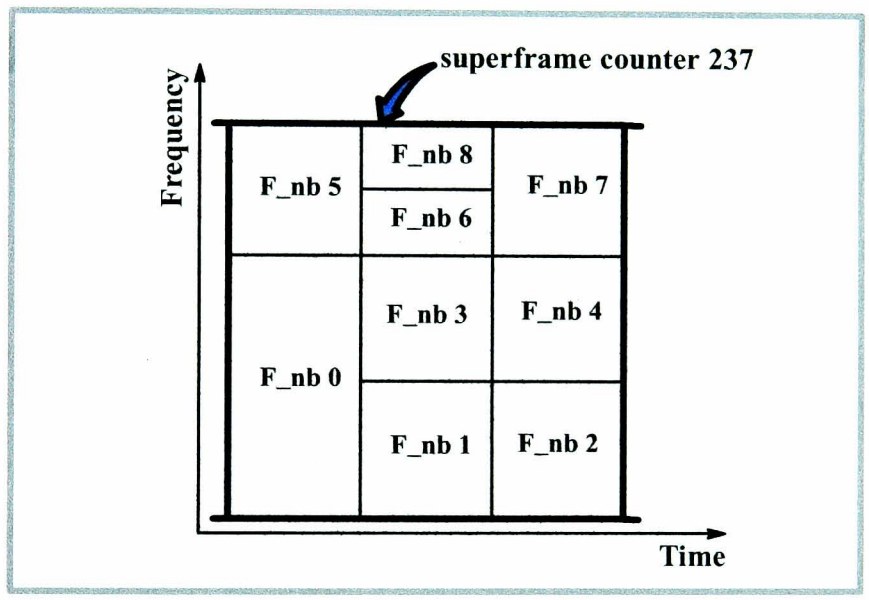

Figure 4.4 Example of superframe composition

Consider the first and second frames of the third superframe in Figure 4.3 (i.e. F_nb 0 and F_nb 1 in SF_counter 3) of SF_ID 1. They are of different duration, different bandwidth and different timeslot composition. Therefore, frames within a superframe may not all have the same duration, bandwidth and timeslot composition. If they all have the same duration, frames can be seen as frequency sub-bands of the superframe. Figure 4.4 shows an example of one superframe lasting 3 times more than each of its frames, which in this example all happen to have the same duration.

C. Timeslots

A frame is composed of timeslots. It may span over several carrier frequencies. In a frame, timeslots are numbered from 0 (lowest frequency, first in time) to M (highest frequency, last in time), ordered in time then in frequency [4.12] (see Figures 4.5 and 4.3).

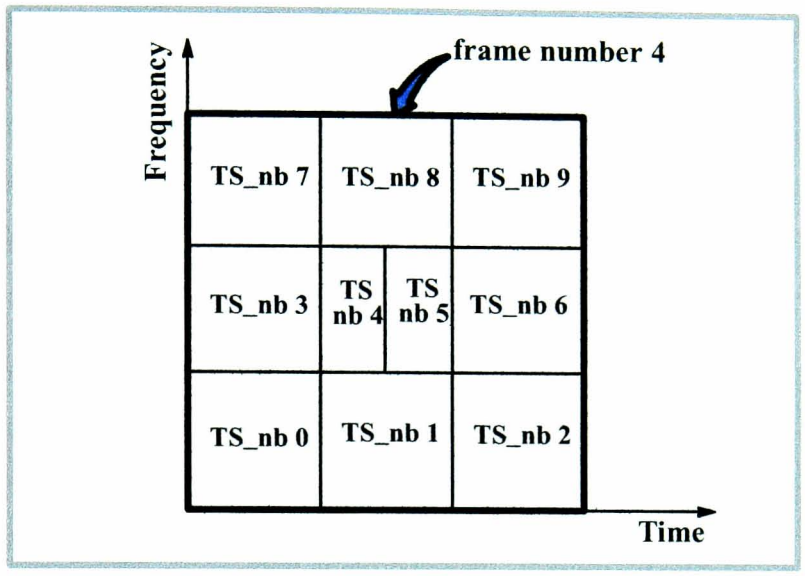

Figure 4.5 Example of frame composition

The number of slots in a frame can be in the range:

$$0 \leq M \leq 2047 \tag{4.4}$$

Again, this numbering scheme was applied and is shown in Figure 4.3. The bandwidth of timeslots shown in the figure is considered to be fixed for simplicity reasons; it is however possible (with flexible RCSTs [4.12]) to have variable bandwidth/variable duration of successive slots allocated to each RCST.

For the purpose of allocation, each timeslot is uniquely identified by its SF_ID, SF_counter, F_nb and timeslot number ("TS_nb"). Each terminal may transmit on any single frequency at a given time; however, as shown in Figure 4.3, a terminal is not allowed to transmit data on more than one carrier at a time, in order to minimise the power output requirement and reduce the hardware complexity of terminals.

The RCST shall process the TBTP message received from the NCC, to extract the assignment count and timeslot allocations for its next uplink transmissions.

4.2.2 Forward Link Signalling and Terminal Burst Time Plan

The forward link carries signalling from the NCC and user traffic to RCSTs. The signalling from the NCC to RCSTs that is necessary to operate the return link system is called

Forward Link Signalling. Both the user traffic and forward link signalling can be carried over different forward link signals. Several RCST configurations are possible depending on the number of forward link receivers present on the RCST.

The terminals access a pattern of time/frequency slots within the frames. Having established knowledge of the MF-TDMA structure via the forward link tables, the terminal accesses the network using a slotted-Aloha burst [4.12] and [4.13]. Thereafter, traffic capacity is allocated dynamically, allowing the terminal to operate in a contentionless mode. A terminal can only transmit once it has forward channel reception. Moreover, the RCST must have been synchronised, logged in, and have allocated capacity (in terms of MF-TDMA slots).

This message is sent by the NCC to a group of terminals. The group is addressed by a logical Group identifier, while each individual terminal is addressed by a logical Logon identifier. Both "Group_ID" and "Logon_ID" are notified to the terminal at logon time. It contains one or more entries for each RCST with each entry defining an assignment of a contiguous block of timeslots. Each traffic assignment is described by the number of the start timeslot in the block and a repetition factor giving the number of consecutive timeslot allocations. The TBTP allows timeslots to be allocated once or continuously. In the latter case a mechanism is provided to add or remove time slot allocations from the TBTP.

The frequency hopping from timeslot to timeslot (as well as from frame to frame) is illustrated in Figure 4.3. The hopping pattern stays the same from superframe to superframe unless a change is communicated to the RCST group through the TBTP that is normally generated every superframe.

The standard document [4.12] states that the TBTP will be updated every superframe, or equivalently, for each increment of the superframe count parameter. When the superframe duration is long (its definition allows superframes to be as long as 93.2 sec), an update rate of once per superframe would lead to unacceptable response times for the DVB-RCS system. This potential problem is remedied by observing that the definition of the TBTP does not preclude it from being transmitted several times per superframe [4.14]. In such a scheme (see Figure 4.3, SF_counter 3 of SF_ID 2) consecutive TBTPs contain the same superframe count value, but different frame number values.

Similarly, if the frames themselves are long in duration, they too could possibly be split up into multiple TBTP assignments. In this case (see Figure 4.3, F_nb 4 in SF_counter 3 of SF_ID 2), the TBTPs would contain the same superframe count and frame number parameter values, but would differ in their "Start_slot" parameter values. So, the third TBTP would also

use SF_counter 3, F_nb 4 with different "Start_slot" values, as well as the extra frame numbers 3, 7 and 9.

The terminals have a specific frequency range for the frequency hopping (usually 20 MHz is referred to as the frequency hopping range for MF-TDMA [4.15]; this range is communicated from a terminal to the NCC in a common signalling channel (CSC) burst (initial slotted ALOHA) during the logon procedure. The NCC can then allocate appropriate slots/frequencies to the terminal.

4.2.3 Simplified Model of BoD in DVB-RCS

The duration of a DVB-RCS slot is linked to the burst rate $R_{burst\ rate}$ according to:

$$R_{burst\ rate} = \frac{(no.\ of\ bits\ per\ ATM\ cell) \times (no.\ of\ ATM\ cells\ per\ slot)}{\Delta T_{SLOT}} \tag{4.5}$$

For the system studied in this thesis, the following are considered:

- 2.048 Mbps burst rate for the return link
- 1 ATM cell per timeslot [4.14] and [4.15]
- ATM cell of 53 bytes length (5 bytes of header and 48 bytes of payload) [4.12], [4.14], and [4.15].

The above formula becomes:

$$2.048 \times 10^6 = \frac{424}{\Delta T_{SLOT}} \tag{4.6}$$

$$\Leftrightarrow \quad \Delta T_{SLOT} = 0.207031 \text{ ms} \tag{4.7}$$

Consider the occurrence of two superframes as illustrated in Figure 4.6. These are similar to the ones shown in Figure 4.3, except for the fact that frames are considered to have fixed bandwidth and duration and timeslots are also of fixed duration.

Suppose that this was the timeslot allocation for a given terminal and that it changed from one superframe to the other through the transmission of an updated TBTP, due to a request of the terminal for more timeslots.

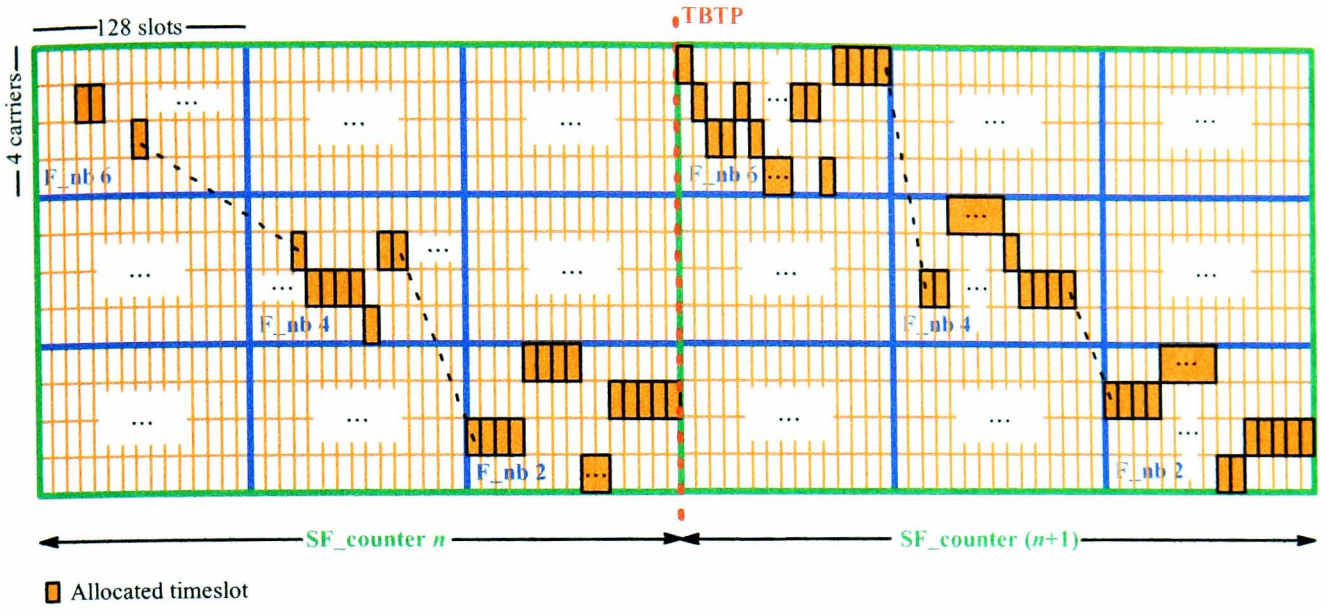

Figure 4.6 Simplified scenario of fixed frames and timeslots: an example of resource allocation

For a burst rate of 2.048 Mbps [4.16] a typical MF-TDMA frame can be assumed, as illustrated above (the scale of the above figure is not realistic and the number of frames within the superframe is just indicative). The frame includes 4 carriers, each consisting of 128 traffic slots, with granularity of 16 kbps.

For SF_counter n, 3 slots in F_nb 6, 8 slots in F_nb 4 and 128 (i.e. all) slots in F_nb 2 are allocated to a particular active terminal, which leads to a total of 139 slots for that super-frame.

For example, for F_nb 6 the average bit rate is:

$$\overline{R}_b = \frac{no.\ of\ allocated\ slots \times bits\ per\ slot}{T_F} = 48 \text{ kbps } (\equiv 3R_{bg}) \tag{4.8}$$

For F_nb 4:

$$\overline{R}_b = 128 \text{ kbps } (\equiv 8R_{bg}) \tag{4.9}$$

For F_nb 2:

$$\overline{R}_b = 2048 \text{ kbps } (\equiv 128R_{bg}) \tag{4.10}$$

The peak bit rate, $\hat{R}_b$, considered over the duration of a frame, would consist of giving contiguous timeslots over a certain duration, i.e.

- 3 slots over a period of $3 \times \Delta T_{SLOT}$ $\equiv$ 2048 kbps over 0.621 ms
- 2048 kbps over a period of 1.656 ms
- 2048 kbps over a period of 26.5 ms (frame duration)

In SF_counter n+1, after the terminal's request for more timeslots, a total of 380 slots is allocated, just 4 slots below the maximum a user can actually get for the particular example of a superframe.

Summarising:

	SF_counter n		SF_counter n+1	
F_nb	$\overline{R}_b$ (kbps)	$\hat{R}_b$ = 2.048 Mbps over:	$\overline{R}_b$ (kbps)	$\hat{R}_b$ = 2.048 Mbps over:
6	48	0.621 ms (3 slots)	2048	26.5 ms (1 frame)
4	128	1.656 ms (8 slots)	1984	25.67 ms (124 slots)
2	2048	26.5 ms (1 frame)	2048	26.5 ms (1 frame)

Table 4.1 Average and peak rate changes for a terminal from one superframe to the other

It is therefore obvious that, thanks to the system's bandwidth-on-demand capability, a user station can vary the bit rate according to its traffic needs. The following section will present the resource allocation algorithm designed for the purpose of simulating the BoD controller of an MF-TDMA network, taking into account the BoD requests from the user stations as well as the rain conditions affecting each connection.

4.2.4 The Resource Allocation Algorithm

The task of the BoD controller, assignment of resources in response to a BoD request, clearly implies the need for an adaptive BoD algorithm. The main issues to be dealt with are fairness, channel efficiency and QoS control for multiple BoD flows. The following summarises the BoD process.

The BoD controller receives all user traffic requests $\overline{R}_b^i$ and, from measured fading conditions, having selected the appropriate ACM mode for each user and corresponding bandwidth B_i, the controller can then calculate the requested burst duration $T_i = \overline{R}_b^i / k'(Att_i)$ for each connection i for the following frame interval (Equation (2.8)). The BoD controller can then group the connections using the same ACM mode (and bandwidth) into ACM request tables shown in Figure 4.7. In practice, every table will have a different size and the entries will depend on actual rain conditions and current traffic requirement of each traffic source. The number of ACM tables may also be variable, depending on the rain conditions. Figure 4.8 shows the top-level block diagram of the simulation model.

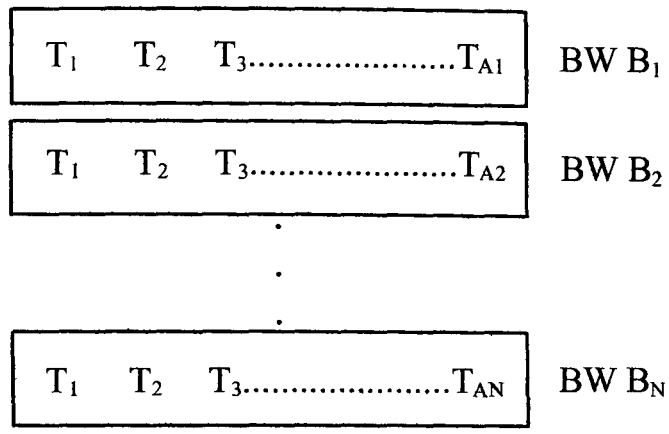

Figure 4.7 ACM request tables (grouped according to their required ACM mode or equivalently their carrier bandwidth)

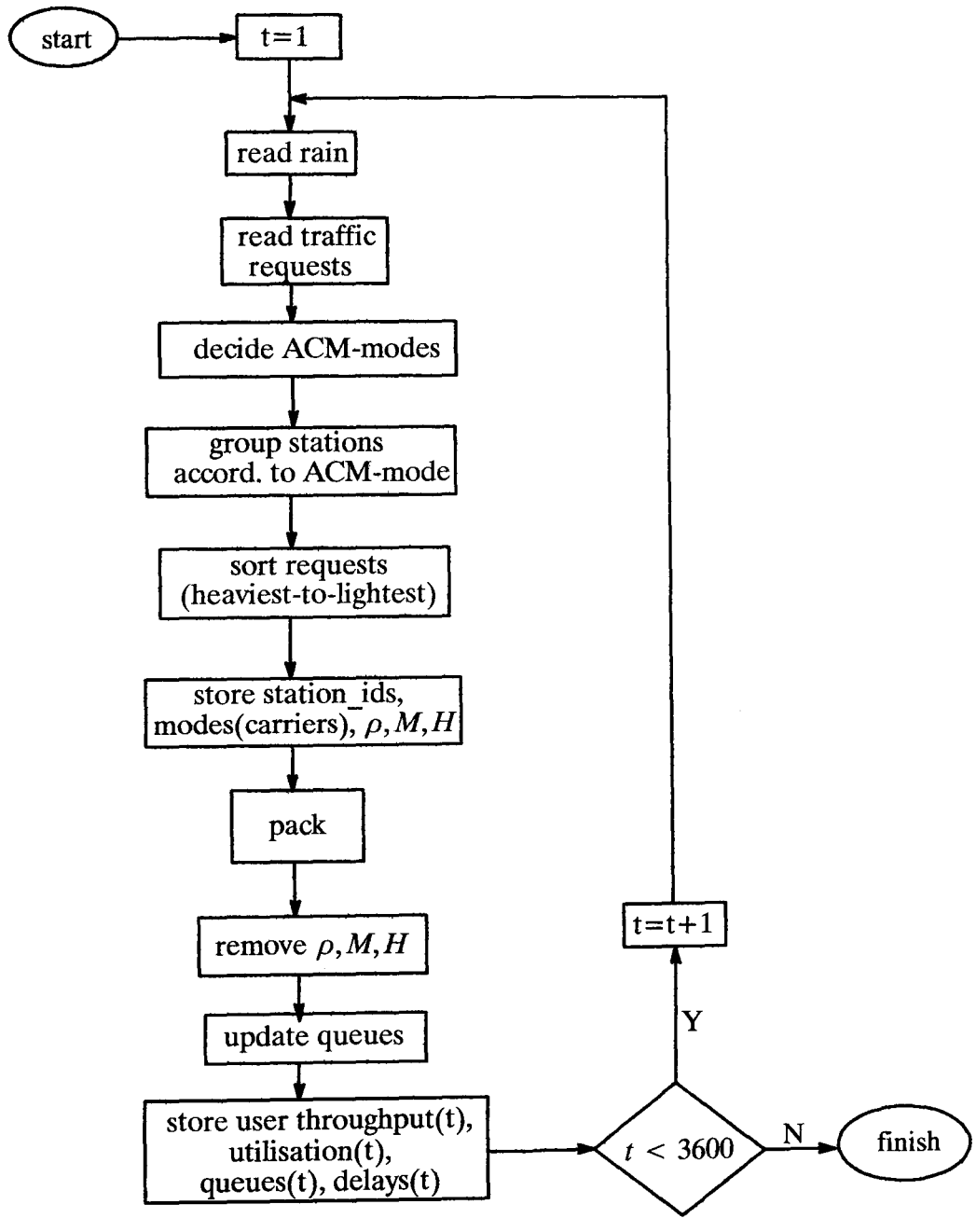

Figure 4.8 Top-level block diagram of RA simulator

The BoD controller's next task is to calculate the proportion of MF-TDMA usage that will be required for each ACM mode (or carrier bandwidth). This ensures that all the flows with different ACM mode are treated fairly. If A_{req} is the total required MF-TDMA area given by:

$$A_{req} = \sum_{j=1}^{N} B_j \times \left[\sum_{i=1}^{A_j} T_i \right] \tag{4.11}$$

then the proportion P_j, $0 \leq P_j \leq 1$, of the MF-TDMA area required for each mode is

$$P_j = \frac{B_j \sum_{i=1}^{A_j} T_i}{A_{req}}, \qquad j = 1,2,...,N \tag{4.12}$$

Therefore the number of channels of width B_j needed in the next MF-TDMA frame is

$$N_j = \left\lfloor \frac{P_j \times B_{\max}}{B_j} \right\rfloor, \qquad j = 1,2,...,N \tag{4.13}$$

where $\lfloor x \rfloor$ means the integer part of x and $B_{\max}$ is the total MF-TDMA bandwidth available to the BoD resource controller.

After the bandwidth is appropriately segmented using the above equations, the controller's next step is to allocate burst durations $\tilde{T}_i \leq T_i$ to each traffic request in the same ACM request table. This is achieved by running a resource allocation algorithm. In this thesis, the requests are first sorted from heaviest-to-lightest (Figure 4.8). Then a round-robin allocation is applied for serving the requests. Figure 4.9 shows the flow-chart of the packing algorithm.

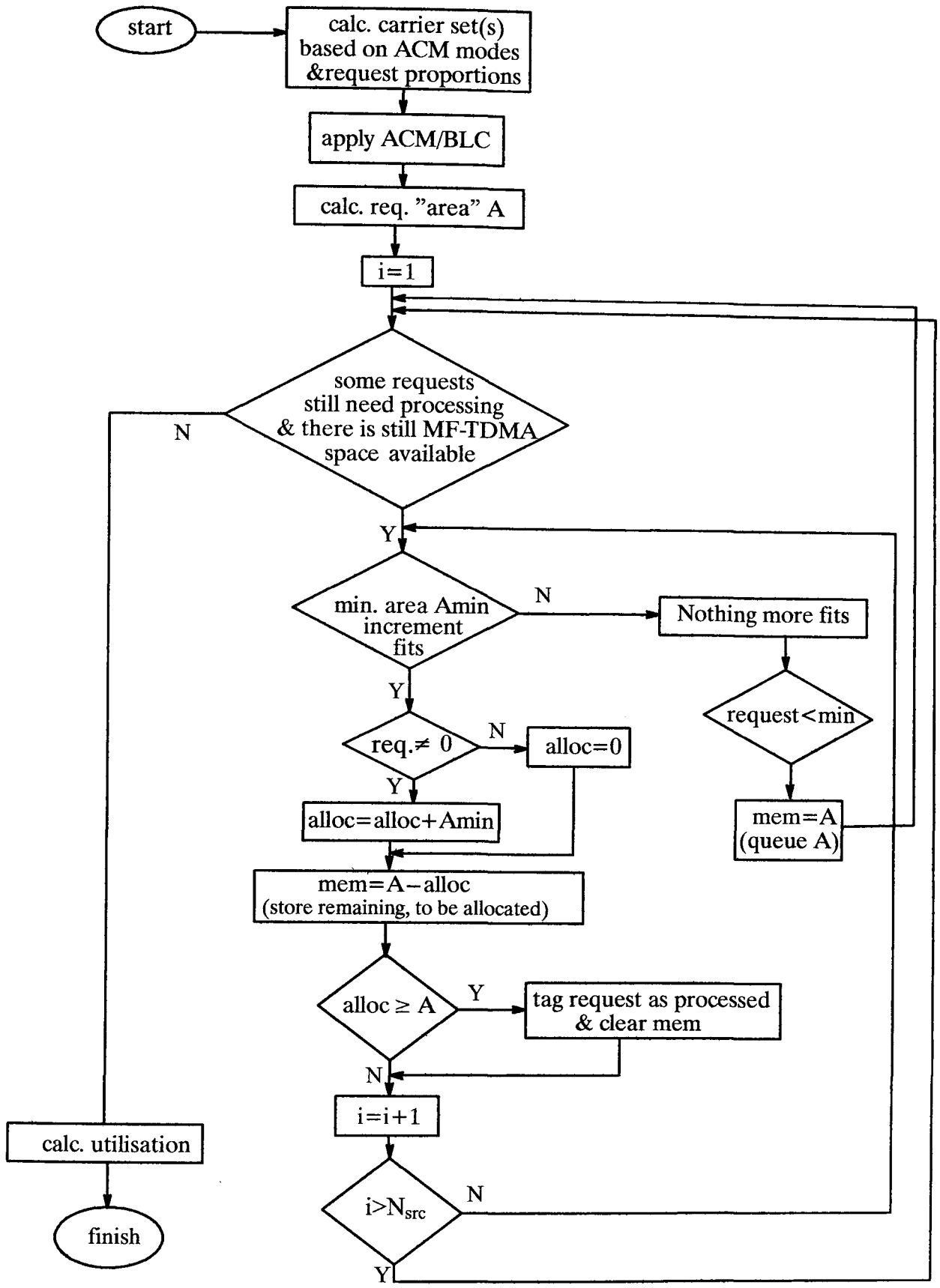

Figure 4.9 Block diagram of packing algorithm

The allocation is performed using a gradual incremental technique in order to ensure fairness. In particular, for each ACM request table, the BoD controller initially gives a

guaranteed minimum cell rate of 16 kbps to all live connections by initially allocating the minimum burst duration $T_{\min} = 207\mu s$. Using a for loop, the granted individual source bit rate is then built-up in steps of 16 kbps in a round-robin way for all the connections, until either (see Figure 4.9):

(i) the resource of MF-TDMA space available to the ACM request table is exhausted, or

(ii) the actual BoD requests for a particular connection has been satisfied by the resource allocation algorithm.

Any request that is not fully granted in the current allocation round is queued by the traffic source to be served in the next allocation (i.e. frame) period. Thus all connections are served, however the very greedy BoD requests may end up as partially queued. Obviously, the above process is repeated for all ACM request tables.

The use of $\lfloor x \rfloor$ ensures that as a best case, just enough MF-TDMA resources are given to a particular ACM request table since in general $\lfloor x \rfloor \leq x$. Thus equation (4.13) tries to make sure that the channel utilisation is maximised. However, the most greedy traffic request will not be fully granted and will therefore need to be queued at the source. Hence the proposed algorithm is trying to maximise channel utilisation at the cost of delay.

An alternative would be to use $\lceil x \rceil$ in equation (4.13) where $\lceil 1.2 \rceil = 2$, for example. In this case, more resources will be reserved than is effectively required. So the system tries to minimize delay at the cost of channel utilization. This approach may prove useful especially when few connections are live in the network making sure that at least one channel is made available for a particular ACM mode. Another alternative, in between the previous two would be to use simple rounding in equation (4.13).

So the basic RA processing of each ACM request table is summarised as follows.

Find the set of granted burst $\tilde{T}_i$ for all connections with the same ACM mode, such that

$$\tilde{T}_i \leq T_i = \frac{\overline{R}_b^i}{k'(Att_i)} \text{ is maximised} \tag{4.14}$$

$$\text{subject to } \begin{cases} (i) \sum_{i=1}^{N} T_i \leq N_i T_F \\ (ii) T_{\min} \leq T_i \leq T_F \end{cases} \tag{4.15}$$

Clearly when $\tilde{T}_i < T_i$ some traffic will be queued at the source.

The proposed allocation algorithm is mainly suitable for types of traffic that can tolerate some variations of the delay (lower QoS types of service with no delay bounds like ABR/UBR/non-real-time VBR, or even some real-time VBR applications that can tolerate some degree of delay and jitter).

In the hopefully rare worst case scenario where the resource allocation cannot be achieved (e.g. when some queues become unstable and start growing exponentially), the BoD controller would have to inform the Call Admission Controller, which is responsible for accepting/shutting-down connections so that the remaining live connections can be serviced adequately. Effective communication between the two controllers, or even merging of the two processes (CAC and BoD) is able to prevent such situations in the first place. As it was seen earlier in section 2.2.3, CAC bases its decision on whether to accept new connections on their QoS requirements and the condition of the network (for example, availability/unavailability of resources based on the TBTP table as well as buffer states of the existing connections).

4.2.5 Resource Allocation under Rain Conditions

The above algorithm applied to the scenario described in the previous chapter has been developed using Matlab to get system performance results. This thesis is focusses on the transport of aggregate Internet traffic that is known to exhibit self-similarity with long-range dependence and high levels of burstiness [4.8]. In the simulations one connection per terminal is assumed, each generating a stream of traffic ATM cells (424 bits) during the activity state (sojourn time) of a Pareto ON/OFF model ($a = 1.2$) with a Peak Cell Rate (PCR) of 2.048 Mbps. Note that in order to simplify the process and speed up the simulation, the dynamic management of a MF-TDMA subspace of bandwidth $B_{\max} = 5.5$ MHz is simulated. In order for this work to be compatible with published DVB-RCS systems [4.17]-[4.20], it has been assumed that $T_{\min} = 207\,\mu$s and $T_F = 26.5\,m$s.

The traffic requests are cumulated over periods of one second and sent to the BoD controller. This update rate is very important when integrating an FMT within DVB-RCS, as it must be able to track the variations of the rain attenuation process. Faster rates may yet be required if the FMT is also to compensate dynamically for interference and/or scintillations.

Depending on the attenuation level on each link, the appropriate FMT mode and bandwidth is selected by the BoD controller. Then the granted burst durations $\tilde{T}_i$ are communicated to each live traffic source via the TBTP table. The new MF-TDMA allocation is implemented in the next TBTP interval.

As it will be seen in the following chapter, correlated and uncorrelated rain events were used, however, even in the uncorrelated case every connection experienced some deep rain attenuation during the simulated time. Therefore the approach of this work is more of a worst case investigation on the system's performance, in order to expose the reaction of the system to rain and varying traffic load and the resulting issues, problems and trade-offs.

An important issue is that the system should be able to support the active connections including their FMT and short-term traffic needs. The available MF-TDMA capacity allocated to flows of the same class is however limited and fixed. As the RA algorithm may not be able to grant 100% of all the individual requests, if the agreed QoS or service level agreement allows it, some connections could perhaps be blocked until resources became available. The intention of this simulation is to prevent this by trying to ensure that all connections will be still kept alive at the cost of delay under bad channel and/or traffic conditions. This solution is acceptable for ABR (Available Bit Rate) traffic and it is also desirable for UBR (Unspecified Bit Rate) connections [4.21] and [4.22].

A key additional requirement is to be able to control the stability of the queues at each of the sources and try to minimise and control the delay in case of extreme network congestion due to very unfavourable traffic or rain conditions. A simple way of achieving this second layer of protection is to apply traffic shaping to all the sources. As an extension to the design, a variable PCR traffic shaping technique was furthermore implemented. When the MF-TDMA network becomes too congested, the sources are made to reduce their traffic by reducing their PCR. Similarly, when conditions improve or buffer occupancy is relatively low, the BoD controller allows the sources to increase their PCR to achieve higher user throughputs. Thus, when the system is very heavily loaded, the throughput of the connections is reduced until the system becomes capable of reducing its queued backlog traffic. More details regarding this mechanism will be seen in the following chapter.

4.3 Conclusion

This chapter has presented the traffic source model developed to be employed in the simulation. The capacity organisation of the return link was then reviewed, as this will provide the basis for the Bandwidth-on-Demand operation.

The chapter finally presented the proposed resource allocation algorithm designed and implemented for the purposes of the simulation that will be presented in detail in the following chapter.

4.4 References

[4.1] Mitchell P. D., Grace D., Tozer T. C., "Comparative Performance of the CFDAMA Protocol with Various Terminal Request Strategies", IEEE Global Telecommunications Conference (GLOBECOM), vol. 4, pp. 2720-2724, 2001.

[4.2] Dukes S., Roberts M., "Predictive Scheduling of TCP ACK Traffic over DVB-RCS", Highland Systems, Inc., retrieved June 11, 2008, from http://www.highsys.com /products/TCP%20over%20DVB-RCS%20v01.pdf

[4.3] Sahinoglu Z., Tekinay S., "On Multimedia Network: Self-Similar Traffic and Network Performance", IEEE Communications Magazine, vol. 37, no. 1, pp. 48-52, 1999.

[4.4] Jiang Z., Leung V. C. M., "A Predictive Demand Assignment Multiple Access Protocol for Internet Access over Broadband Satellite Networks", International Journal of Satellite Communications and Networking, vol. 21, p. 451-467, 2003.

[4.5] Crovella M. E., Bestavros A., "Self-Similarity in World Wide Web Traffic: Evidence, and Possible Causes", IEEE/ACM Transactions on Networking, vol. 5, no. 6, pp. 835-846, 1997.

[4.6] Cardellini V., Colajanni M., Yu P. S., "Geographic Load Balancing for Scalable Distributed Web Systems", IEEE. Proceedings of Mascots 2000, San Francisco, Aug./Sep. 2000.

[4.7] Willinger W., Taqqu M. S., Sherman R., Wilson D. V., "Self-Similarity Through High-Variability: Statistical Analysis of Ethernet LAN Traffic, at the Source Level", IEEE/ACM Transactions on Networking, vol. 5, no. 1, pp. 71-86, 1997.

[4.8] Leland W. E., Taqqu M. S., Willinger W., Wilson D. V., "On the Self-Similar Nature of Ethernet Traffic", IEEE/ACM Transactions on Networking, vol. 2, no. 1, pp. 1-15, 1994.

[4.9] Kramer G., "Self-Similar Network Traffic - The Notions and Effects of Self-Similarity and Long-Range Dependence", May 21, 2001, retrieved January 2003, from http://wwwcsif.cs.ucdavis.edu/~kramer/papers/ss_trf_present2.pdf

[4.10] Paxson V., Floyd S., "Wide Area Traffic: the Failure of Poisson Modelling", IEEE/ACM Transactions on Networking, vol. 3, no. 3, pp. 226-244, 1995.

[4.11] Mitchell P. D., "Effective Medium Access Control for Geostationary Satellite Systems", PhD Thesis, University of York, U.K., 2003.

[4.12] ETSI EN 301 790 (V1.3.1): "Digital Video Braodcasing (DVB); Interaction Channel for Satellite Distribution Systems" (also known as the 'DVB-RCS' specification), Final Draft, 2002-11.

[4.13] Kleinrock L., Lam S. S., "Packet switching in a slotted satellite channel", AFIPS Conference Proceedings, vol. 42, p. 703-710, 1973.

[4.14] ETSI TR 101 790 (V1.2.1): "Digital Video Broadcasting (DVB); Interaction Channel for Satellite Distribution Systems; Guidelines for the use of EN 301 790", 2003-01.

[4.15] Krause J., "The ASTRA BBI System: An overview", retrieved January 2003, from http://www.luxinnovation.lu/presentations/020708_presa_krause.pdf

[4.16] Iuoras A., Takats P., Black C., DiGirolamo R., Wobowo E., Lambadaris J, Devetsikiotis M., "Quality of Service-Oriented Protocols for Resource Management in Packet-Switched Satellites", International Journal of Satellite Communications, vol. 17, no. 3, pp. 129-141, May-June 1999.

[4.17] *"Eutelsat Will Expand Broadband Multimedia Services with Satellite Terminals from ViaSat"*, ViaSat, Press Releases, 05-02-2003, retrieved June 2003, from the ViaSat website: http://www.viasat.com/news/eutelsat-will-expand-broadband-multimedia-services -satellite-terminals-viasat

[4.18] Fairhurst G., "Broadband Multimedia Satellite Systems", Jan. 2001, retrieved January 2003, from http://www.erg.abdn.ac.uk/public_html/research/future-net/digital-video/bband-sat.html

[4.19] Krause J., "The ASTRA BBI System: An overview", retrieved January 2003, from http://www.luxinnovation.lu/presentations/020708_presa_krause.pdf

[4.20] Schweikert R., Wörz A. J., Lücke O., Werner M., "Protocols and Signalling for Adaptive Fade Mitigation Techniques (FMT) in DVB-RCS Multi-Beam Systems": Executive Summary, ESA Study Contract Report, Issue 01, 12 October 2005.

[4.21] ATM Forum, Traffic Management Specification Version 4, af-tm-0056, April 1996, retrieved January 2003, from ftp://ftp.atmforum.com/pub/approved-specs/

[4.22] Awadalla H. O., "Resource Management for Multimedia Traffic over ATM Broadband Satellite Networks", PhD Thesis, Dept. of Electronic Engineering, Queen Mary and Westfield College, University of London, March 2000.

CHAPTER 5

SYSTEM PERFORMANCE ANALYSIS AND EVALUATION

This chapter measures the performance of the resource allocation algorithm in the presence of bursty traffic and rain attenuation. The simulator's typical outputs are first presented as they comprise the basic performance metrics used throughout the chapter. Typical rain events have been selected in order to test the short-term performance of the proposed scheme, mostly to represent scenarios that stretch the system and expose any weaknesses, issues, problems and trade-offs arising. At certain points of the analysis, detailed time-series plots, obtained from a detailed simulation of the proposed algorithm, are presented for a more detailed investigation. The rest of the analysis focuses on results obtained from multiple simulation runs, all averaged and appropriately plotted for discussion.

5.1 System Performance

5.1.1 Simulator Outputs: Performance measures

The first part of the simulation approach was to obtain and observe results in a time-series form. This was the type of output given directly by the simulation and originally played a very essential role in the monitoring and verification of the correct operation and inter-working of the individual models within the simulator; the rain synthesis and application, the traffic/request generation process, the FMT management (type/mode mapping and application), the requests processing and bandwidth dynamic management (on-line partitioning), and finally the resource allocation process. Besides, these results comprise the main metrics used to evaluate the system's performance.

A. Channel Utilisation

Channel utilisation is usually defined as the proportion of the data carrying channel capacity that is effectively used for data throughput, and is generally one of the most

important criteria in the performance evaluation of a MAC scheme. It is understandably important to use the satellite channel as efficiently as possible, either to be able to support a greater number of users or to provide the same number of users with higher data rates. In either case, higher utilisation generates larger revenues for the service provider. With TDMA-based MAC schemes, the objective is to maximise the use of the allocated transmission slots [5.2]. As utilisation refers to the level at which the channel is being used, it was chosen for the purposes of this work to express the percentage of overall channel occupancy. Practically, in this thesis it expresses the percentage of used versus total MF-TDMA space available. Figure 5.1 shows a typical example of the channel utilisation achieved by six connections transmitting in clear-sky conditions over an MF-TDMA network.

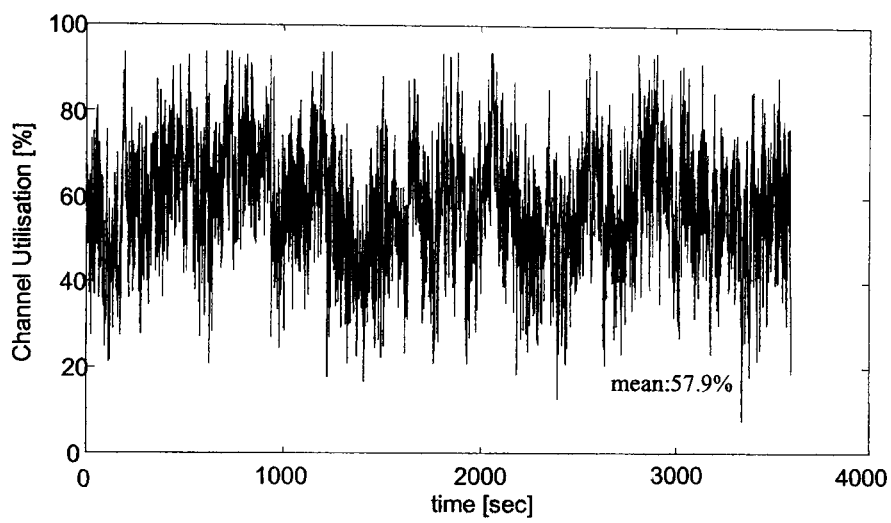

Figure 5.1 MF-TDMA subspace utilisation (6 connections with $\hat{R}_b$=2.048 Mbps)

For scenarios with fixed-size carriers, the used MF-TDMA space can be simply expressed as the number of allocated timeslots over the total number of timeslots available. In this MF-TDMA scenario, where the bandwidth is divided into carriers of different bandwidth as explained previously, channel utilisation is equivalently derived from the proportion of the MF-TDMA area that is allocated and used for overall data throughput, i.e. used for useful user throughput (or goodput) plus FMT overhead.

B. Useful User Throughtput (Goodput)

Another measure used in this thesis is user throughput, which relates to the overall data that effectively carries *useful* user information. This is expressed as a useful bit rate from a certain source address to a certain destination (for a network).

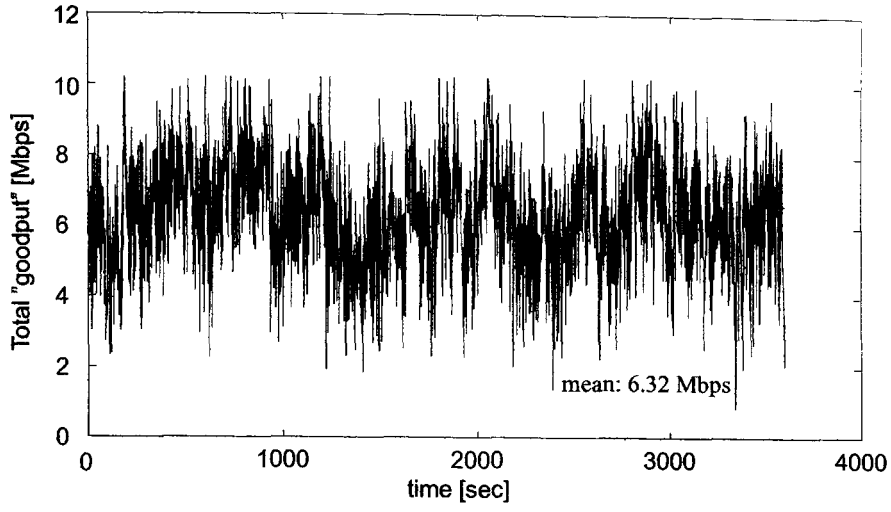

Figure 5.2 Total useful throughput (goodput) of six user connections with $\hat{R}_b$ of 2 Mbps

The intention of a MAC scheme along with maximising the use of the allocated transmission slots, should also be to minimise the frame overhead whenever possible. In this case, total user goodput (see Figure 5.2 above for an example) is the total number of useful bits per unit of time transmitted by all sources across the return satellite link, *excluding* any error-correction/FMT overhead. Other overheads have been neglected.

Figures 5.2 and 5.1 can be related by considering the mean values noted. The maximum total bit rate supported by the network is 10.923 Mbps. Hence the average total goodput value of 6.32 Mbps in Figure 5.2, results in a utilisation of $(6.32/10.923) \simeq 57.9\%$ (see Figure 5.1).

C. End-to-end Delay and Buffer Occupancy

The end-to-end delay of a packet transmission is the time taken for a packet to be successfully received at the destination terminal at the other end of the satellite link from the time it was generated at the source. It consists of a number of components including the queuing delay prior to transmission, the packet transmission duration, and the signal propagation delay. There is always a benefit to be gained from reducing the end-to-end delay of packet transmissions over a satellite link, because even if the user-recognised improvement in the quality of service of an application is minor, any enhancement in the delay distribution of packet transmissions for a given scenario is indicative of a more efficient MAC scheme. In addition, long transmission delays may inhibit the operation of other layers of the protocol stack such as the transport layer in the case of TCP. The mean value of end-to-end delay is commonly used as a performance metric and so an attempt was made in

this thesis to obtain, where possible, the mean end-to-end delay performance as a function of time and as a function of channel load. Figure 5.3 shows examples of the queuing delay as a function of time.

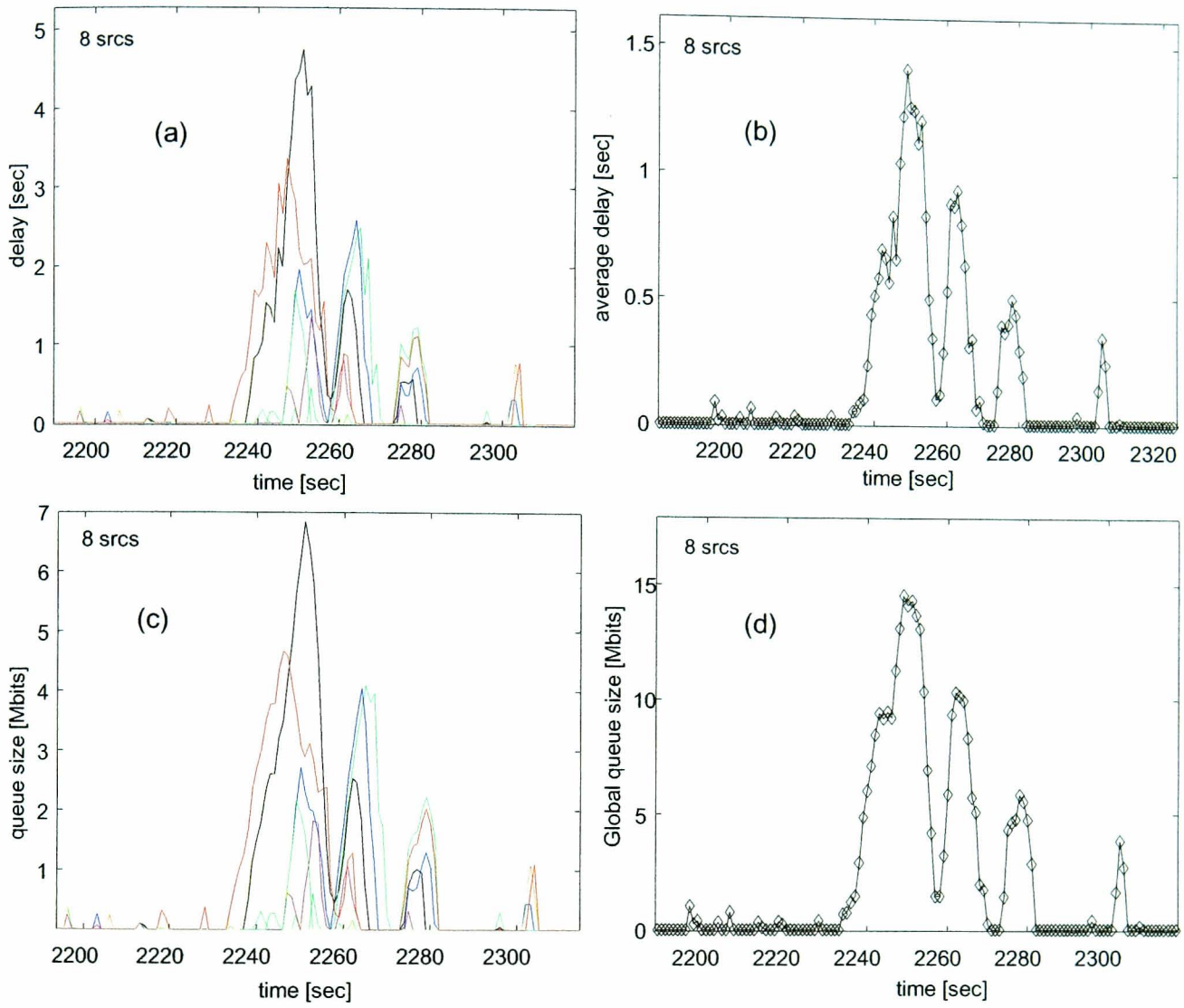

Figure 5.3 Examples of (a) queuing delay time-series output for 8 connections, (b) average queuing delay, (c) individual queue sizes, (d) global queue

Some applications are sensitive to the variation in the end-to-end delay of packet transmissions, often referred to as delay jitter, arising from the fluctuations in the queuing delay at the terminals (Figure 5.4). Audio and video streaming applications commonly require low delay jitter. Buffering at the receiver combined with constant buffer read-out can alleviate the problem but this implies additional hardware and complexity, resulting in an increase in the overall delay of the received stream. Reducing the variation in the delay of packet transmissions through good MAC protocol design is preferred.

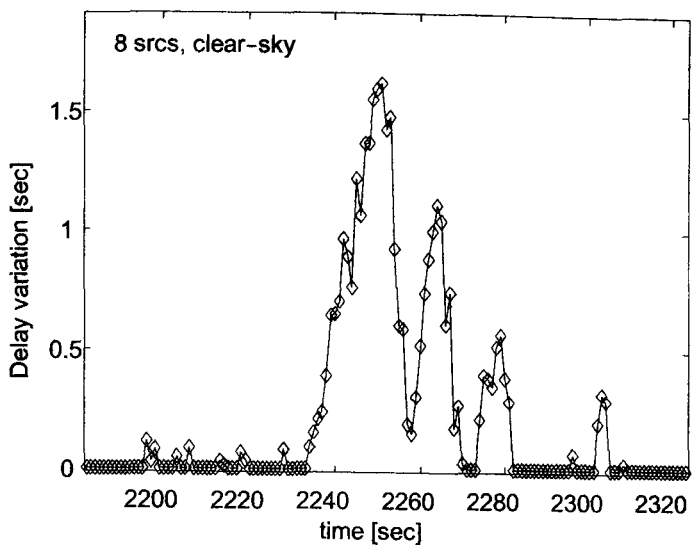

Figure 5.4 Example of delay variation (time-series output)

Assuming a satellite architecture where packets can be immediately transmitted on the downlink following reception on the uplink, the end-to-end delay comprises three components and is given by:

$$D = D_{queue} + 2.T_{pkt} + x.RTD \tag{5.1}$$

where D is the end-to-end delay, D_{queue} is the queuing delay prior to transmission, T_{pkt} is the packet transmission/reception duration, and RTD is the satellite round trip propagation delay.

Setting $x = 1$, this expression corresponds to the simulation model of the free assignment scheme where the downlink data transmission slots occur immediately subsequent to the uplink slots. With DAMA, x can be equal to 2 or 3, for an on-board or ground-based scheduler respectively. The queuing delay incurred at the satellite is equal to a single packet duration, with another packet duration for reception at the destination terminal [5.2]. The values of T_{pkt} and RTD are constant and are known. The queuing delay D_{queue} prior to transmission is an unknown quantity that depends on both the number of packets in the queue at the instant of a packet arrival, and on the time between a packet arrival and the occurrence of the next transmission slot.

5.1.2 Rain Scenarios and Link Availability

The time-series random rain synthesiser introduced in section 3.5.4 was used to simulate typical rain events of various amplitudes and durations (10-15 minutes on average) that were produced and loaded during simulation.

A. Uncorrelated rain simulation case

Figure 5.5 demonstrates a typical sample of the synthesiser's output: a series of rain events were used to simulate the uncorrelated case of a scenario where all links suffer from rain at some point over the simulated period. Although these rain events are not experienced by the links simultaneously, the scenario can still be considered quite severe and unfortunate since it almost always rains somewhere during the period of an hour. Normally, sources from different locations are grouped together so as to provide some statistical multiplexing. It is however an interesting case that can be used to investigate the performance of the system in somewhat unfavourable conditions, so the results can be expected to be conservative.

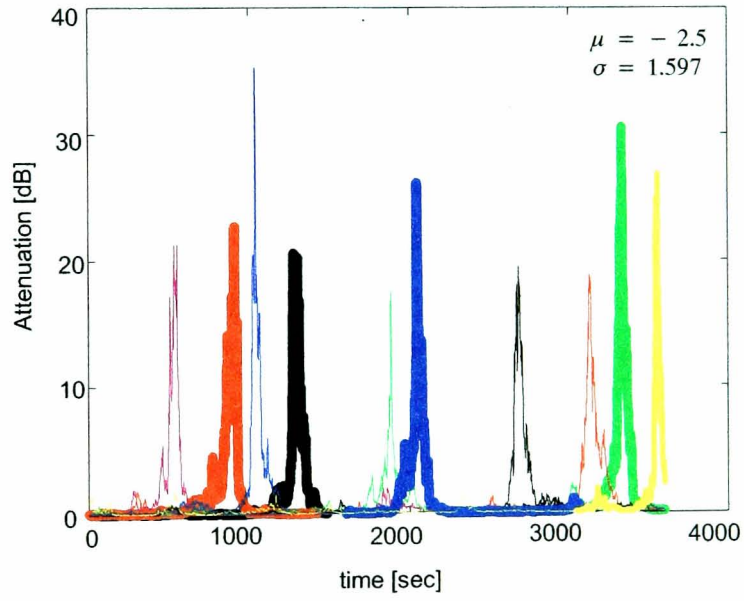

Figure 5.5 Example of 10 uncorrelated (convective) rain events at 30 GHz (rain synthesiser output)

B. Correlated rain simulation case

A worst case scenario was developed, where no geographical multiplexing is involved. All sources transmit within the same MF-TDMA subspace simultaneously and they experience the same rain event (correlated rain). Such an event is shown in Figure 5.6.

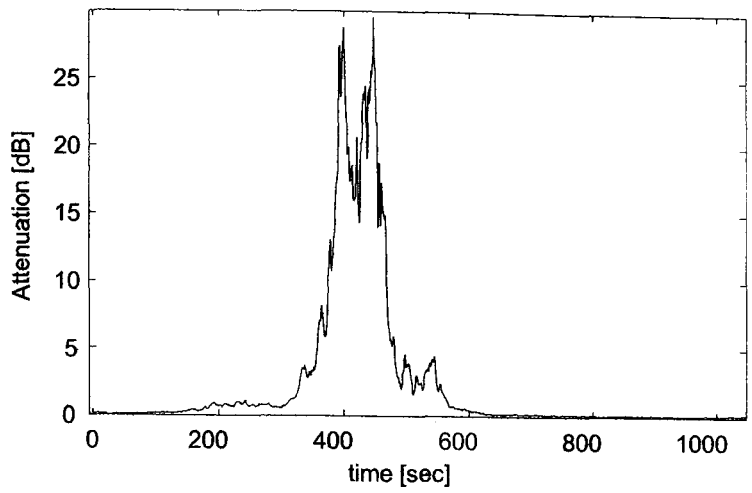

Figure 5.6 Large rain event at 30 GHz used for the correlated rain scenario

The system's performance will be thoroughly examined through numerous simulation runs, either by varying the channel load under rain conditions or "gradually" introducing rain events by increasing the number of rain-affected links for each simulation run, keeping the channel load constant.

C. Link availability

Figure 5.7 shows the potential improvement of the overall availability of all links over the simulated network time of 1 hr, for the pure ACM and combined ACM-BLC schemes in comparison with a traditional small fixed margin system for decorrelated rain, including events with peak attenuation of up to 35 dB (Figure 5.5). Assuming that enough resources are available, the combined ACM-BLC scheme can significantly reduce outages and improve the overall availability.

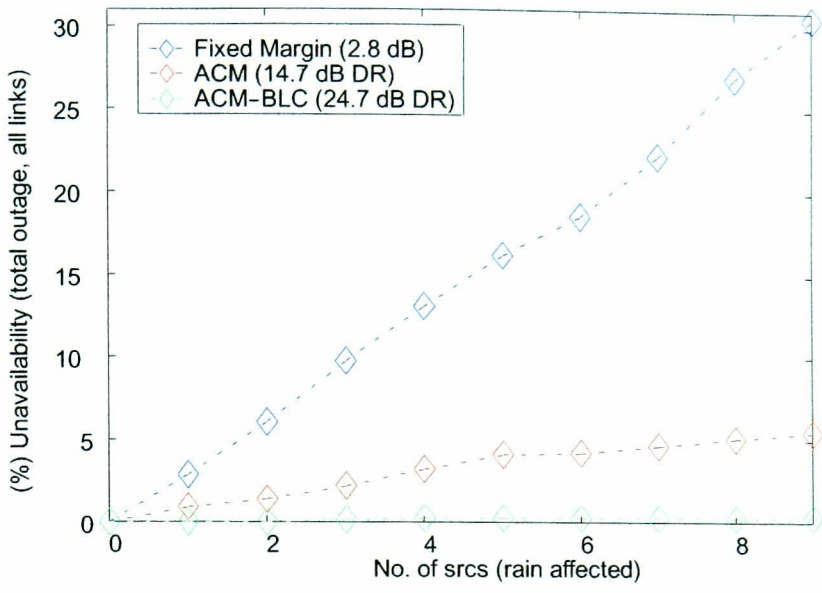

Figure 5.7 Total unavailability (overall outage of all links over the simulated network time of 1 hr) as a function of the number of rain-affected sources

Figure 5.8 shows the outage for each link in the correlated rain case (of a 30 dB rain event). BLC can potentially bring an improvement of the overall system availability over the simulated network time (from 97.9% to 99.6%) compared to the pure ACM scheme.

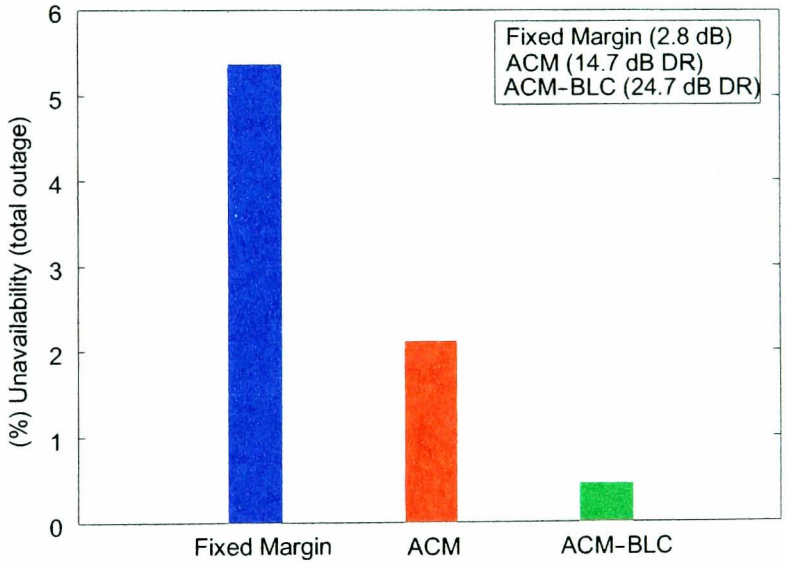

Figure 5.8 Unavailability (over the simulated network time of 1 hr) for each link in correlated rain conditions (30 dB event, Figure 5.6)

This sample result demonstrates very clearly that a small fixed margin is inadequate. Also the result shows that, assuming that enough resources are available, ACM/BLC reduces unavailability by 1.7 % compared to ACM.

5.1.3 Validation of Results

In this thesis, a simulation approach has been chosen as the main research tool for studying a MAC protocol with an FMT. Several factors concerning the complexity of the network studied make both analytical and practically implemented models not adequate and flexible enough (for example the traffic modelling, the combining of both complex traffic and FMTs, the adaptation requirements and applicability of the model for investigating and comparing the performance of different schemes and for examining the various performance trade-offs as different parameters are varied).

The software tool used for both mathematical and simulation purposes is Matlab. In order to validate the simulation techniques, a method is required to provide confidence in the adequacy of the software developed and the resulting measured performance. There are generally two alternative approaches: mathematical modelling, and comparison of results with those published in the literature for models that have a considerable part of their functionality in common.

Effort has been made to validate the models and results presented in this thesis using appropriate methods, i.e. through comparison of theoretical and simulated performance or through comparison with simulation results already published in the literature. This way the software developed in this thesis can be used confidently in further investigations.

A. Validation & Simulation of a Pareto ON/OFF Traffic Source

(i) Setting the Parameters

The choice of parameters in the Pareto distribution determines the degree of self-similarity in the aggregate traffic and the minimum possible ON and OFF periods. A common measure of the degree of self-similarity is the Hurst parameter, H_P, related to the tail parameter of the Pareto distribution by [5.1], [5.2]:

$$H_p = \frac{3-\alpha}{2}, \qquad 0.5 \leq H_p \leq 1 \tag{5.2}$$

Statistical estimation of the Hurst parameter on a comprehensive set of Ethernet LAN traffic measurements in [5.3] and [5.4] gave a value of ~ 0.9, corresponding to a value of 1.2 for the tail parameter, α, for both the ON and OFF periods.

Research on Web traffic [5.1] has shown that ON times are heavy-tailed with $\alpha \approx 1.0\text{-}1.3$ and OFF times are less heavy-tailed with $\alpha \approx 1.5$, so it has been concluded that ON times are more likely responsible for the observed level of traffic self-similarity, rather than OFF times.

In research carried on thereafter [5.2], [5.5], [5.6], [5.7], and [5.8] the most commonly used values for the α-parameters have been $\alpha_{on} = \alpha_{off} = 1.2$, and in some cases, the value of 1.4 has been used for either of the two parameters, for example in [5.7]. So, the α-parameters used in this thesis to simulate highly bursty traffic with different variability of ON/OFF times, ranging from $\alpha = 1.0$ to $\alpha = 2.0$ with 1.2 chosen as the optimum value. Relatively smooth traffic (with $\alpha \gg 2$) has also been simulated as part of the experiment, for comparison purposes.

The parameter k is the starting point of the pareto tail, representing the minimum possible value of the distribution, i.e. it defines the minimum allowable burst length, and, to ensure that all bursts last for at least one timeslot, k is set to the duration of one slot [5.7], [5.8], and [5.9].

(ii) Generating Values Fitting a Pareto PDF

One method of generating values fitting a Pareto probability density function is to derive an expression to translate values obtained from one of the standard distributions into values fitting a Pareto distribution. Mathematical analysis in [5.2] has shown how a set of values fitting a Pareto probability density function can be obtained from a random variable with a uniform distribution of values. The following mapping can be used to generate values fitting a Pareto pdf from a uniform distribution:

$$Y = kX^{-\left(\frac{1}{\alpha}\right)} \tag{5.3}$$

It has been verified that if X is a random variable with a uniform distribution of values between 0 and 1, $p(X)$ will be equal to 1 over the entire range of possible values, and hence the corresponding values of Y will fit a Pareto probability distribution.

A heavy-tailed distribution can also be produced by simply generating a uniform sample and apply the inverse CDF [5.10].

Matlab scripts have been developed to verify both the above methods. The results representing the PDF of the values as well as the theoretical pareto PDF are plotted for comparison in Figure 5.9.

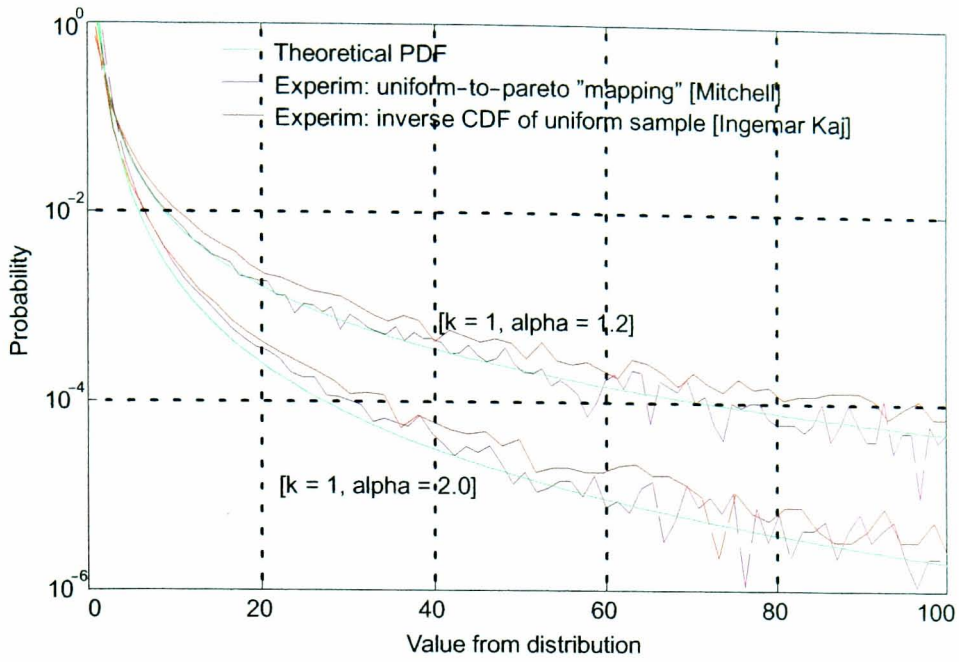

Figure 5.9 Theoretical and experimental Pareto probability distribution functions

(iii) Slots-per-Frame Requirements

The Matlab script mentioned above calls "paretoON_OFF", a function that takes *npoints*, $[\alpha_{on}\ \alpha_{off}]$, $[k_{on}\ k_{off}]$, and T_{pkt} as arguments; *npoints* is the sample size, α_{on}/α_{off} and k_{on}/k_{off} the shape/tail parameter and location parameter of the ON time and OFF time distribution, respectively, and T_{pkt} (207 μ sec) the packet's duration in seconds (where a packet represents one ATM cell). After generating the Pareto distributed ON and OFF times, the slots-per-frame requirement for a single Pareto source was calculated. Figure 5.10 shows a typical output plot of the number of required slots per frame over a period of 140 frames:

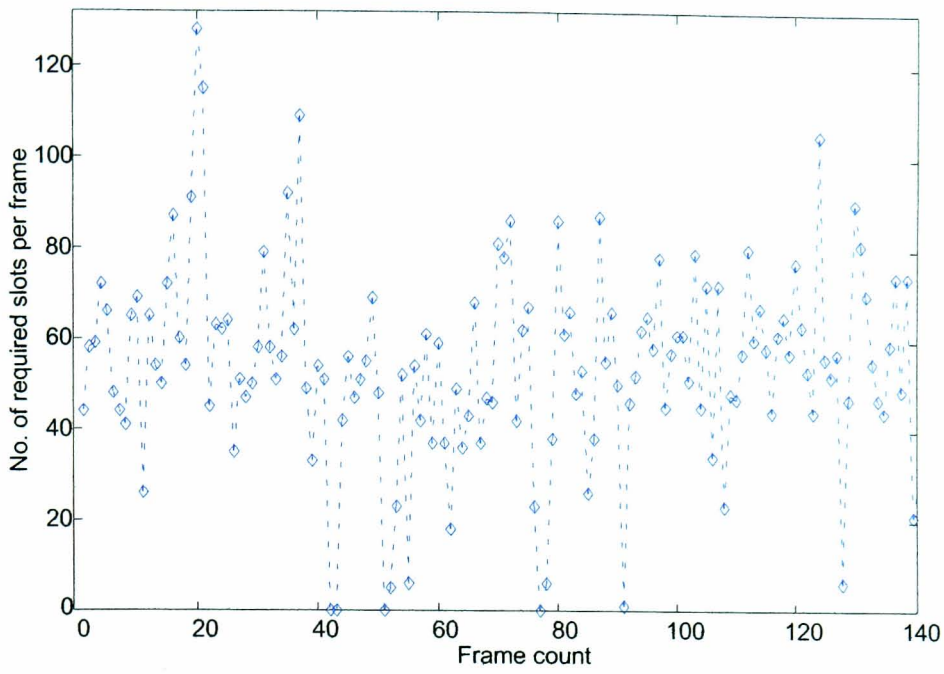

Figure 5.10 ATM slots per frame requirement for a single Pareto source with $\alpha_{on} = \alpha_{off} = 1.2$, over a period of 140 frames

The plots in the following two figures show the outputs produced over longer time ranges, measured in frame durations (frame duration = $T_F \simeq 26.5$ msec $\equiv 128$ timelsots); the α-parameters were used to simulate traffic with different variability of ON/OFF times. Figure 5.11 shows how the shape parameter defines the heaviness of the distribution's tail, i.e. the burstiness of the generated traffic. The lower the shape parameter α_{on} the higher the burstiness of the traffic hence the higher the mean number of required slots per frame:

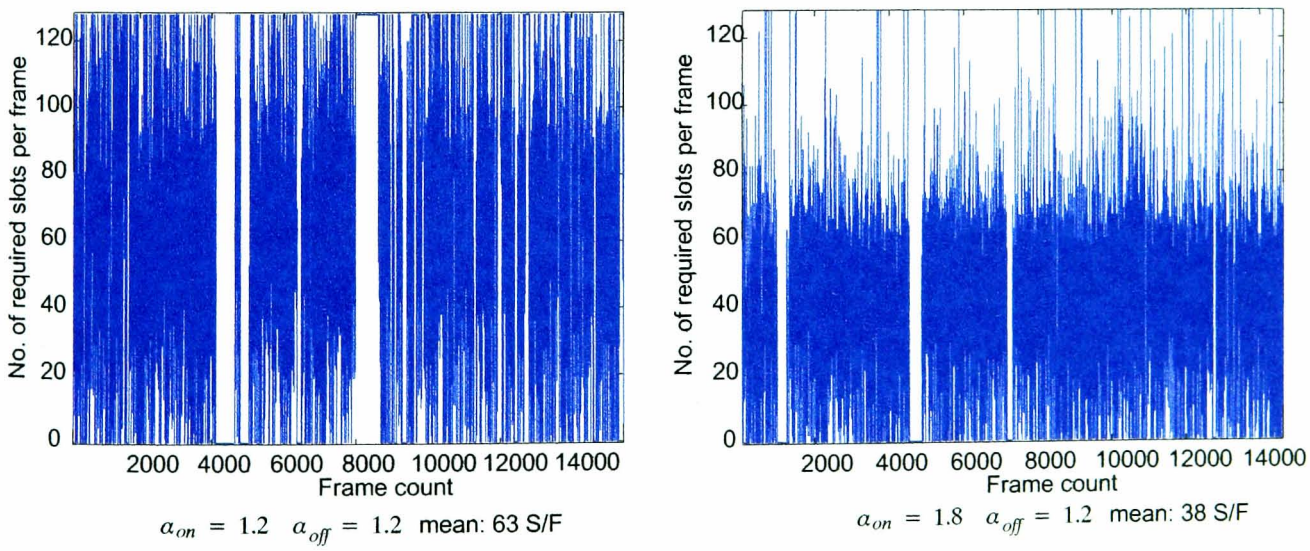

Figure 5.11 Slots per frame requirement for a single Pareto source - effect of α-parameter on traffic burstiness

The above plots show the effect on traffic burstiness when α_{on} changes with α_{off} kept constant. One can easily realise the role of the ratio between the two shape parameters, α_{on}/α_{off}. This becomes obvious in Figure 5.12. The higher this ratio, the lower the mean slot-per-frame requirement (see first pair of plots in Figure 5.12). Furthermore, keeping the ratio constant and changing the value of the α-parameters, again affects the smoothness of the traffic, this time preserving the mean (see second pair of plots):

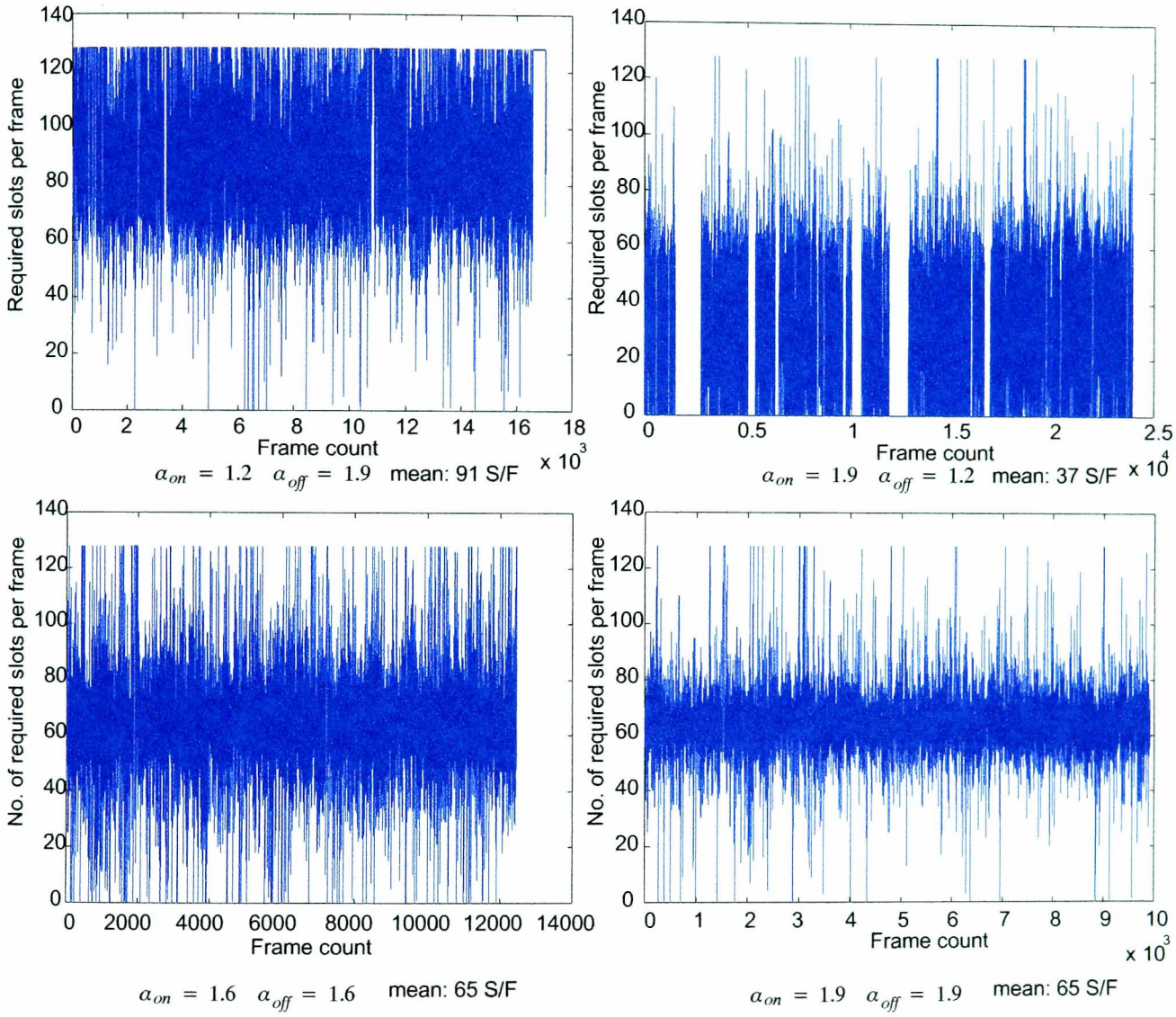

Figure 5.12 Slots per frame requirement for a single Pareto source - the effect of the α-parameter

(iv) Generalisation to Multiple Pareto Sources

The packetised input traffic can be modelled as a superposition of independent ON/OFF Asynchronous Transfer Mode (ATM) slotted sources, with the duration of the ON and OFF

times taken from a Pareto distribution, as discussed above. It is known that the superposition of many ON/OFF sources whose ON and OFF times have infinite variance produces self-similar traffic [5.3] and [5.8]. This concept of aggregation of n sources of Pareto-distributed ON/OFF periods is illustrated in Figure 5.13:

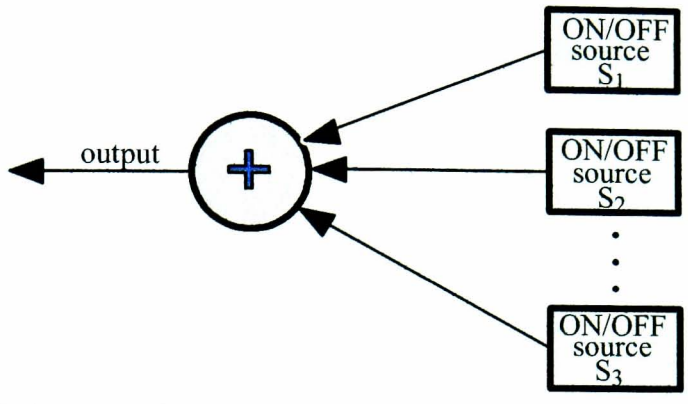

Figure 5.13 Aggregation of n sources of Pareto-distributed ON/OFF periods

For each independent ON/OFF ATM source, the ON and OFF times, T_{on} and T_{off}, were simulated as described above. Channel utilisation, ρ, is given as [5.4]:

$$\rho = \frac{E_{on}}{E_{on} + E_{off}} \tag{5.4}$$

where E_{on} and E_{off} are the mean ON and OFF periods respectively, calculated from Equation (4.2). Figure 5.14 shows aggregate traffic in the form of overall slot-requirement of multiple independent sources.

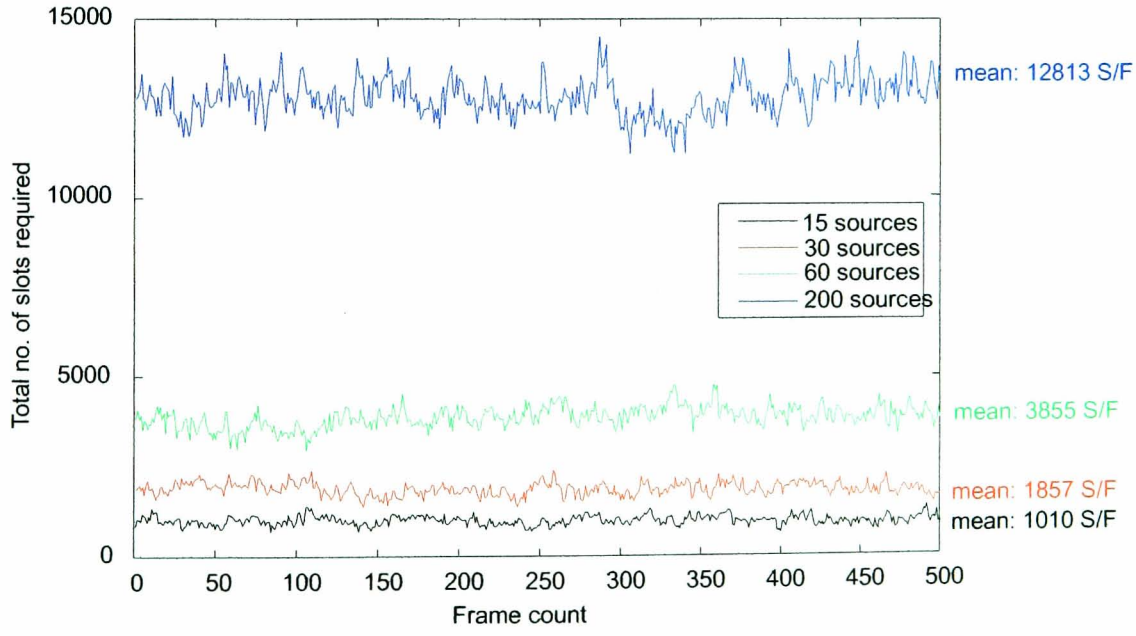

Figure 5.14 Total requirement in slots for 15, 30, 60 and 200 independent Pareto sources with $\alpha_{on} = \alpha_{off} = 1.2$ over a period of 500 frames ($\equiv$ 13 seconds)

B. Validation of the DAMA Simulator

The behaviour and performance of the DAMA algorithm implemented for this thesis is investigated through simulation. In order to test its basic adequacy, the model was validated through comparison with results previously published by Mobasseri presented in [5.11] of both the mean end-to-end delay and delay variation obtained for the BoD algorithm under clear-sky conditions. The values representing Mobasseri's results have been obtained directly from the IEEE paper, through careful measurement of enlarged versions of the original plots.

It should be noted here that load refers to the level of demand placed on the channel expressed as a fraction of the total channel capacity C. It is defined as:

$$L = \frac{N \times Av.\ user\ bit\ rate}{C} \tag{5.5}$$

where N is the number of user connections sharing the uplink bandwidth.

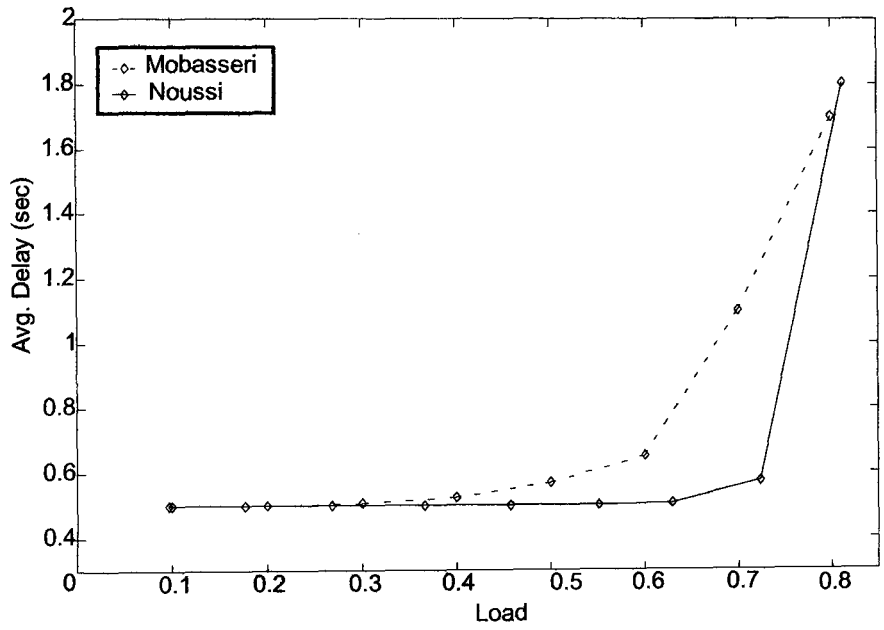

Figure 5.15 Mean end-to-end delay as a function of channel load for DAMA (assuming on-board scheduling)

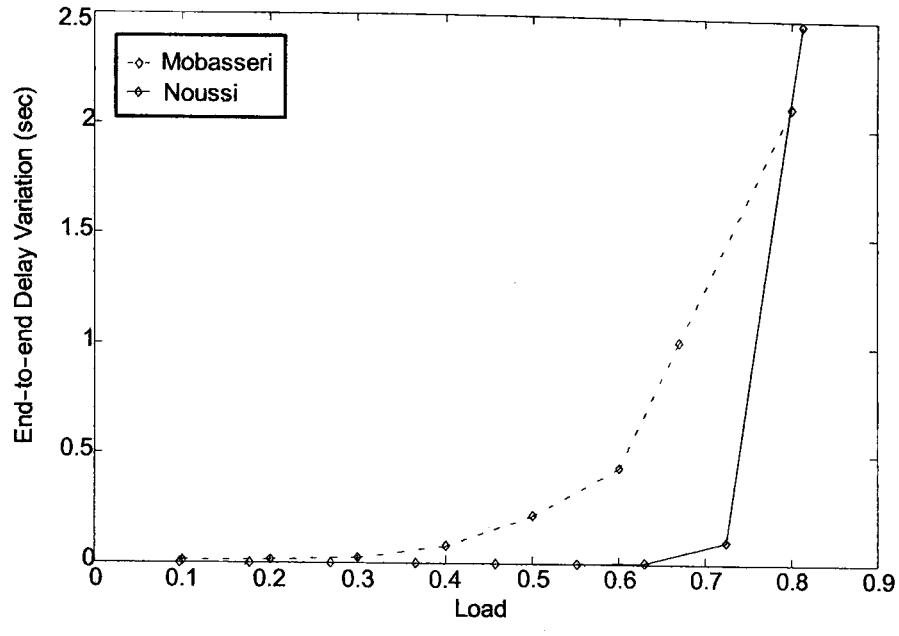

Figure 5.16 Mean end-to-end delay variation as a function of channel load for DAMA (assuming on-board scheduling)

The comparative mean end-to-end delay performance is shown in Figures 5.15 as function of channel load. The variation of the end-to-end delay packet transmissions is shown in Figure 5.16.

It can be seen that the simulation results offer a close match to those of Mobasseri for the lower and higher loads. The discrepancies in the results for the intermediate loads (0.5-0.7) are mainly, as expected, due to different bandwidth segmentation techniques and algorithm performance. Although there is apparently no difference in the bandwidth partitioning (no fixed bandwidth allocated to terminals) in Mobasseri's pure DAMA scenario, there are unavoidable and expected differences that can result from this work's FMT-oriented bandwidth segmentation technique (the MF-TDMA space is dynamically divided into appropriate carriers, based on the required ACM mode of each user terminal every second). An important factor is also the performance and efficiency of the particular packing algorithms used in each case. Note here that for the purpose of Mobasseri's simulations real movie traces had been used as bit-rate video sources and no details were given on the bandwidth segmentation techniques or the packing algorithm employed, hence actual implementation of Mobasseri's algorithm for additional comparison was not viable.

The major similarity and common base between the two models is the MAC protocol used for bandwidth assignment in bursty traffic applications: demand assignment (DAMA). Slots in uplink frames are assigned to the earth terminals based on their traffic demands (or, in other words, queue occupancies). Therefore in the resulting system, the time-varying bandwidth

requirements of the earth terminals can be accommodated and no bandwidth will be wasted. The drawback of this scheme is apparent in both graphs of Figure 5.15, as expected; there is a minimum delay experienced by the data in the queue from the time the earth terminal sends bandwidth request signalling to the BoD scheduler, until the time the data is received at the destination terminal. It is realised at this point that the advantage of an on-board scheduler is reduced delay for DAMA requests and subsequent acknowledgements which improves the QoS of DAMA techniques. With a satellite-based scheduler there is a minimum propagation delay of one satellite hop (0.25 sec for GEO satellites) from the instance a request is made to receiving a request from the scheduler, hence resulting to an end-to-end propagation delay of two hops (0.5 sec until data is received at destination terminal), compared to that of three satellite hops (0.75 sec end-to-end delay) for a ground-based scheduler. However, despite this disadvantage, lower QoS types of service with no delay bounds like ABR/UBR/non-real-time VBR, as well as some real-time VBR applications with some degree of delay and jitter tolerance, can use this scheme.

As a means of additional validation, the queuing behaviour was observed. At the end of each simulation run every individual queue could be probed and examined. As an example, Figure 5.17 shows time-series of the terminal queues for 5 traffic sources. This particular plot is from a simulation run of the complete DAMA model, including 9 traffic sources with a peak rate R_b^i of 2.048 Mbps transmitting over a 5.5 MHz bandwidth in clear-sky conditions (clear-sky mode; $\rho = 2/3$, $M = 16$, 10.92 Mbps link rate).

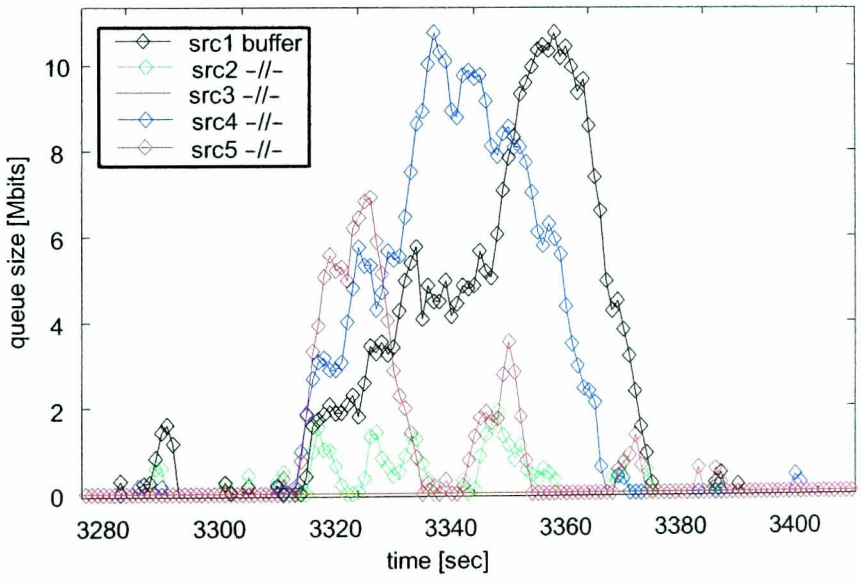

Figure 5.17 Observed queuing behaviour

Thanks to the multiplexing of bursty traffic sources in such a scenario like this, the network can cope, although the bandwidth utilisation is high most of the time (83% average

utilisation) and the queued traffic is large when sources transmit at peak rate simultaneously. Such scenarios, however, offer a great opportunity to examine the behaviour of the system and, in this case, the variation in the queue sizes demonstrating that the enqueuing/dequeuing operations are properly taking place. Below a typical set of results directly obtained through simulation is presented. These results further extend this validation as they are used to thoroughly examine and verify the correct operation and inter-working of all individual models within the simulator.

5.1.4 Performance of the DAMA Model in the Presence of Rain

A. ACM and combined ACM-BLC Scheme

(i) Single Source Simulation

The rain event shown in Figure 5.6 was used for the simulation of the resource allocation scheme when one source transmits over the MF-TDMA subspace. Results from the simulation of three rain scenarios were collected and compared: clear-sky, rain scenario with ACM (DR of 14.7 dB), and then combined ACM-BLC (with DR=20.7 dB).

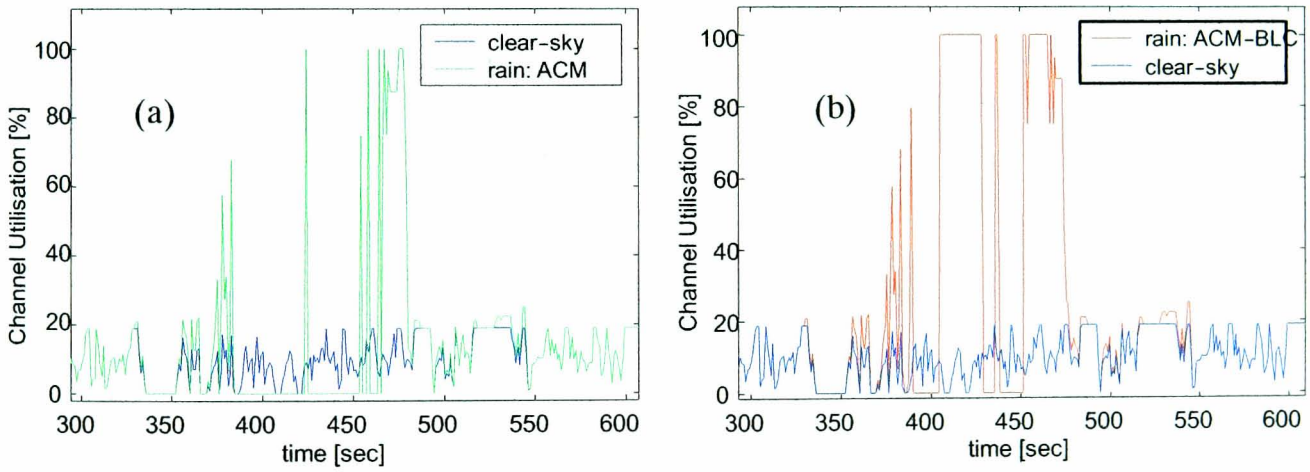

Figure 5.18 Channel utilisation (time-series) of a single traffic source during clear-sky and during severe rain (30 dB rain event) with (a) ACM (b) combined ACM-BLC

The above figure compares the channel utilisation, for one live connection, achieved during clear-sky with that achieved during a rain event, when FMT was employed: pure ACM and BLC-extended ACM. It reveals the expected short-term increase of utilisation during the event due to either FMT in rain conditions. In the first case, the connection transmits using the most robust ACM scheme (i.e. across the widest carrier taking up 5.5 MHz), hence using 100% of the MF-TDMA space available. For most of the period between

t=380 and t=460 sec, the link enters an outage phase, during which no further transmission takes place and thus utilisation drops to 0%. This happens because during this period rain attenuation reaches and exceeds the ACM dynamic range of 14.7 dB. In Figure 5.18(b), when the ACM's dynamic range is exceeded, BLC is employed and manages to compensate for an extra 6 dB of attenuation (extended DR of 20.7 dB). During this period, the utilisation is kept at maximum for longer and transmission continues taking place for longer, unless the extended dynamic range is exceeded (attenuation greater than 20.7 dB).

Figure 5.19 shows the corresponding useful data throughput achieved during this period. The short-term lower values of goodput achieved during rain conditions compared to clear-sky in both cases can be observed. With ACM, around t=375 sec, it is noticed how for the same values of goodput, utilisation (Figure 5.18(a)) reaches up to almost 70%. Compared to the 20% utilisation achieved during clear-sky, for the same goodput values, this extra 50% used at that instant represents the FMT overhead resources needed and in that case used to fully compensate for the respective attenuation at the time.

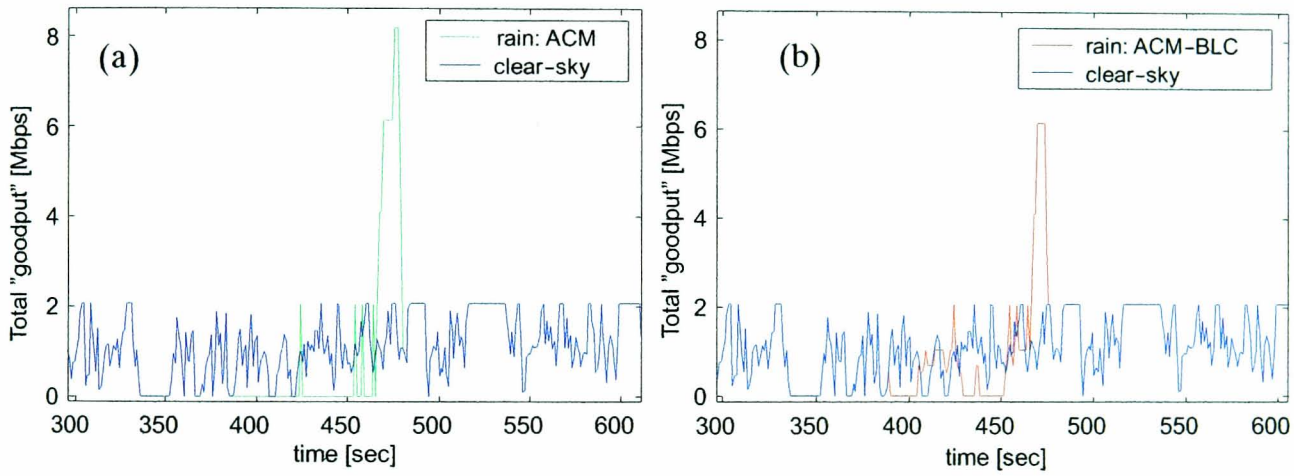

Figure 5.19 Useful data throughput time-series for clear-sky and severe rain with (a) ACM (b) combined ACM-BLC

During the periods of attenuation below 20.7 dB, BLC manages to successfully extend the dynamic range of ACM (from $t \simeq 400$ to $t \simeq 430$ sec in Figures 5.19 and 5.18). It is noticed again how relatively low the values of goodput are considering that utilisation in these periods reaches up to 100%. When in clear-sky utilisation values are below 20% (Figure 5.18), in the ACM-BLC case (around t=475 sec) utilisation reaches up to 100% for similar levels of goodput (Figure 5.19). This means that, at those instants, an extra 60% of the resources is necessary for FMT to successfully compensate for attenuations between 14.7 and 20.7 dB. In both cases of ACM/ACM-BLC, when the rain event is over, all queued useful data that has not been transmitted due to the lower goodput phases, finally gets transmitted, which is confirmed by the short-term increase of goodput around t=475 sec.

The higher short-term values of goodput in Figure 5.19(a) when compared to 5.19(b) around t=475 sec, are expected as the longer outage period of the link with ACM leads to a larger queue of useful data waiting to be transmitted when conditions improve. This is how, by preventing or reducing outage periods, BLC can even keep the queue size lower in comparison, leading to shorter queuing delay. Looking at Figure 5.20 this fact is further confirmed by looking at the total queue length generated during this period.

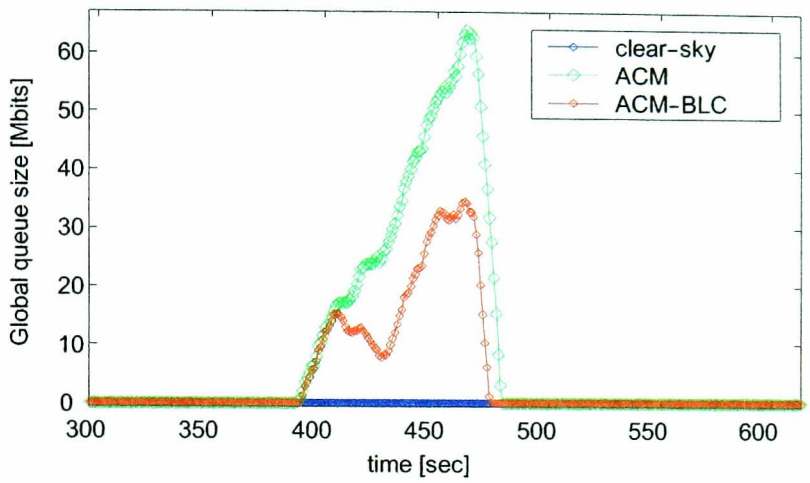

Figure 5.20 Buffer Occupancy time series for clear-sky and heavy rain with ACM, and combined ACM-BLC

So, as long as there are slots resources available, BLC can compensate for an extra attenuation of 6 dB. If there are not enough resources, the resulting queuing and hence delays might increase. Counting on the statistical multiplexing of bursty traffic sources, BLC can however still be introduced. This chapter will investigate the price at which BLC is introduced and whether its advantages can still be enjoyed when traffic load increases.

(ii) Multiple-Links Scenarios

Performance of the model with varying channel load

Figure 5.21 shows the average channel utilisation as a function of channel load in clear-sky as well as rain conditions. It demonstrates and confirms the ability of demand assignment to provide a high channel utilisation level for bursty traffic, as a result of the dynamic allocation of capacity based on short-term requirements.

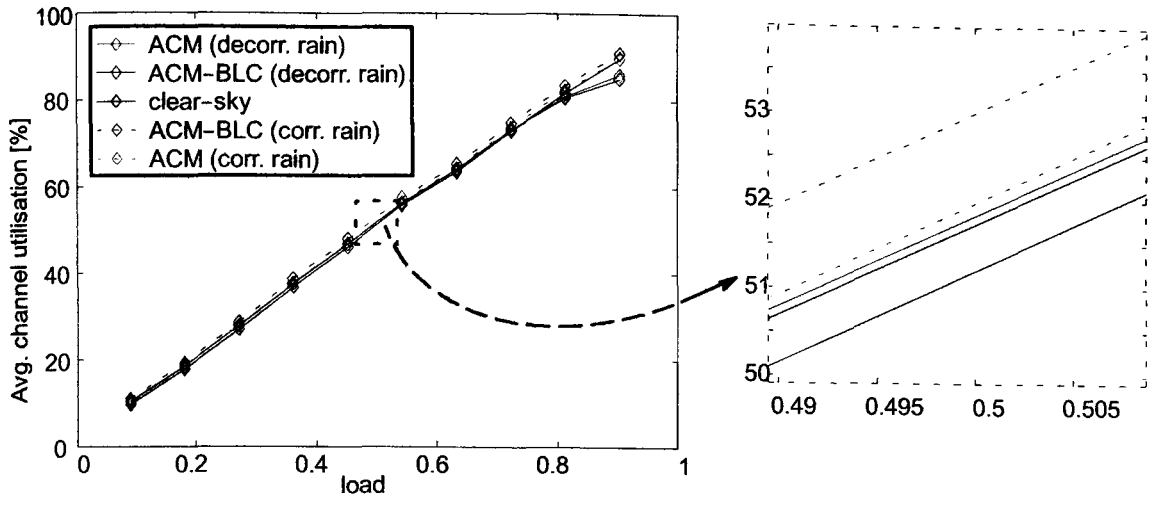

Figure 5.21 Average channel utilisation as a function of channel load for clear-sky and ACM/ACM-BLC in correlated and decorrelated rain scenarios

Looking at the graph it is observed that as the overall load placed on the network is increased, so is the average channel utilisation, in a linear and proportional fashion, as expected. Similarly consistent performance is obtained during rain conditions. Any short-term increase of utilisation during the simulation time due to ACM or combined ACM-BLC in rain conditions (as illustrated earlier in Figure 5.18) only resulted in a small (2%) increase of the average utilisation values. This indicates a better performance of BLC in terms of channel utilisation, when compared to ACM. When the dynamic range of ACM is exceeded, the affected links enter an outage phase where no transmission takes place for them, leading to lower values of channel utilisation. If there are slot resources available, BLC can reduce or prevent outages hence resulting in higher utilisation values.

Apparently, beyond an 80% load, there is a 5% drop in average utilisation values for the uncorrelated rain scenario, possibly due to the specific simulation statistics and/or specific RA algorithm performance in rainy conditions at high traffic. Note that beyond a load of 0.8, even in clear-sky the network is starting to become overloaded, resulting in a very high increase in queue sizes which will be confirmed in the following part (when the queue sizes are examined).

Figure 5.22 shows the average total useful throughput or total goodput transmitted on the network. The average results for all cases are identical, confirming that all useful data gets successfully transmitted in the long-term, even if there are occasional reductions in the overall throughput (for example, due to either allocation algorithm packing efficiency, or system outage during severe rain when no data is transmitted) or occasional reductions in the user data itself due to the changing proportion between FMT and actual traffic resources (as seen in Figure 5.19).

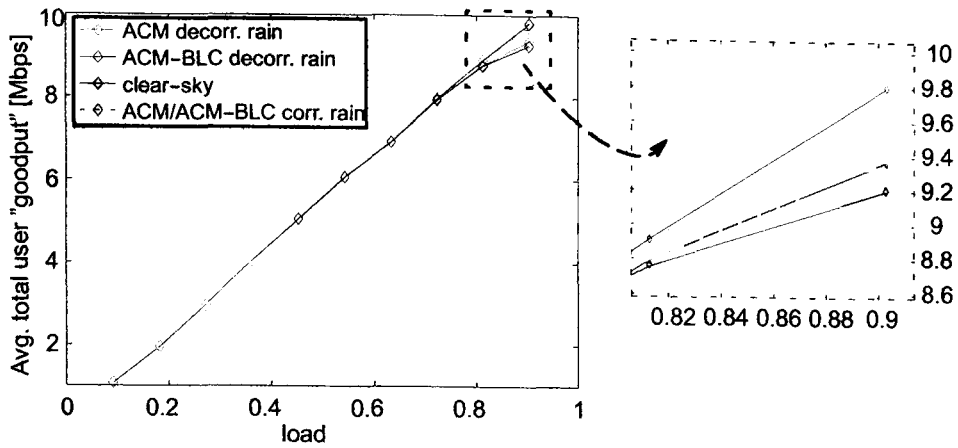

Figure 5.22 Average total user goodput as a function of channel load for clear-sky and ACM/ACM-BLC in correlated and decorrelated rain scenarios

Similarly to the utilisation above, there is also a slight drop of the average throughput values of up to 600 kbits (400 kbits for ACM and 600 kbits for ACM-BLC) which leads to the conclusion that specific traffic statistics together with rain must have caused not all useful data to be transmitted by the time the simulation was over, when compared to the other scenarios.

Next, the queue sizes and resulting delays are discussed. Figure 5.23 illustrates the average size and variation of the global queue and Figure 5.26 shows the resulting average delay and delay variation. The standard deviation, i.e. the dispersion or spread of the delay values away from their mean, is used here as a measure of the delay variation. The curves demonstrate how detrimental rain can be for the system.

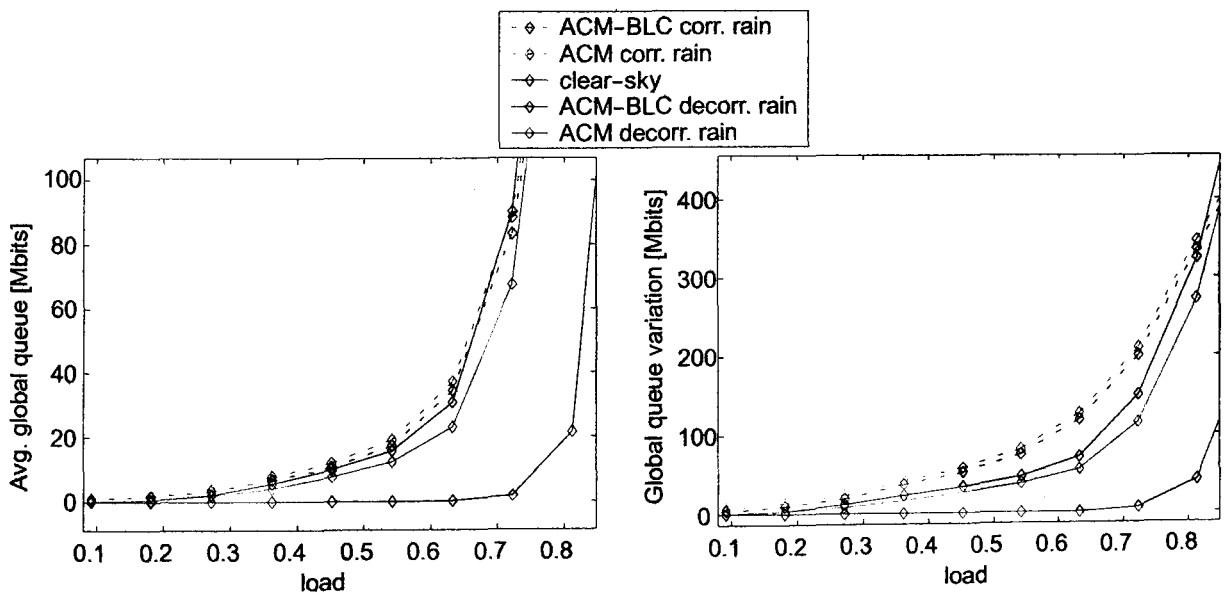

Figure 5.23 Average global queue size and queue variation as a function of channel load for clear-sky and ACM/ACM-BLC in correlated and decorrelated rain scenarios

Something of importance that needs to be pointed out at this stage is that -although the delay results can be confidently used as a general indication of the performance of the FMT schemes- for the comparative part of the analysis between the two schemes, the delay curves do not fairly reflect the potential delay improvement that is brought by BLC. The reason is captured by the following example.

Figure 5.24 shows the utilisation and useful throughput as a function of time, for one connection transmitting over the MF-TDMA subspace, utilising pure ACM and combined ACM-BLC as FMT during rain.

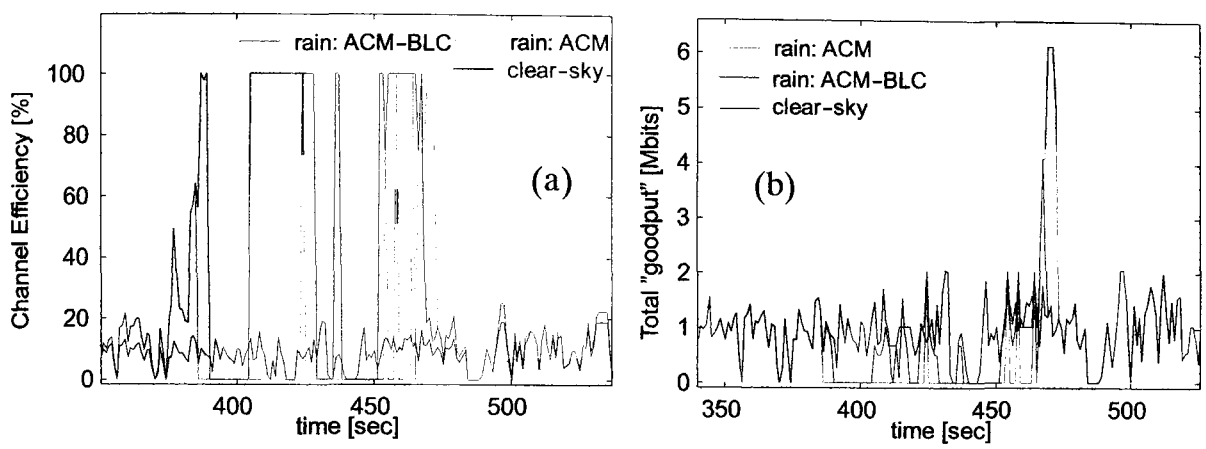

Figure 5.24 Utilisation and useful user throughput (goodput) for clear-sky, and during rain with ACM and ACM-BLC

The longer outage period of the link with pure ACM, when compared to ACM-BLC leads to a larger queue of useful data waiting to be transmitted when conditions improve. This is further confirmed by Figure 5.25(a) that shows how, by preventing or reducing outage periods, the BLC-extended ACM scheme can even keep the queue sizes lower when compared to pure ACM. Figure 5.25(b) shows the resulting queuing delays.

The queuing delay, i.e. the time during which a packet stays in the queue prior to transmission, is calculated using equation (5.6):

$$D_{queue} = \Delta T = \frac{N_{pkt}}{R_{pkt}} \tag{5.6}$$

where $D_{queue} = \Delta T$ is the queuing delay prior to transmission, N_{pkt} is the total number of packets in that queue and R_{pkt} is the current transmission cell rate.

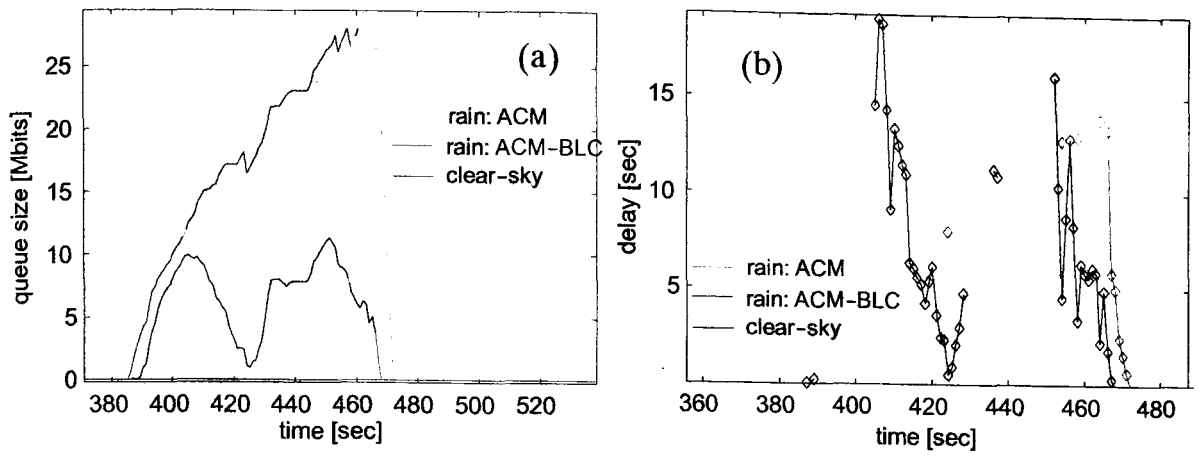

Figure 5.25 Queue size and resulting queuing delay for ACM and ACM-BLC

This is due to the software not being able to capture and quantify the improvement brought by BLC during periods that ACM on its own cannot compensate for attenuation resulting to an outage. Shorter or no outage periods for the extended ACM-BLC scheme, ironically lead to a bigger set of delay results available for averaging (see Figure 5.25(b)), sometimes resulting to a false increase of the average delay calculation outputs for ACM-BLC - while on the other hand, zero allocated data rate values during an outage on ACM mode lead to subsets of undefined delay (divide-by-zero) values that get ignored by the software and generate a smaller set of delay values for averaging, see equation (5.6) and Figure 5.25(b). This is why the queuing delay calculations fail to reflect the potential delay improvement that can be brought by BLC through prevented or reduced outage periods, thus when it comes to the comparison of the performance between the two schemes, the queue size and variation results always have to be considered to be a fairer indication of the comparative performance; as long as the average queue sizes do not grow noticeably or are kept within the same range, BLC is not introduced at the price of any additional delay. This could have been a main disadvantage of BLC with an impact on its dynamic range and the resulting availability improvement. During an ACM outage, whenever there is some MF-TDMA space available, BLC will manage to fit more data slots into the available space thus decreasing the queues (as seen in Figures 5.19 and 5.20).

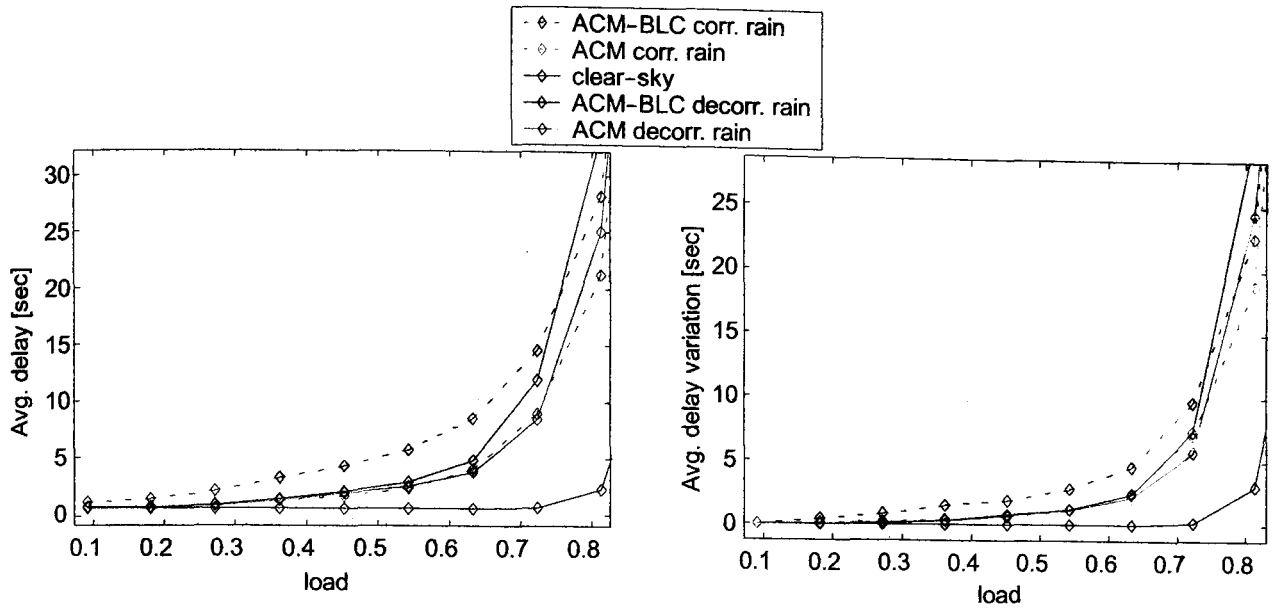

Figure 5.26 Average global delay and delay variation as a function of channel load for clear-sky and ACM/ACM-BLC in correlated and decorrelated rain scenarios

The results show that the mean end-to-end delay performance of a pure variable rate demand assignment scheme is first of all dominated by the fundamental lower bound of the propagation delay of at least two satellite hops. In the clear-sky scenario, and partly in the rainy cases, it exhibits a linear and relatively low variation in the mean delay with channel load that can be explained by considering the scheme's operation. Every connection is provided with regular and periodic request opportunities leading to regular and consistent resource allocations thanks to the BoD controller's direct mapping of requests to slot assignments whilst ensuring this is being done with fairness [gradual incremental technique of guaranteed minimum burst allocations (minimum cell rate of 16 kbps, i.e. $T_{\min} = 207\,\mu s$) to each live connection that build up in a round-robin fashion for all connections].

So thanks to this consistent and predictable behaviour, linearity is observed, even under rain conditions. As the channel load increases, the packet interarrival times are reduced, as a consequence a packet build up is created, the size of requests increases and so does the subsequent length of slot allocations to each terminal. Then the higher numbers of packets queued take slightly longer to be transmitted on the channel, increasing the average delay by a relatively small amount. This is valid up until a channel load of about 0.7 in clear-sky and 0.5 in rain conditions.

The fundamental fairness and adaptability of variable rate DAMA to match changing requirements, combined with periodic out-of-band (OBR) and/or in-band (IBR prefix) request slots, ensures that connections do not suffer any adverse effects such as being blocked from request or data packet transmission for significant periods of time. For example, if a

long burst of packets was generated by a Pareto ON/OFF source and the requests opportunities were infrequent, a large number of packets would build up in the terminal queue resulting in larger requests and subsequent allocations of slots, which would dominate the uplink frame for a long period of time, blocking other terminals from transmitting on the channel. With regular and guaranteed request opportunities, such bursts are taken care of by a higher number of requests for smaller number of slots, which should not dominate the uplink frame. So, the request and assignment process should be very similar irrespective of the nature of traffic and this regular provision of guaranteed request opportunities is what makes this scheme virtually independent from the source traffic characteristics. If only a small number of packet arrivals are able to take place between successive request slots, the packet arrival process between request opportunities is masked [5.2].

Although at the initialisation of the round-robin MAC allocation the requests are initially sorted from heaviest to lightest, thus slightly favouring and giving initial priority to the highest requests, any request that is not fully granted in the current allocation round is queued by the traffic source to be served in the next allocation period. Hence all connections are served, but the very greedy BoD requests may end up as partially queued.

The results show a significant increase in queue sizes and delay for all scenarios at or beyond the 0.8 channel load, with the mean queue and delay values being significantly higher under rain conditions when compared to the clear-sky case, especially beyond a channel load of 0.5 (Figures 5.23 and 5.26). In clear-sky conditions this is due to the specific simulation statistics, with a significant period of time during which the number of terminals generating bursts exceeded the sustainable number. Moreover, it becomes clear that under rain conditions, the FMT is mainly what amplifies this phenomenon of increased queuing delays as the channel load increases. A general observation in all cases is that the DAMA scheme, although constrained by the minimum propagation delay bound, can offer stable delay performance.

In the following part, the consequences of varying the proportion of rain-affected sources in a network is investigated.

Performance of the model with varying number (percentage) of rain-affected sources

The next part of the investigation involves a variable number of rain-affected sources transmitting over an MF-TDMA network with a fixed load (total number of connections and peak transmission rates unchanged hence keeping the product $N\overline{R}_b$ constant). In practical terms, this is representative of a situation where, in a network with N live connections operating, rain starts to gradually affect different terminals that either happen to be located in the same area (correlated rain case, one connection per terminal assumed) or are geographically multiplexed (i.e. terminals belonging to different geographical areas are intentionally grouped together and mapped onto the same MF-TDMA subspace to reduce the probability of raining everywhere at the same time (decorrelated case)). The latter case, with decorrelated rain events being introduced gradually into the simulation, represents an unfortunate scenario of different rain events occurring quite close in time, on different geographical locations. This, although rare, could occur during winter. So, investigating how the performance of the system is affected in such situations is of great interest.

The following figure shows average channel utilisation and useful throughput results, collected and averaged after multiple simulation runs. For the decorrelated cases, both pure and BLC-extended schemes exhibited very similar and stable behaviour in terms of achieved average throughput and utilisation outputs.

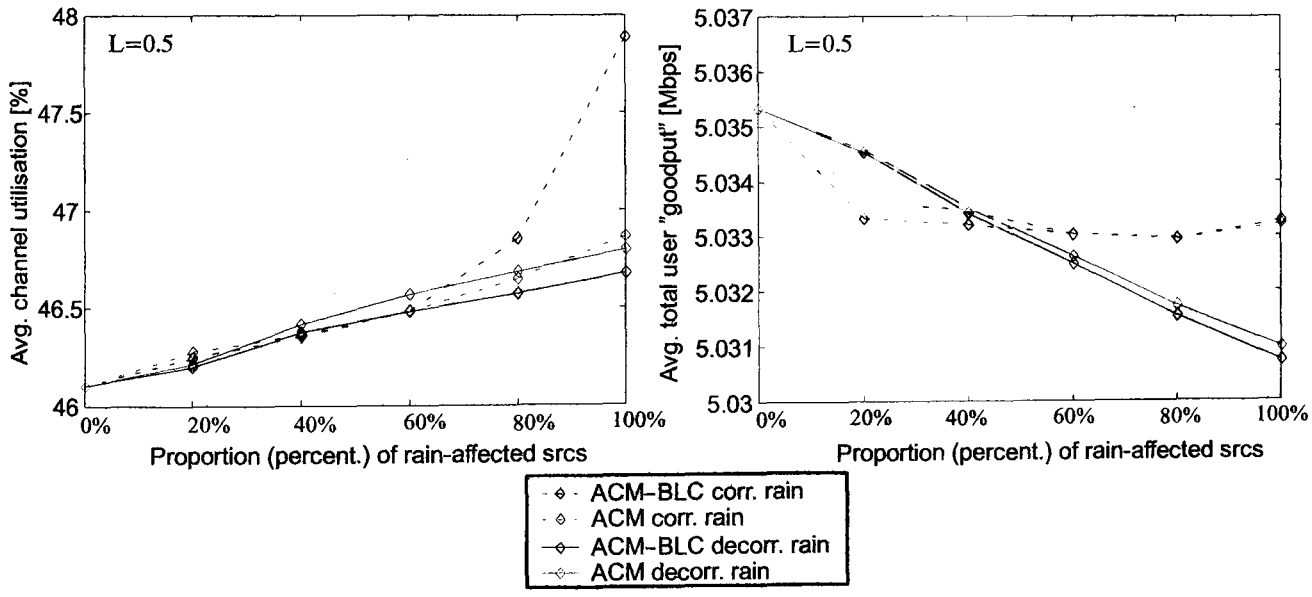

Figure 5.27 Average channel utilisation and average total user goodput as a function of the proportion (percentage) of rain-affected links (L denotes the load)

The average utilisation shows a small, consistent and linear increase for both schemes in the decorrelated rain case and the ACM correlated rain scenario. The BLC extension exhibits

only a slightly higher increase of the average utilisation values when the population of rain affected users exceeds 60% and an increase of 1% when more than 80% of the connections are affected. Generally an increase in average utilisation for an unchanged average goodput indicates added redundancy (noticeably increased FMT resources due to BLC). Note that the particular chosen channel load of L=0.5 was purposefully chosen so that the network was underloaded, but all transmissions could take place rather smoothly and comfortably without any problems/significant queuing delay in the starting clear-sky operation phase. This way, any effects resulting purely from the FMT employment itself during rain, would be easier to identify.

The average goodput values achieved also showed a negligible reduction as the proportion of decorrelated rain-affected users increased, and almost remained unaffected in the correlated case. This indicated that despite any short-term (instantaneous) goodput variations during rain periods for the various users affected (as seen in Figure 5.19 at an individual user level), the system achieved, in the long-term, the overall intended useful data delivery. If a significant drop in goodput had been observed this would indicate data loss or failure to deliver the same useful data that a clear-sky operation would, during one hour of network operation time. As it was earlier seen in this chapter (Figures 5.18 and 5.19), any significant reduction of total goodput during rain (higher FMT/real-traffic proportion for a particular resource utilisation that results from ACM or BLC employment during rain) gets fully recovered straight after, as soon as the weather conditions improve. The fact that even in the correlated case a stable behaviour was observed is quite encouraging.

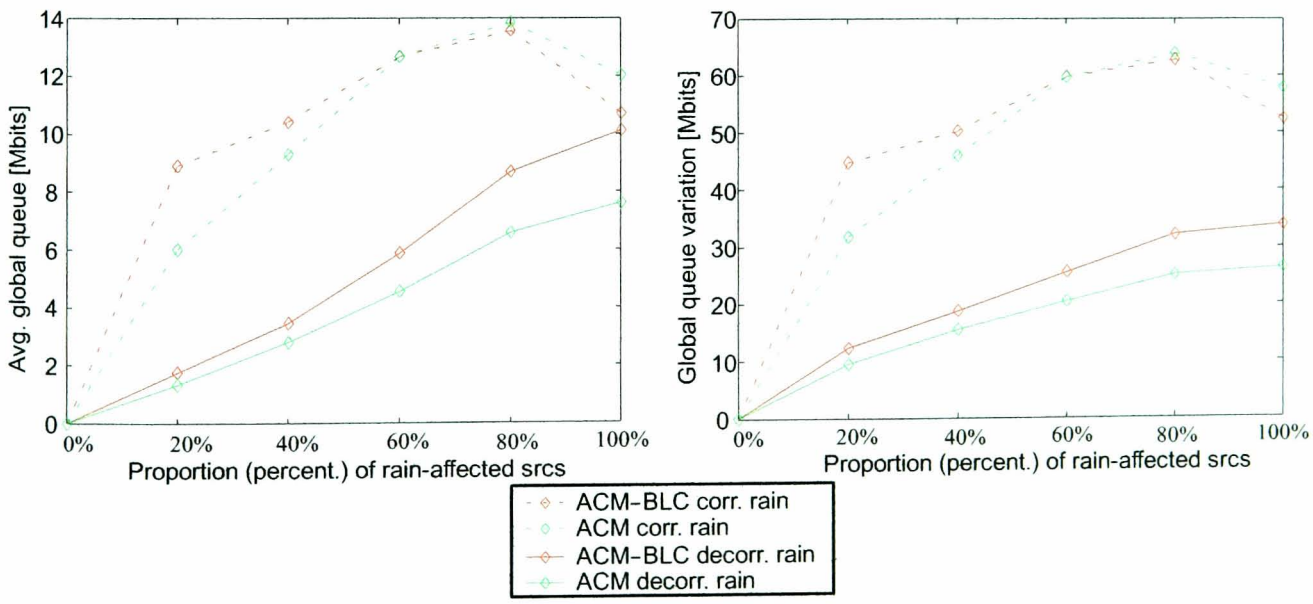

Figure 5.28 Average global queue and global queue variation as a function of the proportion (percentage) of rain-affected links

Figure 5.28 shows the global queue behaviour with the changing rain-affected user population. Considered in combination with Figure 5.29, it indicates that BLC is introduced at the price of queuing and thus delay. In the decorrelated rain case it becomes evident that the mean and variation of the global queue size increases almost linearly with the number of rain-affected users. The correlated case shows increased queuing when only 20% of the users experience rain that requires BLC to be utilised. First of all, the higher values of average queue size and variation compared to the decorrelated cases with both schemes are just a result of the deeper attenuation experienced due to the particular event. Within the correlated rain scenario itself though, when rain is introduced for just 1 out of 5 users, the queue average and variance differ significantly if BLC is used to extend the ACM dynamic range, compared to the pure ACM scheme. The average global queue size appears to have increased by 3 Mbits and its variation by 13 Mbits.

Surprisingly, this significant increase is not observed when more users become rain-affected. This shows how other factors might contribute to the reaction and performance of the system. Such factors are specific traffic statistics and multiplexing of sources as well as RA algorithm performance under different circumstances, such as bandwidth partitioning inefficiency issues. The set(s) of channels that the bandwidth is partitioned into every allocation period are determined by the FMT modes required by the users. This decision is therefore purely FMT oriented and under some circumstances might be seen as unfair with respect to the clear-sky users although the algorithm does its best to make decisions proportional to the requirements. For example, in the particular case where just one connection happens to dominate the MF-TDMA subspace due to severe rain conditions (needing the most robust ACM scheme, i.e. widest possible carrier), the clear-sky connections might end up being put on hold for a long period hence potentially experiencing growing queues and longer delays. This is believed to be the reason why at 20% of rain-affected users the average global queue values showed a significant increase. In that particular case, the bandwidth partitioning and resulting allocation happened to be more favourable to rain-affected stations over the rest, and this was naturally reflected on the rest of the queues and their resulting delays. The fairness with which the users are treated by the resource allocation algorithm increases with the number of users suffering from rain, especially since it is the same rain event they experience (equal opportunity to share the fair amount of common resource they are mapped to, thanks to their common ACM mode). This could be the reason why relatively smaller increments of average queue and variation values were observed in the gradual correlated rain case and why, when all sources suffered from the same event, these values even showed a relative decrease; users were finally all treated equally by being able to proportionally share the MF-TDMA subspace which, during the

worst rain conditions, consisted of just one wide carrier: the one for the most robust ACM mode.

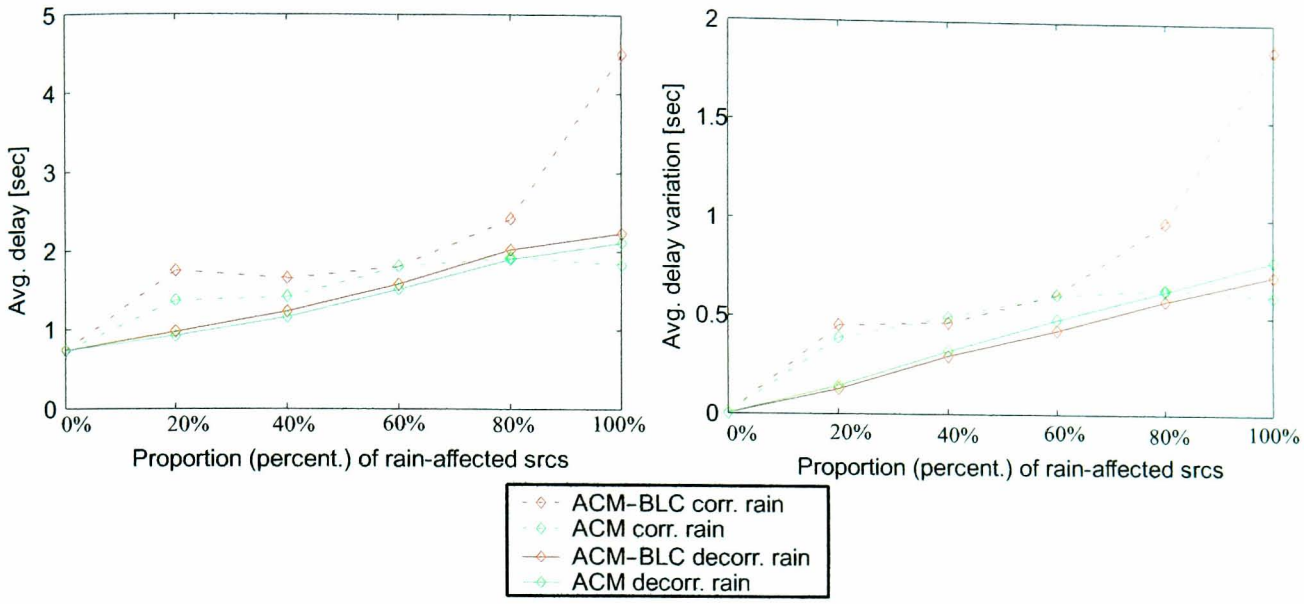

Figure 5.29 Average global delay and delay variation as a function the proportion (percentage) of rain-affected links

Figure 5.29 includes the delay graphs which are not believed to reflect the actual relative performance of the two FMT schemes, especially in the correlated rain scenario. First of all, it is not what would normally be expected due the relatively lower average global queue and queue variation values seen in the 80-100% region (Figure 5.28) whilst the average throughput in Figure 5.27 remained unchanged. Furthermore, as it was discussed earlier, in cases of system outage while on ACM mode, the queuing delay calculations fail to reflect the potential delay improvement that can be brought by BLC. Shorter or no outage periods achieved by the extended ACM-BLC scheme, unfortunately lead to a bigger set of delay results available for averaging hence falsely increasing the average delay value calculated for ACM-BLC.

Despite this, it has become apparent that FMT generally amplifies the potential problem of growing queues and resulting queuing delays as the channel load increases. During a system outage while in ACM mode, if there are resources available (low channel load, users not transmitting at peak rate), BLC can be effectively applied by utilising the available resources and compensating for extra attenuation. At low loads it is possible for BLC not to be introduced at the price of any considerable delay. BLC is introduced as an extension to ACM which can itself exhibit an increasing queuing delay performance in unfavourable channel and traffic conditions. If BLC is introduced at the price of delay, its potential advantage of extending the dynamic range of ACM and improving the availability of the system become uncertain.

B. Managing the Queues: Traffic Shaping

It is well-known that increased traffic can create congestion problems by causing the demand for resources to exceed the available capacity. The Call Admission Control operation is there to ensure, based on the traffic characteristics and requirements of the calling connections, that only connections that can be served within the available capacity of the network will be admitted. It becomes apparent however that unfavourable rain conditions can change the situation for channel loads that could otherwise be served by the network without problems. Queues can increase rapidly and long delays can be generated that can severely limit the advantages obtained by dynamic resource sharing. This might go against the quality of service agreement between certain connections and the network, and even move the FMT dynamic range and their link availability potential improvement to uncertainty.

So, a key additional requirement is to be able to control the stability of the queues at each of the sources and try to minimise and control the delay in case of extreme network congestion due to very unfavourable traffic and/or rain conditions.

A simple way of achieving this second layer of protection is to apply traffic shaping to all the sources. As an extension to the design, a variable Peak Cell Rate (PCR) traffic shaping technique is furthermore implemented here. When the MF-TDMA network becomes too congested, the sources are made to reduce their traffic by reducing their PCR. Similarly, when conditions improve or buffer occupancy is relatively low, the BoD controller allows the sources to increase their PCR to achieve higher user throughputs. Thus, when the system is very heavily loaded, the throughput of the connections is reduced until the system becomes capable of reducing its queued backlog traffic.

Figure 5.30 shows the operation of the dynamic PCR adaptation scheme for a particular traffic source. Whenever the size of the transmission queue for that source exceeds a certain threshold (for this example it was set to 2 Mbits), the BoD controller reduces the peak cell rate of the source by a factor of two. The source is then able to gently increase its peak bit rate in steps of 128 kbps until the next time the queue exceeds the threshold when it is again reduced by factor of two. The increments are allowed by the BoD controller every second. This has the effect of reducing effectively the depth of the queue. Clearly this congestion control mechanism is reminiscent to that used by TCP networks [5.12]. In severe conditions due to either heavy traffic and/or heavy rain, this mechanism is extremely useful as it prevents queues from growing too large. It protects the network from further congestion and reduces the possibility of having to block or shut down individual connections. Thus the main part

of the resource management can be performed by the BoD controller and not the Connection Admission Controller.

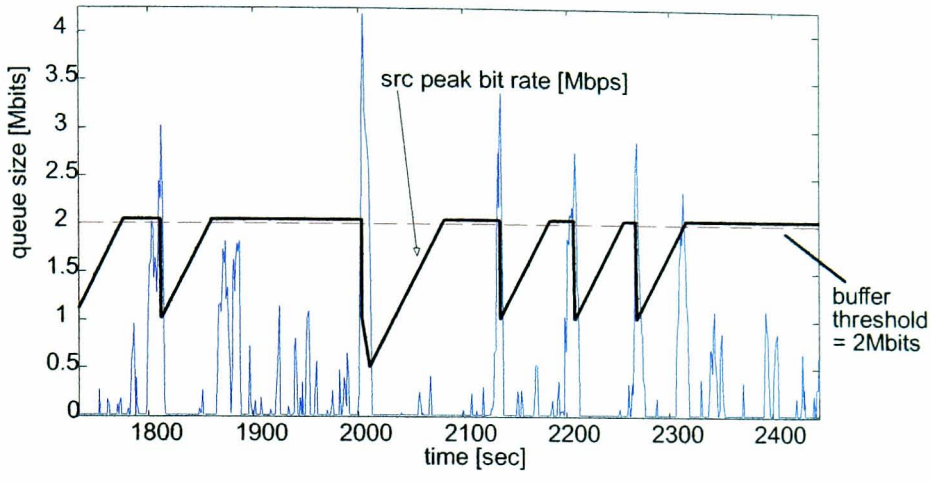

Figure 5.30 Dynamic PCR adaptation to control the queue of an individual connection

The following figure shows examples of significant reductions in global queue size for ACM-BLC with and without dynamic PCR. In fact, figure 5.31(b) shows a severe case where the global queue carries on growing during the whole simulated network time of one hour. A buffer threshold of 6 Mbits was used and proved adequate for queues to reduce rapidly hence reducing the resulting queuing delays for moderate to high loads.

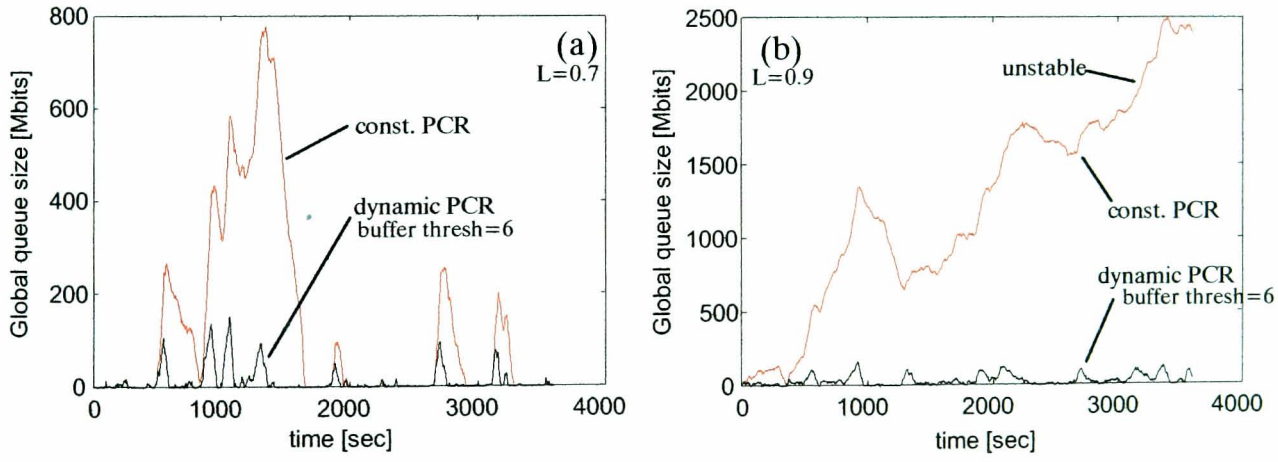

Figure 5.31 ACM-BLC: global queue for channel load of (a) 0.7 and (b) 0.9, before and after employing dynamic peak rate adaptation

Below is an example of multiple individual queues that make up the global queue of Figure 5.31(b). The queues state before and after applying dynamic PCR adaptation is shown in (a) and (b) respectively. Notice how the majority were kept under the buffer threshold of

6 Mbits, with certain queues exceeding it for a short period until the dynamic PCR managed to finally relieve them by gradually shaping the traffic of their corresponding connections.

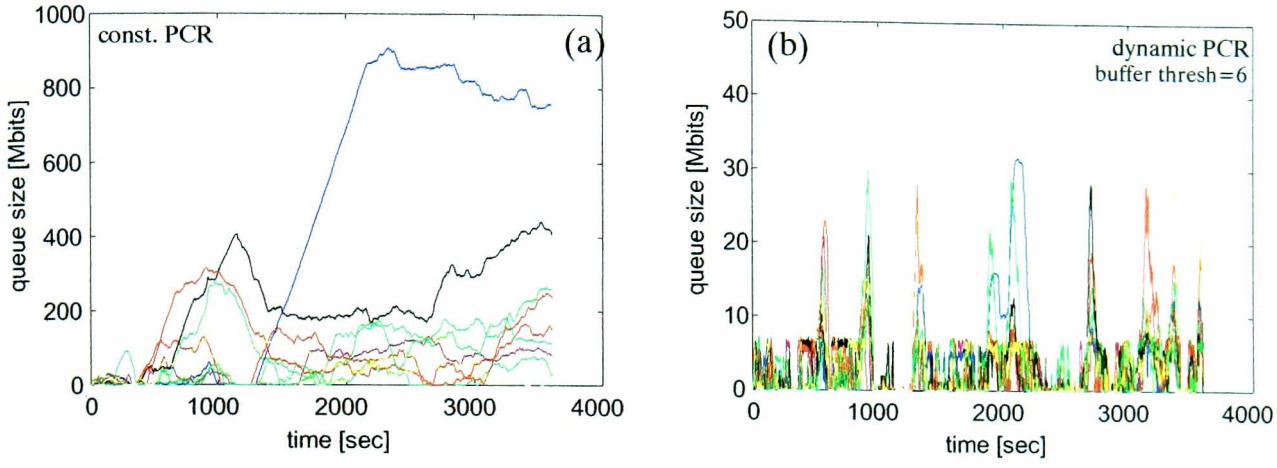

Figure 5.32 ACM-BLC: individual queues for L=0.9 (a) before and (b) after employing dynamic peak rate adaptation

A natural question that arises here is regarding the value of this buffer threshold. The approach that can be taken here is for the designer to set and optimise such threshold in the best possible way, based on practical considerations of the actual buffer sizes that can be incorporated to accommodate each connection's queue. A sensible approach is to assume that these buffers should be able to support packets waiting for transmission for at least as long as the fundamental lower end-to-end delay bound of two satellite hops in case of satellite-based schedulers and three hops for a ground-based scheduler. If buffer sizes only satisfy this minimum, based on the RTT-bandwidth product (2RTT $\times$BW or 3RTT $\times$BW), such buffers should range from 6 to 8 Mbits (for a maximum bit rate of 10.92 Mbps, $M = 16$, $\rho = 2/3$). In that case the buffer threshold would have to be set to an even lower value to ensure that buffer sizes are not exceeded, or else packets that arrive at a full buffer would be dropped. In any case, the congestion control technique applied to such systems would take care of this issue. For the purpose of this thesis, a buffer threshold of 6 Mbits, although quite high if the above practical limitations apply, was adequate to demonstrate significant performance improvements and provides the confidence that an even lower threshold would only further improve the system performance.

Figure 5.33 shows that average utilisation values remain mostly unaffected by traffic shaping, with a slight gradual drop compared to clear-sky values beyond the 0.6 channel load ranging from 1-4% for the decorrelated rain scenarios for both AC and ACM-BLC, possibly caused by larger variation of results due to different resource allocation efficiency (different bandwidth partitioning and packing algorithm decisions).

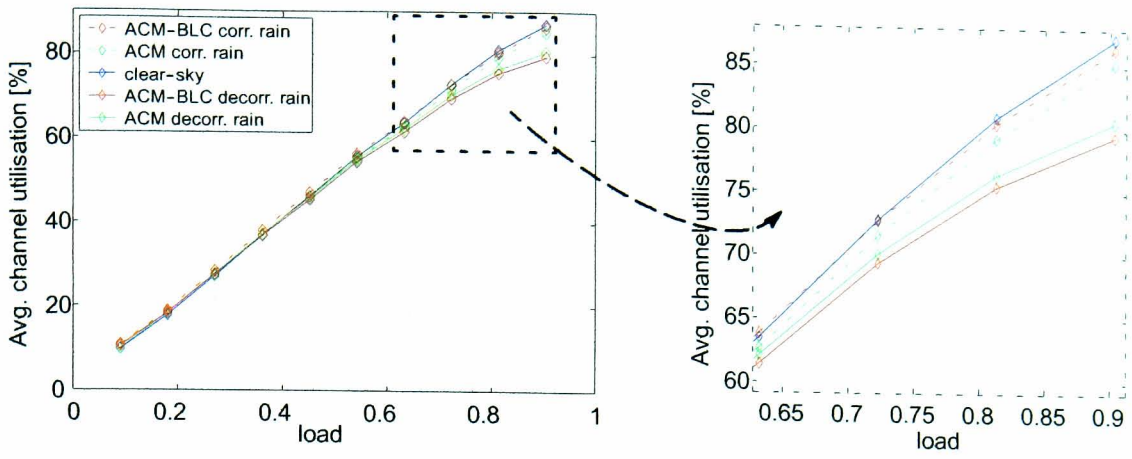

Figure 5.33 Average channel utilisation as a function of channel load for clear-sky and ACM/ACM-BLC with dynamic peak rate adaptation

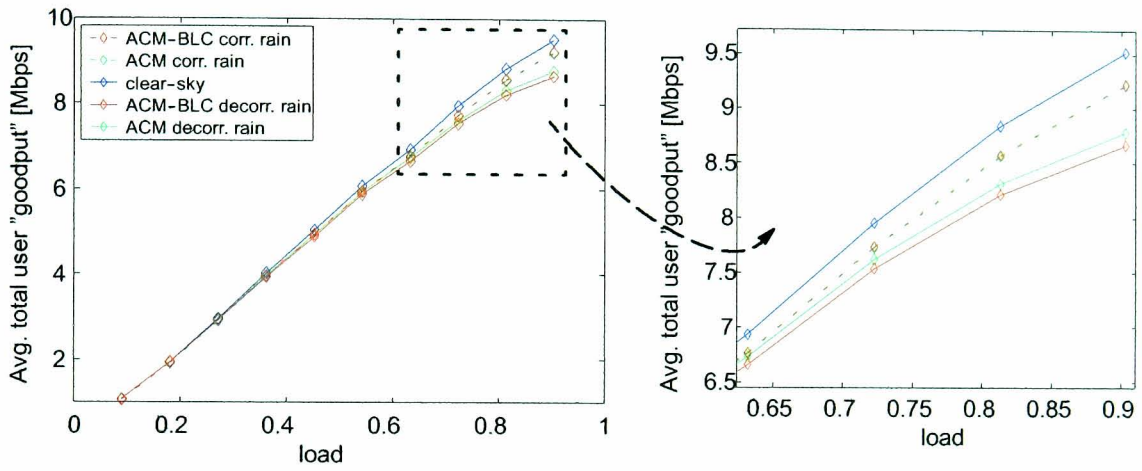

Figure 5.34 Average total useful throughput as a function of channel load for clear-sky and ACM/ACM-BLC with dynamic peak rate adaptation

Similarly for Figure 5.34, the average values for the useful throughput remain mostly unaffected - despite a reduction at the highest channel loads (reaching 1 Mbps at 0.9 load), when compared to clear-sky for the decorrelated case. This happens because in the decorrelated scenarios, the rain events are all spread out during a period of one hour, some happened to occur in the last part of the simulation, with one occurring during the very last minutes before the simulated hour was over. This clearly implies that at the simulation finishing point, some useful data (how much also depends on the specific traffic statistics) still remained in the queues, thus, in the finite simulation time, did not have the chance to get transmitted.

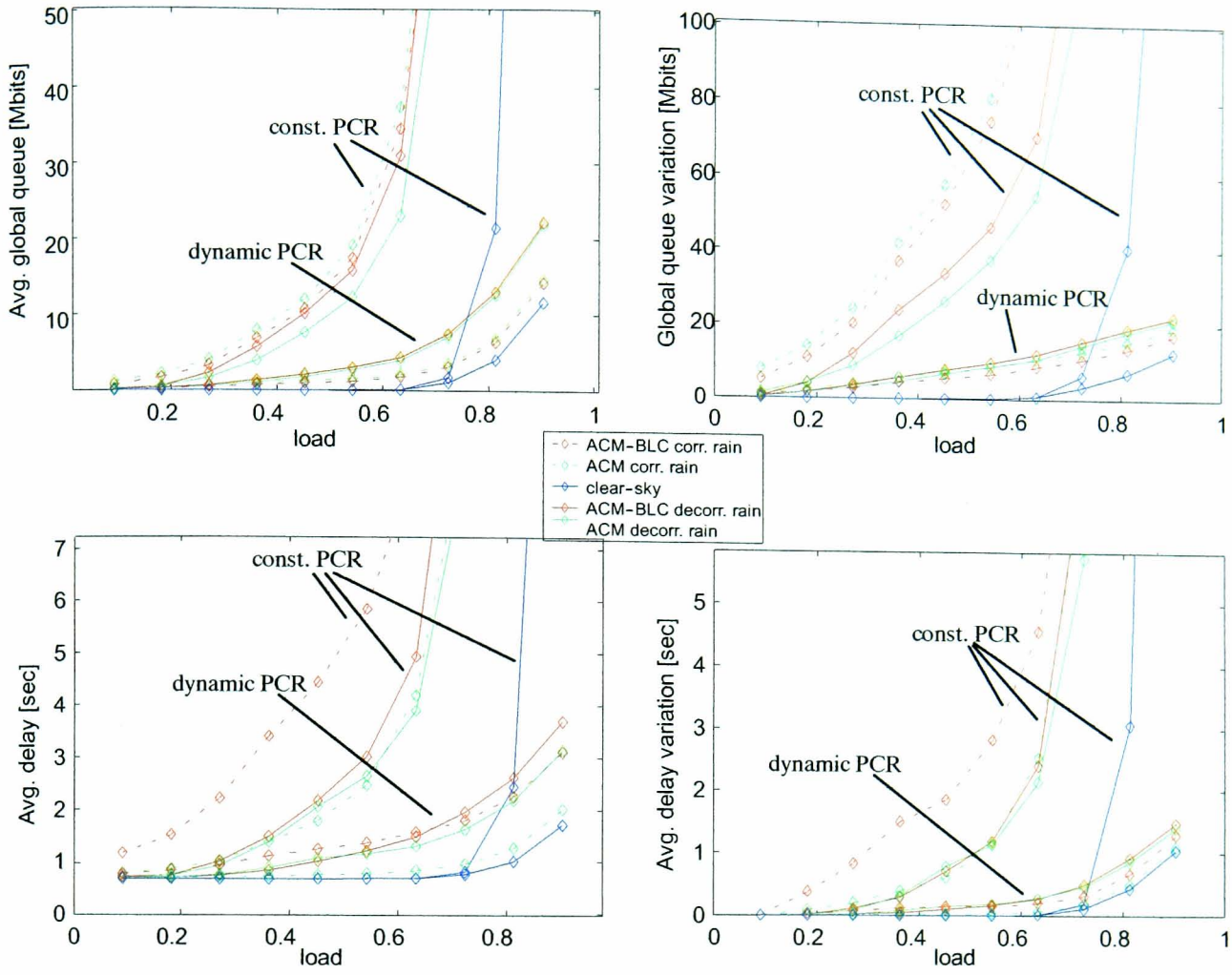

Figure 5.35 Global queue and delay results as a function of channel load

Figure 5.35 shows the significant improvement brought by the dynamic PCR adaptation technique to the system performance. The average values and variations of queues and resulting delays are reduced drastically.

Although there is an independent FMT and queue management approach to the design, traffic shaping is applied in the bad range of (traffic and/or rain) conditions. As it was seen earlier, it is mainly the FMT that increases queuing delays with increasing load. Hence in clear-sky conditions, the dynamic PCR adaptation only gets activated at the highest loads (0.8, 0.9). Even if the buffer threshold had been lower, no noticeable difference would have been made to the resulting delays as they are mainly the result of the fixed minimum propagation delay bound and not the variable delay component resulting from queuing.

In the rainy cases, the PCR adaptation takes place almost straight away starting from low to moderate loads and ending up significantly improving the performance of the system at higher loads, keeping it consistently closer to the more stable clear-sky DAMA scheme.

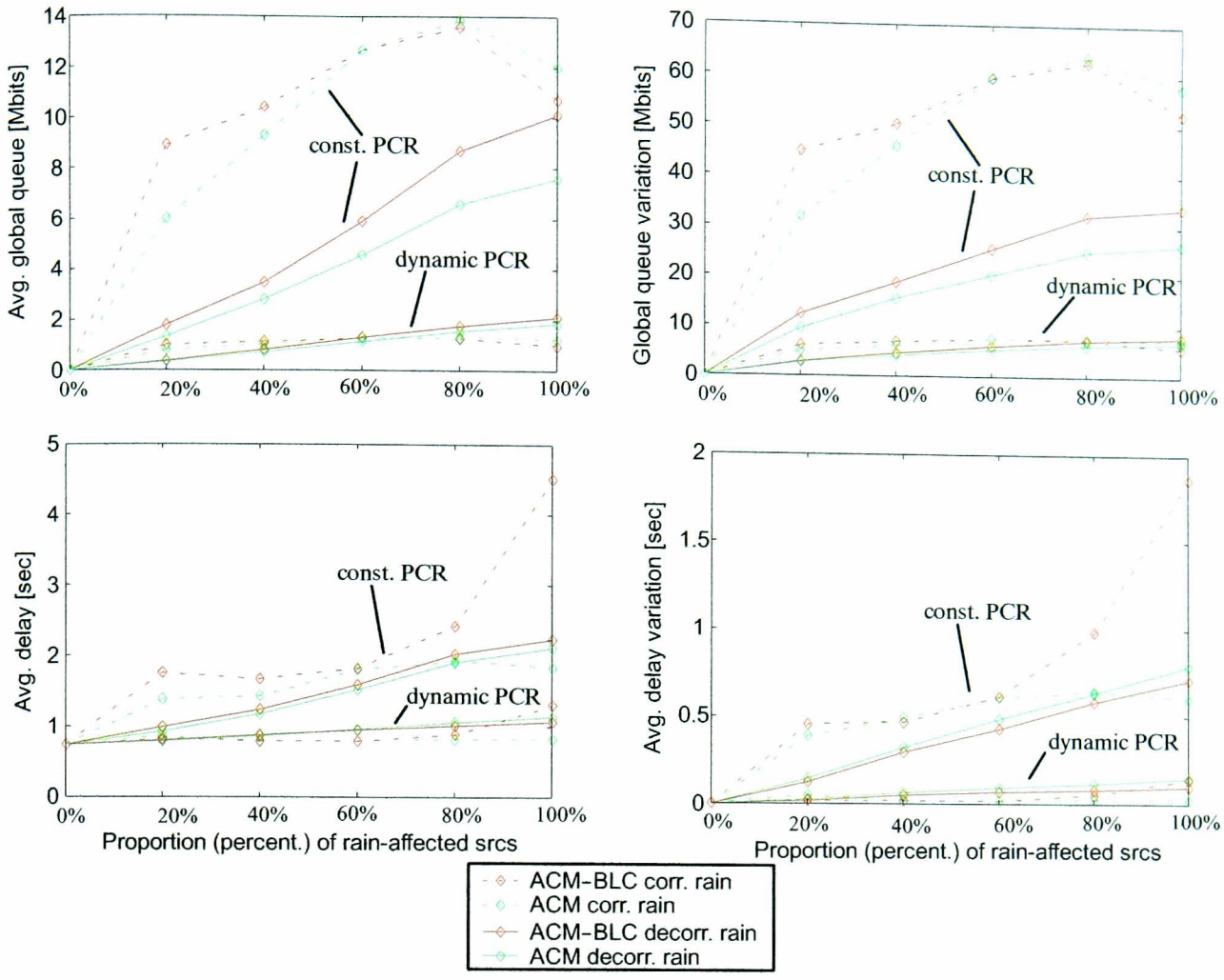

Figure 5.36 Average global queue and delay results as a function of the proportion (percentage) of rain-affected links

The same observations apply to the plots of Figure 5.36. A much more stable and consistent behaviour is noticed as more stations of a fixed network, operating at medium load, are affected by rain. The average global queue values are kept within only a 2 Mbits range when all stations eventually get affected (with the variation kept below 10 Mbits) - an 85% reduction of the average global queue size when compared to the 14 Mbits of maximum queue size (variation up to 60 Mbits), reached in the original simulation runs with constant PCR. Hence the resulting average end-to-end delay with PCR adaptation goes up to 1.2 seconds with a variation of 167 ms when all stations are affected.

5.2 Conclusions

As long as there are resources available, BLC with dynamic range of 14.7 dB will manage to extend ACM's dynamic range and compensate for an extra attenuation of 6 dB. If there are not enough resources, increased queuing might however make things worse resulting in

longer delays. Using the statistical multiplexing of bursty traffic sources that do not always transmit at peak bit rate, BLC can still be introduced. This chapter has investigated the price at which BLC is introduced and whether its advantages can still be exploited when traffic load increases.

BLC can be introduced without generating considerable delay:

- at low loads when there is plenty of spare resource available or
- at the price of variable peak bit rate, through a traffic shaping mechanism.

It is possible to extend the dynamic range of ACM and improve the availability of the suffering power-limited return link. If reducing the peak bit rate is unacceptable for certain types of sources, the first of the two is the only option; and if a certain dynamic range is required by these connections to guarantee a certain link availability, then this option unavoidably comes with the disadvantage of poor channel utilisation in clear-sky, as spare resources would have to be guaranteed at all times for these connections to be able to use them in rainy conditions.

5.3 References

[5.1] Crovella M. E., Bestavros A., "Self-Similarity in World Wide Web Traffic: Evidence, and Possible Causes", IEEE/ACM Transactions on Networking, vol. 5, no. 6, pp. 835-846, 1997.

[5.2] Mitchell P. D., "Effective Medium Access Control for Geostationary Satellite Systems", PhD Thesis, University of York, U.K., 2003.

[5.3] Willinger W., Taqqu M. S., Sherman R., Wilson D. V., "Self-Similarity Through High-Variability: Statistical Analysis of Ethernet LAN Traffic, at the Source Level", IEEE/ACM Transactions on Networking, vol. 5, no. 1, pp. 71-86, 1997.

[5.4] Leland W. E., Taqqu M. S., Willinger W., Wilson D. V., "On the Self-Similar Nature of Ethernet Traffic", IEEE/ACM Transactions on Networking, vol. 2, no. 1, pp. 1-15, 1994.

[5.5] Mitchell P. D., Grace D., Tozer T. C., "Comparative Performance of the CFDAMA Protocol with Various Terminal Request Strategies", IEEE Global Telecommunications Conference (GLOBECOM), vol. 4, pp. 2720-2724, 2001.

[5.6] Jiang Z., Leung V. C. M., "A Predictive Demand Assignment Multiple Access Protocol for Internet Access over Broadband Satellite Networks", International Journal of Satellite Communications and Networking, vol. 21, p. 451-467, 2003.

[5.7] Kramer G., "Self-Similar Network Traffic - The Notions and Effects of Self-Similarity and Long-Range Dependence", May 21, 2001, retrieved January 2003, from http://wwwcsif.cs.ucdavis.edu/~kramer/papers/ss_trf_present2.pdf

[5.8] Bononi A., Tancevski L., Rusch L. A., "Large Power Swings in Doped-Fiber Amplifiers with Highly Variable Data", IEEE Photonics Technology Letters, vol. 11, no. 1, pp. 131-133, 1999.

[5.9] Zukerman M., Neame T. D., Addie R. G., "Internet Traffic Modelling and Future Technology Implications", Proceedings of IEEE INFOCOM 2003, S. Francisco, CA, USA, Apr. 1-4, 2003 (also available at http://www.ieee-infocom.org/2003/papers/15_01.pdf, last access: 11 June 2008).

[5.10] Kaj Ingemar., Gaigalas R., "Stochastic Simulation using Matlab", Seminar and Workshop, November 2001, retrieved May 2003 from the Uppsala University website: http://www.math.uu.se/research/telecom/software/

[5.11] Mobasseri M., Leung V. C. M., "Bandwidth Assignment for VBR Traffic in Broadband Satellite Networks", 2000 Canadian Conference on Electrical and Computer Engineering, Halifax, NS, Canada, vol. 2, pp. 654-658, 2000.

[5.12] Jacobson V., "Congestion Avoidance and Control", ACM, SIGCOMM '88, August 1988.

[5.13] Cardellini V., Colajanni M., Yu P. S., "Geographic Load Balancing for Scalable Distributed Web Systems", IEEE. Proceedings of Mascots 2000, San Francisco, Aug./Sep. 2000.

[5.14] Paxson V., Floyd S., "Wide Area Traffic: the Failure of Poisson Modelling", IEEE/ACM Transactions on Networking, vol. 3, no. 3, pp. 226-244, 1995.

CHAPTER 6

CONCLUSIONS AND FURTHER WORK

6.1 Resource-shared FMTs

Satellite systems have some outstanding challenges to cope with; resource management is a major issue because of the latency and the limited capacity resource available. Solutions have to be mainly based on recognised network protocols and standards in order to reduce costs, and for two-way services the use of the DVB-RCS protocol is a commonly accepted choice.

Improved solutions include use of higher frequency bands and multi-beam coverage to increase throughput and system capacity. Higher frequency satellite systems can however suffer from severe atmospheric impairments and require advanced techniques to compensate for the effects of rain attenuation. Keeping a classical approach, based on a worst case sizing, will result in fixed over-sizing of systems leading to reduced efficiency and unreasonable costs. It is therefore necessary that these systems include adaptive FMTs to counteract propagation impairments in real-time and use system resources efficiently.

DVB-RCS and DVB-S standards have not primarily been defined considering the details of rain FMTs; they have to be adapted to support FMTs, so the study of efficient FMTs and their integration within the standards is necessary. Some FMTs, are already adopted by current systems (e.g. Power Control [6.1] and [6.2]), and others, such as ACM, are still a subject for enhancement of the current DVB-RCS standard (DVB-RCS [6.3]). Adaptive transmission techniques are mostly introduced as a way of achieving efficient BoD. But ACM is also a good framework for deploying FMTs and can provide high availabilities for powerful enough connections. Employing Burst Length Control can be a useful extension of ACM that permits an increase in FMT dynamic range.

6.2 Thesis Overview

This thesis has presented a detailed study of the application of an FMT to an advanced satellite network affected by rain. Through qualitative and quantitative analysis, an attempt has been made to examine the impact of the introduction of a new Fade Mitigation Technique on the interdependent system operations.

6.2.1 FMT Review

Achieving high capacity with limited radio resources is an important focus of investigation for the return link in DVB-RCS systems, since there is neither a broadcasting effect as in the forward link nor reuse efficiency as in cellular systems. Thus the management of radio resources, combined with the need for deployment of FMTs, becomes an outstanding challenge for these systems.

Fade Mitigation Techniques suitable for the enhancement of current standards were reviewed and their important implications on the MF-TDMA resource allocation process were examined. Adaptive Coding and Modulation (ACM) has been identified as an effective FMT whose advantages cannot be fully enjoyed by power-limited return links from small or very small terminals (as high-order modulation schemes cannot be used), hence an extension of the dynamic range of ACM by Burst Length Control (BLC) is particularly useful.

6.2.2 Resource Allocation in the Presence of Rain

A design methodology of a combined FMT with ACM and BLC has been proposed. The analysis shows that the system availability depends not only on the combined FMT performance, but also on the resource allocation scheme performance. For resource management, a resource allocation protocol that incorporates FMT under variable rain conditions is presented, including bursty traffic sources.

Simulation results showed that as long as there are MF-TDMA resources available, BLC will manage to compensate for 6 dB of extra attenuation. By reducing outages compared to ACM, BLC can even achieve lower queue sizes, leading to shorter queuing delays and increased channel utilisation. The price of BLC is reduced goodput (due to FMT resources needed). The average utilisation and average useful throughput performance of the system are not affected in the longer-term, except only slightly for the highest of traffic loads. When it comes to queuing and resulting delays, simulation results showed how detrimental rain can

be, especially at higher traffic loads. The FMT generally amplifies the potential problem of growing queues as the channel load increases. During a possible system outage while on ACM mode, if there are resources available (low channel load, users not transmitting at peak rate), BLC can be effectively be introduced without the price of any considerable delay. BLC is introduced as an extension to ACM which can itself exhibit an increasing queuing delay performance in unfavourable channel and/or traffic conditions. If BLC is introduced at the price of delay, its potential advantage of extending ACM's FMT dynamic range and improving the availability of the system simply become more uncertain. The simulation shows that the equality with which the users are treated increased with the number of users suffering from correlated rain. This happens because they are given equal opportunity to share the fair amount of common resource they are mapped to, due to their common ACM mode. This was expected, as decisions on the bandwidth partitioning are FMT-oriented (determined by the required FMT modes), although the resource allocation algorithm does its best to make fair decisions allocating resources proportionally to the users' traffic requirements.

6.2.3 Traffic Shaping

The Call Admission Control operation of such systems is there to ensure, based on the traffic characteristics and requirements of the calling connections, that only connections which can be served within the available capacity of the network will be admitted. It has been seen, however, that unfavourable rain conditions can change the situation for channel loads that could otherwise be served by the network without problems. Queues increase rapidly and longer delays are caused that can severely limit the advantages obtained by dynamic resource sharing, can go against the quality of service agreement between certain connections and the network, and move the FMT dynamic range to uncertainty.

Controlling the stability of the queues during unfavourable traffic and/or rain conditions becomes necessary. Through a variable PCR traffic shaping queues can be prevented from growing too large, protecting the network from further congestion and reducing the possibility of having to block or shut down greedy connections. While preserving the average channel utilisation and useful throughput performance of the system, traffic shaping brings significant improvement to the network performance at moderate to high loads, keeping it consistently closer to the more stable type of performance of the clear-sky DAMA scheme. Therefore, it is possible to extend the dynamic range of ACM *and* improve the availability of a rain-affected power-limited return link, by introducing BLC at the price of a variable peak bit rate - if this is unacceptable for some types of sources, then BLC can only be

introduced at low loads, when there are spare resources available. The price will then be poor channel utilisation in clear-sky, as spare resources will have to be guaranteed at all times so that they can be used in the case of rain conditions.

6.3 Original Contributions

The author's specific contributions and novel aspects of the work presented in this thesis can be summarised as follows:

- The extension of the FMT dynamic range of ACM with BLC, for improving the link availability of power-limited return channels.
- The identification of the complex problem of the dependence of system availability not only on the combined FMT dynamic range, but also on the resource allocation scheme performance.
- The proposal of a resource allocation protocol that incorporates FMT within a dynamic capacity assignment strategy.
- A detailed computer simulation of the proposed resource allocation scheme under variable rain conditions, including bursty traffic sources that more accurately represent the behaviour of modern Internet traffic.
- A detailed analysis of the short-term performance of the proposed scheme and comparison with pure ACM, through implementation of scenarios that stretch the system and expose relevant issues, problems and trade-offs.
- A novel adaptive bandwidth-partitioning technique, incorporating BLC, which is allowed by the DVB-RCS standard and takes into account the real-time channel conditions and traffic needs of the MF-TDMA network users.

6.4 Further Investigation of Current Work

6.4.1 MAC Scheme and Source Traffic

The performance of the DAMA scheme does not depend on the source traffic characteristics thanks to the regular and guaranteed request opportunities, between which the

packet arrival process is masked. In this thesis, Pareto ON/OFF data traffic is considered, based on the wide support and recognition that modern data traffic is ON/OFF in nature and not Poisson (as traditionally assumed). Different ON/OFF distributions, such as exponential, are not expected to cause significant differences in the performance of this scheme either, as the size and regularity of DAMA requests is what primarily determines its performance. However, other families of MAC schemes that support ON/OFF type data traffic can be utilised for reducing/eliminating the fundamental end-to-end delay bound of traditional DAMA and its hybrid variants (such as Combined Free/DAMA protocols); for example Burst-Targeted DAMA [6.4], whose performance is a strong function of burst duration and inter-burst gaps in the source traffic. It can be extremely useful for delay-intolerant connections. Thus further investigation of such MAC schemes incorporating FMT resource allocation and the dependency of their performance on different source traffic characteristics could help generate further techniques to effectively provide FMT support for different types of source traffic.

6.4.2 User Priority/Preemption Schemes

Although in severe rain conditions the dynamic bandwidth partitioning technique can end up being most favourable to rain-affected users due to the FMT-oriented design approach, the DAMA scheme presented in this thesis was primarily designed to give equal channel access to all user connections in clear-sky conditions, with each user contributing an equal traffic load to the MF-TDMA channel at most times. In practice, differing service level agreements might result to different groups of users requiring permanently different amounts of capacity or different quality of service than others. It is common for networks to provide different levels of service to users at different costs, so that they can match their individual requirements. Similarly, prioritisation techniques might be needed for different applications involved, based on individual resource requirements and delay sensitivity [6.5] and [6.6]. Consideration of this issue, i.e. prioritising user connections and their FMT needs based on their QoS requirements, appears to be a further challenge that can be handled through selection of appropriate request and scheduling strategies within the MAC protocol. For example, access to random or periodically-assigned request slots (OBR method) can be exclusive to high priority users providing them with better delay performance than lower priority ones, and resource requests could be ordered to provide high priority users with preferential treatment so that they always obtain the resources they require.

6.4.3 Different FMTs/Real Network

Some additional studies could be useful in combining the proposed scheme with other FMTs. For example, Up-Link Power Control (ULPC) [6.1] and [6.2] is a suitable candidate that may potentially allow further improvements in system performance. Such goal is particularly significant for future satellite systems operating at V-Band [6.10]. Also, testing the proposed scheme on an actual network would also be very interesting.

6.4.4 Call Admission Control

Call Admission Control is the operation that ensures that, based on the traffic characteristics and requirements of the calling connections, only connections that can be served within the available capacity of the network will be admitted. Although the design of the MAC scheme in this thesis assumed that all live connections have already been admitted by CAC, the work presented in this thesis shows how unfavourable rain conditions can worsen the situation, resulting in issues serving the network. Further investigation of CAC algorithms [6.7], [6.8], and [6.9] would be interesting. Decisions to grant a connection request will be based on the service category, the desired QoS, and information from the BoD controller on the state of the network, i.e.number and traffic/rain conditions of existing connections. Appropriate geographical and rain multiplexing of connections should be applied when possible, i.e. avoiding grouping together connections from the same location to minimise the probability of simultaneously rain-affected links transmitting over the same MF-TDMA subspace.

6.4.5 Additional Considerations

Some additional considerations could be worth exploring, such as the consideration of different elevation angles for users belonging to large footprints. Finally, an extra addition could be the incorporation of hysterisis into the FMT algorithm in order to avoid unnecessary switchings in short periods of time, due to fast changes in attenuation levels, and minimise FMT signalling in the network.

6.5 References

[6.1] Nivens D., "A Novel Uplink Power Scheme for Ka-band Satellite Systems", American Institute of Aeronautics and Astronautics, AIAA 2002-1957, Montreal, 12-13 May 2002.

[6.2] Kastamonitis K., Grémont B., Filip M., "Loop-Back Detection Technique for Uplink Power Control", 22nd AIAA International Communications Satellite Systems Conference, AIAA-2004-3198, Monterey, USA, 9-12 May 2004.

[6.3] Moreau C.: "Protocols and Signalling for Adaptive Fade Mitigation Techniques (FMT) in DVB-RCS Multi-beam Systems" (Executive Summary), EADS Astrium and Space Engineering, 17-06-05, retrieved December 2005, from the ESA Telecommunications website: http://telecom.esa.int/telecom/www/object/index.cfm?fobjectid=11068.

[6.4] Mitchell P. D., "Effective Medium Access Control for Geostationary Satellite Systems", PhD Thesis, University of York, U.K., 2003.

[6.5] Iera A., Molinaro A., Marano S., "Call Admission Control and Resource Management Issues for Real-Time VBR Traffic in ATM-Satellite Networks", IEEE Journal on Selected Areas in Communications, vol. 18, no. 11, November 2000.

[6.6] Iera A., Molinaro A., Marano S., Mignolo D., "Integration of ATMand Satellite Networks: Traffic Management Issues", IEICE Trans. on Commun. (IEICE/IEEE Joint Special Issue on Recent Progress in ATM Technologies), February 2000.

[6.7] Liu K., Petr D. W., Braun C., "A Measurement-based CAC Strategy for ATM Networks", IEEE International Conference on Communications, Towards the Knowledge Millenium, vol. 3, p. 1714-1718, June 1997.

[6.8] Eom D. S., Sugano M., Murata M., Miyahara H., "Call Admission Control for QoS Provisioning in Multimedia Wireless ATM Networks", IEICE Trans. Commun., vol. E82-B, no. 1, January 1999.

[6.9] Iera A., Molinaro A., Pulitano S., "Connection Admission Control Issues in DVB-RCS Systems", Proceedings of the 6th European Workshop on Mobile/Personal SatComs (EMPS 2004) and 2nd Advanced Satellite Mobile Systems (ASMS) Conference, EMPS and ASMS Presentations and Papers, Noordwijk, The Netherlands, 21-22 September 2004.

[6.10] Kastamonitis K., "A Study of Up-Link Power Control for Digital Satellite Links in Rain Conditions", PhD Thesis, University of Portsmouth, 2005.

Appendix A : The Principle of BLC

Running the modem at maximum baud rate at all times, each bit of the burst could be repeated (stored into memory and being re-written contiguously an appropriate number of times, H, depending on the fade depth):

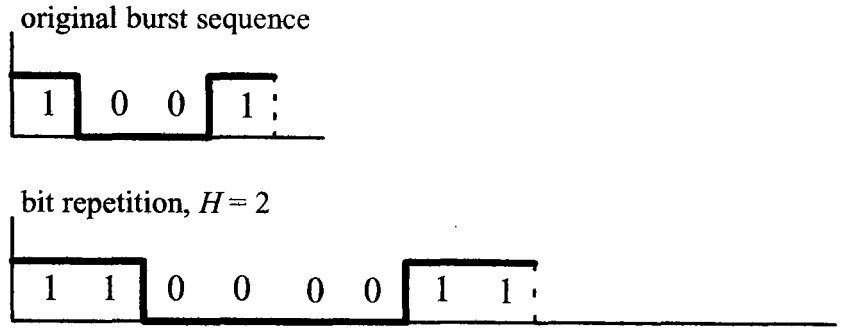

Figure A.1 An example of contiguous bit repetition showing BLC as a time expansion

The transmission bit rate is kept at maximum at all times and adaptive filters are required for the reduction of the noise bandwidth when the bits are spread. At the receiving side, clock recovery performance can be enhanced by switching the channel filter in the demodulator to the appropriate bandwidth depending on the value of H. Here, adaptive symbol and bit recovery as well as adaptive filters are required at the receive end to exploit the reduced noise bandwidth.

A long string of 0s or 1s may cause transmission synchronisation problems. By scrambling the transmitted data symbols, continuous symbol patterns can be eliminated and EMI (Electro-Magnetic Interference) noise removed. This prevents peaks in the spectrum of the modulated signal and ensures that the signal occupies a fixed bandwidth $B = (1 + \alpha) R_s$ where R_s is the symbol rate and α is the roll-off factor. In BLC, the descrambler's clock rate is kept constant with period $T_s = 1/R_s$. However the actual symbol clock used by the demodulator matched filter (after the descrambler) has to be variable and capable of tracking the variable period of the time-spread signals as shown in Figure A.1.

The single-sided power spectral density, $G(f)$, for a modulated signal stream takes the form [2.27]:

$$G(f) \propto Tsinc^2(fT) = T_s\left[\frac{\sin(\pi f T_s)}{\pi f T_s}\right]^2 \qquad (A.1)$$

where T_s is the symbol duration. The general appearance of this power spectral density is shown in Figure A.2.

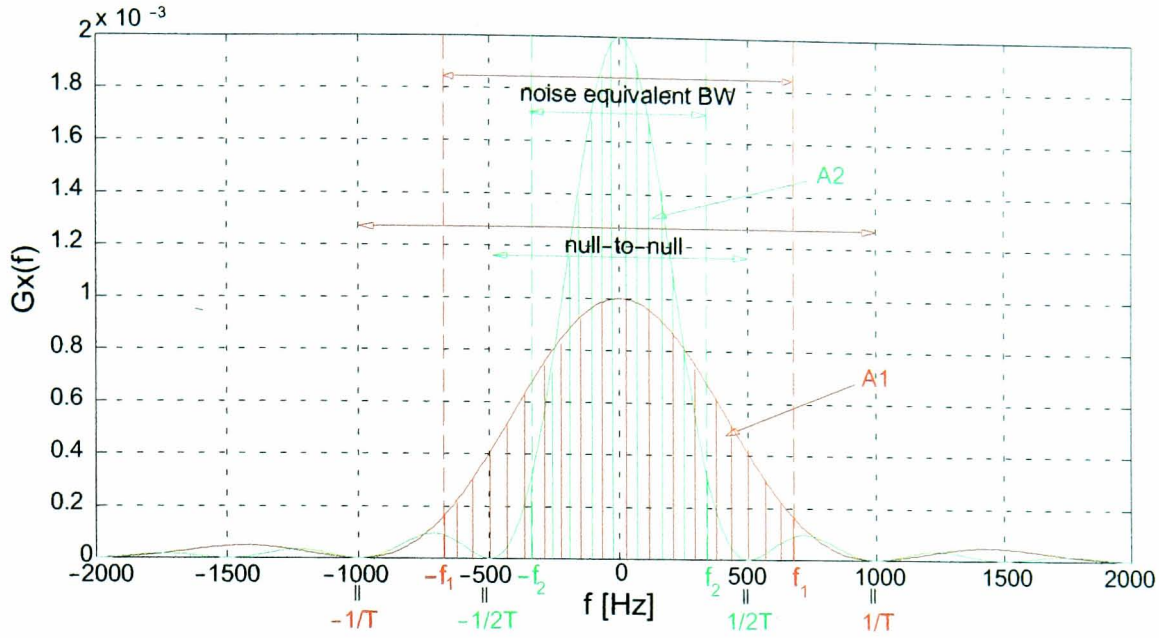

Figure A.2 General shape of Power Spectral Density (PSD) before and after spreading (H=2)

Repeating the bit H times is equivalent to increasing the symbol duration by a factor of H. For a particular expansion one can find the corresponding energy gain (by integrating the PSD function over the appropriate bandwidth and calculating the ratio of the energy after expansion and the original energy), see Figure A.2.

Let us examine the change in signal-to-noise ratio due to spreading. Originally, before BLC spreading we have:

$$SNR_1 = \frac{S_1}{N_1} = \frac{S_1}{N_o B_1} \tag{A.2}$$

where S_1 is the original, average modulation signal power and B_1 is the original equivalent noise bandwidth:

$$B_1 = \frac{(1+\alpha)}{T_{s1}} = R_{s1} \times (1+\alpha) \tag{A.3}$$

Here T_{s1} is the original symbol duration, R_{s1} denotes the original symbol rate in symbols/sec (or Baud), and α=35% is the roll-off factor [1.1].

Similarly, the signal-to-noise ratio after spreading would become:

$$SNR_2 = \frac{S_2}{N_2} = \frac{S_2}{N_o B_2} \tag{A.4}$$

where
$$B_2 = \frac{(1+\alpha)}{T_{s2}} = R_{s2} \times (1+\alpha), \tag{A.5}$$

With a spreading factor of H, we have: $T_{s2} = H \times T_{s1}$, so:

$$B_2 = \frac{(1+\alpha)}{H \times T_{s1}} = \frac{R_{s1}}{H} \times (1+\alpha) \tag{A.6}$$

From equations (A.3) and (A.6): $B_2 = \frac{B_1}{H}$ (A.7)

i.e. the bandwidth after spreading decreases by a factor of H, as expected. The signal-to-noise ratio change due to spreading can now be found using equations (A.3) and (A.4):

$$\Delta SNR = SNR_2[dB] - SNR_1[dB] = 10\log_{10}\left[\frac{S_2 \times B_1}{S_1 \times B_2}\right], \tag{A.8}$$

So, using (A.7) $$\Delta SNR = 10\log_{10}\left[\frac{S_2}{S_1} \times H\right] \tag{A.9}$$

$$\Leftrightarrow \Delta SNR = 10\log_{10}\left[\frac{A_2}{A_1} \times H\right] \tag{A.10}$$

where A_1 and A_2 are the areas shown in Figure A.2.

By integrating the power spectral density (PSD) function over the appropriate bandwidth, it is verified that $A_2 = A_1$, therefore:

$$\Leftrightarrow \Delta SNR = 10\log_{10} H \tag{A.11}$$

i.e. it has been verified that every time the burst duration is doubled in time, there is an increase in average transmitted power of 3 dB (see Figure A.3):

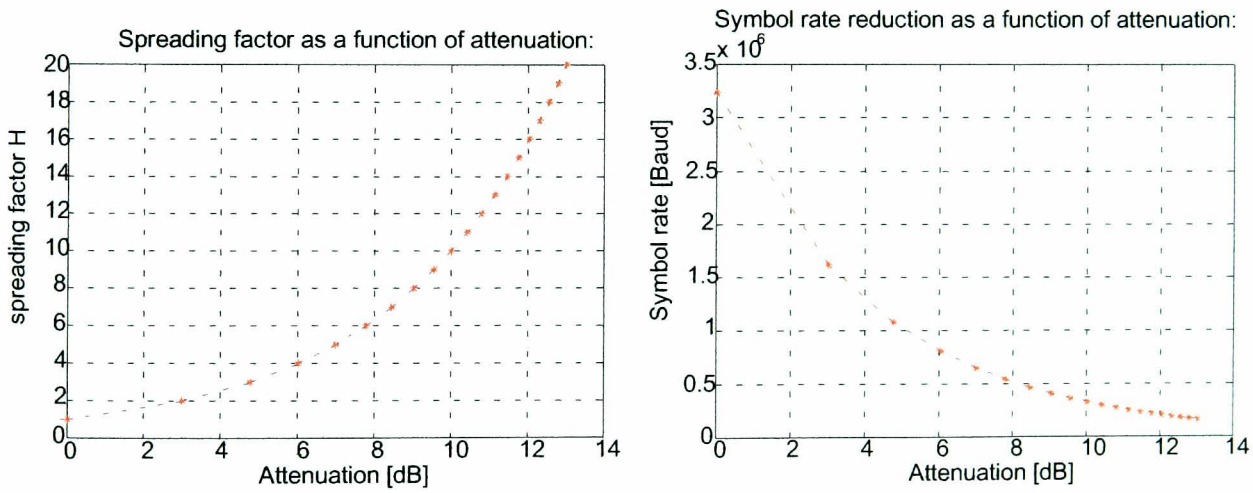

Figure A.3 Spreading as a function of attenuation

Therefore, if G_c is the coding gain obtainable by coding the message, and the burst duration is increased H times [2.27] (i.e. the station is allocated H-1 extra FMT timeslots per traffic slot), then the original power margin, M_o, of the station is increased to:

$$M = M_O + G_H + G_C = M_O + 10\log_{10} H + G_C \tag{A.12}$$

Appendix B: Publications

B.1 Publications and Presentations

(* Papers presented by E. Noussi)

1. * Noussi E., Grémont B., Filip M., Pekou A., "Centrally Managed FMT Built Upon DVB-RCS", COST Action 280, "Propagation Impairment Mitigation for Millimetre Wave Radio Systems", MC#6 Meeting, Paper PM6-006, October 2003, Abingdon, UK.

2. * Noussi E., Grémont B., Filip M., "Centrally Managed MF-TDMA Broadband Network with Fade Mitigation built upon DVB-RCS", 9th Ka and Broadband Communications Conference, p. 215-222, 5-7 November 2003, Island of Ischia, Italy.

3. Noussi E., Grémont B., Filip M., Pekou A., "Rain Compensation for Advanced Satellite Systems", PREP 2004 Proceedings, p. 68-69, 5-7 April 2004, University of Hertfordshire, UK.

4. * Noussi E., Grémont B., Filip M., "Adaptive MF-TDMA: Burst Length Control as a Rain Fade Countermeasure", CSNDSP, 4th International Symposium on Communication Systems, Networks and Digital Signal Processing Proceedings, University of Newcastle upon Tyne, UK, 20-22 July 2004, p. 43-46.

5. * Noussi E., Grémont B., Filip M., "A Demand Assignment Algorithm for FMT Resource Management in DVB-RCS Networks", PREP 2005 Proceedings, 30 March to 1st April 2005, Lancaster University, UK.

6. Noussi E., Grémont B., "FMT Resource Management in DVB-RCS Networks", COST Action 280, Propagation Impairment Mitigation for Millimetre Wave Radio Systems, Final Report, Chapter 3: Mitigation Techniques, 2005.

7. Noussi E., Grémont B., Hewitt A., "DVB-RCS2 Satellite Network with Dual Fade Mitigation Technique", 23rd AIAA International Communications Satellite Systems Conference (ICSSC-2005), 25-28 September 2005, Aurelia Convention Centre Rome, Italy.

B.2 Internal Research Reports

8. Noussi E., Grémont B., "Modelling of Broadband Satellite Links over Rain-Affected Wide Areas: Problem Statement", MTSRG Internal Research Report No. 03/09, University of Portsmouth, Department of Electronic & Computer Engineering, June, 2003.

9. Noussi E., Grémont B., "Basis for Fade Mitigation Technique Implementation over the DVB-Return Channel by Satellite", MTSRG Internal Research Report No. 03/11, University of Portsmouth, Department of Electronic & Computer Engineering, June, 2003.

10. Noussi E., Grémont B., Filip M., Vilar E., "Broadband Satellite Links Over Rain-Affected Wide Areas: Progression from MPhil to PhD Document", MTSRG Internal Research Report No. 03/16, University of Portsmouth, Department of Electronic & Computer Engineering, July 2003.

11. Noussi E., Grémont B., Filip M., "Burst Length Control with Forward Error Correction as a Rain Fade Countermeasure - Single Link Analysis", MTSRG Internal Research Report No. 04/04, University of Portsmouth, Department of Electronic & Computer Engineering, April, 2004.

COST Action 280

"Propagation Impairment Mitigation for Millimetre Wave Radio Systems"

Centrally Managed FMT Built Upon DVB-RCS

Abstract

This paper proposes a methodology on how to design a centrally managed satellite network in the presence of rain fading as encountered on an actual spotbeam area whilst meeting the user-specified QoS requirements. A possible Fade Mitigation Technique applicable to DVB-RCS is described based on mechanisms supported by the Standard.

1. Introduction

A result of the need to accommodate high-rate transmission is to push into increasingly higher frequency bands, namely Ka band (27-40 GHz) and V band (40-75 GHz). This trend is explained by the relatively large segments of frequency spectrum required for supporting the high data rates planned in newer systems, [1]. Most VSAT and Digital Broadcast Satellite TV systems in operation today use portions of the Ku band.

A major drawback to the use of higher frequencies is significant rain attenuation, as this increases rapidly with increasing microwave frequency, [2], [3], [4]. It can cause serious signal quality degradations of earth-space communication links and can therefore have a major impact not only on individual links, but on the whole network, which will be affected on a global basis.

MF-TDMA allows a group of Return Channel Satellite Terminals (RCSTs) to communicate with a Gateway using a set of carrier frequencies. In order to guarantee a Quality of Service, it is important that the NCC gets to know the actual needs of each of the active RCSTs of the network. Therefore each user station needs to monitor and measure its specific traffic requirements that are communicated to the NCC. If resources are available, the NCC will generate a new Terminal Burst Time Plan (TBTP) accommodating the needs of all its active stations at a superframe/frame level, [5].

Eleni Noussi
University Of Portsmouth
ECE Department
Anglesea Road
Portsmouth, PO1 3DJ
United Kingdom
Tel: +44-23-92846028
Fax: +44-23-92842792
E-m: noussie@ee.port.ac.uk

Boris Grémont
Tel: +44-23-92842552
Fax: +44-23-92842792
boris.gremont@port.ac.uk

Misha Filip
Tel: +44-23-92842310
Fax: +44-23-92842561
misha.filip@port.ac.uk

2. Bandwidth on Demand Over MF-TDMA

Most new generation Ka-band satellite systems are being designed to provide low-cost telecommunication services to hundreds of millions of users. In order to maximise the system capacity, frequencies can be allocated dynamically and reused many times. "Bandwidth on Demand" can be employed to support the maximum amount of users possible. On the billing side, bandwidth on demand enables users to pay only for the bandwidth they utilise, [6].

2.1. Segmentation of Return Link Capacity: A Simplified Scenario

The timeslots of the return link are organised and numbered so that the network is able to allocate them to individual active RCSTs. Figure 1 shows how the global return link capacity may be segmented amongst a group of RCSTs; the network will then manage several superframe identifiers, SF_IDs, (i.e. separate sets of carrier frequencies).

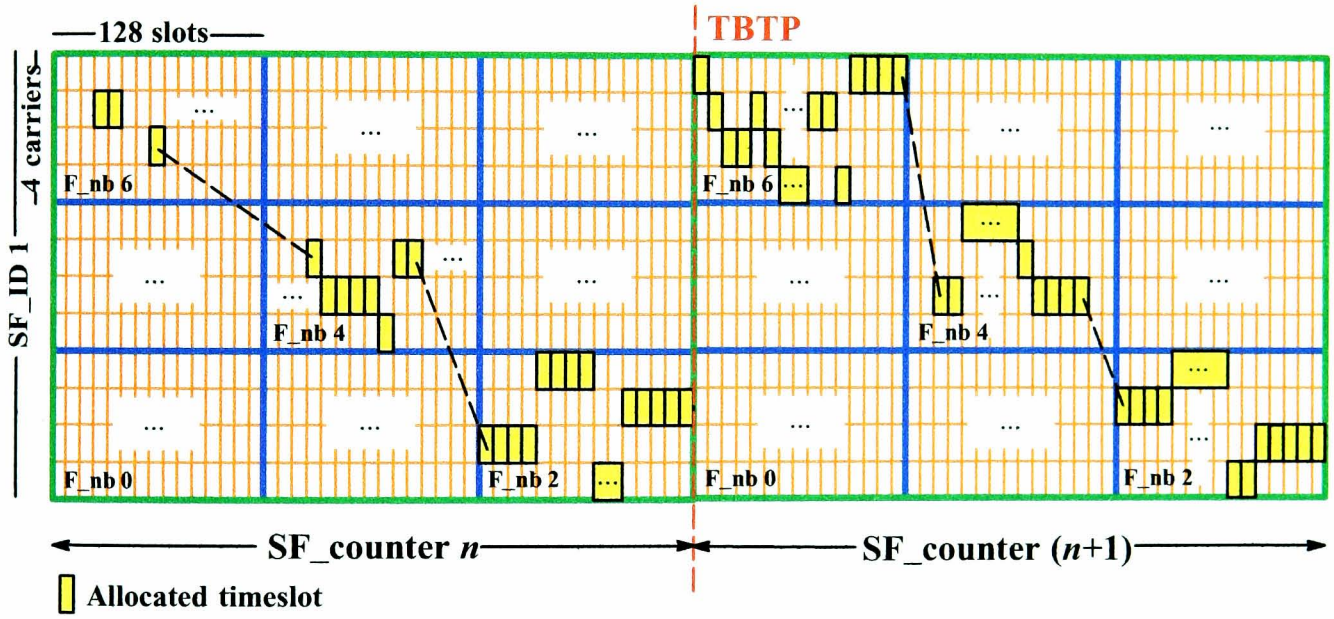

Figure 1: Capacity segmentation and timeslot allocation: an example

For simplicity reasons it is assumed that these frequency sets are fixed, i.e. superframes have a fixed bandwidth (otherwise a change in a superframe's bandwidth would affect the whole arrangement and all RCST groups would then have to be notified and have their superframe bandwidth adjusted appropriately (hence more signalling). For each superframe of a given SF_ID, allocation of timeslots is communicated to the RCSTs via the Terminal Burst Time Plan table. An RCST is there on allowed to transmit data bursts in timeslots, which were allocated to it.

As shown in Figure 1, the consecutive superframes of a given SF_ID are contiguous in time. Each occurrence of a superframe in time is labelled with a number called "SF_counter". These two superframes of this particular SF_ID 1 are of the same composition and duration, unless a notification that a change should be applied is provided; this can occur at the boundary between

two superframes (between two consecutive SF_counters of the SF_ID), so that the next superframe is of different composition and/or duration. This notification involves the TBTP and the Superframe, Frame and Timeslot Composition Tables (SCT, FCT, TCT).

A superframe is composed of frames, themselves composed of timeslots. In a superframe, frames are numbered from 0 (lowest frequency, first in time) to N (highest frequency, last in time), ordered in time then in frequency, (F_nb represents the frame number) and can take the values $0 \leq N \leq 31$. A frame is composed of timeslots. It may span over several carrier frequencies. In a frame, timeslots are numbered from 0 (lowest frequency, first in time) to M (highest frequency, last in time), ordered in time then in frequency. The number of slots in a frame can be in the range $0 \leq M \leq 2047$, [7].

Assuming that the bandwidth and duration of superframes, frames and timeslots is fixed, for an uplink burst rate of 2048 kbps, a typical MF-TDMA frame would last for 26.5 ms. The frame includes 4 carriers of 128 traffic slots each (i.e. 512 slots per frame), with rate granularity of 16 kbps (i.e. the minimum rate that can be achieved over the period of a frame by the allocation of just one timeslot).

Thanks to the system bandwidth-on-demand capability, a user station can vary the average bit rate according to its traffic needs by being allocated 1, 2, 3, ... up to $M_c = 128$ slots/frame leading to 16, 32, 48, ... up to $(M_c \times 16) = (128 \times 16) = 2048$ kbps over a frame duration.

Each terminal may transmit on any single frequency at a given time; it is not allowed to transmit data on more than one carrier at a time, in order to minimise the power output requirement and reduce the hardware complexity of terminals. The RCST will process the TBTP message received from the NCC, to extract the assignment count and timeslot allocations for its next uplink transmissions.

2.2. Satellite Access Control

The synchronisation burst and the optional prefix attached to ATM traffic bursts contain the Satellite Access Control field composed of signalling information added by the RCSTs for the purpose of requesting capacity for the session. The Request sub-field within the SAC accommodates capacity requests signalled from the terminal in terms of uplink payload slots required (either fixed or variable number of slots in each frame, or even total number of uplink payload slots required to empty its queue). Upon receiving the capacity request messages, the NCC generates a TBTP table and sends it, so that each RCST knows what timeslots have been assigned to it. This mechanism can also be used to drive a fade mitigation technique, i.e. for the purposes of FMT slot reservation when a terminal needs more resources under rain conditions.

2.2.1. Mini-slot Out-of-Band Request (OBR)

(i) Periodic Assignment Based OBR

This mechanism is based on a periodic assignment to logged-on RCSTs of bursts smaller than traffic timeslots. It carries control and management information from the RCSTs to the NCC and is also used for maintaining RCST synchronisation. This mechanism is supported by the SAC Request sub-field used in synchronisation bursts.

(ii) Contention Based OBR

In this case, the mini-slot can be accessed by a group of RCSTs on a contention basis. This mechanism is supported by the Satellite Access Control Request, Group_ID and Logon_ID sub-fields used in the synchronisation bursts (see Figures 2 and 3).

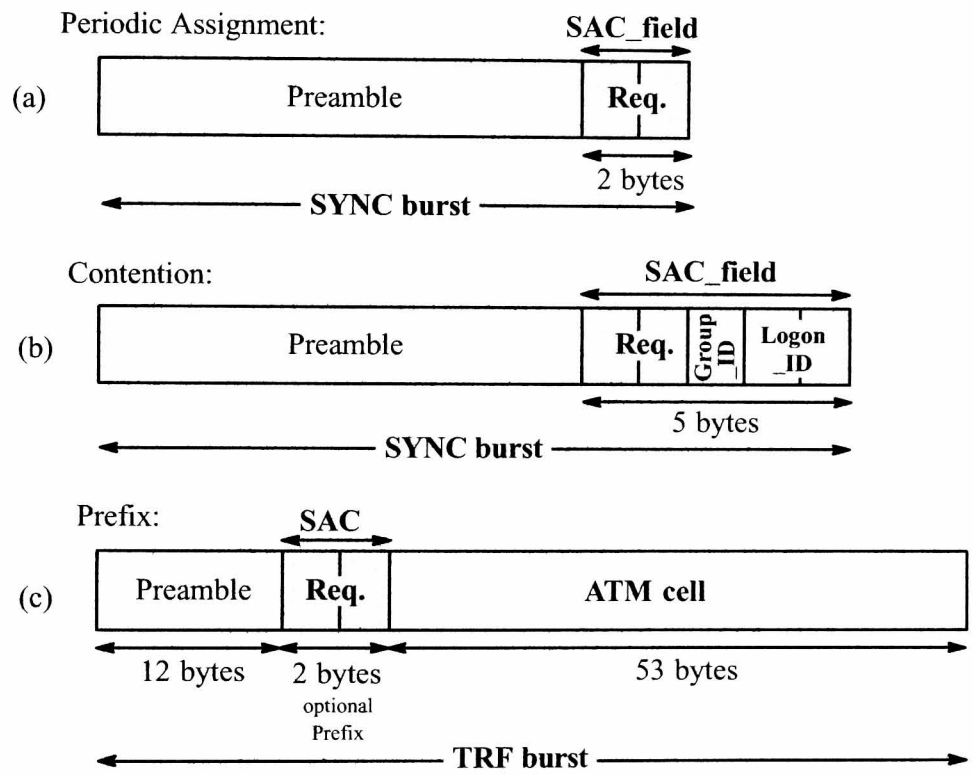

Figure 2: Examples of SAC field composition (a) SYNC mini-slot (b) contention based SYNC mini-slot (c) TRF prefix method

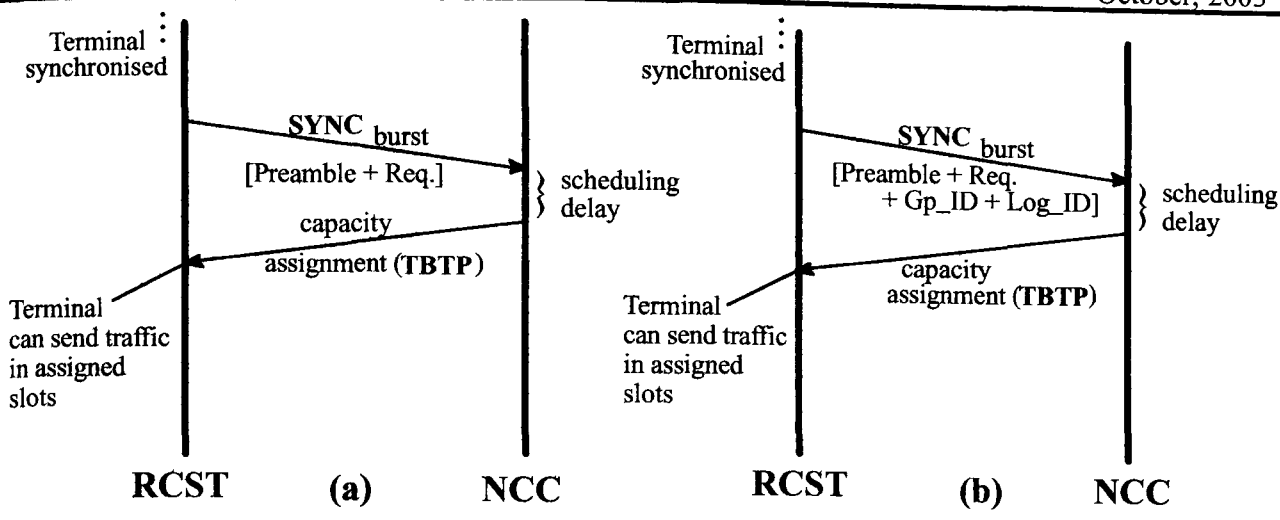

Figure 3: Signalling regarding OBR for capacity through (a) periodically assigned SYNC mini-slot (b) contention based SYNC mini-slot

2.2.2. Prefix Method or In-Band Request (IBR)

This method is based on an optional prefix attached to ATM traffic bursts. If used, the prefix carries control and management information from the RCSTs to the NCC. This mechanism is supported by the SAC Request sub-field when appended to ATM traffic bursts (see Figures 2 and 4).

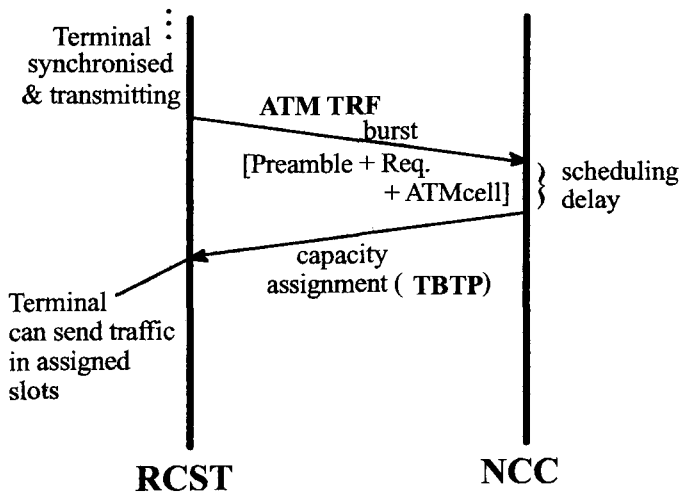

Figure 4: Signalling regarding IBR for capacity through TRF prefix method

Obviously the use of IBR signalling allows for the reduction in the traffic load over the reservation channels, which are normally randomly accessed by terminals to content for bandwidth. IBR has in fact the great advantage of being collision-free. Hence a terminal that has been assigned traffic slot(s) should use IBR (also known as "piggy-backed" requests). In this way, the out-of-band request slots can be shared by terminals that do not have any assigned traffic slot. The waiting time to send a reservation will also be reduced due to the availability of both IBR and OBR slots, [8].

3. Basis for Implementation of a Fade Mitigation Technique

3.1. Forward Link Signalling (FSL) supporting a Fade Countermeasure

The TCT defines parameters concerning the coding for error protection; two coding schemes are supported, Turbo and concatenated coding (outer code: Reed-Solomon, inner code Convolutional).

All sections of the SCT, FCT, TCT, and broadcast Terminal Information Message (TIM) will be transmitted at least every 10 s. This implies that the coding parameters (defined in the TCT) can be updated at least every 10 s; this is of great interest, as in the case of rain, changing the coding or symbol rate is actually a fade countermeasure.

The repetition rate can take any value equal to or greater than 1/(10 sec), i.e. these tables can be transmitted asynchronously as frequently as required, and this can occur at any time during a superframe; only in the case when the inverse of this rate is equal to the superframe duration, the tables will be transmitted synchronously at the exact beginning of every superframe.

In addition, the TIM will be updated as required to reflect system status changes requiring immediate notification of the RCSTs. For example, the transmission of the TIM table with its RCST_status field set to "`00000010`" (`Rain_Fade_detect` bit set to '`1`') would indicate that the NCC is performing a reconfiguration procedure (e.g. increasing the code rate) to establish rain fade settings. Similarly, a "`00000100`" (`Rain_Fade_release` bit set to '`1`') would mean that the NCC is restoring settings due to cessation of a rain fade event, [7].

In the context of FMTs, one can foresee two basic scenarios. In the first scenario, each RCST monitors the channel conditions (in terms of rain attenuation). Based on the detected conditions, the RCST issues a set of new QoS requirements that not only cover its actual traffic needs but also its FMT needs. Thus each RCST would "lie" to the NCC and ask for more resources to accommodate its FMT needs. Here the already built-in reservation mechanisms described above (see Figure 2) can be used for the purposes of FMT slot reservation.

A second approach relies on the monitoring of the whole satellite footprint (using for example a weather radar network) so that, at any time, the NCC has an image of the rain conditions over the whole network. The allocation of timeslots is performed by the NCC from the true traffic and QoS requests of all the RCSTs. The FMT allocation is done independently by the NCC that takes into account the measured rain conditions, [5]. Both methods do not require any additional specific signalling. They are therefore efficient in terms of spectrum utilisation.

3.2. Coding and Burst Length Control (BLC)

Within an adaptive MF-TDMA fade countermeasure scheme a portion of MF-TDMA timeslots is reserved as a shared resource, which can be distributed to any stations within the network that

are subject to rain fading. When a burst within the MF-TDMA frame is subject to fading, it is allocated some extra timeslots into which it can expand. Since the user data rate is not changed this expansion results to an increase in average power (or energy/bit) of the signal and so counteracts the effect of the fade, [9].

If G_c is the coding gain obtainable by coding the message, and the burst duration is increased H times, then the original power margin, M_o, of the station is increased to, [10]:

$$M = M_o + G_H + G_c = M_o + 10\log_{10}H + G_c \quad (1)$$

Every time the burst duration is doubled in time, there is an increase in average transmitted power of 3 dB. Figure 6 illustrates an example of employing coding and bit rate reduction to counteract fading. Switching from no coding to 1/2 coding rate provides a 6 dB increase for a BER threshold of 10^{-8} (see Figure 5).

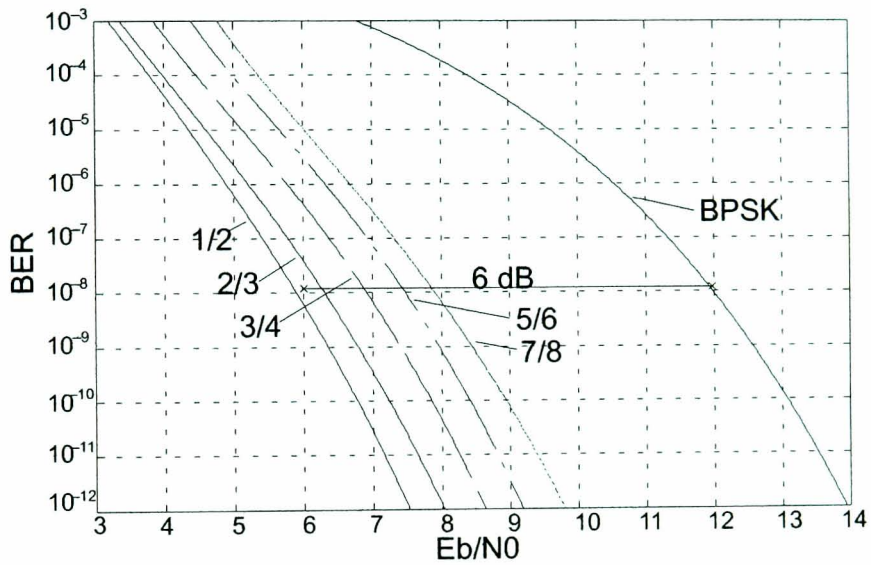

Figure 5: BER vs. E_b/N_0 performance of a convolutional coding system with BPSK, for various code rates

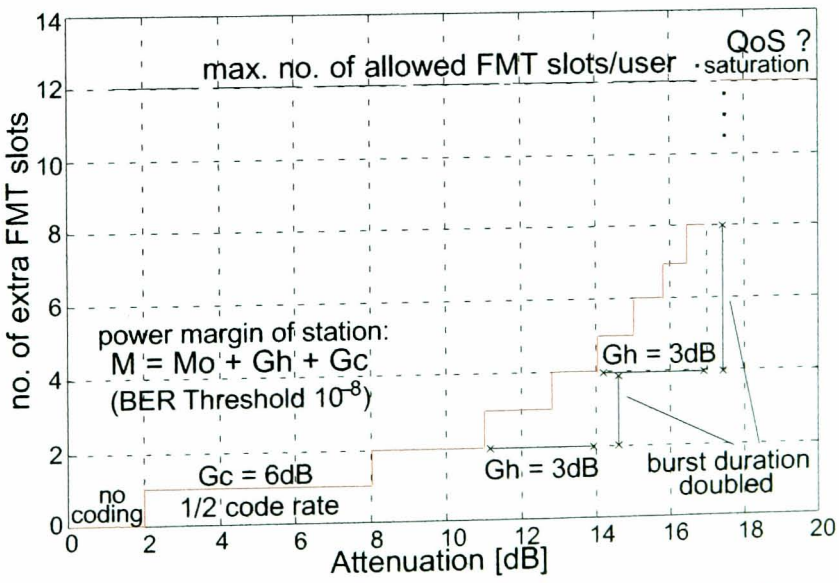

Figure 6: No. of extra FMT slots due to coding or BLC vs. attenuation protection (for a user requiring 1 timeslot/frame in "clear sky" conditions)

In general, if N is the original number of slots/frame being transmitted, reducing the code rate from the baseline code rate r_1 –decided by the clear-sky link budget and the QoS (BER) objective– to a new code rate r_2, results in expanding the transmission over $(r_1/r_2) \times N$ timeslots. For example, if one slot was originally used and the code rate switched from a baseline clear-sky code rate $r_1 = 7/8$ to a lower rate $r_2 = 1/2$ to combat fading, then the total number of slots required would be $(7/8)/(1/2) \times 1 = 1.75 \simeq 2$ slots, i.e. one extra timeslot to fit the coded bits. For a BER objective of 10^{-8} (see Figure 5) this would translate into an extra 2 dB protection against fading. If, in addition, bit rate reduction (or burst length control) was employed, with H=2 (i.e. transmitting the information bits over twice as many slots), an additional 3 dB protection (total of 5 dB) would be provided. In this case, we would need: $(r_1/r_2) \times N \times H = 3.5 \simeq 4$ slots, i.e. 3 extra timeslots in total.

3.3. Linking BER to QoS Performance Parameters

It should be noted, however, that, for new Ka-band systems, the C/N_0 loss due to attenuation does not correspond directly to the degradation of the QoS offered to the end-user, because of a complexity in system architectures and a large variety of multimedia applications. To achieve a good assessment of this QoS information, the parameters derived by propagation models are not sufficient and estimating the distributions of more oriented QoS parameters is required. These parameters (Cell Loss Ratio and other ATM performance parameters) can be directly derived from the physical layer main parameter BER, [11]. The equations for the conversion from the BER into the ITU-T Rec. I.356 parameters, [12], depend on the error pattern model (random or burst errors) and rely on the principle of the Header Error Control mechanism implemented in ATM systems.

3.4. Dimensioning and Management of the FMT Resource at a Network Level

In the event of rain in some portion of the footprint (see Figure 7), the drop in QoS on individual links will require the allocation of spare timeslots to counteract for rain attenuation. Assuming a population of N users, the NCC must be able to learn quickly about the links affected, so that allocation of communication and FMT slots can be achieved. As explained above, service communication can be achieved through OBR and IBR requests.

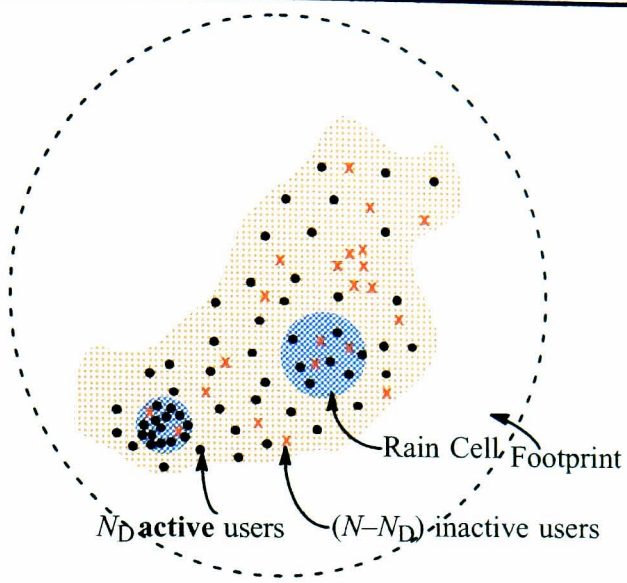

Figure 7: Example of rain cells over areas with active and non-active users inside the footprint of a satellite

A major issue is that the MF-TDMA should be able to support the active users. This implies that if the number of FMT spare slots is limited, there will be a finite blocking probability of not meeting QoS parameters originally agreed. Alternatively, the requests may be queued, in which case, the limited capacity in the presence of rain will result in longer delays or a re-negotiation of QoS between RCST and NCC could be performed depending on the service agreement.

Figure 7 shows an example of rain cells over areas with active and non-active users inside the coverage area of a satellite. It becomes apparent that the total number of required FMT slots depends on:

1. users' density and location (the greater the concentration of users the greater the number of required FMT slots);
2. space and time characteristics of rain (for rain over large areas, more FMT slots are required);
3. magnitude of the rain attenuation;
4. actual traffic characteristics of the user stations;
5. QoS parameters.

Furthermore, depending on the hour of the day or the month, the rain conditions may be quite severe resulting in a much more extensive use of FMT slots. This would get even worse if worst fades occur at times when user traffic is high.

We therefore conclude that the design of MF-TDMA networks with burst-length control requires a detailed study of the impact of rain attenuation on the satellite footprint. Long-term analysis will allow investigating the share between traffic and FMT slots whilst short-term analysis will permit to study the resource allocation algorithms that the NCC needs to run for a rapidly converging and fair management of the MF-TDMA channel.

The performance of FMT resource allocation algorithms described above needs to be evaluated in a network simulator. Such a simulator would need a fine scale simulation of the rain attenuation conditions encountered on a satellite footprint. Recent ptopagation activity has focused on the space-time modelling of rainfields.

A rain attenuation field can be simulated in space and time using a mixture of time and frequency domain signal processing. Such rainfield model can be used to simulate the variations of CNR over the whole footprint. It can consider seasonal/diurnal variations of rain for realistic worst-month and time-of-the-day dependent rain conditions, [5], [13], [14].

4. Conclusions and Future Work

This paper has presented a review of Bandwidth on Demand for MF-TDMA networks with an emphasis on the ability of the NCC to deliver centralised FMT management to a multitude of RCSTs simultaneously affected by rainfield attenuation. A possible FMT compatible with DVB-RCS has been described and the methods and supported by the standard mechanisms through which the proposed FMT can be implemented have been investigated. It is believed that the space-time model of rain attenuation, [13], is appropriate for the analysis of resource allocation for MF-TDMA networks in the presence of fading. The proposed methodology will consider the impact of rain attenuation magnitude, actual traffic characteristics of the user stations, spatial characteristics of rain as well as users' location and density on the overall achievable user capacity.

5. References

[1] M. H. Hadjitheodosiou, A. Ephremides, D. Friedman, *"Broadband Access via Satellite"*, Technical Research Report, CSHCN T.R. 99–2, Centre for Satellite and Hybrid Communication Networks, University of Maryland, 1999, available at http://techreports. isr.umd.edu/TechReports/CSHCN/1999/ CSHCN_TR_99–2/CSHCN_ TR_99–2.pdf

[2] L. J. Ippolito, *"Radio propagation for space communications systems"*, IEEE Proceedings, vol. 69, no. 6, pp. 697-727, U.S.A., June 1981.

[3] S. I. E. Touw, *"Analyses of Amplitude Scintillations for the Evaluation of the Performance of Open-Loop ULPC Systems"*, MSc Thesis, Eindhoven University of Technology, Eindhoven, The Netherlands, 1994.

[4] R.A. Nelson, *"V-band: Expansion of the Spectrum Frontier"*, Via Satellite, February 1998, pp. 66+.

[5] B. C. Grémont, R. J. Watson, P. A. Watson, D. D. Hodges, *"Modelling and Detection of Rain Attenuation for MF-TDMA Satellite Networks Utilising Fade Mitigation*

Techniques", Int. Workshop of COST Actions 272 and 280 Satellite Communications – From Fade Mitigation to Satellite Provision, p. 277-284, 26-28 May 2003, ESTEC, Noordwijk, The Netherlands.

[6] G. Psomas, *"Satellite Communications: An overview"*, http://www.iis.ee.ic.ac.uk/~frank/surp98/report/ hdr1/, last accessed on 23/02/03.

[7] ETSI EN 301 790 (V1.3.1): *"Digital Video Broadcasting (DVB); Interaction Channel for Satellite Distribution Systems"* (also known as the 'DVB-RCS' specification), Final Draft, 2002-11, available at http://www.etsi.org/getastandard/home.htm

[8] T. Le-Ngoc, S. V. Krishnamurthy, *"Performance of Combined Free/Demand Assignment Multiple Access Schemes in Satellite Communications"*, International Journal of Satellite Communications, vol. 14, no. 1, pp. 11-21, January-February 1996.

[9] D. J. Emerson, R. M. Nelhams, B. L. Clark, *"Adaptive TDMA for Fade Countermeasures"*, Olympus Utilisation Conference, ESA SP-292, 12-14 April 1989, Vienna.

[10] F. Carassa, *"Adaptive Methods to Counteract Rain Attenuation Effects in the 20/30 GHz Band"*, Space Communication and Broadcasting 2, pp. 253-269, 1984, North Holland.

[11] P. Pech, L. Castanet, M. Bousquet, *"A Prediction Model to Convert Propagation Distributions in Statistics of Quality of Service Performance Parameters"*, COST Action 280 "Propagation Impairment Mitigation for Millimetre Wave Radio Systems", 1st Int. Workshop, doc. PM3023[R1], 1-3 July 2002, Malvern, UK.

[12] B-ISDN ATM Layer Cell Transfer Performance – ITU-T Recommendation I.356, November 1993.

[13] B. Grémont, *"Simulation of Rainfield Attenuation for Satellite Communication Networks"*, 1st Workshop of the COST Action 280 "Propagation Impairments Mitigation for Millimetre Wave Radio Systems", 1-3 July 2002, Malvern, UK.

[14] B. Grémont, *"Generalised Model of the SatComm Channel for Applications to Fade Countermeasures"*, XXVIIth General Assembly of the International Union of Radio Science, Maastricht, The Netherlands, August 17-24, 2002.

CENTRALLY MANAGED MF-TDMA BROADBAND NETWORK WITH FADE MITIGATION BUILT UPON DVB-RCS

Eleni Noussi, Boris Grémont, Misha Filip
Microwave Telecommunication Systems Research Group
University of Portsmouth, Department of Electronic & Computer Engineering,
Anglesea Road, Portsmouth, PO1 3DJ, U.K. Tel: +44(0)23-92846028,
Email: noussie@ee.port.ac.uk, {boris.gremont, misha.filip}@port.ac.uk

Abstract

This paper proposes a methodology on how to design a centrally managed satellite network in the presence of rain fading as encountered on an actual spotbeam area whilst meeting the user-specified QoS requirements. A possible Fade Mitigation Technique applicable to DVB-RCS is described based on mechanisms supported by the Standard. The paper also presents the development of a novel space-time model of rain attenuation, suitable for application to the dimensioning and real-time management of Ka/V band broadband MF-TDMA networks.

1 INTRODUCTION

A result of the need to accommodate high-rate transmission is to push into increasingly higher frequency bands, namely Ka band (27-40 GHz) and V band (40-75 GHz). This trend is explained by the relatively large segments of frequency spectrum required for supporting the high data rates planned in newer systems, [1]. Most VSAT and Digital Broadcast Satellite TV systems in operation today use portions of the Ku band.

A major drawback to the use of higher frequencies is significant rain attenuation, as this increases rapidly with increasing microwave frequency, [2], [3], [4]. It can cause serious signal quality degradations of earth-space communication links and can therefore have a major impact not only on individual links, but on the whole network, which will be affected on a global basis.

MF-TDMA allows a group of Return Channel Satellite Terminals (RCSTs) to communicate with a Gateway using a set of carrier frequencies. In order to guarantee a Quality of Service, it is important that the NCC gets to know the actual needs of each of the active RCSTs of the network. Therefore each user station needs to monitor and measure its specific traffic requirements that are communicated to the NCC. If resources are available, the NCC will generate a new Terminal Burst Time Plan (TBTP) accommodating the needs of all its active stations at a superframe/frame level, [5].

2 BANDWIDTH ON DEMAND OVER MF-TDMA

Most new generation Ka-band satellite systems are being designed to provide low-cost telecommunication services to hundreds of millions of users. In order to maximise the system capacity, frequencies can be allocated dynamically and reused many times. "Bandwidth on Demand" can be employed to support the maximum amount of users possible. On the billing side, bandwidth on demand enables users to pay only for the bandwidth they utilise, [6].

2.1 Segmentation of Return Link Capacity: A Simplified Scenario

The timeslots of the return link are organised and numbered so that the network is able to allocate them to individual active RCSTs. Figure 1 shows how the global return link capacity may be segmented amongst a group of RCSTs; the network will then manage several superframe identifiers, SF_IDs, (i.e. separate sets of carrier frequencies).

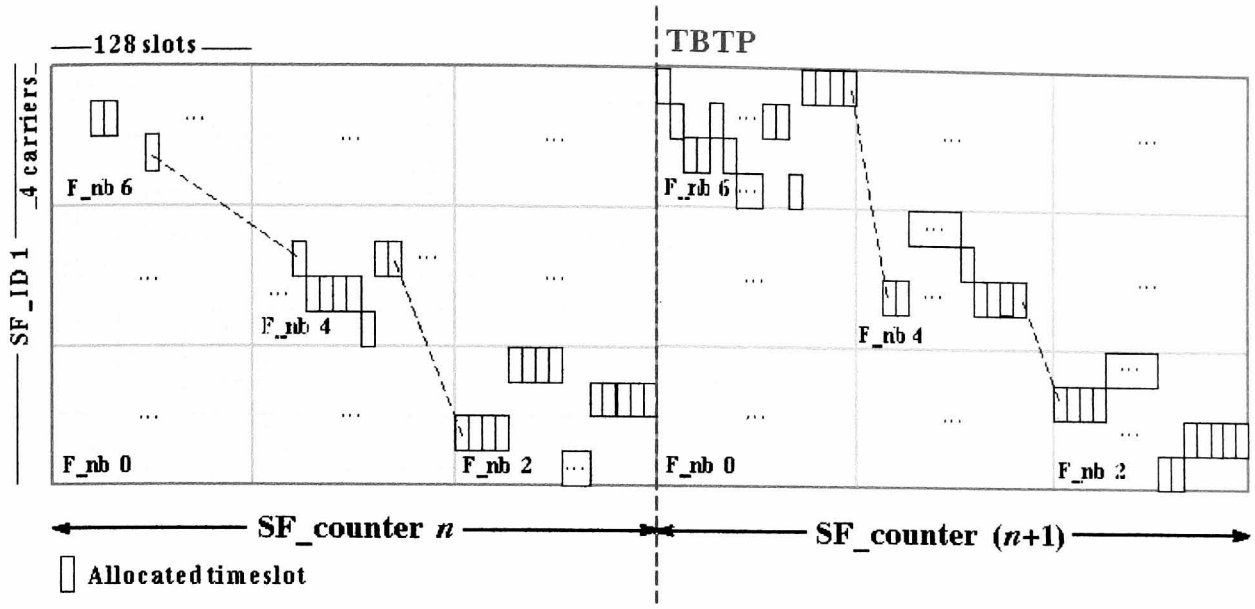

Figure 1. *Capacity segmentation and timeslot allocation: an example*

For simplicity reasons it is assumed that these frequency sets are fixed, i.e. superframes have a fixed bandwidth (otherwise a change in a superframe's bandwidth would affect the whole arrangement and all RCST groups would then have to be notified and have their superframe bandwidth adjusted appropriately (hence more signalling). For each superframe of a given SF_ID, allocation of timeslots is communicated to the RCSTs via the Terminal Burst Time Plan table. An RCST is there on allowed to transmit data bursts in timeslots, which were allocated to it.

As shown in Figure 1, the consecutive superframes of a given SF_ID are contiguous in time. Each occurrence of a superframe in time is labelled with a number called "SF_counter". These two superframes of this particular SF_ID 1 are of the same composition and duration, unless a notification that a change should be applied is provided; this can occur at the boundary between two superframes (between two consecutive SF_counters of the SF_ID), so that the next superframe is of different composition and/or duration. This notification involves the TBTP and the Superframe, Frame and Timeslot Composition Tables (SCT, FCT, TCT).

A superframe is composed of frames, themselves composed of timeslots. In a superframe, frames are numbered from 0 (lowest frequency, first in time) to N (highest frequency, last in time), ordered in time then in frequency, (F_nb represents the frame number) and can take the values $0 \leq N \leq 31$. A frame is composed of timeslots. It may span over several carrier frequencies. In a frame, timeslots are numbered from 0 (lowest frequency, first in time) to M (highest frequency, last in time), ordered in time then in frequency. The number of slots in a frame can be in the range $0 \leq M \leq 2047$, [7].

Assuming that the bandwidth and duration of superframes, frames and timeslots is fixed, for an uplink burst rate of 2048 kbps, a typical MF-TDMA frame would last for 26.5 ms. The frame includes 4 carriers of 128 traffic slots each (i.e. 512 slots per frame), with rate granularity of 16 kbps (i.e. the minimum rate that can be achieved over the period of a frame by the allocation of just one timeslot).

Thanks to the system bandwidth-on-demand capability, a user station can vary the average bit rate according to its traffic needs by being allocated 1, 2, 3, … up to M_c =128 slots/frame leading to 16, 32, 48, ... up to $(M_c \times 16) = (128 \times 16) = 2048$ kbps over a frame duration.

Each terminal may transmit on any single frequency at a given time; it is not allowed to transmit data on more than one carrier at a time, in order to minimise the power output requirement and reduce the hardware complexity of terminals. The RCST will process the TBTP message received from the NCC, to extract the assignment count and timeslot allocations for its next uplink transmissions.

2.2 Satellite Access Control

The synchronisation burst and the optional prefix attached to ATM traffic bursts contain the Satellite Access Control field composed of signalling information added by the RCSTs for the purpose of requesting capacity for the session. The Request sub-field within the SAC accommodates capacity requests signalled from the terminal in terms of uplink payload slots required (either fixed or variable number of slots in each frame, or even total number of uplink payload slots required to empty its queue). Upon receiving the capacity request messages, the NCC generates a TBTP table and sends it, so that each RCST knows what timeslots have been assigned to it. This mechanism can also be used to drive a fade mitigation technique, i.e. for the purposes of FMT slot reservation when a terminal needs more resources under rain conditions.

2.2.1 Mini-slot Out-of-Band Request (OBR)

(i) Periodic Assignment Based OBR

This mechanism is based on a periodic assignment to logged-on RCSTs of bursts smaller than traffic timeslots. It carries control and management information from the RCSTs to the NCC and is also used for maintaining RCST synchronisation. This mechanism is supported by the SAC Request sub-field used in synchronisation bursts.

(ii) Contention Based OBR

In this case, the mini-slot can be accessed by a group of RCSTs on a contention basis. This mechanism is supported by the Satellite Access Control Request, Group_ID and Logon_ID sub-fields used in the synchronisation bursts (see Figures 2 and 3).

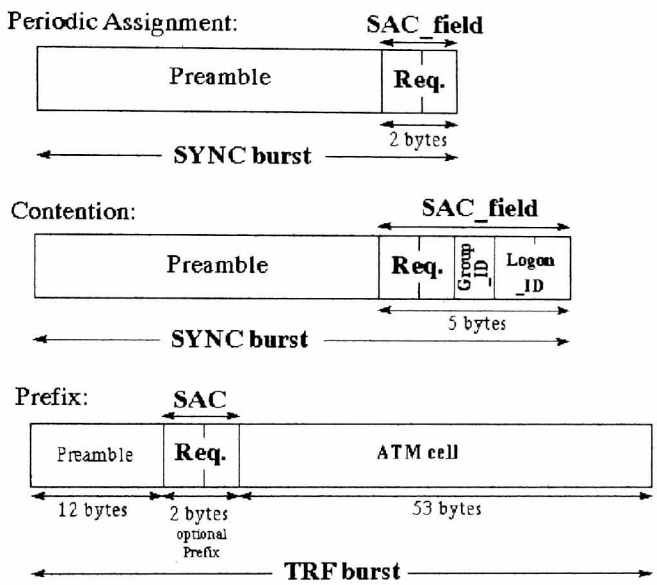

Figure 2. *Examples of SAC field composition (a) SYNC mini-slot (b) contention based SYNC mini-slot (c) TRF prefix method*

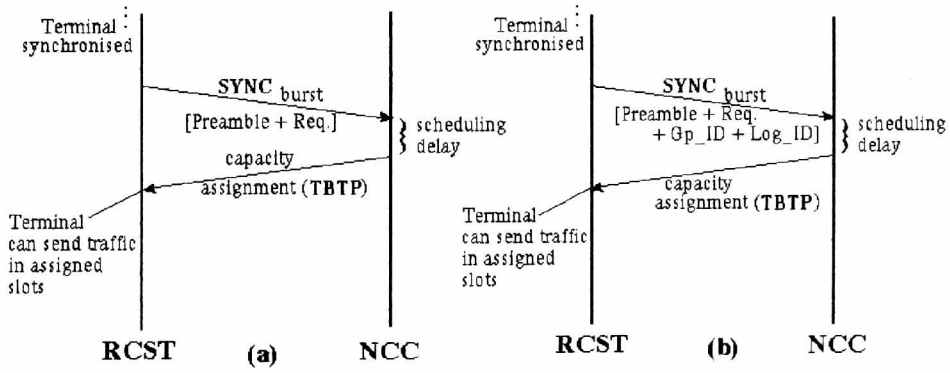

Figure 3. *Signalling regarding OBR for capacity through (a) periodically assigned SYNC mini-slot (b) contention based SYNC mini-slot*

2.2.2 Prefix Method or In-Band Request (IBR)

This method is based on an optional prefix attached to ATM traffic bursts. If used, the prefix carries control and management information from the RCSTs to the NCC. This mechanism is supported by the SAC Request sub-field when appended to ATM traffic bursts (see Figures 2 and 4). Obviously the use of IBR signalling allows for the reduction in the traffic load over

the reservation channels, which are normally randomly accessed by terminals to content for bandwidth. IBR has in fact the great advantage of being collision-free. Hence a terminal that has been assigned traffic slot(s) should use IBR (also known as "piggy-backed" requests). In this way, the out-of-band request slots can be shared by terminals that do not have any assigned traffic slot. The waiting time to send a reservation will also be reduced due to the availability of both IBR and OBR slots, [8].

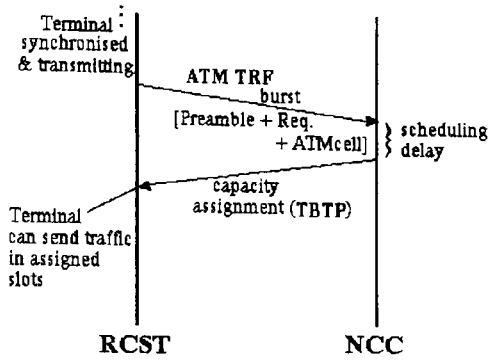

Figure 4. *Signalling regarding IBR for capacity through TRF prefix method*

3 BASIS FOR IMPLEMENTATION OF A FADE MITIGATION TECHNIQUE

3.1 Forward Link Signalling (FSL) supporting a Fade Countermeasure

The TCT defines parameters concerning the coding for error protection; two coding schemes are supported, Turbo and concatenated coding (outer code: Reed-Solomon, inner code Convolutional).

All sections of the SCT, FCT, TCT, and broadcast Terminal Information Message (TIM) will be transmitted at least every 10 s. This implies that the coding parameters (defined in the TCT) can be updated at least every 10 s; this is of great interest, as in the case of rain, changing the coding or symbol rate is actually a fade countermeasure.

The repetition rate can take any value equal to or greater than 1/(10 sec), i.e. these tables can be transmitted asynchronously as frequently as required, and this can occur at any time during a superframe; only in the case when the inverse of this rate is equal to the superframe duration, the tables will be transmitted synchronously at the exact beginning of every superframe.

In addition, the TIM will be updated as required to reflect system status changes requiring immediate notification of the RCSTs. For example, the transmission of the TIM table with its `RCST_status` field set to `"00000010"` (`Rain_Fade_detect` bit set to '1') would indicate that the NCC is performing a reconfiguration procedure (e.g. increasing the code rate) to establish rain fade settings. Similarly, a `"00000100"` (`Rain_Fade_release` bit set to '1') would mean that the NCC is restoring settings due to cessation of a rain fade event, [7].

In the context of FMTs, one can foresee two basic scenarios. In the first scenario, each RCST monitors the channel conditions (in terms of rain attenuation). Based on the detected conditions, the RCST issues a set of new QoS requirements that not only cover its actual traffic needs but also its FMT needs. Thus each RCST would "lie" to the NCC and ask for more resources to accommodate its FMT needs. Here the already built-in reservation mechanisms described above (see Figure 2) can be used for the purposes of FMT slot reservation.

A second approach relies on the monitoring of the whole satellite footprint (using for example a weather radar network) so that, at any time, the NCC has an image of the rain conditions over the whole network. The allocation of timeslots is performed by the NCC from the true traffic and QoS requests of all the RCSTs. The FMT allocation is done independently by the NCC that takes into account the measured rain conditions, [5]. Both methods do not require any additional specific signalling. They are therefore efficient in terms of spectrum utilisation.

3.2 Coding and Burst Length Control (BLC)

Within an adaptive MF-TDMA fade countermeasure scheme a portion of MF-TDMA timeslots is reserved as a shared resource, which can be distributed to any stations within the network that are subject to rain fading. When a burst within the MF-TDMA frame is subject to fading, it is allocated some extra timeslots into which it can expand. Since the user data rate is not changed this expansion results to an increase in average power (or energy/bit) of the signal and so counteracts the effect of the fade, [9].

If G_C is the coding gain obtainable by coding the message, and the burst duration is increased H times (i.e. the station is allocated H extra FMT timeslots), then the original power margin, M_O, of the station is increased to, [10]:

$$M = M_O + G_H + G_C = M_O + 10\log_{10} H + G_C \qquad (1)$$

Every time the burst duration is doubled in time, there is an increase in average transmitted power of 3 dB. Figure 6 illustrates an example of employing coding and bit rate reduction to counteract fading. Switching from no coding to 1/2 coding rate provides a 6 dB increase for a BER threshold of 10^{-8} (see Figure 5). In general, if N is the original number of slots/frame

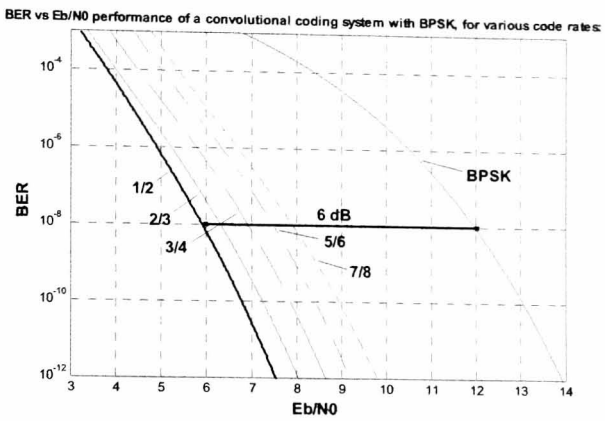

Figure 5. *BER vs. E_b/N_0 performance of a Convolutional coding system with BPSK, for various code rates*

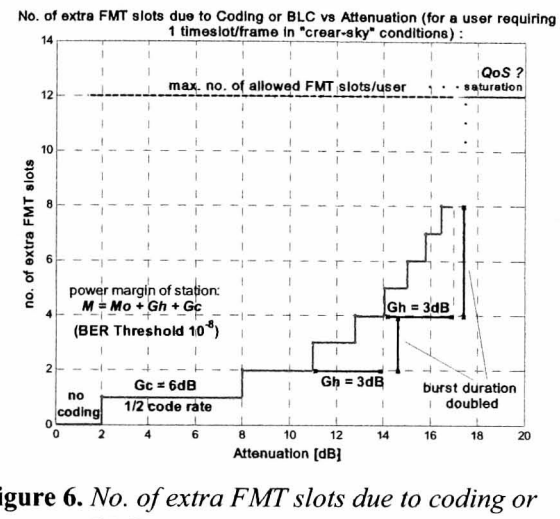

Figure 6. *No. of extra FMT slots due to coding or BLC vs. attenuation protection*

being transmitted, reducing the code rate from the baseline code rate r_1 –decided by the clear-sky link budget and the QoS (BER) objective– to a new code rate r_2, results in expanding the transmission over $(r_1/r_2)\times N$ timeslots. For example, if one slot was originally used and the code rate switched from a baseline clear-sky code rate r_1 = 7/8 to a lower rate r_2 = 1/2 to combat fading,

then the total number of slots required would be $(7/8)/(1/2)\times 1 = 1.75 \approx 2$ slots, i.e. one extra timeslot to fit the coded bits. For a BER objective of 10^{-8} (see Figure 5) this would translate to an extra 2 dB protection against fading. If, on top of this, bit rate reduction (or burst length control) was employed, an additional 3 dB protection (total of 5 dB) would be provided by transmitting the information bits at a speed that is twice as slow, i.e. over twice as many slots: $(r_1/r_2)\times N\times 2 = 3.5 \approx 4$ slots, i.e. 3 extra timeslots in total.

3.3 Linking BER to QoS Performance Parameters

It should be noted, however, that, for new Ka-band systems, the C/N_0 loss due to attenuation does not correspond directly to the degradation of the QoS offered to the end-user, because of a complexity in system architectures and a large variety of multimedia applications. To achieve a good assessment of this QoS information, the parameters derived by propagation models are not sufficient and estimating the distributions of more oriented QoS parameters is required. These parameters (Cell Loss Ratio and other ATM performance parameters) can be directly derived from the physical layer main parameter BER, [11]. The equations for the conversion from the BER into the ITU-T Rec. I.356 parameters, [12], depend on the error pattern model (random or burst errors) and rely on the principle of the Header Error Control mechanism implemented in ATM systems.

3.4 Dimensioning and Management of the FMT Resource at a Network Level

In the event of rain in some portion of the footprint (see Figure 7), the drop in QoS on individual links will require the allocation of spare timeslots to counteract for rain attenuation.

Assuming a population of N users, the NCC must be able to learn quickly about the links affected, so that allocation of communication and FMT slots can be achieved. As explained above, service communication can be achieved through OBR and IBR requests.

A major issue is that the MF-TDMA should be able to support the active users. This implies that if the number of FMT spare slots is limited, there will be a finite blocking probability of not meeting QoS parameters originally agreed. Alternatively, the requests may be queued, in which case, the limited capacity in the presence of rain will result in longer delays or a re-negotiation of QoS between RCST and NCC could be performed depending on the service agreement.

Figure 7 shows an example of rain cells over areas with active and non-active users inside the coverage area of a satellite. It becomes apparent that the total number of required FMT slots depends on: (i) users' density and location (the greater the concentration of users the greater the number of required FMT slots); (ii) space and time characteristics of rain (for rain over large areas, more FMT slots are required); (iii) magnitude of the rain attenuation; (iv) actual traffic characteristics of the user stations; (v) QoS parameters.

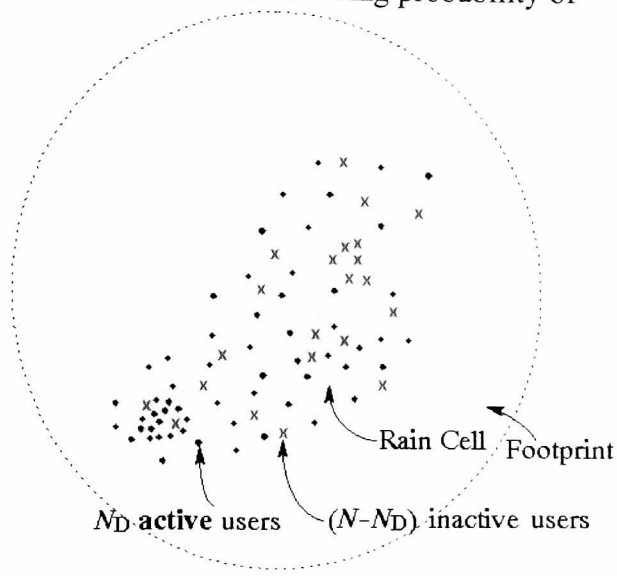

Figure 7. *Example of rain cells over areas with active and non-active users inside the footprint of a satellite*

Furthermore, depending on the hour of the day or the month, the rain conditions may be quite severe resulting in a much more extensive use of FMT slots. This would get even worse if worst fades occur at times when user traffic is high.

We therefore conclude that the design of MF-TDMA networks with burst-length control requires a detailed study of the impact of rain attenuation on the satellite footprint. Long-term analysis will allow investigating the share between traffic and FMT slots whilst short-term analysis will permit to study the resource allocation algorithms that the NCC needs to run for a rapidly converging and fair management of the MF-TDMA channel.

4 SPACE-TIME MODEL OF RAIN ATTENUATION

The performance of FMT resource allocation algorithms described in the previous section needs to be evaluated in a network simulator. Such a simulator would need a fine scale simulation of the rain attenuation conditions encountered on a satellite footprint. Recent propagation activity has focused on the space-time modelling of rain fields.

A rain attenuation field can be simulated in space and time using a mixture of time and frequency domain signal processing. Such rainfield model can be used to simulate the variations of CNR over the whole footprint. It can consider seasonal/diurnal variations of rain for realistic worst-month and time-of-the-day dependent rain conditions.

The proposed model simulates rain attenuation on a (x_1, x_2) grid representing the N^2 locations of interest for the network simulation. It is assumed that it rains on average only a fraction $f(x_1, x_2)$ of the time at any location. When it rains, the attenuation is log-normally distributed with two location dependent parameters $m(x_1, x_2)$ and $\sigma(x_1, x_2)$, which can be easily determined from the ITU-R rain model. These parameters can also encompass diurnal, monthly or seasonal variations, if they are fitted to CCDFs of diurnal, monthly or seasonal rain attenuation. The attenuation field can be synthesised using the non-linear transformation:

$$A(x_1, x_2) = \begin{cases} 0, & \text{if } g(x_1, x_2) < g_0 \\ \exp\left(m(x_1, x_2) + \sigma(x_1, x_2) \otimes g(x_1, x_2)\right), & \text{otherwise} \end{cases} \quad (2)$$

Here $g(x_1, x_2)$ is a 2D Gaussian field with unit variance and zero mean. Whenever $g(x_1, x_2) \geq g_0 = Q^{-1}(f)$, it is raining. Thus $g(x_1, x_2)$ can be transformed to a

lognormal variable using an exponential (array) transformation. This can be achieved by generating a complex field, $a(k_1, k_2)$, and then taking the inverse Fourier transform:

$$g(x,y) = \sum_{k_1=0}^{N} \sum_{k_2 0}^{N} a(k_1,k_2) \exp\left(\frac{i2\pi}{N} (k_1 x + k_2 y) \right) = IFT2\{a(k_1,k_2)\} \qquad (3)$$

To get a good field $g(x_1, x_2)$, we need to consider the spatial cross-correlation function $c_g(d)$ of rain where $d \equiv \left| \vec{x} - \vec{y} \right|$ is the distance between two geographical points $\vec{x} = (x_1, x_2)$ and $\vec{y} = (y_1, y_2)$ of interest. Whilst for short distances the form $c_g(d) = \exp(-d/5 \text{ km})$ is a reasonable model for modelling site diversity in UK, [13], [14], a correlation function considering meso- or synoptic ranges for Italy takes the double exponential form: $c_g(d) = 0.94 \exp(-d/30 \text{ km}) + 0.06 \exp^2(-d/100 \text{ km})$. An alternative approach is to analyse radar data and produce the spectrum of the log of rainfall rate, which is the Fourier transform of the cross-correlation function. Once a suitable correlation function has been chosen, we can calculate its Fourier transform:

$$C_g(k_1,k_2) = \sum_{x_1=0}^{N} \sum_{x_2 0}^{N} c_g(x_1,x_2) \exp\left(-\frac{i2\pi}{N} (k_1 x_1 + k_2 x_2) \right) = FT2\{c_g(x_1,x_2)\} \qquad (4)$$

The complex random field can be obtained by filtering complex 2D noise (zero mean, unit variance) $n(k_1, k_2)$, which in the Fourier domain is a simple multiplication:

$$a(k_1,k_2) = C_g(k_1,k_2) \otimes n(k_1,k_2) \qquad (5)$$

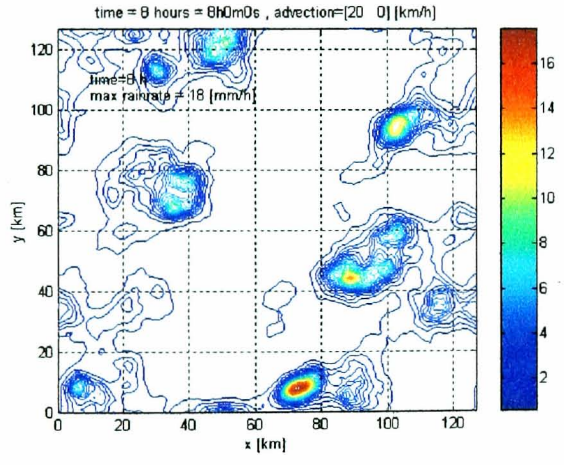

Figure 8. *Typical output of the rainfield simulator*

The model (2) to (5) only generates a single (original) map of the rainfield. A typical output is shown in Figure 8.

It is also important to add two realistic features to simulate time-dependent effects. For this the original rainfield is modified within a "for loop" simulating the passage of time. The first modification is the advection of the rainfall attenuation field. Assuming a velocity $\vec{V} = [V_1 \;\; V_2]$ m/s in the (x_1, x_2) plane, the translated rainfield a short time t later is obtained using:

$$g(x_1 - V_1 t, x_2 - V_2 t) = IFT2\{a(k_1,k_2) \otimes \exp[-it(k_1 V_1 + k_2 V_2)]\} \qquad (6)$$

The second modification takes into consideration the fact that rain effects have random temporal variations related to the natural birth and decay of rain cells over the field. It is well accepted that rain attenuation shows first order spectrum characteristics. One simple way of implementing this is to make $g(x_1, x_2)$ an auto-regressive temporal process that can be synthesised using the following difference equation:

$$a_{\text{new}}(k_1,k_2) = \exp(-\beta t) \otimes a_{\text{old}}(k_1,k_2) + \sqrt{1 - \exp(-\beta t)^2} \otimes n_2(k_1,k_2) \qquad (7)$$

where $n_2(k_1, k_2)$ is complex noise with zero mean and unit variance (uncorrelated with the one in equation (5)). The constant β [1/s] defines the temporal characteristics of rain attenuation and has been estimated from experimental data in [5], [13], [14].

5 CONCLUSIONS AND FUTURE WORK

This paper has presented a review of Bandwidth on Demand for MF-TDMA networks with an emphasis on the ability of the NCC to deliver centralised FMT management to a multitude of RCSTs simultaneously affected by rainfield attenuation. A possible FMT compatible with DVB-RCS has been described and the methods and supported by the standard mechanisms through which the proposed FMT can be implemented have been investigated. It is believed that the space-time model of rain attenuation is appropriate for the analysis of resource allocation for MF-TDMA networks in the presence of rain fading. The proposed methodology will consider the impact of rain attenuation magnitude, actual traffic characteristics of the user stations, spatial characteristics of rain as well as users' location and density on the overall achievable user capacity.

6 REFERENCES

[1] M. H. Hadjitheodosiou, A. Ephremides, D. Friedman, *"Broadband Access via Satellite"*, Technical Research Report, CSHCN T.R. 99-2, Centre for Satellite and Hybrid Communication Networks, University of Maryland, 1999, available at http://techreports.isr.umd.edu/TechReports/CSHCN/1999/ CSHCN_TR_99-2/CSHCN_TR_99-2.pdf

[2] L. J. Ippolito, *"Radio propagation for space communications systems"*, IEEE Proceedings, vol. 69, no. 6, pp. 697-727, U.S.A., June 1981.

[3] S. I. E. Touw, *"Analyses of Amplitude Scintillations for the Evaluation of the Performance of Open-Loop ULPC Systems"*, MSc Thesis, Eindhoven University of Technology, Eindhoven, The Netherlands, 1994.

[4] R.A. Nelson, *"V-band: Expansion of the Spectrum Frontier"*, Via Satellite, February 1998, pp. 66+.

[5] B. C. Grémont, R. J. Watson, P. A. Watson, D. D. Hodges, *"Modelling and Detection of Rain Attenuation for MF-TDMA Satellite Networks Utilising Fade Mitigation Techniques"*, Int. Workshop of COST Actions 272 and 280 Satellite Communications – From Fade Mitigation to Satellite Provision, p. 277-284, 26-28 May 2003, ESTEC, Noordwijk, The Netherlands.

[6] G. Psomas, *"Satellite Communications: An overview"*, http://www.iis.ee.ic.ac.uk/~frank/surp98/report/ hdr1/, last accessed on 23/02/03.

[7] ETSI EN 301 790 (V1.3.1): *"Digital Video Broadcasting (DVB); Interaction Channel for Satellite Distribution Systems"* (also known as the 'DVB-RCS' specification), Final Draft, 2002-11, available at http://www.etsi.org/getastandard/home.htm

[8] T. Le-Ngoc, S. V. Krishnamurthy, *"Performance of Combined Free/Demand Assignment Multiple Access Schemes in Satellite Communications"*, International Journal of Satellite Communications, vol. 14, no. 1, pp. 11-21, January-February 1996.

[9] D. J. Emerson, R. M. Nelhams, B. L. Clark, *"Adaptive TDMA for Fade Countermeasures"*, Olympus Utilisation Conference, ESA SP-292, 12-14 April 1989, Vienna.

[10] F. Carassa, *"Adaptive Methods to Counteract Rain Attenuation Effects in the 20/30 GHz Band"*, Space Communication and Broadcasting 2, pp. 253-269, 1984, North Holland.

[11] P. Pech, L. Castanet, M. Bousquet, *"A Prediction Model to Convert Propagation Distributions in Statistics of Quality of Service Performance Parameters"*, COST Action 280 "Propagation Impairment Mitigation for Millimetre Wave Radio Systems", 1st Int. Workshop, doc. PM3023[R1], 1-3 July 2002, Malvern, UK.

[12] B-ISDN ATM Layer Cell Transfer Performance – ITU-T Recommendation I.356, November 1993.

[13] B. Grémont, *"Simulation of Rainfield Attenuation for Satellite Communication Networks"*, 1st Workshop of the COST Action 280 "Propagation Impairments Mitigation for Millimetre Wave Radio Systems", 1-3 July 2002, Malvern, UK.

[14] B. Grémont, *"Generalised Model of the SatComm Channel for Applications to Fade Countermeasures"*, XXVIIth General Assembly of the International Union of Radio Science, Maastricht, The Netherlands, August 17-24, 2002.

RAIN COMPENSATION FOR ADVANCED SATELLITE SYSTEMS

Eleni Noussi, Boris Grémont, Misha Filip, Afroditi Pekou
Microwave Telecommunications Systems Research Group
Department of Electronic & Computer Engineering, University of Portsmouth,
Anglesea Road, Portsmouth, PO1 3DJ, UK, Tel: +44(0)23-92846028
Email: noussie@ee.port.ac.uk, {boris.gremont, misha.filip}@port.ac.uk, pekoua@ee.port.ac.uk

Key words to describe this work: MF-TDMA, Fade Mitigation, Adaptive Coding, Burst Length Control, QoS.
Key Results: A technique to provide compensation for rain attenuation at the expense of capacity was studied (attenuation protection as a function of spare resource in the form of extra timeslots; single-link analysis).
How does the work advance the state-of-the-art?: Global approach; single-link analysis carried out with the intention to consider a large number of links simultaneously affected by rain.
Motivation (Problems addressed): On-going research is of great importance to system designers as satellite services migrate towards the higher part of the spectrum, where implementation of fade countermeasures becomes necessary.

Introduction

MF-TDMA allows a group of Return Channel Satellite Terminals (RCSTs) to communicate with a Gateway using a set of carrier frequencies. In order to guarantee a Quality of Service, it is important that the Network Control Centre (NCC) gets to know the actual needs of each terminal and generates a new Terminal Burst Time Plan (TBTP), so that each RCST knows its timeslot assignments. This mechanism can also be used to drive a Fade Mitigation Technique, i.e. for the purposes of FMT slot reservation when a terminal needs more resources under rain conditions.

Coding and Burst Length Control (BLC)

Within an adaptive MF-TDMA fade counter-measure scheme, a portion of MF-TDMA timeslots is reserved as a shared resource, which can be distributed to any stations within the network subject to rain fading. When a burst within the MF-TDMA frame is subject to fading, it is allocated some extra timeslots into which it can expand. Since the user data rate is not changed, this expansion results to an increase in average power (or energy/bit) of the signal and so counteracts the effect of the fade, [1].
If G_c is the coding gain obtainable by coding the message, and the burst duration is increased H times (i.e. the station is allocated H extra FMT timeslots), then the original power margin, M_o, of the station is increased to, [2]:

$$M = M_o + G_H + G_c = M_o + 10\log_{10} H + G_c \qquad (1)$$

Every time the burst duration is doubled in time, there is an increase in average transmitted power of 3 dB. Figure 1 illustrates an example of employing coding and bit rate reduction to counteract fading. A baseline coding rate of 1/2 provides a 6 dB protection for a BER threshold of 10^{-8} (see Figure 2).
In general, if S is the original number of slots/frame being transmitted, reducing the code rate from the baseline code rate r_1 -decided by the clear-sky link budget and the QoS (BER) objective- to a new code rate r_2, results in expanding the transmission over $(r_1/r_2)\times S$ timeslots. For example, if one slot was originally used and the code rate switched from a baseline clear-sky code rate r_1=7/8 to a lower rate r_2=1/2 to combat fading, then the total number of slots required would be $(7/8)/(1/2)\times 1 = 1.75 \approx 2$ slots, i.e. one extra timeslot to fit the coded bits. For a BER

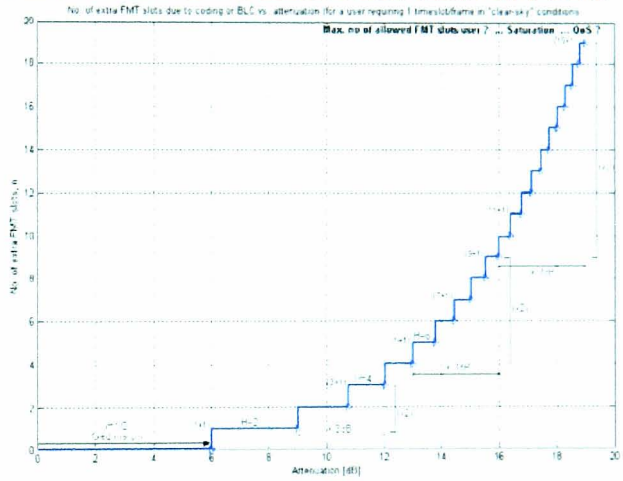

Figure 1. *No. of extra FMT slots due to coding or BLC vs. attenuation protection*

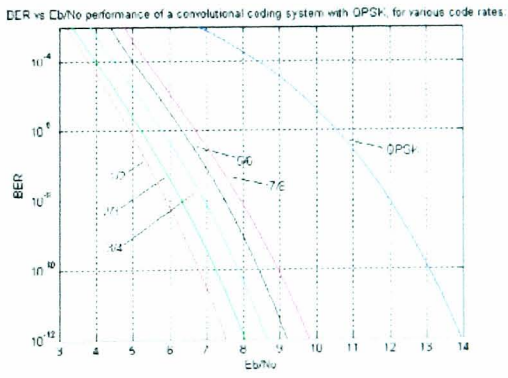

Figure 2. *BER vs. Eb/No performance of a convolutional coding system with QPSK, for various code rates*

objective of 10^{-8} (Figure 2) this would translate to an extra 2 dB protection against fading. If, on top of this, bit rate reduction (or burst length control) was employed, an additional 3 dB protection (total of 5 dB) would be provided by transmitting the information bits at a speed twice as slow, i.e. over twice as many slots: $(r_1/r_2)\times S \times 2 = 3.5 \approx 4$ slots,

i.e. 3 extra timeslots in total.

In the event of rain in some portion of the footprint, the drop in QoS on individual links will require the allocation of spare timeslots to counteract for rain attenuation. Figure 3 shows a typical fade event of 1000 sec duration, i.e. 16-17 minutes of rain; the rain simulator required statistical parameters for rain, μ (mean) and σ (standard deviation) of the distribution, [3].

The signal degradation in terms of E_b/N_o due to rain can be seen in Figure 4; the clear-sky value (achieved E_b/N_o=12.14 dB) was calculated through a return link (RCST to Hub) budget analysis.

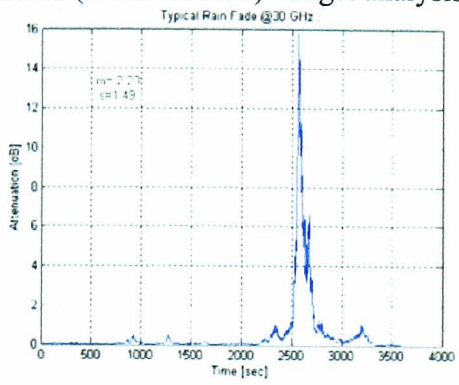

Figure 3. *Simulating rain - typical rain fade event at 30 GHz*

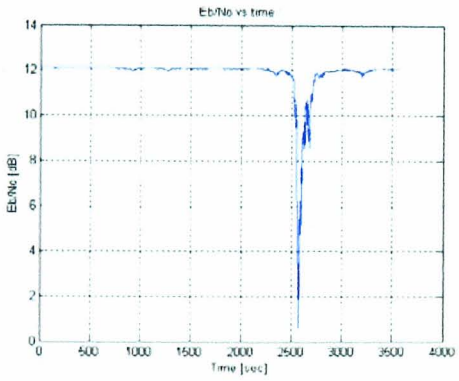

Figure 4. *E_b/N_o degradation due to rain*

Figure 5 illustrates the corresponding BER in time during that event, representing the obvious drop in QoS on the particular link. Depending on the attenuation level, allocation of extra FMT slots will provide the desired compensation (Figure 6). Assuming a population of N users, the NCC must

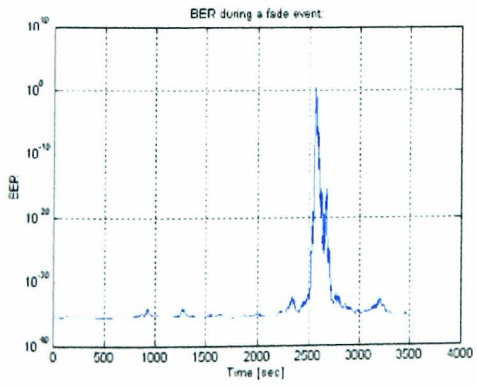

Figure 5. *Bit error rate during rain event*

be able to learn quickly about the links affected, for effective allocation of communication and FMT slots; service communication can be achieved through out-of-band (OBR) and in-band requests (IBR), [4].

A major issue is that MF-TDMA must be able to support the active users. This implies that if the number of FMT spare slots is limited, there will be a finite blocking probability of not meeting the QoS parameters originally agreed. Alternatively, the requests may be queued; in which case, the limited capacity in the presence of rain will result

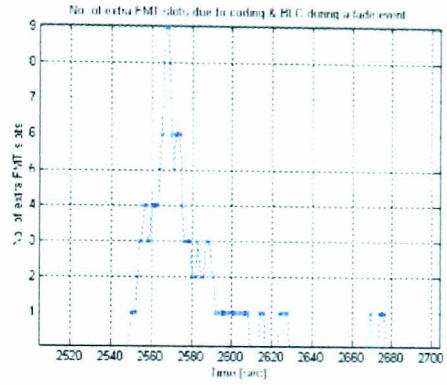

Figure 6. *No. of extra FMT slots for one user during rain*

in longer delays or a re-negotiation of QoS between RCST and NCC could be performed depending on the service agreement. The total number of required FMT slots depends on, [4]: (i) users' density and location; (ii) space and time characteristics of rain; (iii) magnitude of the rain attenuation; (iv) actual traffic characteristics of the user stations; (v) QoS parameters. Furthermore, depending on the hour of the day or the month, the rain conditions may be quite severe resulting in a much more extensive use of FMT slots. This would get even worse if worst fades occur at times when user traffic is high.

Conclusion

The design of MF-TDMA networks with BLC requires a further study of the impact of rain attenuation on the satellite footprint. Long-term analysis will allow investigating the share between traffic and FMT slots whilst short-term analysis will permit to study the resource allocation algorithms that the NCC needs to run for a rapidly converging and fair management of the MF-TDMA channel.

References

[1] D. J. Emerson, R. M. Nelhams, B. L. Clark, *"Adaptive TDMA for Fade Countermeasures"*, Olympus Utilisation Conference, ESA SP-292, 12-14 April 1989, Vienna.

[2] F. Carassa, *"Adaptive Methods to Counteract Rain Attenuation Effects in the 20/30 GHz Band"*, Space Communication and Broadcasting 2, pp. 253-269, 1984, North Holland.

[3] Boris C. Grémont, *"Fade Countermeasure Modelling for Ka-band Satellite Links"*, PhD Thesis, Coventry Univ., Nov. 1997.

[4] E. Noussi, B. Grémont, M. Filip, *"Centrally Managed MF-TDMA Broadband Network with Fade Mitigation built upon DVB-RCS"*, 9th Ka and Broadband Communications Conference, p. 215-222, 5-7 Nov. 2003, Island of Ischia, Italy.

Adaptive MF-TDMA: Burst Length Control as a Rain Fade Countermeasure

Eleni Noussi, Boris Grémont, Misha Filip
Microwave Telecommunication Systems Research Group
University of Portsmouth, Department of Electronic & Computer Engineering,
Anglesea Road, Portsmouth, PO1 3DJ, U.K. Tel: +44(0)23-92846028,
Email: noussie@ee.port.ac.uk, {boris.gremont, misha.filip}@port.ac.uk

Abstract

Satellite services are migrating towards the higher part of the spectrum, where implementation of fade countermeasure becomes necessary. This paper proposes a methodology on how to design a Fade Mitigation Technique (FMT) suitable for application to Ka/V band Multi-Frequency TDMA networks. The technique provides compensation for rain attenuation at the expense of capacity. The attenuation protection as a function of spare resource (extra timeslots) is investigated. Both the advantages and costs of its deployment are demonstrated, with the intention to meet the user-specified Quality of Service requirements when considering a large number of links simultaneously affected by rain.

1 Introduction

A result of the need to accommodate high-rate transmission is to push into increasingly higher frequency bands, namely Ka band (30/20 GHz) and V band (50/40 GHz). This trend is explained by the large segments of frequency spectrum required for supporting the high data rates planned in newer systems, [1]. Most VSAT and Digital Broadcasting Satellite TV systems in operation today use portions of the Ku band.

A major drawback to the use of higher frequencies is significant rain attenuation, which increases rapidly with increasing carrier frequency, [2], [3], [4]. It can cause serious signal quality degradation of earth-space communication links, having a major impact not only on individual links, but also on the global network.

MF-TDMA allows a group of Return Channel Satellite Terminals (RCSTs) to communicate with a Gateway using a set of carrier frequencies. In order to guarantee a Quality of Service, it is important that the Network Control Centre (NCC) gets to know the actual needs of each of the active RCSTs of the network. Therefore each station needs to monitor and measure its specific traffic requirements that are then communicated to the NCC. If resources are available, the NCC generates a new Terminal Burst Time Plan (TBTP) accommodating the needs of all its active stations at a superframe/frame level, so that each RCST knows what timeslots have been assigned to it. This mechanism can also be used to drive a Fade Mitigation Technique, i.e. for the purposes of FMT slot reservation when a terminal needs more resources under rain conditions, [8].

2 Coding & Burst Length Control

Within an adaptive MF-TDMA fade counter-measure scheme, a portion of MF-TDMA timeslots is reserved as a shared resource, which can be distributed to any stations within the network subject to rain fading. When a burst within the MF-TDMA frame is subject to fading, it is allocated some extra timeslots into which it can expand. Since the user data rate is not changed, this expansion results in an increase in average power (or energy/bit) of the signal and so counteracts the effect of the fade, [5].

If G_c is the coding gain obtainable by coding the message, and the burst duration is increased H times (i.e. the station is allocated H extra FMT timeslots), then the original power margin, M_o, of the station is increased to, [6]:

$$M = M_O + G_H + G_C = M_O + 10\log_{10} H + G_C \quad (1)$$

Every time the burst duration is doubled in time (or the symbol rate is halved) there is an increase in average transmitted power of 3 dB.

In the event of a fade, the energy/bit could be increased in either of the following ways: (i) the duration of the transmitted bits could be increased (symbol rate reduction), or equivalently, each bit could be repeated, or (ii) the entire block of bits could be repeated after appropriate expansion:

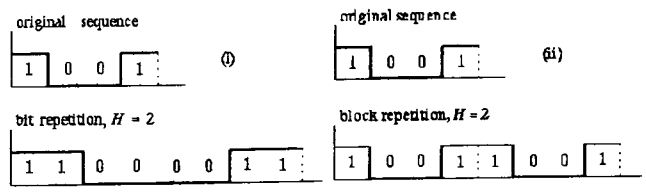

Figure 1. *Example of (i) contiguous bit (ii) data block repetition*

Comparison between the two techniques has shown that (i) is more efficient in terms of the enhancement that can be obtained for a particular utilisation of the shared resource time within the frame.

A baseline coding rate of 7/8 provides a 4 dB protection for a BER threshold of 10^{-8} (see Figure 2).

In general, if S is the original number of slots/frame being transmitted, reducing the code rate from the baseline code rate r_1 (decided by the clear-sky link budget and the QoS (BER) objective) a new code rate r_2, results in expanding the transmission over $\lceil (r_1/r_2)\times S \rceil$ timeslots. For example, if one slot was originally used and the code rate switched from a baseline clear-sky code rate r_1=7/8 to a lower rate r_2=1/2 to combat fading, then the total number of slots required would be $\lceil (7/8)/(1/2)\times 1 \rceil = \lceil 1.75 \rceil = 2$ slots, i.e. one extra timeslot needed to fit the coded bits. For a BER objective of 10^{-8} this would translate into an extra 2 dB protection against fading (Figure 2).

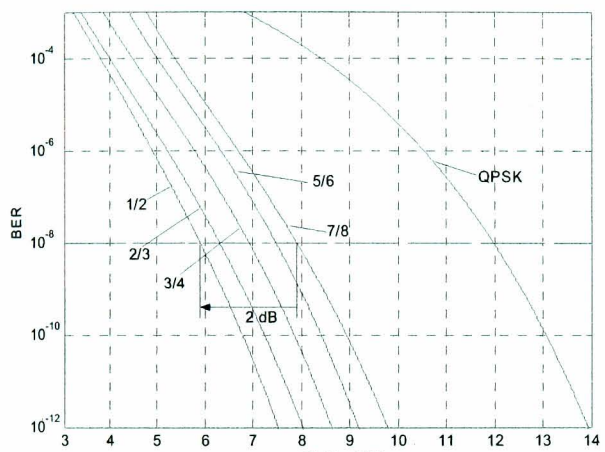

Figure 2. *BER vs. Eb/No performance of a convolutional coding system with QPSK, for various code rates*

If, additionally, burst length control was employed, an extra 3 dB protection (total of 5 dB) would be provided by transmitting the information bits at half the speed, over twice as many slots: $\lceil (r_1/r_2)\times S \times 2 \rceil = \lceil 3.5 \rceil = 4$ slots, i.e. 3 extra timeslots in total.

2.1 Return Link Analysis

Radio frequency link analysis provides the means to calculate the quality of the information contents delivered to the data link control layer. The quality of digital information is measured by the BER, which depends on the type of modulation and coding performed, and on the carrier to noise power spectral density ratio, C/N_o, at the input of the receiver, considered as a quality measure of the link quality. Comparison of what the satellite system can provide in terms of power, noise etc. with the requirements, i.e. comparing the E_b/N_o value achieved with the required value for a specific QoS target, leaves a link margin which should be positive but not excessively so, otherwise the link would be over-engineered. This positive margin represents all those components which it has not been possible to calculate in the budgets but which may affect the link quality (examples may be phase noise, AM/PM conversion in amplifiers, non-Gaussian interference etc.).

Considering the above, QPSK with convolutional code rate of 7/8 is chosen as the system baseline modulation/coding scheme, leaving a positive link margin of 2.73 dB (Table 1). The attenuated values were obtained considering 15-dB rain attenuation (threshold value for 99.91% availability, [7]) on the uplink.

	Uplink	Downlink	
Central T_X frequency, f	29.66	19.7	GHz
Transmitted power, P_{Tx}	2	1.07 (TWTA)	W
Antenna T_X gain, G_{Tx}	49.7	42.6	dB
EIRP	49.8 (ES)	27.02 (SAT)	dBW
Figure of merit, G/T	15 (SAT)	32.7 (HUB)	dB/K
C/N_o	79.74	77.16	dBHz
Mod. scheme, coding	QPSK, convol. ρ = 7/8		
	Overall Link		
Total clear-sky $(C/N_o)_{T,cs}$	75.25		dBHz
Achieved $(E_b/N_o)_{T,cs}$	12.14		dB
Modem implement. losses	1.5		dB
Link Margin, $LM_{(cs)}$	2.73		dB
Total $CNR_{T(rain)}$	64.5		dBHz
Total $(E_b/N_o)_{T(rain)}$	1.39		dB

Table 1. *Return link analysis (RCST to Hub)*

In the event of rain in some portion of the footprint, the drop in QoS on individual links will require the allocation of spare timeslots to counteract the rain attenuation. Figure 3 illustrates an example of employing coding and bit rate reduction to counteract fading.

Note that the original fixed power margin of the station of 2.73 dB is due to the convolutional code rate of 7/8, chosen as a fixed baseline for minimum redundancy and maximum throughput.

Figure 3. *No. of extra FMT slots due to coding and*

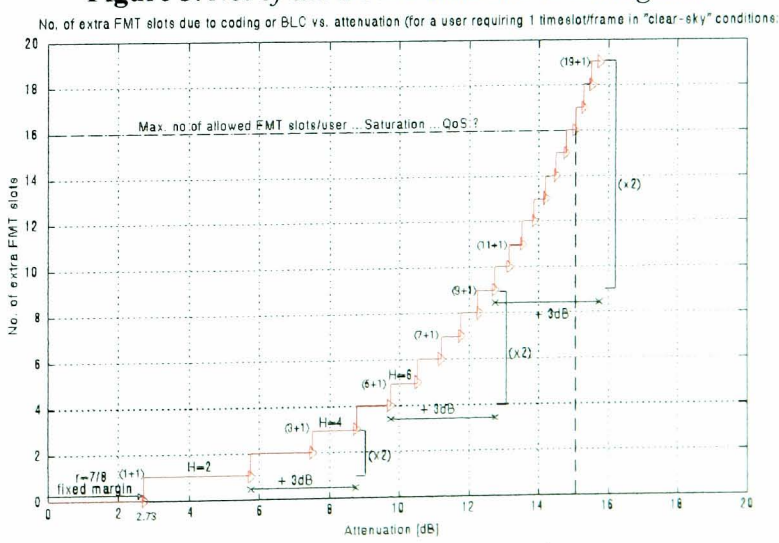

BLC vs. attenuation protection

Attenuation protection is thereafter provided in steps at the expense of capacity; every time the burst duration is doubled (hence the number of timeslots is doubled), an additional 3-dB attenuation protection is provided.

Figure 4 shows an example of carrier-to-noise ratio attenuation for a 30/20 GHz link. The signal degradation in terms of carrier to noise ratio due to rain can be seen; the clear-sky values (available C/N_0=75.25 dBHz, achieved E_b/N_0=12.14 dB) were calculated through the return link (RCST to Hub) budget analysis (Table 1).

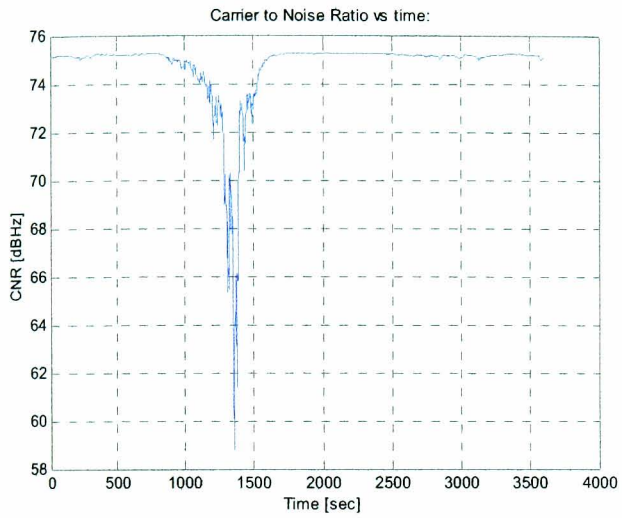

Figure 4. *Simulating rain – an example of CNR degradation for a 30/20 GHz link*

Figure 5 illustrates the corresponding BER in time during that event, showing the drop in QoS on the particular link during rainy conditions.

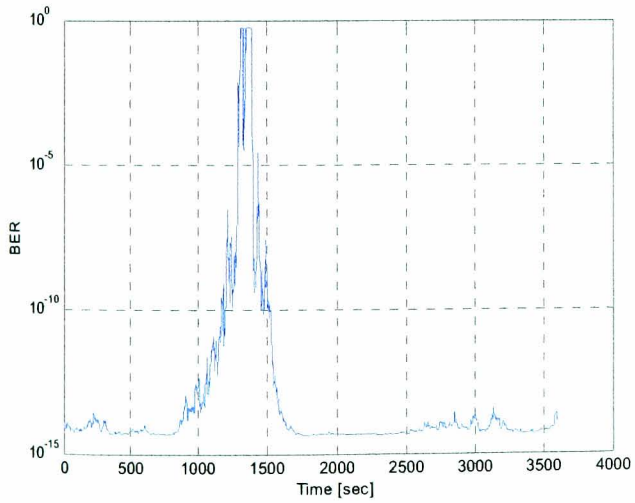

Figure 5. *Bit error rate during rain event*

Depending on the attenuation level, allocation of extra FMT slots will provide the desired compensation (Figure 6 and Figure 7).

We note the advantages of such an adaptive system over a fixed one that would constantly allocate a fixed number of slots (16 extra slots for a 15 dB attenuation threshold).

In the case of an adaptive system, the number of slots will vary in time depending on the actual requirement, as shown in Figure 6. This results in a much more efficient use of spare FMT slots, which can therefore be allocated to other users.

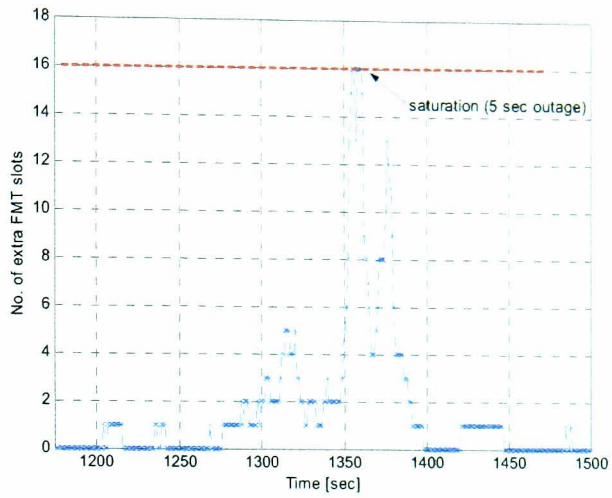

Figure 6. *No. of extra FMT slots for one user during rain*

Maintaining the BER target to achieve long-term availability would then only be limited by the dynamic range of the FMT, i.e. the maximum number of extra slots (16 slots in our example, see also Figure 3); if more slots were required, the system would not perform satisfactorily and there would be network outage as shown in Figure 6. The FMT provides compensation during the fade event, but not for this 5 seconds outage period, the only period during which the QoS threshold of 10^{-8} cannot be maintained (Figure 7):

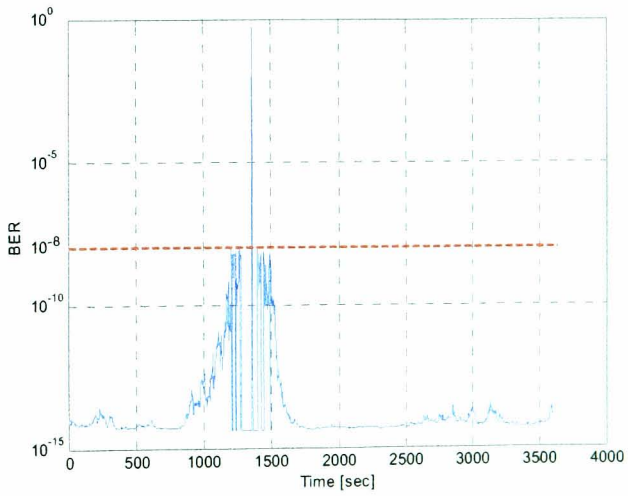

Figure 7. *BER during a fade event with FMT*

It becomes obvious, however, that this adaptiveness of the system should also be controlled, in order to avoid unnecessary "switchings" in short periods of time (see Figure 6) due to rain dynamics (fast changes in attenuation levels), i.e. the number of requests should probably be reduced in order to minimise signalling.

Assuming a population of N users, the NCC must be able to learn quickly about the links affected, for effective allocation of communication and FMT slots; service communication can be achieved through out-of-band (OBR) and in-band requests (IBR), [8].

A major issue is that MF-TDMA must be able to support all the active users. This implies that if the number of FMT spare slots is limited, saturation can occur when many users request slots at the same time. There will therefore be a finite blocking probability of not meeting the QoS parameters originally agreed. Alternatively, the requests may be queued, in which case, the limited capacity in the presence of rain will result in longer delays or a re-negotiation of QoS between RCST and NCC could be performed depending on the service level agreement.

Figure 8 shows an example of rain cells over areas with active and non-active users inside the coverage of area of a satellite.

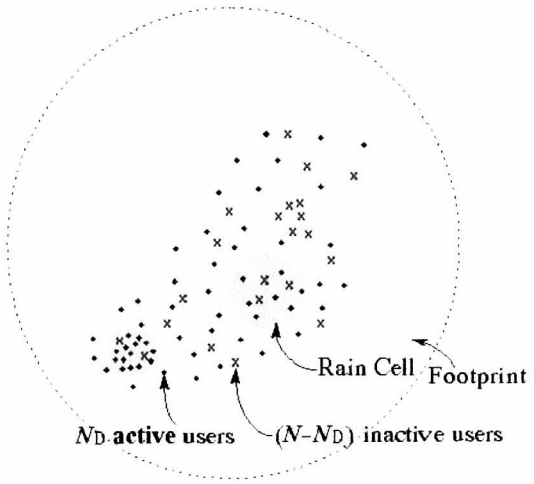

Figure 8. *Example of rain cells over areas with active and non-active users inside the footprint of a satellite*

It becomes apparent that the total number of required FMT slots depends on, [8]: (i) users' density and location (the greater the concentration of users the greater the number of required FMT slots); (ii) space and time characteristics of rain (for rain over large areas, more FMT slots are required); (iii) magnitude of the rain attenuation; (iv) actual traffic characteristics of the user stations; (v) QoS parameters.

Furthermore, depending on the hour of the day or the month, the rain conditions may be quite severe resulting in a more extensive use of FMT slots. This would be detrimental if severe fades occurred at times when user traffic is high.

3 Conclusions & Further Work

This paper has proposed a methodology on how to design a Fade Mitigation Technique suitable for application to Multi-Frequency TDMA networks. It can provide compensation for rain attenuation at the expense of capacity; the attenuation protection as a function of spare resource in the form of extra timeslots has been investigated. The advantages, costs and issues, when it is used, have been demonstrated, with the intention to meet the user-specified QoS requirements.

The design of MF-TDMA networks with Burst Length Control requires a detailed study of the impact of rain attenuation on the satellite footprint. Long-term analysis will allow investigations into the share between traffic and FMT slots. The probability of blocking under severe rain conditions needs be investigated as a measure of the grade of service. Short-term analysis will permit the study of the resource allocation algorithms that the NCC needs to deploy for a rapidly converging and fair management of the MF-TDMA channel.

4 References

[1] M. H. Hadjitheodosiou, A. Ephremides, D. Friedman, *"Broadband Access via Satellite"*, Technical Research Report, CSHCN T.R. 99-2, Centre for Satellite and Hybrid Communication Networks, University of Maryland, 1999, available at http://techreports.isr.umd.edu/TechReports/CSHCN/1999/CSHCN_TR_99-2/CSHCN_TR_99-2.pdf

[2] L. J. Ippolito, *"Radio propagation for space communications systems"*, IEEE Proceedings, vol. 69, no. 6, pp. 697-727, U.S.A., June 1981.

[3] S. I. E. Touw, *"Analyses of Amplitude Scintillations for the Evaluation of the Performance of Open-Loop ULPC Systems"*, MSc Thesis, Eindhoven Univ. of Technology, Eindhoven, The Netherlands, 1994.

[4] R.A. Nelson, *"V-band: Expansion of the Spectrum Frontier"*, Via Satellite, February 1998, pp. 66+.

[5] D. J. Emerson, R. M. Nelhams, B. L. Clark, *"Adaptive TDMA for Fade Countermeasures"*, Olympus Utilisation Conference, ESA SP-292, 12-14 April 1989, Vienna.

[6] F. Carassa, *"Adaptive Methods to Counteract Rain Attenuation Effects in the 20/30 GHz Band"*, Space Communication & Broadcasting 2, pp. 253-269, 1984, North Holland.

[7] E. Noussi, *"Satellite Communication Systems with Up-Link Power Control"*, MSc Thesis, University of Portsmouth, September 2002.

[8] E. Noussi, B. Grémont, M. Filip, *"Centrally Managed MF-TDMA Broadband Network with Fade Mitigation built upon DVB-RCS"*, 9th Ka & Broadband Communications Conference, p. 215-222, 5-7 November 2003, Island of Ischia, Italy.

A DEMAND ASSIGNMENT ALGORITHM FOR FMT RESOURCE MANAGEMENT IN DVB-RCS NETWORKS

Eleni Noussi, Boris Grémont, Misha Filip
Microwave Telecommunications Systems Research Group
Department of Electronic & Computer Engineering, University of Portsmouth,
Anglesea Road, Portsmouth, PO1 3DJ, UK, Tel: +44(0)23-92846028
Email: noussie@ee.port.ac.uk, {boris.gremont, misha.filip}@port.ac.uk

Key words to describe this work: Resource allocation, Burst Length Control (BLC), statistical multiplexing, rain, QoS.
Key Results: A resource allocation algorithm has been developed and applied to a simple MF-TDMA scenario to investigate the effect of different probabilities of rain over different user density areas on channel capacity utilisation.
How does the work advance the state-of-the-art?: Global approach; analysis considers a multiple number of links simultaneously affected by rain.
Motivation (Problems addressed): On-going research is of great importance to system designers, as implementation of fade countermeasures becomes necessary; the proposed technique is particularly suitable for power limited systems.

Abstract: *A Demand Assignment (DA) resource allocation algorithm has been developed and applied to a simple MF-TDMA scenario that investigates the effect of different probabilities of rain over different user density areas on channel capacity utilisation and total user throughput efficiency; two cases, a correlated and an uncorrelated rain scenario, are studied.*

1. Integration of BLC within DVB-RCS

The overall proposed architecture of DVB-RCS with BLC as a rain FMT is depicted in Figure 1. The NCC monitors the traffic bursts from the RCSTs so that it can determine the required BLC multiplication factor H_i. The DAMA algorithm is then run and the new TBTP table is broadcasted.

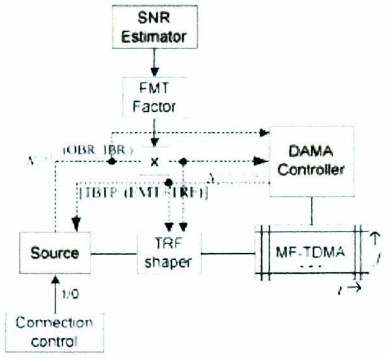

Figure 1. *Architecture of DVB-RCS with BLC*

We focused on the transport of aggregate internet traffic that is known to exhibit self-similarity with long-range dependence and high levels of burstiness, [1]. In our simulations we assumed one connection per terminal, each generating a stream of traffic ATM cells with a Pareto distribution ($\alpha = 1.2$) and Peak Cell Rate of 128 kbps. For the resource allocation phase, a bin-packing algorithm (first fit heaviest to lightest) has been implemented and applied to all traffic requests which are cumulated over a period of 1 sec. Note that in order to simplify the process and speed up calculations, a scaled-down model was used considering only a portion of the MF-TDMA space (2 frequency carriers).

2. Preliminary Results

The following two scenarios were studied in order to investigate the effects of different probabilities of rain over small and large user density areas. Rain events were generated using a random rain simulator, [2]. As the number of active user stations in the area increased, the channel utilisation and total user throughput efficiency were first obtained for clear-sky conditions, Table 1.

N_s	Channel Utilisation (%)		Total (average) user throughput efficiency (b/s/Hz)
	mean	max	
20	30.8	39.7	0.23
30	46.2	57.5	0.34
40	61.7	74.5	0.46
50	77.2	92.5	0.57

Table 1. *Channel utilisation and user throughput efficiency for differing numbers of sources*

2.1 Rain-Uncorrelated Scenario

In this scenario, user density was considered to be uniform and the distance between users to be large. As the probability of uncorrelated rain on this area increased, the overall channel utilisation was monitored for the increasing number of active users. The uncorrelated rain events were up to 13 dB in amplitude, with a duration of 10-20 minutes. Figure 2 shows the slight increase in average capacity utilisation as the rain probability per unit area increases up to 50% (i.e. half of the active users are suffering from uncorrelated rain).

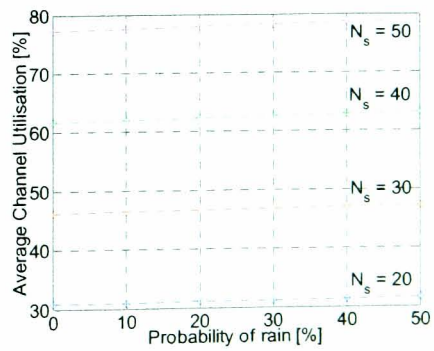

Figure 2. *Average channel utilisation vs. prob. of rain for an increasing number of users (uncorrelated rain)*

As the rain probability increased, the increase noticed for the highest values of channel utilisation

was found to be 10.4% for N_s=20, 8.7% for N_s=30, 6.7% for N_s=40, and 5.2% for N_s=50, see Figure 3.

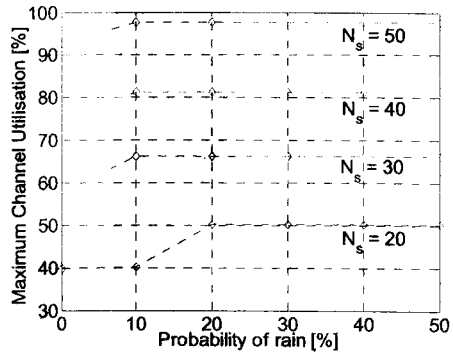

Figure 3. *Maximum channel utilisation vs. prob. of rain for an increasing number of users (uncorrelated rain)*

In order to get a better picture of the utilisation variability as the number of users and rain probability increased, its standard deviation was examined, part of the results will later be shown in comparison with a rain correlated scenario.

It must be noted that, for the purposes of this paper, we ensured that all connections were served every TBTP allocation period without the introduction of any additional delay. Obviously, if some queuing delay had been allowed, more stations would have been able to be served.

2.2 Rain-Correlated Scenario

In this scenario, user density was considered to be large with zero distance between active users. Hence rain-correlated traffic streams were considered. The 7-dB correlated rain event applied had a duration of about 17 minutes. As far as the average channel utilisation is concerned, the results obtained were very similar to those in Figure 2, i.e. only a slight increase in average capacity utilisation was observed as probability of rain on a specific area increased. However, a large increase was observed for the maximum utilisation values, see Figure 4, for N_s=20 and N_s=30 sources. When N_s increased to 40, for rain probability higher than 30%, requests could not be served without queuing. For N_s=50, the requests could be fully granted without any delay only during clear-sky conditions.

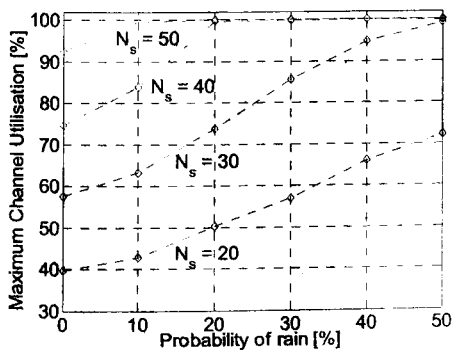

Figure 4. *Maximum channel utilisation vs. prob. of rain for an increasing number of users (correlated rain)*

Figure 5 compares the standard deviation of the channel utilisation for the two scenarios.

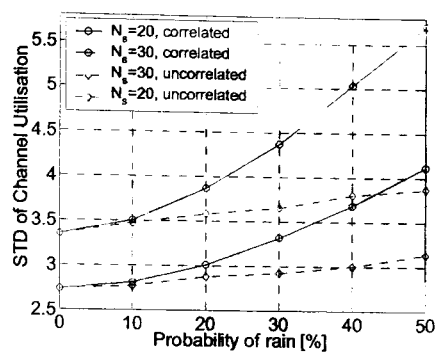

Figure 5. *STD of overall channel utilisation (correlated and uncorrelated rain)*

3. Conclusion

The number of users served within only 2 MF-TDMA channels without any queuing delay was high for the uncorrelated scenario (50 sources, half of them suffering from rain, resulting to an average capacity utilisation of 78.9%), since not all sources happened to transmit at their peak rates simultaneously. This is of great significance and clearly demonstrates the advantages of statistical multiplexing, even in the case when 50% of the links are rain affected (uncorrelated). In the uncorrelated rain scenario, the proposed FMT offers a guaranteed Quality of Service for all served stations. Outage will only occur when the dynamic range of the FMT is exceeded, [2]. In the correlated rain scenario, the algorithm is not able to grant all the requests for the higher numbers of active users; and even when the number of users is low, the high variability in utilisation indicates inefficient use of capacity. In such cases, if the agreed QoS or service level agreement allows it, some connections may be blocked until resources become available, or more likely, the requests may be queued.

The design of MF-TDMA networks with BLC therefore requires a detailed study of the impact of correlated rain attenuation on the satellite footprint. Obviously, the algorithm should avoid multiplexing together requests emanating from rainy regions because this would generate a large amount of total traffic. More detailed simulations and analysis will be required to investigate/solve issues regarding the support of multi-class services, the impact of BLC on QoS, connection admission control and service level agreements.

References

[1] W. E. Leland, M. S. Taqqu, W. Willinger, D. V. Wilson, *"On the Self-Similar Nature of Ethernet Traffic"*, IEEE/ACM Trans.actions on Networking, vol. 2 no. 1, 1994, pp. 1-15.

[2] E. Noussi, B. Grémont, M. Filip, *"Adaptive MF-TDMA: Burst Length Control as a Rain Fade Countermeasure"*, CSNDSP, 4th Int. Symposium Proceedings, University of Newcastle upon Tyne, 20-22 July 2004, p. 43-46.

CHAPTER 3
Mitigation Techniques

Editor: Editor name[1]

Authors:

Chapter 2.2, FMT Resource Management in DVB-RCS Networks
Eleni Noussi[2,3], Boris Grémont[2,4]

[1] Affiliation, Address
Tel.: +xxxxxx, Fax.: + xxxxxx, e-mail: name@addrees
[2] Microwave Telecommunication Systems Research Group, University of Portsmouth, Anglesea Building, Anglesea Road, Portsmouth, Hants, PO1 3DJ, UK
Fax.: +44(0)23-92842792
[3] Tel.: +44(0)23-92846028, email: noussie@ee.port.ac.uk
[4] Tel.: +44(0)23-92842552, email: boris.gremont@port.ac.uk

Contents

2.1 Introduction

A consequence of the need to accommodate higher network capacities is to migrate to higher frequency bands namely Ka band (27-40 GHz) and V band (40-75 GHz). This trend is also justified by the relatively large segments of frequency spectrum required for supporting the high data rates required to deliver advanced multi-class multimedia services, [*Hadjitheodosiou et al., 1999*].

A major drawback is significant rain attenuation that increases rapidly with increasing microwave frequency, [*Ippolito, 1981*], [*Nelson, 1998*], [*Touw, 1994*]. Rain can cause serious signal quality degradations on individual earth-space communication links and this situation will have a major impact on the link availability and the effective throughput of a network, hence the implementation of Fade Countermeasures becomes necessary and is of great importance to system designers.

Studies in the past have developed novel Medium Access Control protocols for Multi-Frequency TDMA satellite channels, [*Iuoras et al., 1999*], [*Li and Chen, 2001*], [*Li et al., 2002*], [*Wibowo et al., 1998*], and dynamic resource allocation algorithms in an MF-TDMA basis for DVB-RCS, [*Lee et al., 2002*], to maximize system throughput. Pech et al., [*Pech et al., 2001*], have conducted one of the very few studies that have taken into account fading conditions. Although the dynamic resource allocation in MF-TDMA systems is of great interest, most studies have not considered the implementation of satellite Fade Mitigation Techniques, necessary for such services and even when FMTs were introduced in resource management protocols, work focused on a single link analysis, lacking a global approach that would consider a large number of links simultaneously affected by rain.

Celandroni et al. have described the concepts and implementation details of a complete fade countermeasure system based on adaptive TDMA, with demand assignment of capacity, [*Celandroni and Potorti, 2000*]. Association of an up-link power control feature with the bit and coding rate variation gives the system an interesting ability to cope with fade conditions, [*Celandroni et al., 1992*], [*Celandroni et al., 1996a*], [*Celandroni et al., 1996b*], [*Celandroni et al., 1997*], [*Celandroni and Potorti, 2000*]. These studies are of great significance as an adaptation of such modelling to the case of MF-TDMA for DVB-RCS is actually essential.

Figure 2.1-1 presents the basic DVB-RCS network architecture, [*ETSI, 2002*].

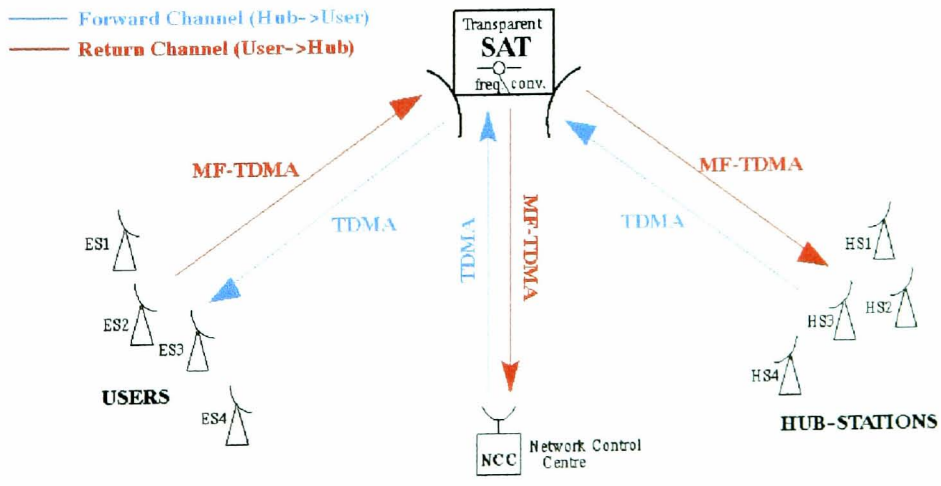

Figure 2.1-1 DVB-RCS network architecture

It consists of the following elements: (i) GEO Ka-Band satellite payload, using the 20/30 GHz band for earth-space communications. We will focus on a bent-pipe system. (ii) The Return Channel Satellite Terminals (RCSTs) can frequency hop across the whole MF-TDMA space and their burst transmission rate is 2.048 Mbps. (ii) The Network Control Centre (NCC) manages in real-time the communications of the whole MF-TDMA satellite system.

MF-TDMA allows a group of Return Channel Satellite Terminals to communicate with a Gateway using a set of carrier frequencies. In order to guarantee a Quality of Service, it is important that the NCC gets to know the actual traffic needs of each of the active RCSTs of the network. Therefore each user station needs to monitor and/or estimate its specific traffic requirements that are then communicated to the NCC. If resources are available, the NCC will generate a new Terminal Burst Time Plan (TBTP) at a superframe/frame level accommodating the needs of all its active stations, so that each RCST learns what timeslots have been assigned to it. Although originally designed to provide bandwidth on demand, this mechanism can also be used to drive a Fade Mitigation Technique. Allocated traffic can be varied not only depending on the RCSTs traffic requirement but it can also be used to carry extra time slots for the purposes of fade mitigation when a link is under rain conditions, [*Grémont et al., 2003*], [*Noussi et al., 2003*].

This paper proposes the integration of a Fade Mitigation Technique that is particularly suitable for power limited systems. It is simple to implement within a centrally managed MF-TDMA satellite network and able to provide compensation for rain attenuation within a large dynamic range, at the expense of capacity. A resource allocation algorithm is applied to a simple MF-TDMA scenario employing suitable multiplexing of rain-uncorrelated traffic streams.

Section 2 introduces Burst Length Control as a Rain Fade Countermeasure. Some background on Bandwidth-on-Demand over DVB-RCS is provided in Section 3. Details regarding the integration of the proposed FMT within DVB-RCS and the simulation model are included in Section 4. Performance results are reported in Section 5. Section 6 concludes the paper.

2.2 Burst Length Control as a Rain Fade Countermeasure

This Section will introduce the principles of the proposed FMT. Considering an adaptive MF-TDMA system with a built-in fade countermeasure, a variable portion of MF-TDMA burst plan will be allocated to carry additional FMT timeslots whose role is to compensate for the attenuation suffered by a set of links undergoing rain. In particular, when a traffic burst is subject to fading, the burst will be allocated extra time slots in which the original traffic burst can be expanded. This time expansion results in an increase in average power (or energy/bit) of the signal and so it counteracts the effect of the fade, [*Emerson et al., 1989*].

If the duration of S_i traffic slots (emanating from one single source labelled i) is spread by a factor H_i then the number of extra FMT slots required by the i^{th} return connection is:

$$N_{FMT}^{i} = S_i \times (H_i - 1) \qquad \text{FMT slots} \qquad 2.2\text{-}1$$

By using spreading, the total power margin M_i is increased to:

$$M_i = M_0^i + 10\log_{10} H_i \qquad [\text{dB}] \qquad 2.2\text{-}2$$

where M_0^i denotes the clear-sky power margin while the second term is the extra power gain brought by the FMT. We note that when we spread by an additional factor of two the FMT produces an increase in average transmitted power of 3 dB. This technique known as Burst Length Control (BLC) was described in [*Carassa, 1984*].

BLC can be implemented in two ways. For the first approach, the duration of the transmitted bits and corresponding symbols can be increased by a factor of H_i (adaptive modem scenario), or equivalently, each bit can be played H_i times and these are passed consecutively to the modulator (operating at fixed symbol rate). The second approach is to contiguously repeat packets of traffic slots by the spreading factor H_i as shown in Figure 2.2-1.

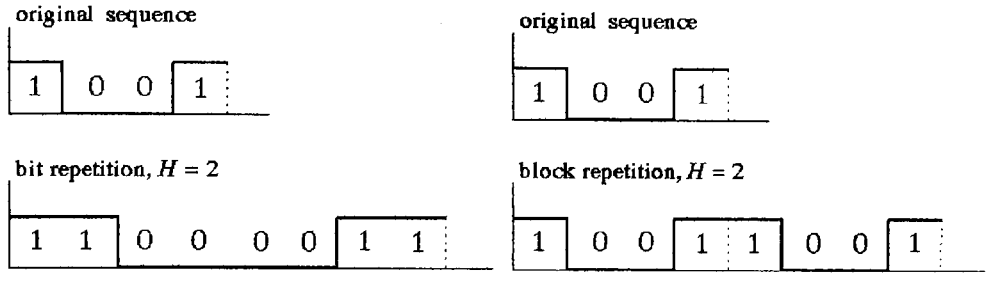

Figure 2.2-1 Example of (i) contiguous bit (ii) data block repetition

Comparison between the two techniques showed that the first technique is less greedy in required FMT slots whereas the second approach only offers power gains for odd numbers of block bit repetition.

In a previous study of a typical Ka band return channel (see [*Noussi et al., 2004*] for details), QPSK with rate 7/8 convolutional coding was chosen as the system baseline (clear-sky) modulation/coding scheme providing maximum user throughput at a BER better than 10^{-8}. This system leaves a positive clear-sky link margin of $M_0^i = 2.73$ dB with a clear-sky CNR_0^i of 75.25 dB.Hz.

In order to deploy in real-time the BLC mitigation technique, the system needs to determine the required spreading factor H_i for each active connection. This in turn will depend on the combined impact of up- and down-link attenuation on the overall CNR on the return link. This will also depend on the clear-sky CNR_0^i and the desired/agreed maximum allowed BER of the return link i.e. in general:

$$H_i = f(BER_{\max}, CNR) = g(A_i, BER_{\max}) \qquad 2.2\text{-}3$$

where $A_i \equiv CNR_0 - CNR_i$ denotes the total drop in CNR at the Hub/NCC station for link i with respect to clear-sky conditions and $H_i \geq 1$. The total number of FMT slots in terms of A_i is $N_{FMT}^i = S_i \times \left[g(A_i, BER_{req}) - 1\right]$. Combining Equations 2.2-4 and 2.2-5, we can express the power fade margin as a function of the drop in CNR. This has been evaluated in [*Noussi et al., 2004*] and is shown in Figure 2.2-2 with S_i is set to unity. Therefore Figure 2.2-2 shows the number of required FMT slots per traffic slot for a typical return channel.

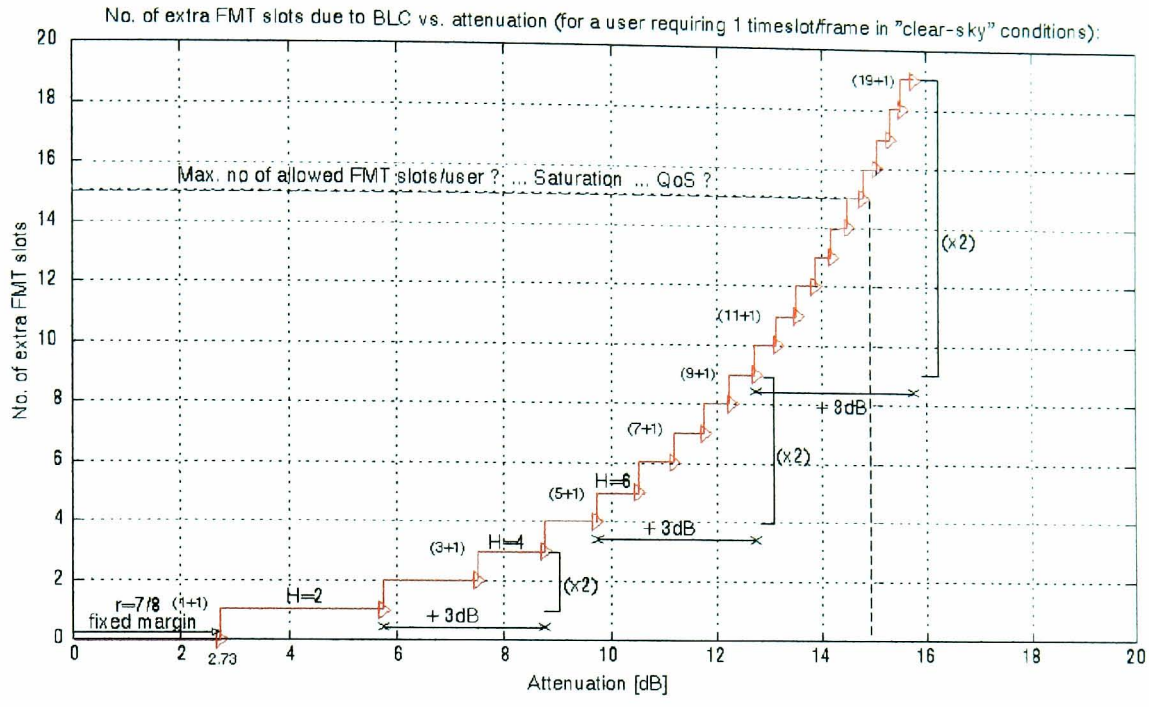

Figure 2.2-2 Number of required FMT slots per traffic slots vs. attenuation protection

It shows that every time the burst duration is doubled in time, the FMT offers an extra 3-dB attenuation protection. For example, spreading by a factor of 2 (i.e. using 1 FMT slot per traffic timeslot) will make the system capable of coping with attenuations that are up to 3 dB higher than the fixed margin of the system; a spreading factor of 4 (i.e. 3 FMT slots per traffic timeslot) will provide with an additional 3 dB attenuation protection and so on.

We call H_i the BLC spread factor or equivalently the BLC multiplication factor. The latter term emphasises that H_i will increase the traffic demand of the source by a factor H_i. We will see later how increasing the capacity requests for the RSCT affected by rain can be achieved within DVB-RCS. Finally, the availability of a typical return link, $A_i^{\%}$, needs to be achieved by the BLC mitigation technique. In our context, we need to make sure that the range of the FMT multiplication is large enough to cope for the long-term drop in overall CNR on the return channel.

As we will see later on, the maximum BLC multiplication factor offered by the system under consideration is 16, i.e. from Figure 2.2-2, the FMT will be able to cope for attenuations of up to 15 dB (15 FMT slots per traffic slot). This will result in a 99.92% link availability (providing 1.92% improvement, when compared with the 98% availability achieved without BLC).

Before proceeding to implementation details of the proposed technique, the following section will provide us with some background on DVB-RCS and the built-in mechanisms that will be used to drive the proposed FMT.

2.3 Bandwidth-on-Demand over DVB-RCS Background [*ETSI, 2002*]

Most new generation Ka-band satellite systems are designed to provide low-cost telecommunication services to hundreds of users. In order to maximise the system capacity,

frequencies and time slots can be allocated dynamically so as to exploit statistical multiplexing of the sources. Bandwidth on Demand (BoD) can be employed to support the maximum amount of users possible. On the billing side BoD may enable users to pay only for the capacity they utilise, [*Psomas and Rees, 1998*].

The timeslots of the return link are organised and numbered so that the network is able to allocate them to individual active RCSTs. Figure 2.3-1 shows how the global return link capacity may be segmented amongst a group of RCSTs; the network will then manage several superframe identifiers, SF_IDs, (i.e. separate sets of carrier frequencies).

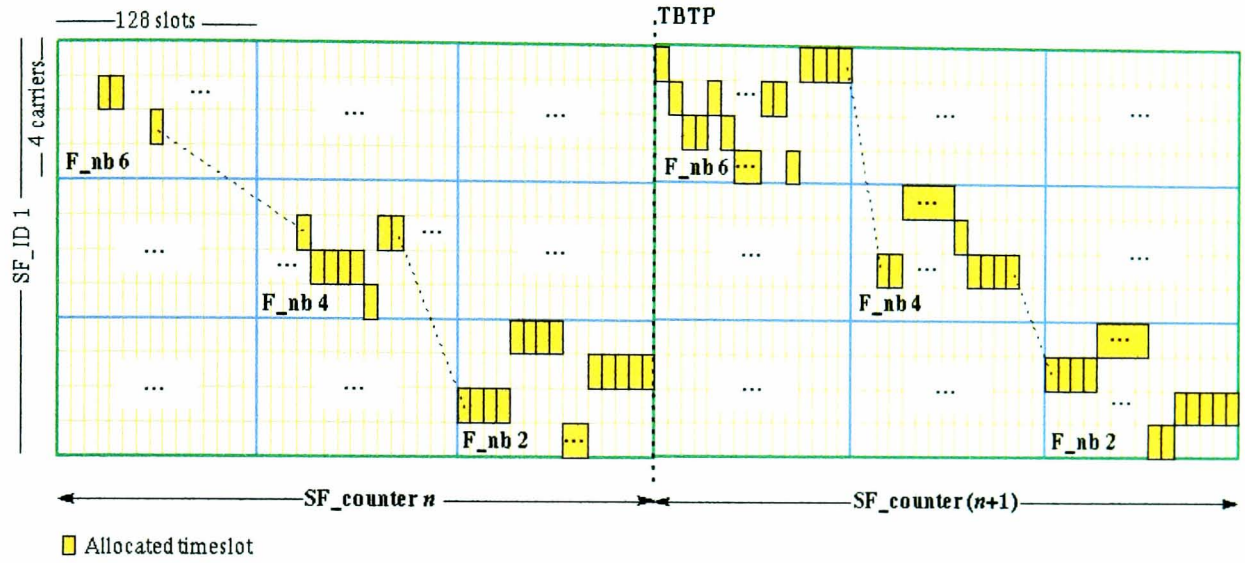

Figure 2.3-1 Capacity segmentation and timeslot allocation: an example

Without loss of generality, it is assumed that these frequency sets are fixed, i.e. superframes/frames have a fixed bandwidth (otherwise a change in a superframe's bandwidth would affect the whole arrangement and all RCST groups would then have to be notified and have their superframe bandwidth adjusted appropriately via additional service signalling). For each superframe of a given SF_ID, allocation of timeslots is communicated to the RCSTs via the Terminal Burst Time Plan table. An RCST is there on allowed to transmit data bursts in the timeslots that have been allocated to it.

As shown in Figure 2.3-1, the consecutive superframes of a given SF_ID are time-contiguous. Each occurrence of a superframe is labelled with a number called "SF_counter". These two superframes of this particular SF_ID 1 are of the same composition and duration, unless a notification that a change should be applied is provided; this can occur at the boundary between two superframes (between two consecutive SF_counters of the SF_ID) so that the next superframe is of different composition and/or duration. This notification involves the TBTP and the Superframe, Frame and Timeslot Composition Tables (SCT, FCT, TCT). The DVB-RCS standard specifies that these service information tables will be transmitted at least every 10 seconds. Alternatively the tables can be transmitted synchronously at the exact beginning of every superframe. In fact, if required, the TBTP can even be updated at the beginning of every frame. These tables can therefore be transmitted as frequently as required to provide detailed network information, transmission parameters and timeslot properties (such as symbol rate, code rate, payload content). This is of importance as it is directly related to the achievable update rates when deploying FMTs for the compensation of rain attenuation.

A superframe is composed of frames, themselves composed of timeslots. In a superframe, frames are numbered from 0 (lowest frequency, first in time) to N (highest frequency, last in time), ordered in time then in frequency, (F_nb represents the frame number) and can take the values $0 \leq N \leq 31$. A frame is composed of timeslots that may span over several carrier frequencies. In a frame, timeslots are numbered from 0 (lowest frequency, first in time) to M (highest frequency, last in time), ordered in time then in frequency. The number of slots in a frame can be in the range $0 \leq M \leq 2047$, [*ETSI, 2002*], [*Noussi et al., 2004*].

In our scenario, the bandwidth and duration of superframes, frames and timeslots are fixed providing burst data rate of 2048 kbps and a typical MF-TDMA frame lasts for 24 ms. The frame includes 4 carriers of 128 traffic slots each (i.e. 512 slots per frame) with rate granularity of 16 kbps (i.e. the minimum rate that can be achieved over the period of a frame by the allocation of just one timeslot). Due to the system's BoD capability a user station can vary the average bit rate over each frame according to its traffic needs by being allocated 1, 2, 3, ... up to 128 slots/frame leading to average bit rates of 16, 32, 48, ... up to 2048 kbps. Each terminal may only transmit on any single frequency (or channel) at a given time; it is not allowed to transmit data on more than one carrier at a time in order to minimise the power output requirement and reduce the hardware complexity of terminals. The RCST processes the TBTP message received from the NCC, to extract the assignment count and timeslot allocations for its next uplink transmissions.

The synchronisation burst and the optional prefix attached to S-ATM traffic bursts contain the Satellite Access Control (SAC) field composed of signalling information added by the RCSTs for the purpose of requesting capacity for the session. The Request sub-field within the SAC field accommodates the capacity requests from the terminals.

There are two main mechanisms available to the RCST for issuing data traffic requests to the NCC (see Figure 2.3-2). The mini-slot *Out-of-Band Requests* (OBR) are small bursts that can be periodically assigned to logged-on RCSTs. It carries control and management information from the RCSTs to the NCC and it is also used for maintaining RCST synchronisation. As an alternative to the round-robin approach, OBR may also be used in contention-based mode.

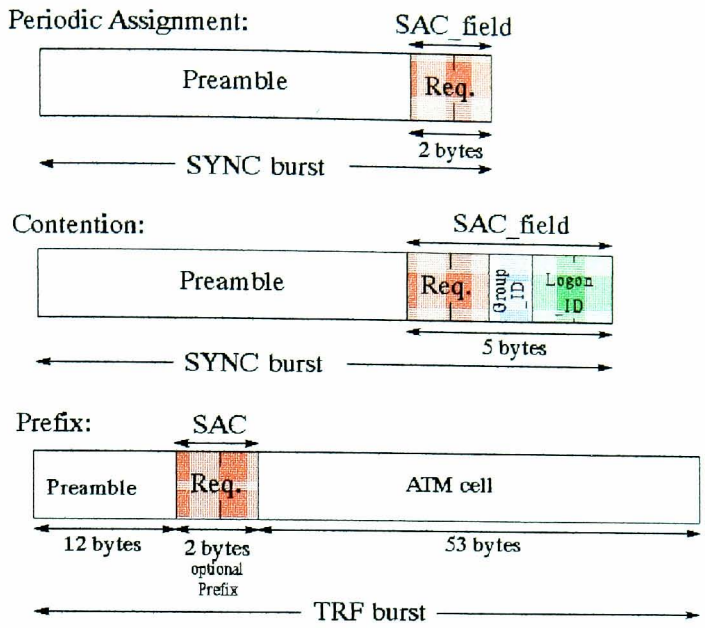

Figure 2.3-2 Traffic request SAC Fields for OBR and IBR

The other method called the *Prefix* or *In-Band Request* (IBR) is based on an optional prefix attached to ATM traffic bursts. The prefix carries control and management sub-field (see Figure 2.3-2). Obviously, the use of IBR signalling allows for the reduction in the traffic load over the OBR reservation channels as IBR is readily available. IBR has in fact the great advantage of being collision-free. Hence a terminal that has been assigned traffic slot(s) should preferably use IBR. In this way the OBR slots can be shared by terminals that do not yet have any assigned traffic slot. The waiting time to send a reservation will also be reduced due to the availability of both IBR and OBR slots, [*Le-Ngoc and Krishnamurthy, 1996*].

2.4 Integration within DVB-RCS

Here, the integration of the proposed FMT within the existing DVB-RCS standard will be described and details of the model used to simulate it will be discussed.

2.4.1 The BLC Concept

The overall proposed architecture for DVB-RCS with Burst-Length Control as a rain fade mitigation technique is depicted in Figure 2.4-1.

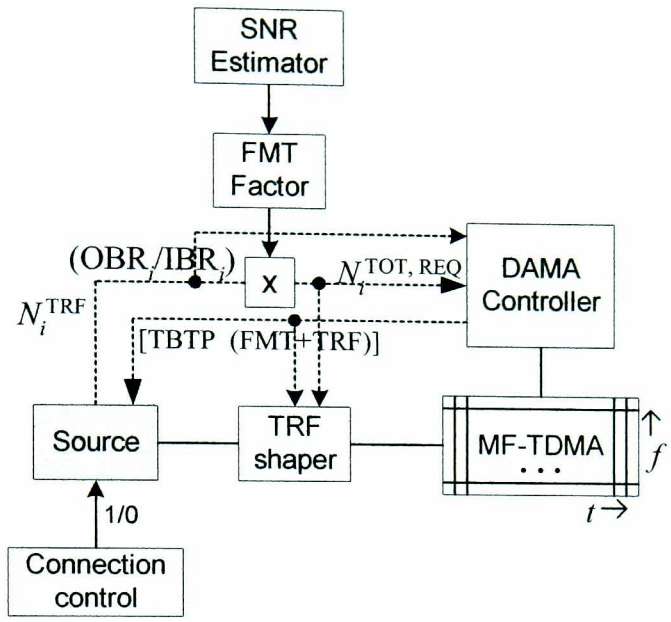

Figure 2.4-1 Architecture of BLC DVB-RCS

The traffic bursts from the RCSTs are independently monitored by the NCC so that it can determine H_i (see Equation 2.4-1) and the required BLC multiplication factor H_i. For this, the NCC measures the received SNR from all the bursts from all active RCSTs .

2.4.2 SNR Estimator

The operation can be achieved using a non-data aided SNR estimation technique at the NCC. To improve further the estimation, estimates from multiple bursts for a same connection can be averaged together to reduce the estimation error. One main concern is that the amount of traffic (average number of symbols per unit time) from a RSCT can be very sporadic and small which would have an impact on the accuracy of the burst SNR estimator. We have therefore simulated the ML-RxDA estimator applied to QPSK described in [*Pauluzzi and Beaulieu, 2000*], (Maximum-Likelihood Data-Aided estimator using an estimate of the transmitted data from receiver decisions) with the addition of a correction for the bias of the estimator at low SNRs. As a worst case we have assumed that only one traffic slot is processed every second. Figure 2.4-2 shows the simulation results.

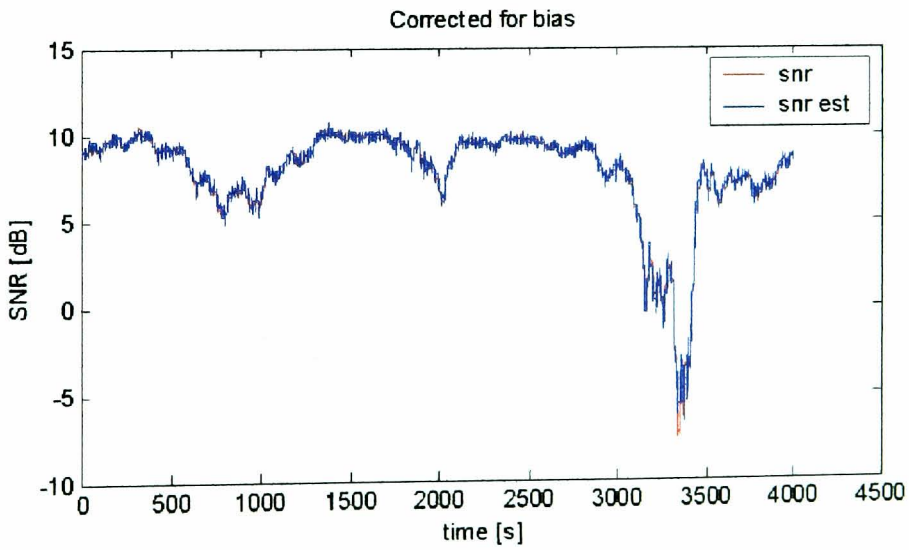

Figure 2.4-2 Estimated and true SNR

For a typical Ka band 15 dB event, the estimated SNR remains within 1 dB of the true SNR. This shows the appropriateness of the technique even for very low traffic.

2.4.3 Simulation Model

Depending on the current need of the source, the RCST issues normal traffic requests to the NCC via either the IBR or OBR signalling channels. Upon receiving the capacity requests from each active connection, the DAMA then evaluates the total number of required slots by multiplying each traffic request S_i by the BLC multiplication factor H_i that has been determined from the SNR estimator subsystem. The DAMA then performs its resource allocation algorithm to generate the new TBTP table. This is then broadcasted on the forward channel so that each RCST can switch to its new frequency/time positions within the next MF-TDMA space including the fade mitigation technique.

Note that BLC does not require any additional specific signalling. The technique is therefore efficient in terms of spectrum utilisation.

Another important point is that, provided that the request can be serviced, the RCST can work out what BLC spreading factor without requiring extra signalling. The RCST should apply using the following procedures: (i) the RCST issues a request to the NCC for S_i traffic slots. This request is processed by the NCC that applies the BLC multiplication factor from the measured SNR. If the DAMA algorithm can service the request, it allocates $S_{tot} = S_i \times H_i$ traffic slots to the RCST. By comparing S_i and S_{tot}, the RCST can calculate the required BLC expansion factor it has to use over the next allocation period. However, the RCST will not be able to calculate the BLC spreading factor itself in all cases. If the request cannot be immediately serviced and some of it needs to be queued, the RCST will not be able to work out the BLC factor. In such cases, the timeslot type (i.e. payload content) explicitly defined for each timeslot in the TCT sent to the terminals will help the station know exactly how many normal traffic and FMT slots have been assigned to it.

We assume that the update rate of the FMT is one second. This update rate is very important when integrating an FMT within DVB-RCS, as it must be able to track the variations of the rain attenuation process. Therefore the source traffic will have to be queued for one second at the source. The source will emit a traffic request and the new allocation will be implemented in the next FMT interval (1 second later).

An important issue is that the MF-TDMA should be able to support the active connections including their FMT needs. If the MF-TDMA capacity allocated to flows of the same class is limited and fixed the DAMA algorithm may not be able to grant all the requests. If the agreed QoS or service level agreement allows it, some connections may be blocked until resources become available. More likely the requests may be queued, in which case, the limited capacity in the presence of rain will result in possible delays. To control this delay, it is important to make sure the sources do not generate too much traffic (including FMT).

We consider as a baseline case that N connections with peak traffic rate of 128 kbps share a subspace of the entire MF-TDMA space. In order to show how the system can be dimensioned, we assume that the DAMA controller will group N traffic requests so that only one of those requires full FMT support while all other connections operate at maximum bit rate. We consider that each connection transmits at a peak rate much lower that the burst rate of the MF-TDMA system. In our system, if they operated at burst data rate of 2 Mbps, they

would require 5333 traffic slots per second. If the peak rate of each terminal is reduced to 128 kbps, they only need 333 slots per second. Furthermore if one of these terminals is attenuated and requires maximum FMT protection it will need 16 times as many slots (i.e. traffic and FMT slots) therefore a fully attenuated return link would require 5328 slots per second. We note that this single attenuated link would occupy a very large portion of one MF-TDMA channel (5333 slots/sec). This simplifies greatly the DAMA algorithm and means that our FMT is introduced with no extra queuing since the traffic plus FMT can be supported within one TBTP allocation period.

Assuming that we also multiplex 16 return links in clear-sky conditions with one link experiencing maximum rain attenuation, the total traffic of this network would be 10656 slots/second. Bearing in mind that any MF-TDMA channel can only have 5333 slots per second, this means that we could fit our 17 links within two MF-TDMA frequency channels (half of a frame width which has four channels). Obviously, when the faded link returns to clear-sky conditions, much capacity is freed since FMT slots are required and, assuming all connections are rain free, we can support at least 32 individual 128 kbps connections in our two MF-TDMA channels.

In this simplified scenario the DAMA algorithm should (i) partition the MF-TDMA in areas of width of two MF-TDMA channels. Multiplex different traffic sources by (ii) choosing one request requiring FMT support and (iii) Multiplexing it with a variable number of unaffected return links so as to occupy as best as possible the two MF-TDMA channels of the subspace.

The described FMT offers a *guaranteed* quality of service for all served stations. The parameters chosen to be monitored in this work were the BER (as an indirect way of measuring quality of service), the delay of communication, and the link availability. As it will be seen, outage will only occur when the dynamic range of the FMT is exceeded. Additional connections may be brought in whenever rain conditions over the footprint are good enough or are improving. By partitioning the entire MF-TDMA space accordingly and applying appropriate multiplexing (see (i)-(iii) above), the proposed FMT can be applied to a large number of connections. However, as this assignment strategy is clearly at the price of a variable number of supportable connections and perfect statistical multiplexing may not always be possible for the entire network, ultimately, some connections may need to be queued or dropped, which will be acceptable as long as the QoS or service level agreement allows it. Figure 2.4-3 shows an example of rain cells over areas with active and non-active users inside the coverage area of a satellite.

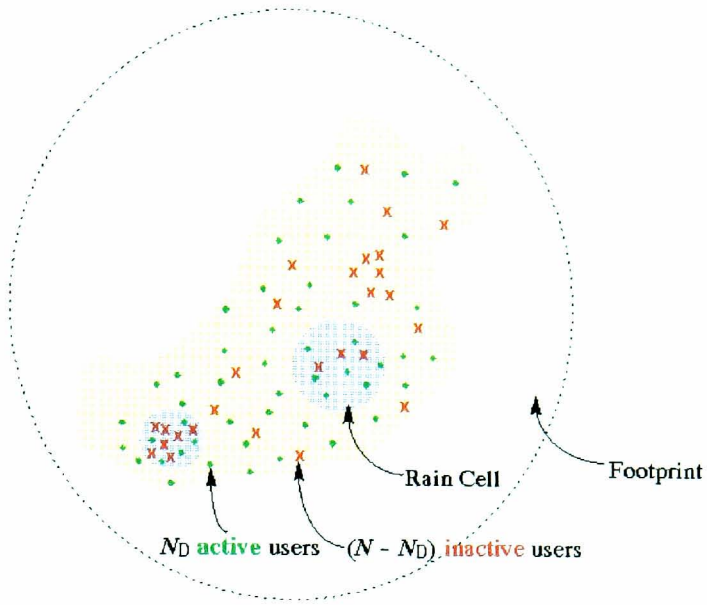

Figure 2.4-3 Active and non-active users in the footprint in the presence of rain

It becomes apparent that the total number of required FMT slots depends on: (i) users' density and location (the greater the concentration of users the greater the number of required FMT slots when it rains); (ii) space and time characteristics of rain (for rain over large areas, more FMT slots are required); (iii) magnitude of the rain attenuation; (iv) actual traffic characteristics of the user stations; (v) agreed QoS parameters.

Furthermore, depending on the hour of the day or the month, the rain conditions may be quite severe resulting in a much more extensive need of FMT slots. This would be detrimental if severe fades occurred at times when user traffic is high. In order to study the impact of correlated rain attenuation on the satellite footprint, we have developed a rainfield stochastic simulator described in the Appendix. A typical snapshot of the synthesised rainfield is shown in Figure 2.4-4.

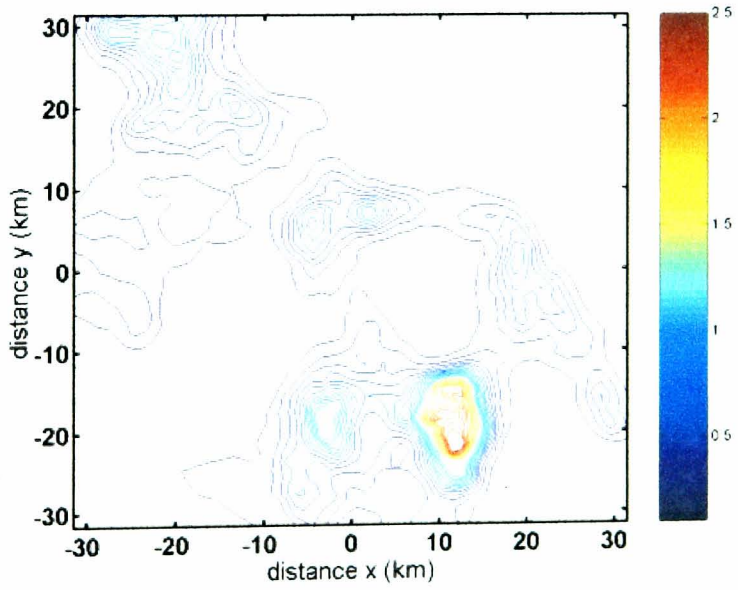

Figure 2.4-4 Example of synthesised rainfield

In this particular case, there is a raincell in the lower right quadrant with a small peak attenuation of about 2.5 dB. Obviously the DAMA algorithm should avoid multiplexing

together requests emanating from rainy regions because this would generate a large amount of total traffic (TRF and FMT slots). A uniform density of users has been assumed, so that suitable rain-decorrelated traffic streams can be (geographically) multiplexed.

The following Section will present the performance results of the algorithm.

2.5 FMT Resource Management – Performance Results

We focus on the transport of aggregate internet traffic that is known to exhibit self-similarity with long-range dependence and high levels of burstiness, [*Cardellini and Colajanni, 2000*], [*Crovella and Bestavros, 1997*], [*Jiang and Leung, 2003*], [*Kramer, 2001*], [*Leland et al., 1994*], [*Sahinoglu and Tekinay, 1999*], [*Willinger et al., 1997*]. In our simulations we assumed one connection per terminal, each generating a stream of traffic ATM cells with a Pareto distribution with Peak Cell Rate equal to 128 kbps. The shape parameter of the distribution, α , was set to 1.2.

For the resource allocation phase, a bin-packing algorithm (first fit heaviest to lightest) has been implemented. This has been applied to all the traffic requests which are cumulated over periods on 1 second. As mentioned above, only one out of N stations experiences rain. Figure 2.5-1 shows the variations of the carrier-to-noise ratio for the rain-affected 30/20 GHz return link.

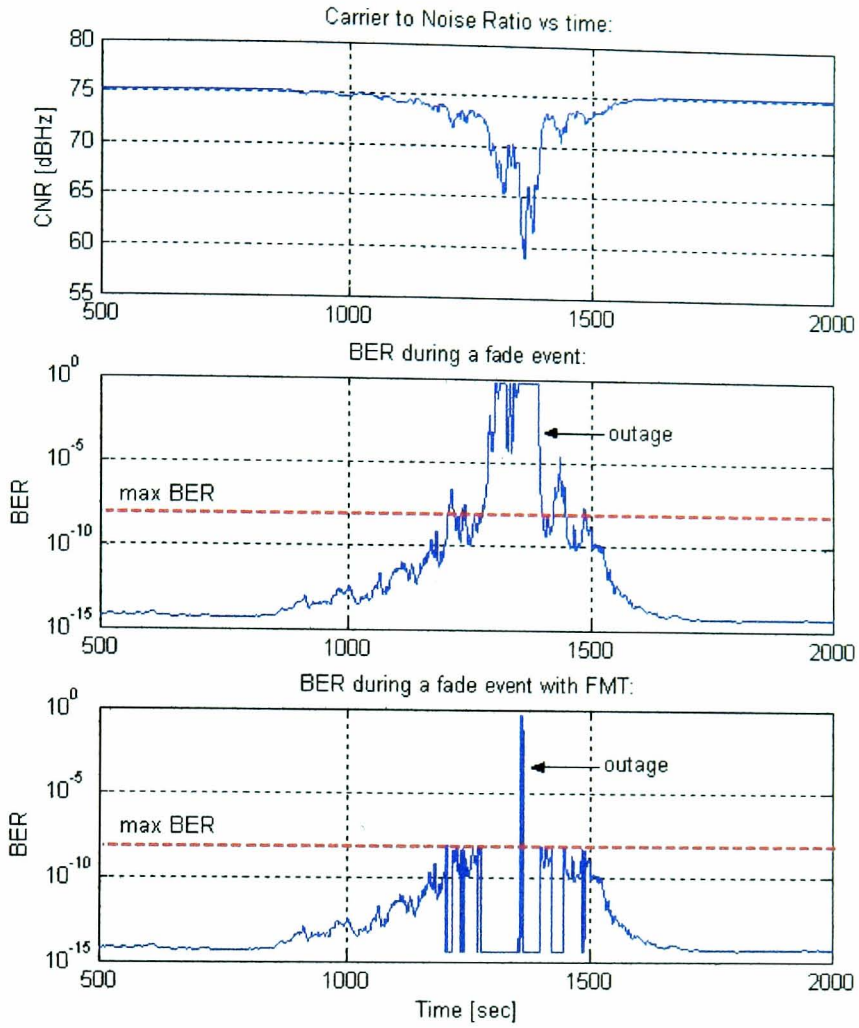

Figure 2.5-1 Example of synthesised rainfield

The link is attenuated by rain for about 10 minutes and the CNR drop slightly exceeds 16 dB.

Figure 2.5-1 also compares the variable BER of the link with and without FMT. Only by employing the FMT, the link can maintain the BER below the maximum BER threshold of 10^{-8} for most of the time. However when the total drop in CNR exceeds the 15 dB dynamic range of the FMT (see Figure 2.2-2), the BER grows to a large value. This corresponds to an outage that will ultimately contribute towards the long-term unavailability of the return link.

Figure 2.5-2 shows the corresponding number of FMT slots per normal traffic slot for the link undergoing rain attenuation.

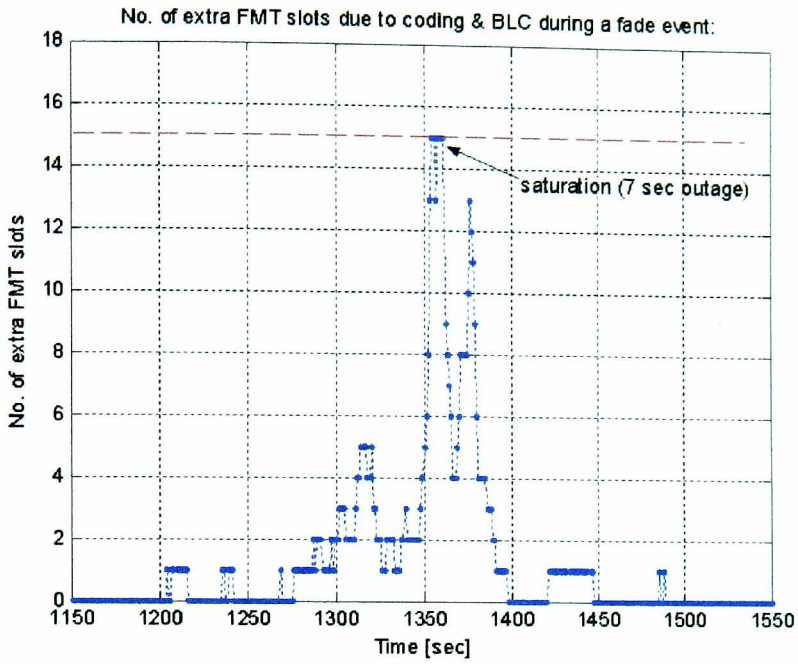

Figure 2.5-2 Variations of the number of FMT slots per traffic slot during rain event for one return link

This shows results including the DAMA allocation process. We see that at time 1300 seconds, the FMT saturates to its maximum value. The FMT is not able to offer enough protection and hence the link enters an outage state.

We see that for most of the time, the link does not need any fade mitigation. This implies that channel capacity should be used by other links as long as they can fit within the available total bandwidth.

As it has been discussed earlier, during our simulations, the DAMA controller grouped traffic requests so that only one required FMT support. Figure 2.5-3 illustrates the MF-TDMA subspace occupancy during this multiplexing.

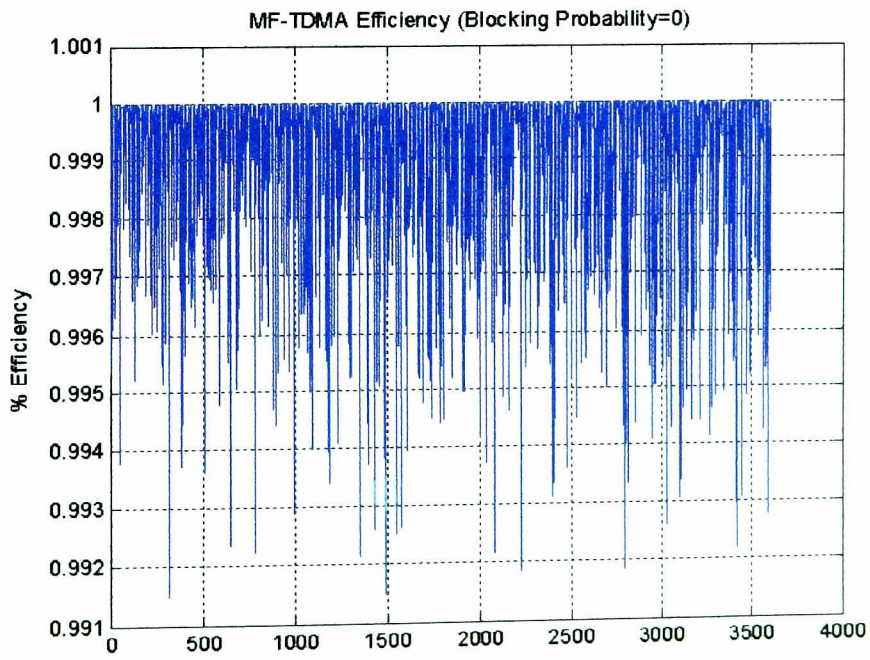

Figure 2.5-3 MF-TDMA subspace utilisation during multiplexing of one affected link with a variable number of unaffected links

As it can be realised, even though one of the links suffered from rain during some period of time (around t = 1300 sec) the throughput utilisation remains pretty much unaffected and was generally kept at an average of 99.9%.

The number of multiplexed connections within our subspace of two channels is illustrated in Figure 2.5-4.

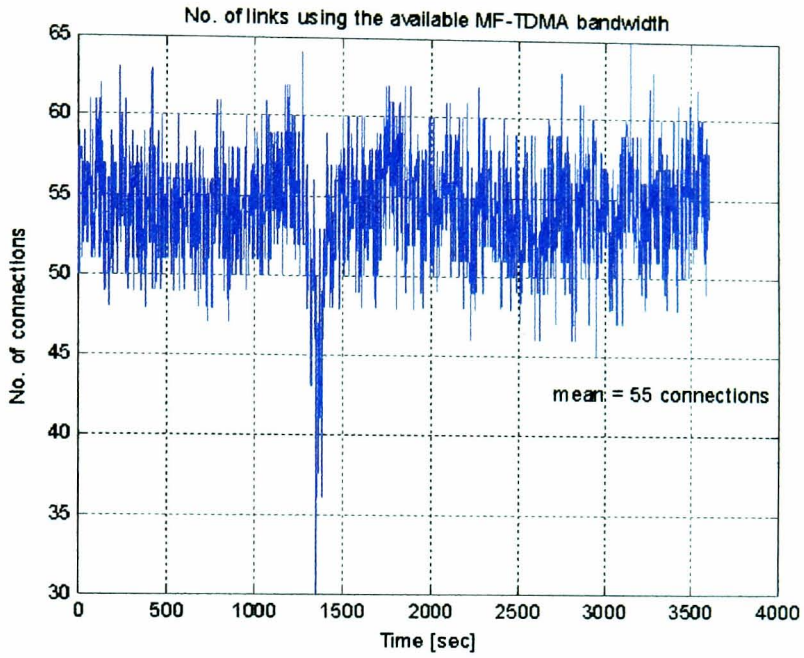

Figure 2.5-4 Connections multiplexed in time to occupy the available MF-TDMA bandwidth

This number varies significantly in time in order to achieve the best possible utilisation. In fact, this number was impressively high since not all sources happened to transmit at their peak rates simultaneously as it had been assumed in the previous "worst case" calculations that considered maximum transmission rates for all sources as well as a perfect allocation process. This is of great significance and it clearly demonstrates the advantages of statistical multiplexing even in the case of a "rainy" link. It should be repeated that this mechanism ensures that all connections are served every TBTP allocation period without the introduction of any additional delay.

2.6 Conclusions

This paper has discussed the integration of a Fade Mitigation Technique within a centrally managed MF-TDMA satellite network in the context of guaranteed QoS delivery. The objective is to determine a way of achieving the integration without requiring any modification of the existing DVB-RCS standard.

Burst Length Control is proposed as a suitable FMT. This technique is relatively simple to implement and it provides a large dynamic range that can be arbitrarily chosen depending on requirements. This is not the case of other techniques like adaptive coding/modulation where the dynamic range is limited to a maximum value. For BLC, outage will only occur when the dynamic range of the FMT is exceeded and by limiting the capacity of individual connections, BLC can be introduced without inducing any additional delay.

Burst length control provides compensation for rain attenuation at the expense of normal traffic capacity. This is encapsulated by the derivation of the required number of FMT time slots as a function of the total attenuation on the return link. The appropriate existing mechanisms defined in the ETSI standard were extracted and examined in order to achieve the sought integration of FMTs within DVB-RCS. We indicate that in-band requests (IBR) and possibly out-of-band requests (OBR) can be used for issuing normal traffic requests. In this paper, we have considered that the burst time plan has an update rate of 1 second as this is sufficient to track the variations of rain attenuation.

The Network Control Center then centrally detects the fades by applying the ML-RxDA SNR estimation algorithm with a bias correction to all incoming bursts. By simulation, this detector was shown to achieve sufficient accuracy despite the possibly sporadic and scarce traffic from the remote terminals. The measured SNRs are then used by the Network Control Centre to calculate the BLC multiplication factor that is applied to the IBR/OBR traffic requests by the NCC prior to running the resource allocation algorithm.

The DAMA resource allocation algorithm was applied to a simple MF-TDMA scenario for which geographical multiplexing has been applied. In particular, the DAMA algorithm groups one rain-attenuated link with a variable number of un-attenuated links so as to maximise the channel capacity within a fixed subspace/partition of the MF-TDMA channel. This requires the dynamic selection of appropriate links based on the outputs of a space-time rain attenuation field simulator. This selection can be performed without knowing the actual locations of the RCSTs simply by sorting the FMT multiplied traffic order from largest to smallest.

We have finally quantified the achieved channel capacity utilisation and the variable number of 128 kbps connections that can be serviced within the MF-TDMA subspace. Our results indicate that an average utilisation of 99.9% can be achieved while the average number of connections is around 55. The proposed FMT offers a guaranteed quality of service for all served stations. The BER, the delay of communication and the link availability have been monitored; as it was seen, by limiting the capacity of individual connections, BLC was introduced without inducing any additional queuing delay and both traffic and FMT were supported within one TBTP allocation period. As long as the dynamic range of the FMT is not exceeded, the BER will be kept below the maximum threshold and no outage will occur, guaranteeing the long-term availability of the link.

Current work includes extension of the algorithm into a multi-class scenario with differentiated services involving traffic streams with different QoS levels (for example different delay tolerance). The basis is the same but further investigation is required to control the increased queuing delays induced due to differing priorities and limited capacity allocated to flows of different classes, especially in the presence of rain.

More detailed simulations and analysis will be required to investigate/solve issues regarding the support of multi-class services, the impact of BLC on Quality of Service, Connection Admission Control and Service Level Agreements. The full details and implications on QoS, CAC and SLA will clearly require further investigations into alternative assignment strategies. This will require a detailed analysis of the whole MF-TDMA system in the presence of rainfield attenuation. Future work will involve a detailed study of the impact of correlated rain attenuation on the satellite footprint.

2.7 References

[*Carassa, 1984*]
F. Carassa, "Adaptive Methods to Counteract Rain Attenuation Effects in the 20/30 GHz Band", Space Communication and Broadcasting 2, North Holland, 1984, pp. 253-269.

[*Cardellini and Colajanni, 2000*]
V. Cardellini, M. Colajanni, P. S. Yu, "Geographic Load Balancing for Scalable Distributed Web Systems, IEEE. Proceedings of Mascots 2000, San Francisco, Aug./Sep. 2000.

[*Celandroni et al., 1996a*]
N. Celandroni, E. Ferro, F. Potorti, "Comparison between Distributed and Centralised Demand Assignment TDMA Satellite Access Schemes", International Journal of Satellite Communications, vol. 14, no. 2 , pp. 95-112, 1996.

[*Celandroni et al., 1996b*]
N. Celandroni, E. Ferro, F. Potorti, "Experimental Results of a Demand-Assignment Thin Route TDMA System", International Journal of Satellite Communications, vol. 14, no. 2, pp.113-126, 1996.

[*Celandroni et al., 1997*]
N. Celandroni, E. Ferro, F. Potorti, G. Maral, "Delay Analysis for InterLAN Traffic using two suitable TDMA Satellite Access Schemes", International Journal of Satellite Communications, vol. 15, no. 4, pp. 141-153, 1997.

[*Celandroni et al., 1992*]
N. Celandroni, E. Ferro, N. James, F. Potorti, "FODA/IBEA-TDMA: A Flexible Fade Countermeasure System for Integrated Services in User Oriented Networks", International Journal of Satellite Communications, vol. 10, pp. 309-323, 1992.

[*Celandroni and Potorti, 2000*]
N. Celandroni, F. Potorti, Fade Countermeasure using Signal Degradation Estimation for Demand-Assignment Satellite Systems, Journal of Communications and Networks, Korean Institute of Comm. Sciences, vol. 2, no. 3, pp. 230-238, September 2000.

[*Celandroni et al., 1996c*]
N. Celandroni, F. Potorti, S. T. Rizzo, "An inexpensive Fade Countermeasure Technique for DA-TDMA Satellites Systems", Proceedings of the IEEE Global Telecommunications Conference GLOBECOM'96, vol. 2, pp. 1001-1005, London, U.K., November 18-22, 1996.

[*Crovella and Bestavros, 1997*]
M. E. Crovella, A. Bestavros, "Self-Similarity in WorldWide Web Traffic: Evidence, and Possible Causes", IEEE/ACM Transactions on Networking, vol. 5, no. 6, pp. 835-846, 1997.

[*Emerson et al., 1989*]
D. J. Emerson, R. M. Nelhams, B. L. Clark, "Adaptive TDMA for Fade Countermeasures", Olympus Utilisation Conference, ESA SP-292, Vienna, 12-14 April 1989.

[*ETSI, 2002*]
ETSI EN 301 790 (V1.3.1): "Digital Video Broadcasting (DVB); Interaction Channel for Satellite Distribution Systems" (also known as the DVB-RCS specification), Final Draft, 2002-11, available at http://www.etsi.org/getastandard/home.htm

[*Grémont, 2002a*]
B. C. Grémont, "Generalised Model of the SatComm Channel for Applications to Fade Countermeasures", XXVIIth General Assembly of the International Union of Radio Science, Maastricht, The Netherlands, August 17-24, 2002.

[*Grémont, 2002b*]
B. C. Grémont, "Simulation of Rainfield Attenuation for Satellite Communication Networks", 1st Workshop of the COST Action 280 Propagation Impairment Mitigation for Millimetre Wave Radio Systems, Malvern, UK, 1-3 July 2002.

[*Grémont and Filip, 2004*]
B. C. Grémont, M. Filip, "Spatio-Temporal Rain Attenuation Model for Application To Fade Mitigation Techniques", IEEE Transactions on Antennas and Propagation, vol. 52, no 5, pp 1245-1256, May 2004.

[*Grémont et al., 2003*]
B. C. Grémont, R. J. Watson, P. A. Watson, D. D. Hodges, "Modelling and Detection of Rain Attenuation for MF-TDMA Satellite Networks Utilising Fade Mitigation Techniques", Int. Workshop of COST Actions 272 and 280 Satellite Communications - From Fade Mitigation to Satellite Provision, ESTEC, Noordwijk, The Netherlands, 26-28 May 2003, p. 277-284.

[*Hadjitheodosiou et al., 1999*]
M. H. Hadjitheodosiou, A. Ephremides, D. Friedman, "Broadband Access via Satellite", Technical Research Report, CSHCN T.R. 99-2, Centre for Satellite and Hybrid Communication Networks, University of Maryland, 1999, available at http://techreports.isr.umd.edu/TechReports/CSHCN/1999/CSHCN_TR_99-2/CSHCN_TR_99-2.pdf.

[*Ippolito, 1981*]
L. J. Ippolito, "Radio propagation for space communications systems", IEEE Proceedings, vol. 69, no. 6, pp. 697-727, U.S.A., June 1981.

[*Iuoras et al., 1999*]
A. Iuoras, P. Takats, C. Black, R. DiGirolamo, E. Wobowo, J. Lambadaris, M. Devetsikiotis, "Quality of Service-Oriented Protocols for Resource Management in Packet-Switched Satellites", vol. 17, no. 3, pp. 129-141, May-June 1999, available at http://www.emssatnet.com/pub/whitepapers.asp

[*Jiang and Leung, 2003*]
Z. Jiang, V. CM Leung, "A Predictive Demand Assignment Multiple Access Protocol for Internet Access over Broadband Satellite Networks", International Journal of Satellite Communications and Networking, vol. 21, p. 451-467, 2003.

[*Kramer, 2001*]
G. Kramer, "Self-Similar Network Traffic - The Notions and Effects of Self-Similarity and Long-Range Dependence", 2001, available at http://wwwcsif.cs.ucdavis.edu/~kramer/papers/ss_trf_present2.pdf

[*Lee et al., 2002*]
K. D. Lee, Y. H. Cho, H. J. Lee, H. Jeong, "Optimal Scheduling for Timeslot Assignment in MF-TDMA Broadband Satellite Communications", IEEE-56th Vehicular Technology Conference Proceedings, vol. 3, p. 1560-1564, Piscataway, NJ, USA, 2002.

[*Leland et al., 1994*]
W. E. Leland, M. S. Taqqu, W. Willinger, D. V. Wilson, "On the Self-Similar Nature of Ethernet Traffic", IEEE/ACM Transactions on Networking, vol. 2, no. 1, pp. 1-15, 1994.

[*Le-Ngoc and Krishnamurthy, 1996*]
T. Le-Ngoc, S. V. Krishnamurthy, "Performance of Combined Free/Demand Assignment Multiple Access Schemes in Satellite Communications", International Journal of Satellite Communications, vol. 14, no. 1, pp. 11-21, January-February 1996.

[*Li and Chen, 2001*]
K. H. Li, C. Chen, "An adaptive MAC protocol for satellite ATM", IEEE Proceedings, 15th International Conference on Information Networking, 2001, p. 119-126.

[*Li et al., 2002*]
Y. Li, Z. Jiang, V. C. M. Leung, "Performance Evaluations of PRR-CFDAMA for TCP Traffic over Geosynchronous Satellite Links", IEEE Wireless Communications and Networking Conference Record, vol. 2, p. 844-8, U.S.A., 2002.

[*Nelson, 1998*]
R. A. Nelson, V-band: "Expansion of the Spectrum Frontier", Via Satellite, February 1998, pp. 66+.

[*Noussi et al., 2003*]
E. Noussi, B. Grémont, M. Filip, "Centrally Managed FMT Built Upon DVB-RCS", Cost Action 280, Propagation Impairment Mitigation for Millimetre Wave Radio Systems, MC#6 Meeting, PM6-006, October 2003, Abington, UK.

[*Noussi et al., 2004*]
E. Noussi, B. Grémont, M. Filip, "Adaptive MF-TDMA: Burst Length Control as a Rain Fade Countermeasure", Communication Systems, Networks and Digital Signal Processing (CSNDSP), 4th Int. Symposium Proceedings, University of Newcastle upon Tyne, 20-22 July 2004, p. 43-46.

[*Pauluzzi and Beaulieu, 2000*]
D. R. Pauluzzi, N.C. Beaulieu, "A comparison of SNR Estimation Techniques for the AWGN Channel", IEEE Trans. on Communications, vol. 48, no. 10, pp. 1681-1691, Oct. 2000.

[*Pech et al., 2001*]
P. Pech, M. Bousquet, L. Castanet, J. Radzik, B. Fabre, "Methodology to Optimise Techniques of Resource Management for Ka-band GEO Satellite Networks from the Introduction of Propagation Information", COST 280, doc. PM2015[R1], October 2001.

[*Psomas and Rees, 1998*]
G. Psomas, H. Rees, "Satellite Communications: An overview, SURPRISE'98", Imperial College, May-June 1998, available at http://www.iis.ee.ic.ac.uk/~frank/surp98/report/hdr1/, last accessed on 23/02/03.

[*Sahinoglu and Tekinay, 1999*]
Z. Sahinoglu, S. Tekinay, "On Multimedia Network: Self-Similar Traffic and Network Performance", IEEE Communications Magazine, vol. 37, no. 1, pp. 48-52, 1999.

[*Spillard et al., 2004a*]
C. Spillard, D. Grace, G. P. White, B. Grémont, T. C. Tozer, "High Altitude Platforms at York", International Conference on Next Generation Teletraffic and Wired/Wireless Advance Networking (NEW2AN'04), February 02-06, 2004, St. Petersburg, Russia.

[*Spillard et al., 2004b*]
C. L. Spillard, B. C. Grémont, D. Grace, T. C. Tozer, "High Altitude Platforms in Rainy Conditions", submitted to IEEE Transactions on Antennas and Propagation, under review, July 2004.

[*Spillard et al., 2004c*]
C. Spillard, T. Tozer, B. Grémont, D. Grace, "The Performance of High-Altitude Platform Networks in Rainy Conditions", 22nd AIAA International Communications Satellite Systems Conference, Monterey, USA, 9-12 May 2004, AIAA-2004-3220.

[*Touw, 1994*]
S. I. E. Touw, "Analyses of Amplitude Scintillations for the Evaluation of the Performance of Open-Loop ULPC Systems", MSc Thesis, Eindhoven University of Technology, Eindhoven, The Netherlands, 1994.

[*Wibowo et al., 1998*]
E. A. Wibowo, A. Iuoras, P. Takats, J. Lambadaris, M. Devetsikiotis, "Guaranteeing QoS in Packet-Switched Satellites by Medium Access Control", CCBR'98, p. 31-43, available at http://www.emssatnet.com/pub/whitepapers.asp

[*Willinger et al., 1997*]
W. Willinger, M. S. Taqqu, R. Sherman, D. V. Wilson, "Self-Similarity Through High-Variability: Statistical Analysis of Ethernet LAN Traffic, at the Source Level", IEEE/ACM Transactions on Networking, vol. 5, no. 1, pp. 71-86, 1997.

2.7.1 Annex 1: Space-Time Model of Rain Attenuation

The performance of FMT resource allocation algorithms described in the previous section needs to be evaluated in a network simulator (for additional information see [*Grémont and Filip, 2004*]). Such a simulator would need a fine scale simulation of the rain attenuation conditions encountered on a satellite footprint. A rain attenuation field can be simulated in

space and time using a mixture of time and frequency domain signal processing. Such rainfield model can be used to simulate the variations of CNR over the whole footprint. It can consider seasonal/diurnal variations of rain for realistic worst-month and time-of-the-day dependent rain conditions. The proposed model simulates rain attenuation on a (x_1, x_2) grid representing the N^2 locations of interest for the network simulation. It is assumed that it rains on average only a fraction $f(x_1, x_2)$ of the time at any location. When it rains, the attenuation is log-normally distributed with two location dependent parameters $m(x_1, x_2)$ and $\sigma(x_1, x_2)$, which can be easily determined from the ITU-R rain model. These parameters can also encompass diurnal, monthly or seasonal variations, if they are fitted to CCDFs of diurnal, monthly or seasonal rain attenuation. The attenuation field can be synthesised using the non-linear transformation:

$$A(x_1, x_2) = \begin{cases} 0, & \text{if } g(x_1, x_2) < g_0 \\ \exp\left(m(x_1, x_2) + \sigma(x_1, x_2) \otimes g(x_1, x_2)\right), & \text{otherwise} \end{cases} \qquad 2.7\text{-}1$$

Here $g(x_1, x_2)$ is a 2D Gaussian field with unit variance and zero mean. Whenever $g(x_1, x_2) \geq g_0 = Q^{-1}(f)$, it is raining. Thus $g(x_1, x_2)$ can be transformed to a lognormal variable using an exponential (array) transformation. This can be achieved by generating a complex field, $a(k_1, k_2)$, and then taking the inverse Fourier transform:

$$g(x, y) = \sum_{k_1=0}^{N} \sum_{k_2 0}^{N} a(k_1, k_2) \exp\left(\frac{i2\pi}{N}(k_1 x + k_2 y)\right) = IFT2\{a(k_1, k_2)\} \qquad 2.7\text{-}2$$

To get a good field $g(x_1, x_2)$, we need to consider the spatial cross-correlation function $c_g(d)$ of rain where $d \equiv \left|\vec{x} - \vec{y}\right|$ is the distance between two geographical points $\vec{x} = (x_1, x_2)$ and $\vec{y} = (y_1, y_2)$ of interest. Whilst for short distances the form $c_g(d) = \exp(-d/5 \text{ km})$ is a reasonable model for modelling site diversity in UK, [*Grémont, 2002a, 2002b*], a correlation function considering meso- or synoptic ranges for Italy takes the double exponential form: $c_g(d) = 0.94 \exp(-d/30 \text{ km}) + 0.06 \exp^2(-d/100 \text{ km})$. An alternative approach is to analyse radar data and produce the spectrum of the log of rainfall rate, which is the Fourier transform of the cross-correlation function. Once a suitable correlation function has been chosen, we can calculate its Fourier transform:

$$C_g(k_1, k_2) = \sum_{x_1=0}^{N} \sum_{x_2 0}^{N} c_g(x_1, x_2) \exp\left(-\frac{i2\pi}{N}(k_1 x_1 + k_2 x_2)\right) = FT2\{c_g(x_1, x_2)\} \qquad 2.7\text{-}3$$

The complex random field can be obtained by filtering complex 2D noise (zero mean, unit variance) $n(k_1, k_2)$, which in the Fourier domain is a simple multiplication:

$$a(k_1, k_2) = C_g(k_1, k_2) \otimes n(k_1, k_2) \qquad 2.7\text{-}4$$

The model (2) to (5) only generates a single (original) map of the rainfield. It is also important to add two realistic features to simulate time-dependent effects. For this the original rainfield is modified within a "for loop" simulating the passage of time. The first modification is the advection of the rainfall attenuation field. Assuming a velocity $\vec{V} = [V_1 \;\; V_2]$ m/s in the (x_1, x_2) plane, the translated rainfield a short time t later is obtained using:

$$g(x_1 - V_1 t, x_2 - V_2 t) = IFT2\{a(k_1, k_2) \otimes \exp[-it(k_1 V_1 + k_2 V_2)]\} \qquad 2.7\text{-}5$$

The second modification takes into consideration the fact that rain effects have random temporal variations related to the natural birth and decay of rain cells over the field. It is well accepted that rain attenuation shows first order spectrum characteristics. One simple way of implementing this is to make $g(x_1, x_2)$ an auto-regressive temporal process that can be synthesised using the following difference equation:

$$a_{\text{new}}(k_1, k_2) = \exp(-\beta t) \otimes a_{\text{old}}(k_1, k_2) + \sqrt{1 - \exp(-\beta t)^2} \otimes n_2(k_1, k_2) \qquad 2.7\text{-}6$$

where $n_2(k_1, k_2)$ is complex noise with zero mean and unit variance (uncorrelated with the one in Equation 2.7-7). The constant $\beta\,[1/\text{s}]$ defines the temporal characteristics of rain attenuation and has been estimated from experimental data in [*Grémont, 2002a*], [*Grémont, 2002b*], [*Grémont et al., 2003*].

The space-time model has been also used in studies regarding the performance of High Altitude Platforms (HAPs) in rainy conditions, [*Spillard et al., 2004a*], [*Spillard et al., 2004b*], [*Spillard et al., 2004c*].

DVB-RCS2 Satellite Network with Dual Fade Mitigation Technique

E. Noussi*, B. Grémont† and A. Hewitt†
University of Portsmouth, Anglesea Building, Anglesea Road, Portsmouth, Hampshire, PO1 3DJ, U.K.

This paper addresses the simulation and performance of a Fade Mitigation Technique (FMT) within a centrally managed MF-TDMA/DVB-RCS satellite network. The core mitigation technique is Adaptive Coding and Modulation (ACM) as specified in the recently enhanced DVB-RCS standard (thereon referred to as DVB-RCS2). We also propose an extension of the DVB-RCS2 standard (called BLC-DVB-RCS2), where Burst Length Control (BLC) is also used to further extend the FMT dynamic range and improve overall link availability. This additional FMT is particularly suitable in the case of power-limited communication scenarios over return channels from very small Earth stations. A resource allocation (RA) algorithm based on MF-TDMA subspace utilization areas is described and simulated demonstrating the use of the DVB-RCS2's MAC layer in its full flexibility. In particular, simulation results of the dynamic management of a 5.5 MHz MF-TDMA subspace are presented. The intention is to demonstrate how QoS (delay), channel utilization and FMT can be managed in real time at network level by the MAC controller. The RA algorithm takes into account the Bandwidth on Demand (BoD) requests from user stations, the rain conditions affecting each connection, and also manages the queuing delay for each source via a simple traffic shaping mechanism. The study presented here therefore applies directly to UBR/ABR traffic flows.

Nomenclature

α	=	roll-off factor
a	=	Pareto distribution shape parameter
A	=	dimensionless "area" in the MF-TDMA space (time-bandwidth product)
ABR	=	Available Bit Rate
ACM	=	Adaptive Coding and Modulation
ATM	=	Asynchronous Transfer Mode
Att	=	Attenuation
B	=	Bandwidth
BER	=	Bit Error Rate
BLC	=	Burst Length Control
BoD	=	Bandwidth on Demand
BPSK	=	Binary Phase Shift Keying
CAC	=	Connection Admission Control
CBR	=	Constant Bit Rate
DR	=	Dynamic Range (of FMT)
DRA	=	Dynamic Rate Adaptation
DVB-RCS	=	Digital Video Broadcasting – Return Channel by Satellite
E_s/N_0	=	symbol energy to noise power density ratio
f	=	frequency
FDMA	=	Frequency Division Multiple Access
FMT	=	Fade Mitigation Technique

---

* Research Student, Department of Electronic and Computer Engineering, Microwave Telecommunication Systems (MTS) Research Group.
† Senior Lecturer, Department of Electronic and Computer Engineering, MTS Research Group.

GEO	=	Geostationary (orbit)
H_i	=	Burst Length Control factor
m	=	mode
M	=	M-arity (modulation order)
MAC	=	Medium Access Control
MF-TDMA	=	Multi-Frequency Time Division Multiple Access
MPEG	=	Moving Picture Experts Group
NCC	=	Network Control Centre
nrt-VBR	=	non-real time Variable Bit Rate
PCR	=	Peak Cell Rate
PER	=	Packet Error Rate
QoS	=	Quality of Service
QPSK	=	Quaternary Phase Shift Keying
RA	=	Resource Allocation
R_b	=	(source) information bit rate, BoD request from the source
$\hat{R}_b^i$	=	maximum bit rate, assuming transmission over the full frame duration T_F
RCST	=	Return Channel Satellite Terminal
ρ	=	coding rate
SNR	=	Signal-to-Noise Ratio
TBTP	=	Terminal Burst Time Plan
T_F	=	frame duration
T_i	=	transmission burst duration for connection i in the next frame
TRF	=	traffic
UBR	=	Unspecified Bit Rate

I. Introduction

A consequence of the need to accommodate higher network capacities is the migration to higher frequency bands such as Ka band (27-40 GHz) and V band (40-75 GHz)[1]. A major drawback is that rain attenuation increases rapidly with carrier frequency[2-4] and can cause significant signal quality degradation on individual earth-space links. This will have a major impact on the achievable throughput of a network. Hence Fade Mitigation Techniques (FMTs) are necessary to maintain the reliability of the communications during deep fading.

FMTs are required to improve the long-term availability of a connection. The larger the dynamic range of the FMT the better the availability will be. However, the FMT protection against rain/interference is introduced at the cost of a greater usage of the MF-TDMA communication resources (transmission duration or bandwidth). So, all active connections have to share or compete for use of the MF-TDMA space. Thus the FMTs may force a reduction in the number of active connections that can be supported by the network. If FMT and traffic requirements are too high, the Connection Admission Controller (CAC) may have to shut down some of the connections, so that reasonable QoS can be achieved for the remaining live connections.

Depending on the depth and correlation of the rain attenuation among the active links, it is desirable to queue the traffic sources that would require large FMT resources or that are too traffic intensive at a particular moment in time. This can be done by the BoD controller by avoiding allocating MF-TDMA resources to these hungry connections for periods of time. Thus FMT protection can be postponed at the cost of delay (i.e. reduced QoS).

This management of FMTs must be achieved in parallel with a Bandwidth-on-Demand (BoD) philosophy, i.e. the BoD controller must be able to grant the instantaneous bit rate requested by an active traffic source. Adaptive resource[5] control can allow exploitation of statistical multiplexing to maximize achievable network throughputs. However, in cases where delay becomes unacceptable, it may, as a last resort, be required to further restrain the source through a traffic shaper or shut down some connections. This type of issue will be amplified when using FMTs. From this description, it can be concluded that it is important to develop a detailed simulation of MF-TDMA networks with FMTs and examine the trade offs between availability, QoS and channel management and utilization. This is the objective of this paper.

II. Adaptive Coding and Modulation (ACM)

Adaptive coding and modulation is used by satellite systems to maintain the bit-error ratio (BER) or packet error ratio (PER) below an agreed level while permitting a reduction of the required energy per information bit when fading conditions get worse.

Parallel concatenated convolutional coding with interleaving (turbo coding[7]) has attracted the interest of the satellite communications industry, leading to the standardization of such codes for second-generation DVB-RCS terminals.[5,8,9] This extends the dynamic range of the FMT and also allows the link throughput to be increased. Lower coding rates and/or reduced constellations can be selected when the carrier-to-noise power ratio at the input of the demodulator decreases due to propagation effects.

In a BoD scenario, the instantaneous information bit rate requested by the source should be granted if it is within the bounds agreed by CAC. This implies a reduction of the total throughput when multiple links experience fading simultaneously,[6] since the links compete for limited resources. Alternatively, some connections could be shut down, but this should remain a last resort solution.

For MF-TDMA, ACM offers a trade off between time/bandwidth and power. For M-PSK with code rate ρ, the user information bit rate R_b in [bps] is proportional to $B\rho\log_2 M$, where B is the bandwidth and ρ the code rate. If the M-arity M can be increased from 2 to 4, 8 or 16, then R_b can be increased by a factor of 1, 2, 3 or 4 respectively. Similarly, the information bit rate can be matched by varying the code rate ρ. But higher-level constellations and reduced coding require higher signal-to-noise ratios, so this is only feasible whenever atmospheric conditions are good enough:[10] typically close to clear-sky (provided the link power budget is large enough). Therefore, ACM is particularly useful for increasing the (clear-sky) throughput of a connection. It may increase the dynamic range of the FMT by about 0 to 17 dB depending on the link budget. So in general, ACM should be able to provide high availabilities for powerful connections. The advantage of ACM for power-limited connections is virtually non-existent.

III. DVB-RCS2 FMT

The overall architecture for DVB-RCS2 with ACM as a rain fade mitigation technique is depicted in Fig. 1. Provided the user station has been allowed connection by the Connection Admission Controller (CAC) it sends its traffic request (TRF Req), typically expressed as a bit rate or multiples of payload size (53 bytes for ATM or 188 bytes for MPEG packets, according to the encapsulation mode defined at logon) to the BoD controller. If granted, this will translate into the allocation of an "area", A_i, in the MF-TDMA subspace of a frame, as shown in Fig. 1.

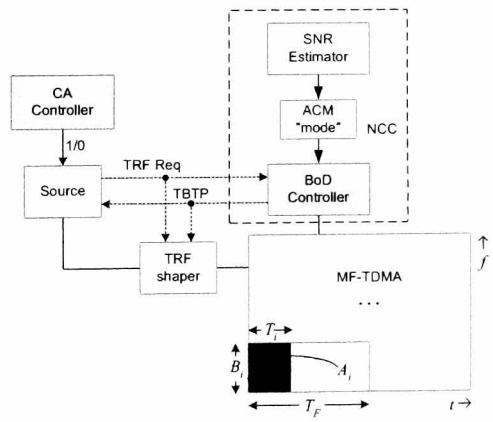

Figure 1. Architecture of ACM DVB-RCS2.

The dimensionless area A_i can be expressed as a time-bandwidth product:

$$A_i = B_i \times T_i \qquad (1)$$

where B_i is the allocated carrier bandwidth (Hz) and T_i is the period over which the connection i will be allowed to transmit during the next frame period T_F.

In addition, the Network Control Centre (NCC), where the BoD controller resides, measures the received SNR on the return channels from the received bursts of all active RCSTs (Return Channel Satellite Terminals). This operation can be achieved using, for example, a non-data aided SNR estimator such as in Ref. 11 and 12.

Depending on the attenuation level, the appropriate ACM "mode" (i.e. modulation and coding) is chosen by the NCC for a particular connection from the range of available ACM schemes. This is done using the look-up graph shown in Fig. 2 (the cases where BLC is used, with BLC > 1, will be explained later). We assume here that the system has a large enough link power budget to support 16APSK code rate 9/10 in clear-sky (no rain) conditions. When the SNR degrades, a more robust ACM scheme is selected to keep the PER below 10^{-7}, with the bit rate kept constant at $R_b^i = \hat{R}_b^i = 2.048$ Mbps. The dynamic range of the ACM FMT is therefore of the order of 17 dB. It is important that a change in ACM mode must also be accompanied by a change in bandwidth whose values are given in Table 1. For power limited systems, we could use the original DVB-RCS system[8]. In this case, the required link power budget would be reduced by 9 dB but the FMT dynamic range would fall to 8 dB (Fig. 2).

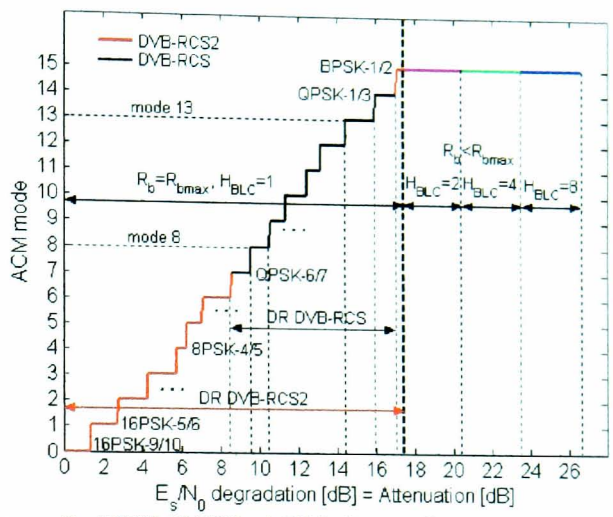

Figure 2. DVB-RCS2 ACM "mode" selection vs. SNR degradation w.r.t. clear-sky (PER=10^{-7}) and FMT Dynamic Range extension due to Burst Length Control.

Having selected the ACM mode based on measured SNRs (including fading conditions) and having received the BoD traffic requests R_b^i from the remote stations, the NCC can then allocate a carrier of appropriate bandwidth and duration to each connection for transmission of its bursts in the following frame period. This assignment and mode setting is achieved through the TBTP (Terminal Burst Time Plan) table broadcast to all stations as often as required (e.g. every superframe/frame period).

The maximum bit rate $\hat{R}_b^i$ available to a connection i assuming transmission over the full frame duration (T_F) is given by:

$$\hat{R}_b^i = \frac{B_i \cdot \rho(Att_i) \cdot \log_2 M(Att_i)}{(1+\alpha)} \quad \text{[bps]} \tag{2}$$

where $\alpha \approx 0.35$ is the roll-off factor, and B_i is the allocated bandwidth for connection i. When using a portion of the frame lasting only T_i seconds, ($T_i \le T_F$) the average bit rate $\overline{R}_b^i$ over the duration of a frame, T_F, is given by:

$$\overline{R}_b^i = \frac{B_i(Att_i)\rho_i(Att_i)\log_2 M_i(Att_i)}{T_F(1+\alpha)} \times T_i = k(Att_i) \times B_i T_i \tag{3}$$

where we have emphasized on the right hand side that bandwidth, code rate and M-arity are chosen based on attenuation (see Fig. 2). Note that in the original DVB-RCS[8] system, the BoD is restricted to QPSK (modes 7 to 14, see Table 1). In the context of DVB-RCS2, the system can be assumed to vary the carrier bandwidth and ACM modes over a wider range according to Table 1 which was obtained assuming transmission over the full frame duration T_F of 26.5 ms ($\overline{R}_b^i = \hat{R}_b^i = 2.048$ Mbps). If the signal bursts can be increased in steps of $T_{\min}$ 207 μs (one ATM cell/slot at 2 Mbps),[13] the bit rate $\overline{R}_b^i$ can vary between 16 kbps and 2.048 Mbps with a granularity of 16 kbps. So the BoD controller can match the required bit rate $\overline{R}_b^i$ by changing the duration of the burst for a connection.

Table 1. DVB-RCS2 carrier bandwidth variation depending on selected ACM mode ($\overline{R}_b^i = \hat{R}_b^i = 2.048$ kbps).

mode m	Modulation	ρ	B [kHz]	"area", A [-]
0	16-APSK	$\frac{9}{10}$	768	A_0
1		$\frac{5}{6}$	829.44	1.08 A_0
2		$\frac{3}{4}$	921.6	1.2 A_0
3		$\frac{2}{3}$	1036.8	1.35 A_0
4	8-PSK	$\frac{4}{5}$	1152	1.5 A_0
5		$\frac{3}{4}$	1228.8	1.6 A_0
6		$\frac{2}{3}$	1382.4	1.8 A_0
7	QPSK	$\frac{6}{7}$	1612.8	2.1 A_0
8		$\frac{4}{5}$	1728	2.25 A_0
9		$\frac{3}{4}$	1843.2	2.4 A_0
10		$\frac{2}{3}$	2073.6	2.7 A_0
11		$\frac{3}{5}$	2304	3 A_0
12		$\frac{1}{2}$	2764.8	3.6 A_0
13		$\frac{2}{5}$	3456	4.5 A_0
14		$\frac{1}{3}$	4147.2	5.4 A_0
15	BPSK	$\frac{1}{2}$	5529.6	7.2 A_0

In practice, assuming a BoD traffic request of $\overline{R}_b^i$ from a source and taking into account the selected ACM mode, the BoD controller can then calculate the requested MF-TDMA burst duration T_i that this request corresponds to. It is then up to the BoD controller to determine the allocated bandwidth and burst duration $\widetilde{T}_i \le T_i$ for the connection, taking into account all user connections and the limited MFTDMA space.

To explain the FMT scenario, let us assume that the connection is currently in mode 8 ($E_s/N_0 \approx 10$ dB below clear sky). Due to rain conditions, the SNR degrades further to 14.5 dB below clear-sky. Using Fig. 2 the system would switch to mode 13. This switching from mode 8 to mode 13 corresponds to halving the code rate from 4/5 to 2/5 with QPSK and has the effect of increasing the required MF-TDMA area from A_i to $A'_i = 2A_i$, expanding the carrier bandwidth by a factor of 2 (see case (a) in Fig. 3). The duration T_i of the burst is always chosen so as to match the required $\overline{R}_b^i$. Case (b) in Fig. 3 where BLC is employed will be discussed in the following section.

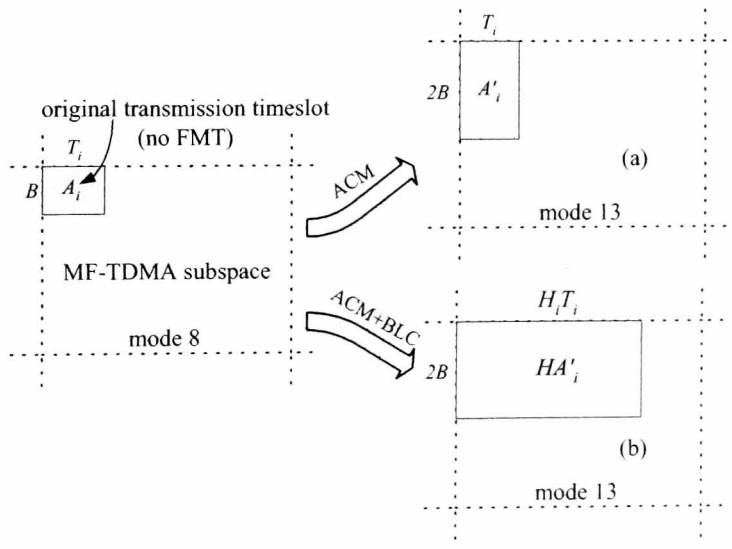

Figure 3. Simple example of equivalent area expansions (the source bit rate remains unchanged).

It should be noted that, from the user's perspective, the BoD capability of DVB-RCS2 can offer a wide range of transmission rates if resources are available. DVB-RCS2 provides the possibility of achieving high peak rates, if required, whenever weather conditions and the link power budget allow it. For example, with a modulator operating at its maximum supported symbol rate of 4.096 MBaud[14], a user can achieve a maximum bit rate $\hat{R}_b^i = 14.75$ Mbps ($\rho = 9/10$, $M = 16$), if allowed to transmit exclusively over a 5.5 MHz carrier bandwidth. Such increase in throughput can be used to boost the overall throughput or possibly to reduce the transmission queues.

IV. Resource management for BLC-DVB-RCS2 system

Looking at Eq. (3), the DVB-RCS2 system can be operated in the following ways.

ACM: The switching to a more robust ACM mode can be accompanied with an increase of the B_iT_i product (through an increase of the carrier bandwidth B_i) that allows the source bit rate to be kept constant. In particular, if the burst duration T^i is kept constant, then the bandwidth B_i (hence the symbol rate) must be chosen to counter-balance the change of ACM mode, as discussed in the previous section and Table 1.

Moreover, additional redundancy or lower order constellations can be introduced by changing to a more robust ACM mode whilst keeping the carrier bandwidth B_i for connection i constant. This implies a reduction in source bit rate and goes against the BoD philosophy as in this case we need to temper the required source bit rate. This technique, however, will have little effect on the actual packing of the live connections in the MF-TDMA space.

DRA: Similarly, if the ACM mode is kept unchanged, a decrease of the symbol rate (through reduction of the bandwidth B_i) will result in a reduced source bit rate. This countermeasure technique is known as Dynamic Rate Adaptation[5,9] (DRA). Here, the reduced symbol rate during fading conditions translates in an increase of the energy-per-symbol to noise-spectral-density ratio E_s/N_0. It is however introduced at the cost of a reduced user bit rate.

A further extension of the dynamic range of the FMT would be particularly useful in the case of power-limited systems for which high-order modulation schemes cannot be used. The ACM-BLC scheme can achieve this.

ACM-BLC: The source bit rate is maintained. However the change in ACM mode is accompanied with a change of the burst duration to $H_i \times T_i \le T_F$ while the bandwidth B_i is kept constant. Therefore the MF-TDMA area used by the connection becomes $H_iB_iT_i$. The factor H_i is called the BLC factor. The increased duration is used to transmit a time-expanded version of the original symbol stream. This FMT technique applied to DVB-RCS was described in detail, with simulations, in Ref. 12 and 16. Whenever the bust is increased by H_i we gain an extra $10\log_{10} H_i$ dB of protection against fading. The BLC is due to an apparent change of the symbol clock effectively increasing the symbol energy by a factor H_i. The impact of ACM-BLC scheme on the mode selection look-up graph is shown on the top-right of Fig. 2. When the ACM system's dynamic range is exhausted, time expansion by a factor H_i of 2, 4, 8 provides 3, 6 and 9 dB respectively of extra protection. We should repeat that BLC can only be applied when the bit rate of the source is below the peak bit rate $\hat{R}_b^i$, in order to allow for the necessary expansion from T_i to $H_i \times T_i \le T_F$. This is generally possible since most traffic sources are bursty and therefore they rarely transmit at peak bit rate.

The impact of BLC on the utilization of the MFTDMA space is illustrated in Fig. 3(b). BLC with $H_i = 3$ is applied in addition to a change to ACM mode 13. As a consequence, BLC brings an extra 4.77-dB fade protection, making the system capable of coping with up to 20.5 dB of attenuation.

Fig. 4 shows the attenuation the system would be able to cope with, by applying BLC, as a function of $\overline{R}_b^i$.

As explained before, BLC can only be applied when the traffic source requires a bit rate $\overline{R}_b^i$ smaller than its peak. Clearly, the lower the $\overline{R}_b^i$, the greater the extension to the FMT's dynamic range that BLC can offer.

Thus the ACM-BLC system, with its greater dynamic range, will be able to achieve greater link availabilities. This is at the cost of increased channel capacity utilization. Clearly, this will make it even more difficult to pack all the live connections within the MF-TDMA subspace.

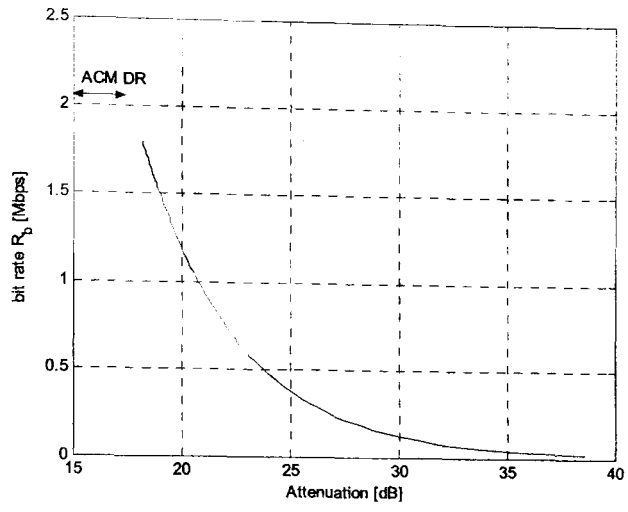

Figure 4. FMT Dynamic Range extension, offered by Burst Length Control, as a function of $\overline{R}_b^i$.

When BLC is used in addition to ACM, Eq. (3) becomes:

$$\overline{R}_b^i = k'(Att_i) \times T_i \tag{4}$$

where $k'(Att_i) = k(Att_i)/H_i(Att_i)$. So a BLC expansion factor H_i will result in an area expansion by the same factor H_i, so that $\overline{R}_b^i$ is still kept constant ($H_i(Att_i) = 1$, if no BLC is applied.)

H_i has to be chosen by the NCC, which, depending on the attenuation level, will select and apply the appropriate BLC factor using the graph shown in Fig. 2.

In our particular study, BLC is only applied when the most robust ACM scheme cannot provide the required rain margin.

The task of the BoD controller, assignment of resources in response to a BoD request, clearly implies the need for an adaptive BoD algorithm. The main issues to be dealt with are fairness, channel efficiency and QoS control for multiple BoD flows. The following summarizes the BoD process.

The BoD controller receives all user traffic requests $\overline{R}_b^i$ and, having selected the appropriate ACM mode for each user and corresponding bandwidth B_i. The BoD controller can then calculate the requested burst duration $T_i = \overline{R}_b^i / k'(Att_i)$ for each connection i for the following frame interval. The BoD controller can then group the connections using the same ACM mode (and bandwidth) into ACM request tables shown in Fig. 5. In practice, every table will have a different size and the entries will depend on actual rain conditions and current traffic requirement of each traffic source. The number of ACM tables may also be variable, depending on the rain conditions.

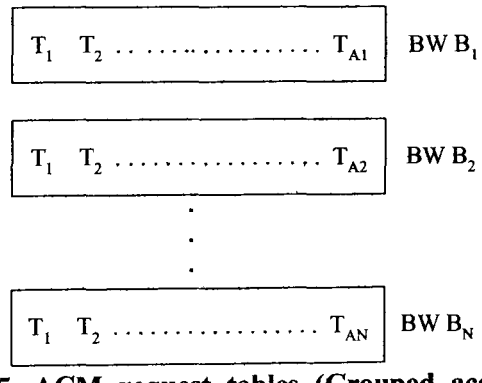

Figure 5. ACM request tables (Grouped according to their required ACM mode or equivalently their carrier bandwidth).

The BoD controller's next task is to calculate the proportion of MF-TDMA usage that will be required for each ACM mode (or carrier bandwidth). This ensures that all the flows, with different ACM mode are treated fairly. If A_{req} is the total required MF-TDMA area given by:

$$A_{req} = \sum_{j=1}^{N} B_j \times \left(\sum_{i=1}^{A_j} T_i \right) \tag{5}$$

then the proportion P_i of the MF-TDMA area required for each mode is

$$P_j = \frac{B_j \sum_{i=1}^{A_j} T_i}{A_{req}}, \quad j = 1,2,...N \tag{6}$$

Therefore the number of channels of width B_j needed in the next MF-TDMA frame is

$$N_j = \left\lfloor \frac{P_j \times B_{\max}}{B_j} \right\rfloor, \quad j = 1,2,...N \tag{7}$$

where $\lfloor x \rfloor$ means the integer part of x and $B_{\max}$ is the total MF-TDMA bandwidth available to the BoD resource controller.

After the bandwidth is appropriately segmented using the above equations, the controller's next step is to allocate burst durations $\widetilde{T}_i \le T_i$ to each traffic request in a same ACM request table.

This is achieved by running a resource allocation algorithm. In this paper, the requests are first sorted from heaviest-to-lightest. Then a round-robin allocation is applied for serving the requests. The allocation is performed using a gradual incremental technique in order to ensure fairness. In particular, for each ACM request table, the BoD controller initially gives a guaranteed minimum cell rate of 16 kbps to all live connections by initially allocating the minimum burst duration $T_{\min} = 207\mu s$. Using a "for" loop, the granted individual source bit rate is then built-up in steps of 16 kbps in a round robin way for all the connections until either (i) the resource of MF-TDMA space available to the ACM request table is exhausted or (ii) the actual BoD requests for a particular connection has been satisfied by the RA. Any request that is not fully granted in the current allocation round is queued by the traffic source to be served in the next allocation (i.e. frame) period. Thus all connections are served, however the very greedy BoD requests may end up as partially queued. Obviously, the above process is repeated for all ACM request tables.

The use of $\lfloor x \rfloor$ ensures that as a best case, just enough MF-TDMA resources are given to a particular ACM request table since in general $\lfloor x \rfloor \le x$. Thus Eq. (7) makes sure that the channel utilization is maximized. However, the most greedy traffic request will not be fully granted and thus they will need to be queued at the source. Thus our proposed algorithm is trying to maximize channel utilization at the cost of delay.

An alternative would be to use $\lceil x \rceil$ in Eq. (7) where $\lceil 1.2 \rceil = 2$ for example. In this case, more resources will be reserved than is effectively required. So the system tries to minimize delay at the cost of channel utilization. This approach may prove useful especially when few connections are live in the network making sure that at least one channel is made available for a particular ACM mode. Another alternative, in between the previous two would be to use simple rounding in Eq. (7).

So the basic RA processing of each ACM request table is as follows.

Find the set of granted burst $\widetilde{T}_i$ for all connections with the same ACM mode such that

$$\widetilde{T}_i \le T_i = \frac{\overline{R}_b^i}{k'(Att_i)} \text{ is maximized} \tag{8}$$

subject to

$$\begin{cases} (i) & \sum_{i=1}^{N} T_i \le N_i T_F \\ (ii) & T_{\min} \le T_i \le T_F \end{cases} . \tag{9}$$

Clearly when $\widetilde{T}_i \le T_i$ some traffic will be queued at the source.

The above allocation algorithm applies mainly to UBR or ABR types of traffic since they have to be able to tolerate some variations of the delay.

In the (hopefully rare) cases when the resource allocation cannot be achieved (e.g. when some queues become unstable and start growing exponentially), the BoD controller will have to inform the Call Admission Controller, which is responsible for accepting/shutting-down connections so that the remaining live connections can be serviced adequately.

V. Simulation of DVB-RCS2 with FMT

The scenario described in the above two sections has been simulated in order to obtain some system performance results. We focus on the transport of aggregate internet traffic that is known to exhibit self-similarity with long-range dependence and high levels of burstiness[17]. In our simulations we assume one connection per terminal, each generating a stream of traffic ATM cells during the activity state (sojourn time) of a Pareto ON/OFF model ($a = 1.2$) with a baseline Peak Cell Rate (PCR) of 2.048 Mbps. Note that in order to simplify the process and speed up the simulation, we simulate only the dynamic management of a MF-TDMA space of bandwidth $B_{\max} = 5.5$ MHz. In this paper, to be compatible with known DVB-RCS systems, we have assumed that $T_{\min} = 207\,\mu s$ and $T_F = 26.5$ ms. In order to get reasonable utilization, this required fifteen 2.048 Mbps connections.

The resource allocation algorithm described in section IV has been implemented. Any request that has only been partially met by the BoD controller is queued to be served in the next allocation (i.e. frame) period. Thus all connections are served, however the very greedy BoD request may end up as partially queued. The RA algorithm is applied in a round robin fashion to each of the ACM request tables. The traffic requests are cumulated over periods of one second and sent to the BoD controller. This update rate is very important when integrating an FMT within DVB-RCS, as it must be able to track the variations of the rain attenuation process. Faster rates may yet be required if the FMT is also to compensate dynamically for interference and/or scintillations.

Depending on the attenuation level on each link, the appropriate FMT mode and bandwidth based on Fig. 2 is selected by the BoD controller. Then the granted burst durations, $\widetilde{T}_i$ are communicated to each live traffic source via the TBTP table. The new MF-TDMA allocation is implemented in the next TBTP interval (1 second after the cumulated source request).

In this paper, the fifteen rain events were uncorrelated, however every connection experienced some rain attenuation during the simulation which covered one hour of network time. The deepest rain event was up to 15 dB in amplitude, with a duration of 10-20 minutes. So, based on Fig. 2, the system has a large enough link power budget in order to fully utilize ACM at its full range of possible modes (0 to 15). Therefore the extra level of protection offered by BLC, although available, is not needed as the FMT dynamic range is not exhausted due to the relatively low magnitude of the particular rain events.

An important issue is that the system should be able to support the active connections including their FMT and short-term traffic needs. The available MF-TDMA capacity allocated to flows of the same class is limited and fixed. As the RA algorithm may not be able to grant 100% of all the individual requests, if the agreed QoS or service level agreement allows it, some connections could be blocked until resources became available. The present simulation prevents this by trying to ensure that all connections will be still kept "alive" at the cost of delay under bad channel/traffic conditions. This solution is acceptable for ABR (Available Bit Rate) traffic and it is also desirable for UBR (Unspecified Bit Rate) connections.

As a baseline case, we first consider an MF-TDMA system with Pareto traffic sources with a fixed peak cell rate (PCR) of 2.048 Mbps. However, a key additional requirement is to be able to control the stability of the queues at each of the sources in case of extreme network congestion due to very unfavourable traffic or rain conditions.

A simple way of achieving this second layer of protection is to apply some simple traffic shaping to all the sources. In this paper, we implement a variable PCR traffic shaping technique. When the MF-TDMA network becomes too congested, the sources are made to reduce their traffic by reducing their PCR. Similarly, when

conditions improve or buffer occupancy is relatively low, the BoD controller allows the sources to increase their PCR to achieve higher user throughputs. Thus, when the system is very heavily loaded, the throughput of the connections is reduced until the system becomes capable of reducing its queued backlog traffic.

Fig. 6 shows the operation of the variable PCR scheme for a particular traffic source. Whenever, the size of the queue for that source exceeds 2 Mbits, the BoD controller reduces the peak cell rate of the source by a factor of two. The source is then able to gently increase its peak bit rate in steps of 128 kbps until the next time the queue exceeds the threshold when it is again reduced by factor of two. The increments are allowed by the BoD controller very 6 seconds. This has the effect of reducing quickly the depth of the queue. Clearly this congestion avoidance mechanism is very reminiscent to that used by TCP/IP networks. In severe conditions due to either heavy traffic and/or heavy rain, this mechanism is extremely useful as it prevents queues from growing too large, it protects the network from further congestion and reduces the possibility of having to block or shut down individual connections. Thus the main part of the resource management can be performed by the BoD controller and not the CA Controller.

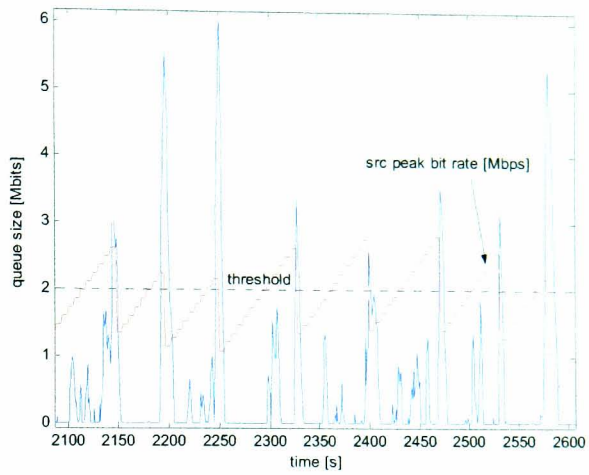

Figure 6. Dynamic PCR adaptation to control the queue of an individual connection (zoom).

Fig. 7 shows the basic behaviour of our 15 Pareto sources for fixed PCR and variable PCR traffic shaping cases. These traces demonstrate the different behaviour of the fifteen queues with and without variable PCR traffic shaping. In the fixed PCR case (a), some individual queue sizes vary over larger ranges. These queue depths are significantly reduced with the variable PCR scheme. Thus variable PCR improves the QoS of the connections.

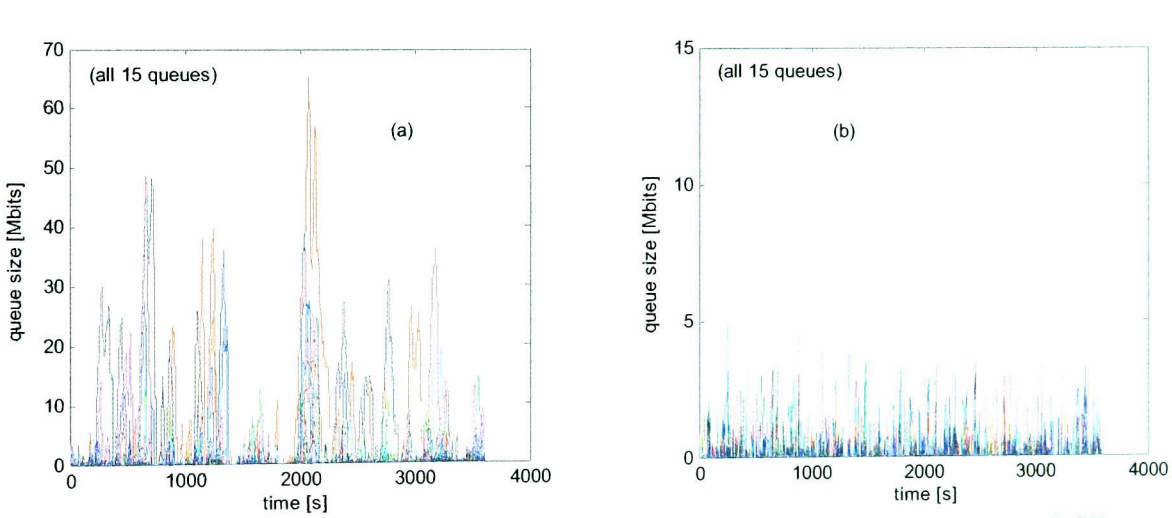

Figure 7. All 15 connection queues in the case of (a) constant PCR (b) variable PCR.

Fig. 8 compares the global queues (i.e. the sum of the queues from all sources) for fixed and variable PCR traffic shapers. In the fixed PCR case, there are significant queuing events at about t=2100 and 3200 seconds. These large peaks are due to a combination of large traffic requests from all the sources. The mean global queue size in the dynamic PCR case is significantly lower than that of the constant PCR scenario. Also, the fixed PCR system takes a long time to reduce the backlog. This long backlog is directly linked to the duration and depth of the rain event affecting the connection. This type of queue behaviour is not desirable since a deeper or longer rain event may result in large queuing delays and long tailbacks. Further investigations are required in order to formalize a way of selecting suitable queue thresholds in the variable PCR scheme.

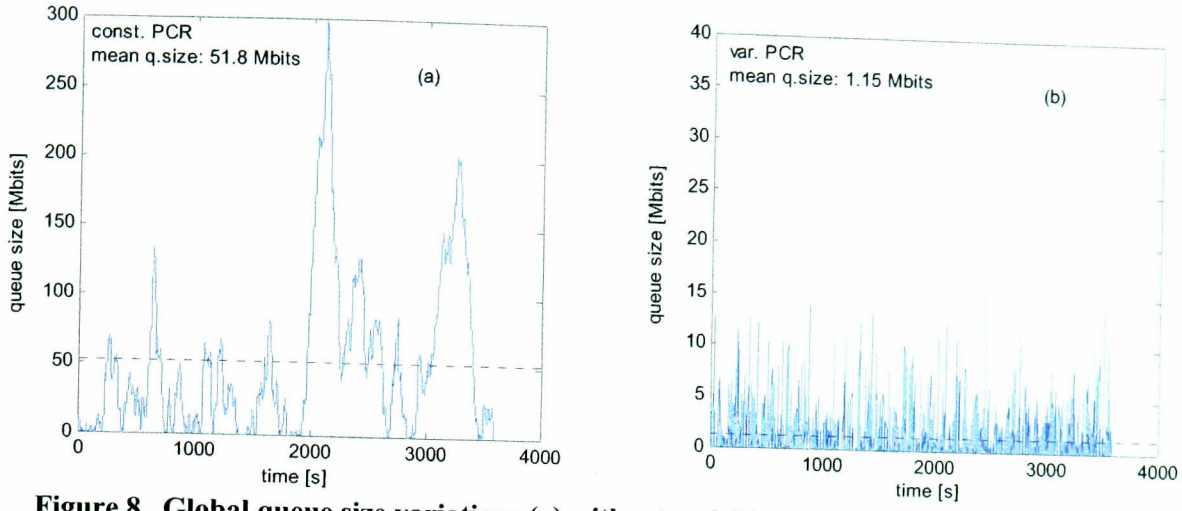

Figure 8. Global queue size variations (a) without and (b) with dynamic PCR adaptation.

We have also considered the trade-off between delay and channel utilization to verify that the variable PCR technique does not have much of a negative effect on the efficiency of the channel. This is exemplified in Fig. 9(b).

We can see that when using the variable PCR traffic shaper, there is an instantaneous drop of the minimum utilization value to about 43%. However although the channel utilization is more erratic with variable PCR, the network can achieve an average channel efficiency of 93%.

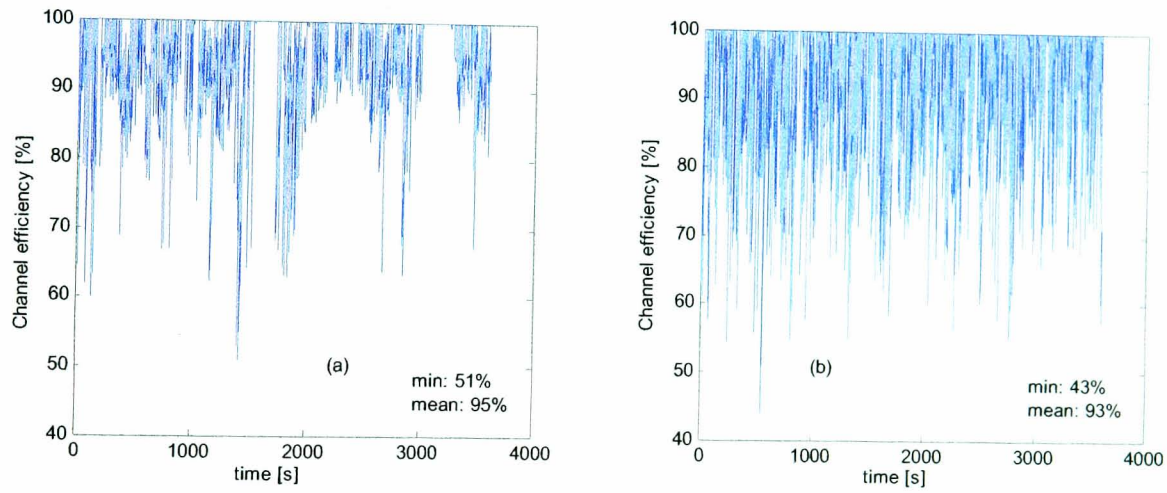

Figure 9. MF-TDMA utilization (a) without and (b) with dynamic PCR adaptation.

Thus traffic shaping has decreased the average channel utilization by only 2%. This seems a reasonable price to pay for improved delay/QoS performance.

VI. Conclusions

BLC offers an extra 3-dB protection every time the burst duration is doubled. This permits the dynamic range of the FMT to be increased, thereby increasing the availability of MF-TDMA connections. This is particularly desirable for power-limited return links from very small terminals. In such cases, ACM, DRA or even power control will not be able to provide the required availabilities. BLC can easily be integrated within the DVB-RCS2 standard.

This paper has described a resource management algorithm supporting standard bandwidth-on-demand and FMT control. The resource allocation (RA) algorithm relies on a simple fair round-robin technique. Its main objective is to try and keep any accepted connections alive irrespective of traffic and/or rain conditions. To achieve high channel utilizations, the RA must be able to allocate resources thereby using the DVB-RCS2 with its full flexibility. In this paper we focused on the servicing of UBR/ABR sources. Although in principle no QoS is required for such traffic, a simple adaptive traffic shaping mechanism still seems desirable to control the queues and delays of UBR/ABR

connections. This proves useful for reducing the time required to reduce backlogs in the network. Such adaptive mechanism provides a failsafe strategy in cases where the BoD traffic is too high, the rain conditions are severe or too many connections are live within the network.

Future work includes extension of the algorithm to a multi-class scenario with differentiated services involving traffic streams with different QoS levels (for example different delay tolerance). The basis is the same but further investigation is required to control queuing delays for traffic with differing priorities. The dynamic management of sub-partitions of the MF-TDMA may also need studying in multi-class traffic scenarios.

Finally the design of MF-TDMA DVB-RCS2 networks with BLC also requires a detailed study of the impact of correlated rain attenuation on the practically achievable network performance. This will require use of more realistic rain attenuation simulators[18].

References

[1]Hatdjitheodosiou M. H., Ephremides A., Friedman D.: "Broadband Access via Satellite", Technical Research Report, *CSHCN* T.R. 99-2, Centre for Satellite and Hybrid Communication Networks, University of Maryland, 1999, available at http://techreports.isr.umd.edu/TechReports/ CSHCN/1999/CSHCN_TR_99-2/CSHCN_TR_99-2.pdf

[2]Ippolito L. J.: "Radio propagation for space communications systems", *IEEE Proceedings*, Vol. 69, No. 6, pp. 697-727, U.S.A., June 1981.

[3]Nelson R. A.: "V-band: Expansion of the Spectrum Frontier", *Via Satellite*, February 1998, pp. 66+.

[4]Touw S. I. E.: "Analyses of Amplitude Scintillations for the Evaluation of the Performance of Open-Loop ULPC Systems", MSc Thesis, Eindhoven University of Technology, Eindhoven, The Netherlands, 1994.

[5]Panagopoulos A. D., Arapoglou P. D. M., Cottis P. G.: "Satellite Communications at Ku, Ka and V Bands: Propagation Impairments and Mitigation Techniques", *IEEE Communications Surveys & Tutorials*, 3rd quarter 2004, Vol. 6, No. 3, available at http://www.comsoc.org/livepubs/surveys/public/2004/jul/pdf/ panagopoulos.pdf.

[6]Alamanac, A. B., Bousquet M.: "Millimetre-Wave Radio Systems: Guidelines on Propagation Modelling and Impairment Mitigation Techniques Research Needs", *MC#3 Meeting and 1st COST280 Int. Workshop*, Malvern, U.K., 1-3 July 2002.

[7]Proakis J. G.: *Digital Communications*, McGraw Hill, 4th Ed., 2001, Chapter 8.

[8]ETSI EN 301 790 (V1.3.1): "Digital Video Broadcasting (DVB); Interaction Channel for Satellite Distribution Systems" (also known as the DVB-RCS specification), Final Draft, 2002-11, available at http://www.etsi.org/getastandard/home.htm

[9]"Protocols and Signalling for Fade Mitigation Techniques (FMT) in DVB-RCS Multi-beam Systems", *ESA Workshop on 'Fade Mitigation Techniques for DVB-S2/DVB-RCS systems'*, Noordwijk, The Netherlands, 13-14 December 2004.

[10]Grémont B.: "Fade Countermeasure Modelling for Ka-band Satellite Links", PhD Thesis, Coventry Univ., Nov. 1997.

[11]Pauluzzi D. R., Bealieu N. C.: "A comparison of SNR Estimation Techniques for the AWGN Channel", *IEEE Trans. on Communications*, Vol. 48, No. 10, pp. 1681-1691, Oct. 2000.

[12]Noussi E., Grémont B., Filip M.: "Integration of Fade Mitigation within Centrally Managed MF-TDMA/DVB-RCS Networks", Special Issue on 'Satellite Network Protocols and Performances', *International Journal of Space Communications* (full manuscript accepted by the editorial board), to be published in 2005, available on demand from the authors.

[13]Krause J.: "The ASTRA BBI System: An Overview", SES ASTRA S. A., available at http://www.luxinnovation.lu/presentations/020708_presa_Krause.pdf

[14]Spacebridge Semiconductor, "SB7088 Broadband Wireless Return Channel Modulator", *Advance Product Information*, available at http://www.spacebridge.com/products/sb7088.htm

[15]Carassa F.: "Adaptive Methods to Counteract Rain Attenuation Effects in the 20/30 GHz Band", *Space Communication and Broadcasting 2*, North Holland, 1984, pp. 253-269.

[16]Noussi E., Grémont B., Filip M.: "Adaptive MF-TDMA: Burst Length Control as a Rain Fade Countermeasure", *CSNDSP, 4th Int. Symposium Proceedings*, University of Newcastle upon Tyne, 20-22 July 2004, p. 43-46.

[17]Leland W. E., Taqqu M. S., Willinger W., Wilson D. V., "On the Self-Similar Nature of Ethernet Traffic", *IEEE/ACM Transactions on Networking*, Vol. 2, No. 1, pp. 1-15, 1994.

[18]Grémont B.: "Simulation of Rainfield Attenuation for Satellite Communication Networks", *1st Workshop of the COST Action 280 Propagation Impairments Mitigation for Millimetre Wave Radio Systems*, Malvern, UK, 1-3 July 2002.